

Dissertation zur Erlangung des Doktorgrades der Fakultät für
Chemie und Pharmazie der Ludwig-Maximilians-Universität
München

**Systematic Studies to Correlate Microcalorimetry with Stability Studies on
Liquid Formulations of Various Protein Drugs.**

Vorgelegt von
Ahmed Moustafa Kamal Youssef Mohamed
Aus Assiut, Ägypten

München 2010

Erklärung

Diese Dissertation wurde im Sinne von § 13 Abs. 3 bzw. 4 der Promotionsordnung vom 29. Januar 1998 von Herrn Prof. Dr. G. Winter betreut.

Ehrenwörtliche Versicherung

Diese Dissertation wurde selbständig, ohne unerlaubte Hilfe erarbeitet.

München, den 29.03.2010

.....
Ahmed M. K. Youssef

Dissertation eingereicht am: 29.03.2010

1. Gutachter: Prof. Dr. Gerhard Winter
2. Gutachter: Prof. Dr. Wolfgang Frieß

Mündliche Prüfung am: 21.05.2010

Acknowledgements

The present thesis was written at the department of Pharmacy, Pharmaceutical technology and Biopharmaceutics at the Ludwig-Maximilians-University in Munich under the supervision of Prof. Dr. Gerhard Winter.

First of all, I would like to express my deepest appreciation to my supervisor Prof. Dr. Gerhard Winter for giving me the opportunity to join his research group. Especially, I want to thank him for his professional guidance and scientific support. I appreciate very much that he offered me great opportunities to present the work at numerous congresses all over the world. Thank you for giving me the chance to integrate in a highly productive scientific environment which I wouldn't be able to join without your help.

I am also deeply grateful for the German Scientific Exchange Service (DAAD) for funding my stay with my family in Germany. I want to especially thank Mrs. Margret Leopold for her patience and for being very helpful during my stay in Germany. Additionally, I would like to express my great appreciation for the DAAD for offering me a six month intensive German language course before my study in Munich. Being a German speaker I was definitely able to communicate better and to integrate in the German culture.

Special Thanks to Dr. Friedrich Gruber for the guidance in the first year of my PhD work. Above all, his friendship during that period helped me very much to integrate in the group. Many thanks are extended to Dr. Sandra Schulze for rendering every help and assistance.

Especially thanks to all my colleagues in the research group of Prof. Dr. Gerhard Winter and Prof. Dr. Wolfgang Frieß for the cooperative and convenient atmosphere. I especially thank Dr. Michael Wiggenhorn, Dr. Stefan Gottschalk, Dr. Reiner Lang, Dr. Kathrin Schersch, Kathrin Mathis and Timm Serno of all the support and the numerous discussions.

I want to especially thank Katja Schmid and Dr. Julia Myschik for the proof reading of the thesis.

Thanks are extended to Roche Diagnostics GmbH, Penzberg, Germany for the donation of the protein drugs used in this thesis.

I would like also to thank Prof. Dr. W. Frieß, Prof. Dr. F. Bracher, Prof. Dr. C. Wahl-schott, Prof. Dr. M. Biel and Prof. Dr. F. F. Paintner for serving as members of my thesis advisor committee.

I would like to express my great thanks to my father Prof. Dr. M. K. Youssef setting to me an example that I am trying to follow in all my life. I want to thank my mother Prof. Dr. S.M. Abo El Soud and my sister Heba for their continuous care and support.

Very special thanks to my small family, my wife Nauras and my little daughter Salma. Without both of you I would not be able to achieve this work. Your love and encouragements gave me the power to complete it till the end.

Table of Contents

Chapter 1: General Introduction and objective of the thesis

1. Introduction.	1
2. Protein stability	2
2.1. Chemical protein stability	2
2.2. Physical protein stability	2
2.2.1. Protein conformational stability	3
2.2.2. Protein colloidal stability	4
2.3. Factors affecting protein stability	4
3. Analytical techniques for protein formulation development	5
3.1. Monitoring techniques	5
3.1.1. Chromatography	5
3.1.1.1. <i>Reversed phase chromatography (RPC)</i>	5
3.1.1.2. <i>Size exclusion chromatography (SEC)</i>	6
3.1.1.3. <i>Ion exchange chromatography (IEC)</i>	6
3.1.2. Particle analysis	6
3.1.3. Gel electrophoresis	7
3.1.3.1. <i>Native gel electrophoresis</i>	7
3.1.3.2. <i>Sodium dodecyl sulphate polyacrylamide gel electrophoresis (SDS-PAGE)</i>	7
3.1.3.3. <i>Isoelectric focusing (IEF)</i>	7
3.1.3.4. <i>Two dimensional (2D) gel electrophoresis</i>	8
3.2. Stability prediction techniques	8
3.2.1. Spectroscopy	8
3.2.2. Calorimetry	9
4. Differential scanning microcalorimetry (μDSC)	11
4.1. μDSC parameters	11
4.1.1. Protein unfolding temperature (T_m)	11
4.1.2. Protein unfolding reversibility	12
4.1.3. Denaturation heat capacity	13
4.1.4. Gibbs free energy	13
4.2. Application of μDSC in protein formulation development	13
5. Objective of the thesis	15
6. References	16

Chapter 2: Microcalorimetry as a predictive tool for physical stability of granulocyte colony stimulating factor (GCSF) in solution at different pH values.

1. Introduction.	25
2. Materials and Methods.	27
2.1. Materials.	27
2.2. Formulations.	27
2.3. Thermal stability using microcalorimetry (μ DSC).	27
2.4. Accelerated stress stability study.	28
2.4.1. Mechanical stress.	28
2.4.2. Thermal stress.	28
2.5. Analytical methods.	29
2.5.1. Size exclusion high performance liquid chromatography (SE-HPLC).	29
2.5.2. Light obscuration.	30
2.5.3. Sodium dodecyl sulphate polyacrylamide gel electrophoresis (SDS-PAGE).	30
2.6. Correlation.	30
2.6.1. Ranking of formulations according to μ DSC.	31
2.6.2. Ranking of formulations according to stress stability studies.	31
3. Results and discussion.	33
3.1. μ DSC measurements.	33
3.2. Accelerated stress stability studies.	34
3.2.1. Mechanical stress.	34
3.2.2. Thermal stress.	35
3.3. Correlation.	37
3.3.1. Predictive power of the μ DSC parameters.	38
3.3.2. Predictive power of the μ DSC based rankings.	39
4. Conclusion.	43
5. References.	44
6. Appendix 2.I.	45
7. Appendix 2.II.	48

Chapter 3: A critical evaluation of microcalorimetry as a predictive tool for long term stability of liquid protein formulations

1. Introduction.	51
I. Granulocyte Colony Stimulating factor (GCSF).	53

I.1. Materials and methods.	53
I.1.1. Materials.	53
I.1.2. Formulations.	53
I.1.3. Thermal stability using microcalorimetry (μDSC).	54
I.1.4. Isothermal stability study (IsoSS).	56
I.1.4.1. Reversed - Phase high performance liquid chromatography (RP-HPLC).	56
I.1.4.2. Size-Exclusion HPLC (SE-HPLC).	56
I.1.4.3. Turbidity measurements.	57
I.1.4.4. Light obscuration.	57
I.1.4.5. Sodium dodecyle sulphate polyacrylamide gel electrophoresis (SDS-PAGE).	57
I.1.5. Correlation.	58
I.1.5.1. Ranking of formulations according to μ DSC.	58
I.1.5.2. Ranking of formulations according to IsoSS.	58
<i>I.1.5.2.1. Ranking based on physical stability (R_p).</i>	<i>59</i>
<i>I.1.5.2.2. Ranking based on chemical stability (R_c).</i>	<i>59</i>
<i>I.1.5.2.3. Ranking based on overall stability (R_s).</i>	<i>59</i>
I.1.6. Prediction quality.	60
I.2. Results and discussion.	62
I.2.1. μDSC measurements.	62
I.2.2. Isothermal stability study (IsoSS).	64
I.2.3. μDSC as a predictive tool for IsoSS.	65
I.2.3.1. Correlation coefficients.	66
I.2.3.2. Prediction quality.	69
I.2.4. μDSC in comparison with classical accelerated IsoSS.	71
I.2.4.1. Correlation coefficients.	71
I.2.4.2. Prediction quality.	73
II. Monoclonal Antibody (MAB).	76
II.1. Materials and methods.	76
II.1.1. Materials.	76
II.1.2. Formulations.	76
II.1.3. Thermal stability using μDSC.	77
II.1.4. Isothermal stability study (IsoSS).	78
II.1.4.1. Size-exclusion HPLC (SE-HPLC).	78
II.1.4.2. Light obscuration.	78
II.1.4.3. Sodium dodecyle sulphate polyacrylamide gel electrophoresis (SDS-PAGE).	79
II.1.4.4. Isoelectric focusing gel electrophoresis (IEF).	79
II.1.5. Correlation.	79
II.1.5.1. Ranking of formulations according to μ DSC.	79
II.1.5.2. Ranking of formulations according to IsoSS.	80

II.1.6. Prediction quality.	81
II.2. Results and discussion.	82
II.2.1. μ DSC measurements.	82
II.2.2. Isothermal stability study (IsoSS).	84
II.2.3. μ DSC as a predictive tool for IsoSS.	85
II.2.3.1. Correlation coefficients.	85
II.2.3.2. Prediction quality.	89
II.2.4. μ DSC in comparison with classical accelerated IsoSS. ...	91
III. Pegylated Interferon α2a. (PEG-INF)	94
III.1. Materials and methods.	94
III.1.1. Materials.	94
III.1.2. Formulations.	94
III.1.3. Thermal stability using (μ DSC).	95
III.1.4. Isothermal stability study (IsoSS).	95
III.1.4.1. Size-exclusion high performance liquid chromatography (SE-HPLC).	96
III.1.4.2. Reversed phase - HPLC (RP-HPLC).	96
III.1.4.3. Light obscuration.	96
III.1.4.4. Sodium dodecyl sulphate polyacrylamide gel electrophoresis (SDS-PAGE).	97
III.1.5. Correlation.	97
III.1.5.1. Ranking of formulations according to μ DSC.	97
III.1.5.2. Ranking of formulations according to IsoSS.	97
III.1.5.2.1. Ranking based on physical stability (R_p).	97
III.1.5.2.2. Ranking based on chemical stability (R_c).	98
III.1.5.2.3. Ranking based on overall stability (R_s).	98
III.1.6. Prediction quality.	98
III.2. Results and discussion.	100
III.2.1. μ DSC measurements.	100
III.2.2. Isothermal stability study (IsoSS).	100
III.2.3. μ DSC as a predictive tool for IsoSS.	101
III.2.3.1. Correlation coefficients.	102
III.2.3.2. Prediction quality.	105
III.2.4. μ DSC in comparison with classical accelerated IsoSS.	105
2. Conclusion.	110
3. References.	112
4. Appendix 3.I.	117
5. Appendix 3.II.	132

Chapter 4: Other strategies for the prediction of long term stability of GCSF liquid formulations

1. Introduction.	149
2. Materials and methods.	150
2.1. Materials.	150
2.2. Formulations.	150
2.3. Fourier Transform Infrared Spectroscopy (FTIR).	150
2.4. 2 nd derivative UV spectroscopy.	152
2.5. Non-Isothermal accelerated stability study (Non-IsoSS).	153
2.6. Isothermal stability study (IsoSS).	154
2.7. Ranking.	155
2.7.1. Ranking for the IsoSS.	155
2.7.2. Predictive rankings.	155
2.7.2.1. Individual ranking.	155
2.7.2.2. Combined ranking.	156
2.8. Correlation.	157
3. Results and discussion.	158
3.1. Measured parameters.	158
3.2. Correlation.	158
3.2.1. Prediction based on individual rankings.	159
3.2.1.1. Differential scanning microcalorimetry (μ DSC.)	160
3.2.1.2. Fourier Transform Infrared spectroscopy (FTIR)	161
3.2.1.3. 2 nd derivative UV spectroscopy.	161
3.2.1.4. Non-IsoSS measured Temp ⁵⁰ .	162
3.2.1.5. IsoSS40°C.	162
3.2.2. Prediction based on combined ranking.	163
3.2.2.1. Physical stability	166
3.2.2.2. Chemical stability.	166
3.2.2.3. Overall stability.	166
4. Conclusion.	167
5. References.	168
6. Appendix 4.I.	170
Chapter 5: Summary of the thesis.	183

List of Abbreviations

SD	Standard deviation
μ DSC	Differential scanning microcalorimetry
T_m	Unfolding temperature
ΔH	Enthalpy change
SDS-PAGE	Sodium dodecyl sulphate polyacrylamide gel electrophoresis
IEF	Isoelectric focusing
FTIR	Fourier transform infrared spectroscopy
FNU	Formazin Nephelometric units
DOE	Design of Experiment
HP- β -CD	Hydroxy propyl beta cyclodextrin
GCSF	Granulocyte Colony Stimulating Factor
MAB	Monoclonal Antibody
PEG-INF	Pegylated Interferon
SE-HPLC	Size-Exclusion high performance liquid chromatography
RP-HPLC	Reversed phase high performance liquid chromatography
R^2	Pearson product moment correlation coefficient
R_{T_m}	Ranking based on T_m
R_{opT_m}	Optimized R_{T_m}
R_{Rev}	Ranking based on the Degree of unfolding reversibility
R_{opRev}	Optimized R_{Rev}
R_{com}	Combined ranking
R_p	Ranking based on physical stability
R_c	Ranking based on chemical stability
R_s	Ranking based on overall stability
K_p	Monomer denaturation rate constant
K_c	Chemical degradation rate constant
IsoSS	Isothermal stability study
Non-IsoSS	Non isothermal stability study
$T_{m\mu DSC}$	Unfolding temperature determined by μ DSC
T_{mFTIR}	Unfolding temperature determined using FTIR
T_{mUV}	Unfolding temperature determined by 2 nd derivative UV spectroscopy
Temp ⁵⁰	Temperature at which 50% of the protein is denaturated

Chapter 1

General Introduction and objective of the thesis

The production of proteins needs much effort in developing a stable formulation, as proteins are complex molecules whose stability is governed by several thermodynamic and kinetic aspects. Therefore, a protein molecule would show in most cases several degradation pathways which almost happen simultaneously. Stability prediction is thus expected to be a highly complicated and tricky process and therefore mastering such a process is a valuable criterion in protein formulation development laboratories. An overview about protein stability general issues, including reported analytical and predictive scenarios in protein formulation development is given in chapter 1.

1. Introduction:

Biotechnologically developed medicines and vaccines offered millions of people new hope to cure their often life threatening diseases. More than 100 registered biopharmaceutical medications are already used in treating serious indications including, for example, cancer, hepatitis and rheumatoid arthritis. More than 30 years ago the first recombinant peptide hormone was successfully produced¹, followed by many success stories including recombinant human insulin² which was in 1982 the first approved genetically engineered biopharmaceutical. The process developed very fast and nowadays the number of biopharmaceuticals under development is extremely magnified to 633 biotechnological medicines in 2008³.

Therefore, the need to develop clear and reliable strategies in stabilizing proteins became mandatory and one of the great challenges is to prevent denaturation processes including protein unfolding and aggregation during the time of shelf life. However, the prediction of the overall protein stability is not trivial and therefore real time stability studies are conducted, which are very costly and time consuming. Due to the complex formation mechanisms and structure of protein degradation products it is quite hard to characterize and furthermore to quantify such species accurately with a single analytical method. In fact, many analytical techniques have to be involved to get reliable decisions. Moreover, predictive strategies are still not well evaluated with respect to real long term stability of proteins. For successful

prediction of protein long term stability the selected analytical method(s) should be able to predict the rates of main protein degradation processes.

2. Protein stability:

The term protein stability was defined by many authors⁴⁻⁶. Most of them refer the protein stability to its resistance towards chemical and physical structure modifications. It should be emphasized that chemical and physical stability events are not necessarily separated processes that take place independently, but in most cases they occur simultaneously. There are many published data where physical instability events were caused by chemical modification and vice versa. For example, human relaxin aggregates after oxidation⁷. The reactivity of the sulphhydryl group in B-lactoglobulin-A is slower in native than in partially folded state⁸.

2.1. Chemical protein stability:

Chemical stability refers to any process involving modification via bond formation or cleavage. Proteins are susceptible to many chemical reactions including deamidation, oxidation, hydrolysis, isomerisation and proteolysis⁹⁻¹¹. One of these reactions can dominate in certain proteins as for example deamidation in lysozyme and epidermal growth factor^{12,13} and oxidation in parathyroid hormone¹⁴. However, more than one chemical reaction can happen simultaneously in a protein such as insulin⁷. The location of the chemical labile amino acid in the protein affects its reactivity and consequently the chemical stability of the whole protein molecule. Therefore, the presence of such labile amino acids in a protein molecule might cause no chemical instability if they are buried inside the hydrophobic core of the protein molecule¹⁵. The dominant degradation pathway of a protein like recombinant human macrophage colony-stimulating factor was highly dependent on solution pH where significantly different degradation products were found at different pHs¹⁶.

2.2. Physical protein stability:

Physical protein stability, which is often the main determinant of the overall protein stability, refers to changes in protein secondary, tertiary or quaternary structures⁹. In contrast to small molecule drugs, proteins can undergo structural physical changes independent of chemical modification. Native proteins occur normally in a folded form where the exposure of hydrophobic groups is minimized¹⁷. Many forces are involved in preserving the native protein confirmation, including hydrophobic interactions, electrostatic interactions, hydrogen bonding

and van der Waals forces¹⁸. The loss of its natively folded structure is referred to as protein denaturation which is usually characterized by aggregate formation. As protein aggregates are usually malfunctioned or could even cause immunological problems, such denatured protein species are not accepted in pharmaceutical protein preparations. Protein physical stability is linked to two main thermodynamic aspects: conformational and colloidal stability of proteins.

2.2.1. Protein conformational stability:

Protein conformation stability is a major aspect in protein physical stability in which a protein undergoes irreversible structural transformation from native to denatured species through the reversible formation of unfolded transition state¹⁹⁻²². Such behaviour mainly depends on the protein structural thermodynamic stability^{23,24}. Protein structure stability is affected by two main opposing forces. Stabilizing enthalpic and destabilizing entropic forces^{6,18} in which the later is the main force opposing protein folding processes.

Thermodynamic stability of the native protein structure is typically quantified by the free energy of unfolding (ΔG_{unf}), also called Gibbs free energy of unfolding, which represents the total work required to transform the native proteins to denatured species. This value is highly dependent on temperature and shows a parabolic profile when plotted against temperature^{25,26}. ΔG_{unf} is determined from calorimetric techniques including differential scanning microcalorimetry (μDSC) by direct measurement of thermodynamic parameters involved in the Gibbs-Helmholtz equation²⁷

$$\Delta G_{\text{unf}} = \Delta H_{\text{unf}} (1 - T/T_m) - \Delta C_p [(T_m - T) + T \ln(T/T_m)]$$

Where, ΔH_{unf} is the enthalpy change during unfolding and calculated from the area under the apparent denaturation curve. T_m , the temperature at the mid of the unfolding peak is defined as the temperature at which 50% of the protein is unfolded and is well known as protein unfolding or melting temperature^{9,10,28}. ΔC_p is the difference in heat capacity between folded and unfolded state of protein. Determination of this parameter using μDSC is possible in all reversible proteins where positive ΔC_p could be measured directly from the protein thermal denaturation curve. Most protein molecules undergo irreversible denaturation which makes the accurate determination of the above mentioned thermodynamic parameters impossible and only unfolding temperature (T_m) can be determined. However, the extraction of meaningful thermodynamic data from such irreversible systems was proved to be applicable^{29,30}.

2.2.2. Protein colloidal stability:

Proteins may undergo intermolecular assembly to form higher molecular weight aggregates as a result of protein-protein interaction. The osmotic second virial coefficient (B_{22}) is a thermodynamic solution parameter that directly quantifies overall protein-protein interaction³¹. Positive B_{22} means more repulsive forces between protein molecules³² indicating favored protein-solvent interaction rather than protein-protein interaction. In contrast a negative B_{22} indicates higher protein-protein interaction and more aggregation. B_{22} has been used to predict solution conditions for protein assembly^{32,33}.

2.3. Factors affecting protein stability:

Protein stability, either chemical or physical, is affected to a great extent by temperature. In general, the higher the temperature, the lower the stability of a protein is. High temperatures are reported to cause denaturation of many proteins including recombinant keratinocyte growth factor³⁴, procaine growth hormone³⁵ and recombinant consensus α -interferon³⁶. Furthermore, chemical degradation of RNase A and lysozyme is accelerated by increasing the temperature⁶. However, the same protein molecule may undergo different degradation mechanism at different temperatures³⁷.

One of the most critical aspects concerning protein stability is the solution pH. Near the isoelectric point (pI), proteins tend to self associate and aggregation increases^{24,38}. On the other hand, far away from the pI electrostatic repulsion increases and proteins tend to unfold^{18,39}.

Protein molecules are surface active and tend to adsorb on surfaces and interfaces. Such behaviour leads in most cases to protein denaturation and aggregation⁴⁰.

Applying mechanical stress like shaking on proteins causes air entrapment which in turn introduces air/water interface in the bulk solution at which proteins can be adsorbed and aggregate¹⁰. Aggregation caused by shaking is reported for several proteins for example, human growth hormone⁴¹ and haemoglobin⁴².

Protein aggregation is affected to a great extent by protein concentration. Increased aggregation rate at high protein concentration was reported for interleukin 1B³⁷. In contrast, bovine insulin at 0.1 mg/ml at pH 7.4 aggregates more readily than at 0.6 mg/ml during shaking. This is attributable to the more favourable formation of insulin hexamers at 0.6 mg/ml, which are less susceptible to hydrophobic surface induced adsorption aggregation than insulin monomers^{43,44}.

3. Analytical techniques for protein formulation development:

Studying the stability of proteins, analytical techniques should be able to quantify denaturation and degradation products during long term stability studies. Registration of new active pharmaceutical products requires long term stability for two or more years to be performed. Usually such data is not available until the clinical program is in late stage. Therefore, additional techniques are extremely required to predict instability events early enough before starting the long term stability studies. The main target would be to reduce the risk of late stage changes in formulation, which is quite costly in term of time and material, and to avoid unexpected aggregation during storage⁴⁵.

Protein analytical techniques can be classified into two main categories based on their role in the formulation development process.

3.1. Monitoring techniques:

Monitoring techniques include techniques used to monitor a certain stability character such as monomer content or particle count in accelerated stress studies. These techniques, which are mostly applied in long term stability studies as well, include i.e. chromatographic techniques, particle analysis and gel electrophoresis. Such methods are fundamental in all protein formulation studies. Using a single technique in such predictive strategy is usually not enough for a decision concerning formulation stability.

3.1.1. Chromatography:

Chromatographic analysis of protein pharmaceuticals is commonly used for screening of impurities formed during protein purification, manufacturing and storage. These could be formed already due to minor chemical or major physical instability events⁴⁶. Chromatographic separation techniques provide a sensitive and reliable method to monitor the resulting impurities and are consistently applied during stability studies or in quality control of the final product. Many chromatographic methods are now on hand which differ in the separation mode.

3.1.1.1. Reversed phase chromatography (RPC):

Reversed phase chromatography is the most applied technique in pharmaceutical development laboratories both for protein and small drug molecules. Reversed phase chromatography employs a non-polar stationary phase and a polar mobile phase and separation happens due to

the so called solvophobic theory⁴⁷ where the protein (the solute) molecule is excluded from the polar solvent and retains on the non polar stationary phase. Reversed phase chromatography is used in protein formulation development mainly to observe chemical degradation such as oxidation and deamidation⁴⁸. That was extensively published as for example oxidation of bovine parathyroid hormone⁴⁹ and recombinant human granulocyte colony stimulating factor⁵⁰, and disulphide bridging for Nonglycosylated interleukin – 2⁵¹.

3.1.1.2. Size exclusion chromatography (SEC):

In Size exclusion or gel permeation chromatography non-interactive porous solid (mostly carbohydrate gels⁵²) is used as a stationary phase whereas the mobile phase consists normally of a buffer system in a pH of 2-8 with addition of salts in order to increase the ionic strength. Separation is based on molecular shape and size. Smaller molecules are easily entrapped in the pores of the column and then retained for longer time whereas the larger ones diffuse faster out of the column and are detected first by the detector. Size exclusion chromatography is applied mainly in protein formulation development to monitor physical changes like aggregation but also fragmentation as a result of chemical degradation. The use of SEC in protein formulation development is extensively published where various protein stability aspects were studied^{35,53-56}.

3.1.1.3. Ion exchange chromatography (IEC):

Ion exchange chromatography is based on electrostatic interactions between positively or negatively charged amino acids in protein and oppositely charged stationary phase molecules. During storage, a protein molecule is susceptible to chemical changes leading to the formation of isoforms. These isoforms are approximately similar in molecular weight and therefore difficult to be separated using SEC. However, the resulting small differences in charge properties could be determined using IEC^{57,58}.

3.1.2. Particle analysis:

A major concern during protein formulation development is the formation of either visible or invisible particles which may be introduced in the formulation during manufacturing procedures and/or storage. Such particles may devastate the safety of the final formulation since they not only may affect capillaries⁵⁹ but also could induce immunogenicity^{60,61}. Therefore, particle count in the final protein formulation is essential for product release. The

United state pharmacopeia has set requirements for the particle contents in parenterals⁶² and has specified the method of light obscuration as the preferred one.

3.1.3. Gel electrophoresis:

The principle known as electrophoresis is very commonly applied to study the structural changes of proteins. High resolution discontinuous electrophoresis was first developed by Ornstein⁶³ and Davis⁶⁴. There are many types of gel electrophoresis depending on the separation mode.

3.1.3.1. *Native gel electrophoresis:*

In native electrophoresis, where no denaturant is used, separation takes place according to the protein net charge and its Stokes' radius and therefore the basis of separation is the difference in mass-to-charge ratio⁶⁵.

3.1.3.2. *Sodium dodecyl sulphate polyacrylamide gel electrophoresis (SDS-PAGE):*

SDS-PAGE is the most common gel electrophoresis technique in protein formulation development. Sodium dodecyl sulphate (SDS) molecules carry negative charge and complex with protein molecules to equalize their mass-to-charge ratios and consequently the separation is based only on the particle size⁶⁵. SDS-PAGE is common in assessing protein purity and determining molecular weight^{66,67}. In protein formulation development SDS-PAGE is used mainly in stability studies to allow the detection of proteolytic degradation events and covalent aggregates which was reported for many proteins such as bovine growth hormone⁶⁸.

3.1.3.3. *Isoelectric focusing (IEF):*

Protein migration in electric field is mainly derived, as mentioned above, by its net charge which is dependent on the pH of the solution. At the protein isoelectric point (pI) the net charge is zero and no mobility in an electric field is shown. Therefore, in a pH gradient electric field the protein will migrate till its pI and migration will stop. Such phenomenon is called isoelectric focusing (IEF)⁶⁹ which is used in protein formulation development mainly to determine modifications leading to formation of species having different pI.

3.1.3.4. *Two dimensional(2D) gel electrophoresis:*

The combination of both SDS-PAGE and IEF in the 2D gel electrophoresis represents higher resolution for complex protein mixtures where the resolution provided by one dimensional analysis is not enough⁷⁰. The samples are allowed to separate first by IEF in a thin tube which is laid after special treatments across a slab gel which is run as one-dimensional SDS-PAGE.

3.2. Stability prediction techniques:

Stability prediction techniques comprise techniques in which conformational changes in protein molecules are monitored during heat cycles. Such methods are able in short time, compared to classical accelerated stress studies, to obtain stability predictive parameters through either spectroscopic or calorimetric measurements. It is to be highlighted that spectroscopic predictive techniques are also used in monitoring protein structural changes during and after stress, i.e. in both stress and long term stability studies.

3.2.1. Spectroscopy:

Spectroscopic techniques are able to measure changes in protein secondary and/or tertiary structures based on different aspects. The most commonly applied techniques in protein formulation development are described below.

The ultraviolet (UV) protein absorption spectra between 240 – 300 nm is composed of multiple overlapping spectra bands arising from the absorbance of several amino acid residue⁷¹. After being able to isolate the multiple components of the zero order spectra by derivative analysis⁷² the peak position of each amino acid residue is used to identify changes in the microenvironment around the aromatic residue and therefore conformational changes in tertiary structure could be monitored⁷³.

Circular dichroism (CD) spectroscopy is widely used to monitor both secondary and tertiary structures of protein molecules. The basics of CD measurements depends on the difference in absorption between left- and right-handed circularly polarized light exerted by asymmetric optically active materials⁷⁴. Protein molecules are normally asymmetric and therefore their structure can be studied by CD where far-UV CD spectra (190-250 nm) are sensitive to changes in protein secondary structures and near-UV CD spectra (over 250 nm) are used for monitoring changes in protein tertiary structures⁷⁵.

Fluorescence spectroscopy is a highly sensitive method for protein analysis. Monitoring protein structural changes takes place either by intrinsic fluorescence of the naturally

fluorescent amino acid residues which expose during unfolding and show fluorescence, or by addition of various extrinsic fluorescent dyes which combine with the hydrophobic residues after protein unfolding increasing their fluorescence as well^{76,77}.

The use of infrared spectroscopy in studying protein structure was first recognized by Elliott and Ambrose⁷⁸ in 1950. The advent and availability of Fourier transform infrared (FTIR) increased the sensitivity of this method. Furthermore, the advancement in computer systems enabled more applications in protein formulation development. FTIR is used in monitoring changes in protein secondary structure obtained mainly from absorbance originating from C=O stretching vibrations (amide I band)⁷⁹. Infrared spectroscopy has the advantage of being suitable for a variety of sample forms including solids and powder. However, the main drawback is the interference of overlapping H₂O bands⁸⁰.

Raman spectroscopy is an alternative vibrational spectroscopic technique where the overlapping H₂O band is not interfering. Raman is based on the scattering of light. A sample will transmit light either unchanged (elastically) or, a small amount is scattered inelastically. This is called “Raman Effect” which causes photons to gain or lose energy and accordingly the Raman spectra could be recorded. Raman requires a centre of symmetry for a band to be seen while IR requires a dipole. The water molecule has a strong permanent dipole which is the reason why it is not seen by Raman⁸¹

All the above mentioned analytical techniques are widely used in monitoring structural changes of proteins after applying stresses such as heat, mechanical stress or freeze thaw cycles having the advantage over traditional monitoring methods in obtaining fast information. However, advancement in spectroscopic methodology has enabled most of them to be used in determining the protein unfolding temperature (T_m) where the structural changes in protein are monitored during heating cycles. Based on spectroscopic determination of T_m prediction of protein stability could be achieved.

3.2.2. Calorimetry:

Calorimetry in protein formulation development incorporates two main techniques, Differential scanning calorimetry (DSC) and Isothermal titration calorimetry (ITC). Due to the low energy accompanied by biochemical reactions, high sensitivity DSC instruments lead to be available known as differential scanning micro- or nanocalorimetry (μ DSC or NDSC). In the next section the use of such sensitive techniques in protein formulation development will be discussed in more details.

ITC allows thermodynamic characterization of binding processes including protein-protein and protein-ligand bindings and nowadays both techniques are essential in protein formulation laboratories⁸².

Many authors have reported the use of DSC and/or ITC in many protein stability aspects⁸³⁻⁸⁵. The use of DSC in protein formulation development is mainly to predict the rank order of different potential formulations having the advantage of being able to achieve that without any need to apply extra stress protocols. The use of such techniques in monitoring changes in protein conformation after stress is however reported by few authors^{86,87}.

4. Differential scanning microcalorimetry (μ DSC):

Differential scanning microcalorimetry (μ DSC) provides direct measurement for enthalpy changes and therefore many thermodynamic parameters can be determined. Due to its high sensitivity, μ DSC is able to measure changes in protein conformational structure which might be too weak for spectroscopic detections.

A typical instrument is composed of two cells: a sample cell containing the protein solution and a reference cell containing buffer. During the experimental, a heating element is used to increase the temperature in both cells while the individual temperature of each cell is monitored continuously. Any difference in heat capacity of the sample compared to the reference cell will give rise to a temperature difference that triggers a feedback system to supply additional heat to the cell that has the lower temperature. The feedback power necessary to keep the temperature difference equal to zero between cells is the measured signal and has the unit $\mu\text{J/s}$ or $\mu\text{cal/s}$ prior to any normalization by the scan rate. For a well matched system with the two cells containing identical buffers, the only difference being the protein in the sample cell, heating of the cells can be seen as an increase in temperature that monotonic in both cells until the protein starts to denature. Because the denaturation of a protein is an energy-requiring process, the feedback system will supply the heat necessary to keep the sample cell at the same temperature as the reference cell until all the protein has unfolded. Subtracting a separate scan where both cells are filled with the same buffer eliminates instrumental effects.

Figure 1.1⁸² shows the result normalized by the scan rate and by the total amount of protein present in the calorimetric sample cell. From such a measurement several parameters could be extracted.

4.1. μ DSC parameters:

4.1.1. Protein unfolding temperature (T_m):

Applied heat during a μ DSC measurement introduces enthalpy that loosens the protein stabilizing forces including hydrogen bonds and hydrophobic interaction^{88,89}. A typical protein denaturation transition is shown by μ DSC as endothermic event where the peak maximum is the protein melting or unfolding temperature (T_m). T_m is defined as the temperature at which 50% of the protein is unfolded^{90,91} and is a very important parameter for each protein with regard to its conformational stability. Different solution conditions can

cause shifts in T_m ^{84,92}. Lower T_m values indicate easier unfolding and in turn lower stability. On the other hand, T_m shift to higher values indicates stronger native structure which resists denaturation^{16,93}. Protein unfolding may catalyze many other denaturation processes including aggregations⁹⁴⁻⁹⁶, or chemical instabilities including deamidation⁹⁷, oxidation and proteolysis⁹⁸.

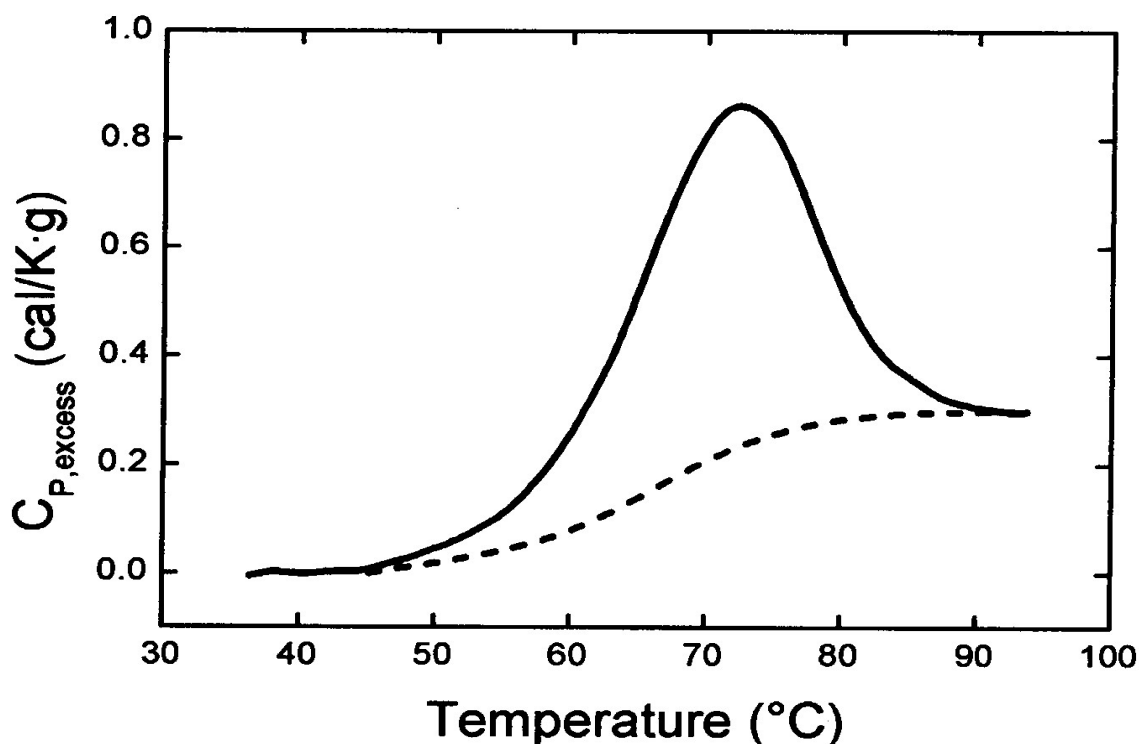


Figure 1. 1: A typical DSC experiment showing the excess heat capacity of a protein⁸²

4.1.2. Protein unfolding reversibility:

The ability of a protein to refold after unfolding can be determined using μ DSC by applying 2 subsequent scans and the degree of reversibility is calculated from the percentage of the enthalpy of the second up-scan (ΔH_2) in relation to the first up-scan enthalpy (ΔH_1). Protein unfolding reversibility was determined for several molecules⁹⁹⁻¹⁰¹.

4.1.3. Denaturation heat capacity:

The heat capacity of unfolding or denaturation (ΔC_p) is the difference between the heat capacity of the folded state and that of the unfolded or denatured state. This value is always positive due to the larger heat capacity of the unfolded state resulting from the high exposure of the hydrophobic amino acids to the solvent where in the folded native state all hydrophobic residues are imbedded inside the molecule¹⁰². ΔC_p is typically measured from the heat capacity differences between the pre and post transition base line⁹⁰. Provided that ΔC_p is not constant and does not change with temperature¹⁰³, an alternative method to determine ΔC_p is obtained from the slope of the linear plot between T_m and ΔH as a function of pH^{96,104}.

4.1.4. Gibbs free energy:

Protein conformational stability is quantified in terms of free energy change of unfolding ΔG_{unf} ^{10,31}. This value is calculated using the above mentioned parameters in the Gibbs-Helmholtz Equation^{27,98}:

$$\Delta G_{unf} = \Delta H_m (1 - T/T_m) - \Delta C_p [(T_m - T) + T \ln(T/T_m)] \quad (1)$$

At a temperature where $T = T_m$ $\Delta G_{unf} = 0$, the parabolic curve obtained from the effect of temperature on ΔG_{unf} suggests that there is lower temperature where ΔG_{unf} would be equal to zero which is called cold denaturation temperature²⁵.

4.2. Applications of μ DSC in protein formulation development:

Once the eligibility of a new active pharmaceutical protein is proved, a formulator would be responsible to introduce such candidate in a suitable formulation to be used in the early clinical phases. During preclinical formulation development, time is very critical and the formulator should be able, in stiff timelines, to answer a very important question: what excipients and solution conditions offer the best stabilization? Microcalorimetry can, in a short time, screen excipients to find the best stabilizer for the native protein state. Moreover, it is well suited and already established to access how different solution conditions perturb protein unfolding. The main objective is to maintain the protein molecule in its native state in the desired dosage form.

At early phases of protein liquid formulation development the optimum pH where the protein will best maintain its native structure is to be determined. By examining the behavior of T_m

the optimum pH was determined for recombinant human macrophage colony stimulating factor¹⁶. The optimum T_m in this case correlated well with the pH value in which aggregation was minimized. The destabilizing effect of pH on protein was estimated by determining T_m of several proteins such as myoglobin¹⁰⁵, rhDNase⁸⁴, RNase A^{106,107} and thrombin¹⁰⁸. The effect of pH and ionic strength of a variant of protein G B1 domain¹⁰⁹ was investigated using T_m . Determining the unfolding reversibility (if possible) within the region of optimum pH was a successful approach in the development of a stable formulation of Flt3L¹¹⁰

Once the optimum pH is determined further augmentation of T_m by screening different buffer and stabilizing excipients is possible. Generally, most excipients behave as protein stabilizers by being preferentially excluded from the vicinity of protein molecules, thus making the denatured state more thermodynamically unfavorable than the native state. These excipient shift the equilibrium to the native conformation and exhibit high melting temperature⁹⁸. Screening several excipients, NaCl showed to increase the T_m of Interleukin 1 receptor (IL-1R) to its highest level⁹³. Additionally, investigating the effect of excipients on the degree of unfolding reversibility was of some benefit for the stabilization of recombinant human megakaryocyte growth and development factor¹¹¹. A variety of osmolytes and salts were screened to find the best stabilizer for of the recombinant human keratinocyte growth factor where NaCl, sodium phosphate, ammonium sulfate and sodium citrate were highly effective in increasing T_m ¹¹². However, quite a lot of data were reported about excipient screening for proteins based on T_m measured from μ DSC¹¹³⁻¹¹⁸

The use of preservatives in a protein formulation might be needed if the formulated dosage form is to be a multidose presentation. The choice of the suitable excipient that does not affect the protein stability can be achieved based on T_m . The effect of preservatives on the sterility of IL-1R was investigated using T_m ⁹³. Protein unfolding as a function of preservative concentration generally shifts the T_m to lower temperature¹¹⁹.

It is important to remember that the use of T_m as a stability marker is based on the notion that higher T_m represents greater resistance of protein to unfold and that this behavior holds at lower temperatures where protein is to be stored. Many of the previously mentioned examples^{16,110,112} proved a correlation between the optimum conditioned determined by T_m and that in which aggregation was minimized. On the other hand, few studies showed unsuccessful T_m prediction. A typical example for such behavior is the negative effect of polysorbate 20 on T_m of recombinant growth hormone although the aggregation formation after agitation was reduced⁴¹.

5. Objectives of the thesis:

In theory, long term stability studies are the best strategy to find the best formulation. However, applying such an experimental plan for all stabilizing factors would be very costly and time consuming. Therefore, accelerated stability studies are applied to obtain preliminary information about formulation factors (such as pH, ionic strength, buffer and stabilizers). In such studies different formulations are subjected to different stresses such as elevated temperatures, mechanical stress and freeze-thaw cycles. However, how the resulting data can be correlated with the real time stability is debated. Although stabilization of protein formulations at elevated temperatures was extensively investigated^{35,110,120}, none of these studies has proved reliable prediction of the real time stability. Furthermore, the work load for a broad accelerated stability study is still considerably high. Therefore, predictive stability studies are extremely valuable in biopharmaceutical industry. μ DSC represents a predictive tool which is believed to be successful in such issues depending on measured T_m s but till now systematic data from real time studies correlated with T_m determined by μ DSC have not been published before.

Therefore, the main objective of this thesis is to find out how far a formulator can rely on T_m as a marker for protein stability. Systematic studies to correlate μ DSC data with long term stability as well as short term stress studies are performed and the quality of the obtained prediction is evaluated.

The following topics are covered:

1. Microcalorimetry as a predictive tool for physical stability of granulocyte colony stimulating factor (GCSF) in solution at different pH values.
2. A Critical evaluation of μ DSC as a predictive tool for long term stability of liquid protein formulations (GCSF, Monoclonal antibody and Pegylated Interferon)
3. Other predictive strategies for the prediction of long term stability of GCSF liquid formulations.

6. References:

1. Itakura, K.; Hirose, T.; Crea, R.; Riggs, A. D.; Heyneker, H. L.; Bolivar, F.; Boyer, H. W. Expression in *Escherichia coli* of a chemically synthesized gene for the hormone somatostatin. *Science* 198[4321], 1056-1063. 1977.
2. Goeddel, D. V.; Kleid, D. G.; Bolivar, F.; Heyneker, H. L.; Yansura, D. G.; Crea, R.; Hirose, T.; Kraszewski, A.; Itakura, K.; Riggs, A. D. Expression in *Escherichia coli* of chemically synthesized genes for human insulin. *Proc.Natl.Acad.Sci.U.S.A.* 76[1], 106-110. 1979.
3. "Medicines in development, Biotechnology, report 2008", available at <http://www.pharma.org/files/attachments/Biotech%202008.pdf> (2009).
4. Fagain, C. O. Understanding and increasing protein stability. *Biochimica et Biophysica Acta, Protein Structure and Molecular Enzymology* 1252[1], 1-14. 1995.
5. Jaenicke, R. Protein stability and molecular adaptation to extreme conditions. *European Journal of Biochemistry* 202[3], 715-728. 1991.
6. Kristjansson, M. M.; Kinsella, J. E. Protein and enzyme stability: structural, thermodynamic, and experimental aspects. *Advances in Food and Nutrition Research* 35, 237-316. 1991.
7. Strickley, R. G.; Anderson, B. D. Solid-State Stability of Human Insulin II. Effect of Water on Reactive Intermediate Partitioning in Lyophiles from pH 2-5 Solutions: Stabilization against Covalent Dimer Formation. *J.Pharm.Sci.* 86[6], 645-653. 1997.
8. Apenten, R. K. O. Protein stability function relations: beta -lactoglobulin-A sulfhydryl group reactivity and its relationship to protein unfolding stability. *Int.J.Biol.Macromol.* 23[1], 19-25. 1998.
9. Manning, M. C.; Patel, K.; Borchardt, R. T. Stability of protein pharmaceuticals. *Pharmaceutical Research* 6[11], 903-918. 1989.
10. Wang, W. Instability, stabilization, and formulation of liquid protein pharmaceuticals. *International Journal of Pharmaceutics* 185[2], 129-188. 1999.
11. Daniel, R. M.; Dines, M.; Petach, H. H. The denaturation and degradation of stable enzymes at high temperatures. *Biochem.J.* 317[1], 1-11. 1996.
12. Tallan, H. H.; Stein, W. Chromatographic studies on lysozyme. *J.Biol.Chem.* 200, 507-514. 1953.
13. DiAugustine, R. P.; Gibson, B. W.; Aberth, W.; Kelly, M.; Ferrua, C. M.; Tomooka, Y.; Brown, C. F.; Walker, M. Evidence for isoaspartyl (deamidated) forms of mouse epidermal growth factor. *Anal Biochem* 165[2], 420-429. 1987.
14. Coltrera, M.; Rosenblatt, M.; Potts, J. T., Jr. Analogs of parathyroid hormone containing D-amino acids: evaluation of biological activity and stability. *Biochemistry* 19[18], 4380-4385. 1980.

15. Mozhaev, V. V.; Martinek, K. Structure-stability relationships in proteins: new approaches to stabilizing enzymes. *Enzyme and Microbial Technology* 6[2], 50-59. 1984.
16. Schrier, J. A.; Kenley, R. A.; Willians, R.; Corcoran, R. J.; Kim, Y.; Northey, R. P.; D'Augusta, D.; Huberty, M. Degradation pathways for recombinant human macrophage colony-stimulating factor in aqueous solution. *Pharmaceutical Research* 10[7], 933-944. 1993.
17. Dill, K. A. Theory for the folding and stability of globular proteins. *Biochemistry* 24[6], 1501-1509. 1985.
18. Dill, K. A. Dominant forces in protein folding. *Biochemistry* 29[31], 7133-7155. 1990.
19. Lumry, R.; Eyring, H. Conformation changes of proteins. *Journal of Physical Chemistry* 58, 110-120. 1954.
20. Kendrick, B. S.; CLeland, J. L.; Lam, X.; Nguyen, T.; Randolph, T. W.; Manning, M. C.; Carpenter, J. F. Aggregation of Recombinant Human Interferon Gamma: Kinetics and Structural Transitions. *J.Pharm.Sci.* 87[9], 1069-1076. 1998.
21. Sanchez-Ruiz, J. M. Theoretical analysis of Lumry-Eyring models in differential scanning calorimetry. *Biophysical Journal* 61[4], 921-935. 1992.
22. Zale, S. E.; Klibanov, A. M. On the role of reversible denaturation (unfolding) in the irreversible thermal inactivation of enzymes. *Biotechnol.Bioeng.* 25[9], 2221-2230. 1983.
23. Krishnan, S.; Chi, E. Y.; Webb, J. N.; Chang, B. S.; Shan, D.; Goldenberg, M.; Manning, M. C.; Randolph, T. W.; Carpenter, J. F. Aggregation of Granulocyte Colony Stimulating Factor under Physiological Conditions: Characterization and Thermodynamic Inhibition. *Biochemistry* 41[20], 6422-6431. 2002.
24. Chi, E. Y.; Krishnan, S.; Kendrick, B. S.; Chang, B. S.; Carpenter, J. F.; Randolph, T. W. Roles of conformational stability and colloidal stability in the aggregation of recombinant human granulocyte colony-stimulating factor. *Protein Science* 12[5], 903-913. 2003.
25. Graziano, G.; Catanzano, F.; Riccio, A.; Barone, G. A reassessment of the molecular origin of cold denaturation. *J.Biochem.* 122[2], 395-401. 1997.
26. Southall, N. T.; Dill, K. A.; Haymet, A. D. J. A View of the hydrophobic effect. [Erratum to document cited in CA136:130291]. *J.Phys.Chem.B* 106[10], 2812. 2002.
27. Bechtel, W. J.; Schellman, J. A. Protein stability curves. *Biopolymers* 26[11], 1859-1877. 1987.
28. Privalov, P. L. Stability of proteins. Small globular proteins. *Advances in Protein Chemistry* 33, 167-241. 1979.
29. Remmele, R. L., Jr.; Zhang-van Enk, J.; Dharmavaram, V.; Balaban, D.; Durst, M.; Shoshitaishvili, A.; Rand, H. Scan-Rate-Dependent Melting Transitions of Interleukin-1 Receptor (Type II): Elucidation of Meaningful Thermodynamic and Kinetic Parameters of

- Aggregation Acquired from DSC Simulations. *Journal of the American Chemical Society* 127[23], 8328-8339. 2005.
30. Sanchez-Ruiz, J. M.; Lopez-Lacomba, J. L.; Cortijo, M.; Mateo, P. L. Differential scanning calorimetry of the irreversible thermal denaturation of thermolysin. *Biochemistry* 27[5], 1648-1652. 1988.
 31. Chi, E. Y.; Krishnan, S.; Randolph, T. W.; Carpenter, J. F. Physical Stability of Proteins in Aqueous Solution: Mechanism and Driving Forces in Nonnative Protein Aggregation. *Pharmaceutical Research* 20[9], 1325-1336. 2003.
 32. George, A.; Chiang, Y.; Guo, B.; Arabshahi, A.; Cai, Z.; Wilson, W. W. Second virial coefficient as predictor in protein crystal growth. *Methods in Enzymology* 276[Macromolecular Crystallography, Part A], 100-110. 1997.
 33. Pjura, P. E.; Lenhoff, A. M.; Leonard, S. A.; Gittis, A. G. Protein Crystallization by Design: Chymotrypsinogen Without Precipitants. *J.Mol.Biol.* 300[2], 235-239. 2000.
 34. Chen, B. L.; Arakawa, T.; Hsu, E.; Narhi, L. O.; Tressel, T. J.; Chien, S. L. Strategies To Suppress Aggregation of Recombinant Keratinocyte Growth Factor during Liquid Formulation Development. *J.Pharm.Sci.* 83[12], 1657-1661. 1994.
 35. Charman, S. A.; Mason, K. L.; Charman, W. N. Techniques for assessing the effects of pharmaceutical excipients on the aggregation of porcine growth hormone. *Pharmaceutical Research* 10[7], 954-962. 1993.
 36. Ip, A. Y.; Arakawa, T.; Silvers, H.; Ransone, C. M.; Niven, a. R. Stability of Recombinant Consensus Interferon to Air-Jet and Ultrasonic Nebulization. *J.Pharm.Sci.* 84[10], 1210-1214. 1995.
 37. Gu, L. C.; Erdos, E. A.; Chiang, H. S.; Calderwood, T.; Tsai, K.; Visor, G. C.; Duffy, J.; Hsu, W. C.; Foster, L. C. Stability of interleukin 1beta (IL-1beta) in aqueous solution: analytical methods, kinetics, products, and solution formulation implications. *Pharm.Res.* 8[4], 485-490. 1991.
 38. Striolo, A.; Bratko, D.; Wu, J. Z.; Elvassore, N.; Blanch, H. W.; Prausnitz, J. M. Forces between aqueous nonuniformly charged colloids from molecular simulation. *J.Chem.Phys.* 116[17], 7733-7743. 2002.
 39. Goto, Y.; Fink, A. L. Conformational states in b-lactamase: molten-globule states at acidic and alkaline pH with high salt. *Biochemistry* 28[3], 945-952. 1989.
 40. Burke, C. J.; Steadman, B. L.; Volkin, D. B.; Tasi, P. K.; Bruner, M. W.; Middaugh, C. R. The adsorption of proteins to pharmaceutical container surfaces. *Int.J.Pharm.* 86[1], 89-93. 1992.
 41. Bam, N. B.; CLeland, J. L.; Yang, J.; Manning, M. C.; Carpenter, J. F.; Kelley, R. F.; Randolph, T. W. Tween Protects Recombinant Human Growth Hormone against Agitation-Induced Damage via Hydrophobic Interactions. *Journal of Pharmaceutical Sciences* 87[12], 1554-1559. 1998.

42. Kerwin, B. A.; Akers, M. J.; Apostol, I.; Moore-Einsel, C.; Etter, J. E.; Hess, E.; Lippincott, J.; Levine, J.; Mathews, A. J.; Revilla-Sharp, P.; Schubert, R.; Looker, D. L. Acute and Long-Term Stability Studies of Deoxy Hemoglobin and Characterization of Ascorbate-Induced Modifications. *Journal of Pharmaceutical Sciences* 88[1], 79-88. 1999.
43. Sluzky, V.; Tamada, J. A.; Klibanov, A. M.; Langer, R. Kinetics of insulin aggregation in aqueous solutions upon agitation in the presence of hydrophobic surfaces. *Proc.Natl.Acad.Sci.U.S.A.* 88[21], 9377-9381. 1991.
44. Sluzky, V.; Klibanov, A. M.; Langer, R. Mechanism of insulin aggregation and stabilization in agitated aqueous solutions. *Biotechnol.Bioeng.* 40[8], 895-903. 1992.
45. Weiss, W. F., IV; Young, T. M.; Roberts, C. J. Principles, approaches, and challenges for predicting protein aggregation rates and shelf life. *J.Pharm.Sci.* 98[4], 1246-1277. 2009.
46. Patel, K.; Borchardt, R. T. Deamidation of asparaginyl residues in proteins: a potential pathway for chemical degradation of proteins in lyophilized dosage forms. *J.Parenter.Sci.Technol.* 44[6], 300-301. 1990.
47. Horvath, C.; Melander, W.; Molnar, I. Solvophobic interactions in liquid chromatography with nonpolar stationary phases. *J.Chromatogr.* 125[1], 129-156. 1976.
48. Wehr, T. Use of reversed-phase liquid chromatography in biopharmaceutical development. *Anal.Tech.Biopharm.Dev.* 27-65. 2005.
49. Frelinger, A. L., III; Zull, J. E. Oxidized forms of parathyroid hormone with biological activity. Separation and characterization of hormone forms oxidized at methionine 8 and methionine 18. *J.Biol.Chem.* 259[9], 5507-5513. 1984.
50. Ohgami, Y.; Nagase, M.; Nabeshima, S.; Fukui, M.; Nakazawa, H. Characterization of recombinant DNA-derived human granulocyte macrophage colony stimulating factor by fast atom bombardment mass spectrometry. *J.Biotechnol.* 12[3-4], 219-229. 1989.
51. Kunitani, M.; Hirtzer, P.; Johnson, D.; Halenbeck, R.; Boosman, A.; Koths, K. Reversed-phase chromatography of interleukin-2 muteins. *J.Chromatogr.* 359, 391-402. 1986.
52. Unger, K. K.; Anspach, B.; Giesche, H. Optimum support properties for protein separations by high-performance size exclusion chromatography. *J.Pharm.Biomed.Anal.* 2[2], 139-151. 1984.
53. Brange, J.; Havelund, S.; Hougaard, P. Chemical stability of insulin. 2. Formation of higher molecular weight transformation products during storage of pharmaceutical preparations. *Pharmaceutical Research* 9[6], 727-734. 1992.
54. Fatouros, A.; Oesterberg, T.; Mikaelsson, M. Recombinant factor VIII SQ-influence of oxygen, metal ions, pH and ionic strength on its stability in aqueous solution. *International Journal of Pharmaceutics* 155[1], 121-131. 1997.
55. Sah, H.; Bahl, Y. Effects of aqueous phase composition upon protein destabilization at water/organic solvent interface. *Journal of Controlled Release* 106[1-2], 51-61. 2005.

56. Kerwin, B. A.; Heller, M. C.; Levin, S. H.; Randolph, T. W. Effects of Tween 80 and Sucrose on Acute Short-Term Stability and Long-Term Storage at -20 DegC of a Recombinant Hemoglobin. *Journal of Pharmaceutical Sciences* 87[9], 1062-1068. 1998.
57. Frenz, J.; Wu, S. L.; Hancock, W. S. Characterization of human growth hormone by capillary electrophoresis. *J.Chromatogr.* 480, 379-391. 1989.
58. Clogston, C. L.; Hsu, Y. R.; Boone, T. C.; Lu, H. S. Detection and quantitation of recombinant granulocyte colony-stimulating factor charge isoforms: comparative analysis by cationic-exchange chromatography, isoelectric focusing gel electrophoresis, and peptide mapping. *Anal.Biochem.* 202[2], 375-383. 1992.
59. Lehr, H.; Brunner, J.; Rangoonwala, R.; Kirkpatrick, C. J. Particulate matter contamination of intravenous antibiotics aggravates loss of functional capillary density in postischemic striated muscle. *Am J Respir Crit Care Med* 165[4], 514-520. 2002.
60. Denis, J.; Majeau, N.; costa-Ramirez, E.; Savard, C.; Bedard, M. C.; Simard, S.; Lecours, K.; Bolduc, M.; Pare, C.; Willems, B.; Shoukry, N.; Tessier, P.; Lacasse, P.; Lamarre, A.; Lapointe, R.; Lopez Macias, C.; Leclerc, D. Immunogenicity of papaya mosaic virus-like particles fused to a hepatitis C virus epitope: Evidence for the critical function of multimerization. *Virology* 363[1], 59-68. 2007.
61. Rosenberg, A. S. Effects of protein aggregates: an immunologic perspective. *AAPS J.* 8[3], No. 2006.
62. U.S.Pharamcopeia.2006 <788> Particulate matter in injections. In *The United States Pharamcopeia - National Formulary*, 24 ed.; 2006.
63. Ornstein, L. Disk electrophoresis. I. Background and theory. *Ann.N.Y.Acad.Sci.* 121[2], 321-349. 1964.
64. Davis, B. J. Disk electrophoresis. II. Method and application to human serum proteins. *Ann.N.Y.Acad.Sci.* 121[2], 404-427. 1964.
65. Jones, A. J. S. Analytical methods for the assessment of protein formulations and delivery systems. *ACS Symposium Series* 567[Formulation and Delivery of Proteins and Peptides], 22-45. 1994.
66. Shapiro, A. L.; Vinuela, E.; Maizel, J. V., Jr. Molecular weight estimation of polypeptide chains by electrophoresis in sodium dodecyl sulfate-polyacrylamide gels. *Biochem.Biophys.Res.Commun.* 28[5], 815-820. 1967.
67. Weber, K.; Osborn, M. Reliability of molecular weight determinations by dodecyl sulfate--polyacrylamide-gel electrophoresis. *J.Biol.Chem.* 244[16], 4406-4412. 1969.
68. Hageman, M. J.; Bauer, J. M.; Possert, P. L.; Darrington, R. T. Preformulation studies oriented toward sustained delivery of recombinant somatotropins. *J.Agric.Food Chem.* 40[2], 348-355. 1992.

69. Bjellqvist, B.; Ek, K.; Righetti, P. G.; Gianazza, E.; Goerg, A.; Westermeier, R.; Postel, W. Isoelectric focusing in immobilized pH gradients: principle, methodology and some applications. *J.Biochem.Biophys.Methods* 6[4], 317-339. 1982.
70. O'Farrell, P. H. High resolution two-dimensional electrophoresis of proteins. *J.Biol.Chem.* 250[10], 4007-4021. 1975.
71. Ichikawa, T.; Terada, H. Estimation of state and amount of phenylalanine residues in proteins by second derivative spectrophotometry. *Biochim.Biophys.Acta, Protein Struct.* 580[1], 120-128. 1979.
72. Ichikawa, T.; Terada, H. Second derivative spectrophotometry as an effective tool for examining phenylalanine residues in proteins. *Biochim.Biophys.Acta, Protein Struct.* 494[1], 267-270. 1977.
73. Ragone, R.; Colonna, G.; Balestrieri, C.; Servillo, L.; Irace, G. Determination of tyrosine exposure in proteins by second-derivative spectroscopy. *Biochemistry* 23[8], 1871-1875. 1984.
74. Cotton, A. Absorption and dispersion of light. *Ann.Chim.Phys.* 8[7], 347. 1896.
75. Bloemendal, M.; Johnson, W. C., Jr. Structural information on proteins from circular dichroism spectroscopy: possibilities and limitations. *Pharm.Biotechnol.* 7[Physical Methods to Characterize Pharmaceutical Proteins], 65-100. 1995.
76. Jiskoot, W.; Hlady, V.; Naleway, J. J.; Herron, J. N. Application of fluorescence spectroscopy for determining the structure and function of proteins. *Pharm.Biotechnol.* 7[Physical Methods to Characterize Pharmaceutical Proteins], 1-63. 1995.
77. Hawe, A.; Sutter, M.; Jiskoot, W. Extrinsic Fluorescent Dyes as Tools for Protein Characterization. *Pharmaceutical Research* 25[7], 1487-1499. 2008.
78. Elliott, A.; Ambrose, E. J. Structure of synthetic polypeptides. *Nature (London, U.K.)* 165, 921-922. 1950.
79. Krimm, S.; Bandekar, J. Vibrational spectroscopy and conformation of peptides, polypeptides, and proteins. *Adv.Protein Chem.* 38, 181-364. 1986.
80. Cooper, E. A.; Knutson, K. Fourier transform infrared spectroscopy investigations of protein structure. *Pharmaceutical Biotechnology* 7[Physical Methods to Characterize Pharmaceutical Proteins], 101-143. 1995.
81. Ciurczak, E. W. Vibrational spectroscopy in bioprocess monitoring. *Anal.Tech.Biopharm.Dev.* 383-400. 2005.
82. Schon, A.; Velazquez-Campoy, A. Calorimetry. *Biotechnol.: Pharm.Aspects* 3[Methods for Structural Analysis of Protein Pharmaceuticals], 573-589. 2005.
83. Shiraki, K.; Kudou, M.; Nishikori, S.; Kitagawa, H.; Imanaka, T.; Takagi, M. Arginine ethyl ester prevents thermal inactivation and aggregation of lysozyme. *European Journal of Biochemistry* 271[15], 3242-3247. 2004.

84. Chan, H. K.; Au-Yeung, K. L.; Gonda, I. Effects of additives on heat denaturation of rhDNase in solutions. *Pharmaceutical Research* 13[5], 756-761. 1996.
85. Morton, T. A.; Bennett, D. B.; Appelbaum, E. R.; Cusimano, D. M.; Johanson, K. O.; Matico, R. E.; Young, P. R.; Doyle, M.; Chaiken, I. M. Analysis of the interaction between human interleukin-5 and the soluble domain of its receptor using a surface plasmon resonance biosensor. *J.Mol.Recognit.* 7[1], 47-55. 1994.
86. Welzel, P. B. Investigation of adsorption-induced structural changes of proteins at solid/liquid interfaces by differential scanning calorimetry. *Thermochimica Acta* 382[1-2], 175-188. 2002.
87. Al-Tahami, K.; Meyer, A.; Singh, J. Poly Lactic Acid Based Injectable Delivery Systems for Controlled Release of a Model Protein, Lysozyme. *Pharm.Dev.Technol.* 11[1], 79-86. 2006.
88. Pace, C. N.; Shirley, B. A.; McNutt, M.; Gajiwala, K. Forces contributing to the conformational stability of proteins. *FASEB J.* 10[1], 75-83. 1996.
89. Tanford, C. *The Hydrophobic Effect: Formation of Micelles and Biological Membranes.* 240. 1973.
90. Privalov, P. L.; Gill, S. J. Stability of protein structure and hydrophobic interaction. *Adv.Protein Chem.* 39, 191-234. 1988.
91. Sturtevant, J. M. Biochemical applications of differential scanning calorimetry. *Annual Review of Physical Chemistry* 38, 463-488. 1987.
92. Maneri, L. R.; Low, P. S. Structural stability of the erythrocyte anion transporter, band 3, in different lipid environments. A differential scanning calorimetric study. *J.Biol.Chem.* 263[31], 16170-16178. 1988.
93. Remmele, R. L., Jr.; Nightlinger, N. S.; Srinivasan, S.; Gombotz, W. R. Interleukin-1 receptor (IL-1R) liquid formulation development using differential scanning calorimetry. *Pharmaceutical Research* 15[2], 200-208. 1998.
94. De Young, L. R.; Dill, K. A.; Fink, A. L. Aggregation and denaturation of apomyoglobin in aqueous urea solutions. *Biochemistry* 32[15], 3877-3886. 1993.
95. D'Avio, S. R.; Kienle, K. M.; Collins, B. E. Interdomain interactions in the chimeric protein toxin sCD4(178)-PE40: a differential scanning calorimetry (DSC) study. *Pharmaceutical Research* 12[5], 642-648. 1995.
96. Martinez, J. C.; Harrous, M. E.; Filimonov, V. V.; Mateo, P. L.; Fersht, A. R. A Calorimetric Study of the Thermal Stability of Barnase and Its Interaction with 3'GMP. *Biochemistry* 33[13], 3919-3926. 1994.
97. Wearne, S. J.; Creighton, T. E. Effect of protein conformation on rate of deamidation: ribonuclease A. *Proteins: Struct., Funct., Genet.* 5[1], 8-12. 1989.

98. Remmele, R. L., Jr. Microcalorimetric approaches to biopharmaceutical development. *Analytical Techniques for Biopharmaceutical Development*, 327-381. 2005.
99. Zaiss, K.; Jaenicke, R. Thermodynamic Study of Phosphoglycerate Kinase from *Thermotoga maritima* and Its Isolated Domains: Reversible Thermal Unfolding Monitored by Differential Scanning Calorimetry and Circular Dichroism Spectroscopy. *Biochemistry* 38[14], 4633-4639. 1999.
100. Beldarrain, A.; Lopez-Lacomba, J. L.; Furrázola, G.; Barberia, D.; Cortijo, M. Thermal Denaturation of Human gamma -Interferon. A Calorimetric and Spectroscopic Study. *Biochemistry* 38[24], 7865-7873. 1999.
101. Blaber, S. I.; Culajay, J. F.; Khurana, A.; Blaber, M. Reversible thermal denaturation of human FGF-1 induced by low concentrations of guanidine hydrochloride. *Biophysical Journal* 77[1], 470-477. 1999.
102. Livingstone, J. R.; Spolar, R. S.; Record, M. T., Jr. Contribution to the thermodynamics of protein folding from the reduction in water-accessible nonpolar surface area. *Biochemistry* 30[17], 4237-4244. 1991.
103. Sturtevant, J. M. Differential scanning calorimetry. Processes involving proteins. *NATO Adv.Study Inst.Ser., Ser.C 55[Bioenerg. Thermodyn.: Model Syst.]*, 391-395. 1980.
104. Liggins, J. R.; Sherman, F.; Mathews, A. J.; Nall, B. T. Differential Scanning Calorimetric Study of the Thermal Unfolding Transitions of Yeast Iso-1 and Iso-2 Cytochromes c and Three Composite Isoenzymes. *Biochemistry* 33[31], 9209-9219. 1994.
105. Chan, H. S.; Dill, K. A. Polymer principles in protein structure and stability. *Annual Review of Biophysics and Biophysical Chemistry* 20, 447-490. 1991.
106. Liu, Y.; Sturtevant, J. M. The Observed Change in Heat Capacity Accompanying the Thermal Unfolding of Proteins Depends on the Composition of the Solution and on the Method Employed To Change the Temperature of Unfolding. *Biochemistry* 35[9], 3059-3062. 1996.
107. McIntosh, K. A.; Charman, W. N.; Charman, S. A. The application of capillary electrophoresis for monitoring effects of excipients on protein conformation. *J.Pharm.Biomed.Anal.* 16[6], 1097-1105. 1998.
108. Boctor, A. M.; Mehta, S. C. Enhancement of the stability of thrombin by polyols: microcalorimetric studies. *J.Pharm.Pharmacol.* 44[7], 600-603. 1992.
109. Lindman, S.; Xue, W. F.; Szczepankiewicz, O.; Bauer, M. C.; Nilsson, H.; Linse, S. Salting the charged surface: pH and salt dependence of protein G B1 stability. *Biophysical Journal* 90[8], 2911-2921. 2006.
110. Remmele, R. L., Jr.; Bhat, S. D.; Phan, D. H.; Gombotz, W. R. Minimization of Recombinant Human Flt3 Ligand Aggregation at the T_m Plateau: A Matter of Thermal Reversibility. *Biochemistry* 38[16], 5241-5247. 1999.

111. Narhi, L. O.; Philo, J. S.; Sun, B.; Chang, B. S.; Arakawa, T. Reversibility of heat-induced denaturation of the recombinant human megakaryocyte growth and development factor. *Pharm.Res.* 16[6], 799-807. 1999.
112. Chen, B. L.; Arakawa, a. T. Stabilization of recombinant human keratinocyte growth factor by osmolytes and salts. *J.Pharm.Sci.* 85[4], 419-422. 1996.
113. Graves, R. L.; Makoid, M. C.; Jonnalagadda, S. The effect of coencapsulation of bovine insulin with cyclodextrins in ethyl cellulose microcapsules. *Journal of Microencapsulation* 22[6], 661-670. 2005.
114. Branchu, S.; Forbes, R. T.; York, P.; Petren, S.; Nyqvist, H.; Camber, O. Hydroxypropyl-b-cyclodextrin Inhibits Spray-Drying-Induced Inactivation Of b-Galactosidase. *Journal of Pharmaceutical Sciences* 88[9], 905-911. 1999.
115. Cooper, A. Effect of cyclodextrins on the thermal stability of globular proteins. *Journal of the American Chemical Society* 114[23], 9208-9209. 1992.
116. Kang, F.; Jiang, G.; Hinderliter, A.; DeLuca, P. P.; Singh, J. Lysozyme Stability in Primary Emulsion for PLGA Microsphere Preparation: Effect of Recovery Methods and Stabilizing Excipients. *Pharmaceutical Research* 19[5], 629-633. 2002.
117. Kang, F.; Singh, J. Conformational stability of a model protein (bovine serum albumin) during primary emulsification process of PLGA microspheres synthesis. *International Journal of Pharmaceutics* 260[1], 149-156. 2003.
118. Singh, S.; Singh, J. Effect of polyols on the conformational stability and biological activity of a model protein lysozyme. *AAPS PharmSciTech* 4[3], 334-342. 2003.
119. Remmele, R. L., Jr.; Gombotz, W. R. Differential scanning calorimetry: a practical tool for elucidating the stability of liquid biopharmaceuticals. *Biopharm Eur.* [June], 56, 58-60, 62. 2000.
120. Bartkowski, R.; Kitchel, R.; Peckham, N.; Margulis, L. Aggregation of recombinant bovine granulocyte colony stimulating factor in solution. *Journal of Protein Chemistry* 21[3], 137-143. 2002.

Chapter 2

Microcalorimetry as a predictive tool for physical stability of granulocyte colony stimulating factor (GCSF) in solution at different pH values

1. Introduction:

Differential scanning microcalorimetry (μ DSC), one of the main techniques in protein stability predictive studies, permits an accurate measurement of the overall thermodynamic parameters and facilitates the study of energetics of biomolecular processes. Many parameters can be measured using μ DSC including unfolding temperature (T_m), also called denaturation or melting temperature, heat of reaction, denaturation heat capacity and free energy change between native and unfolded states. T_m is widely used nowadays in predicting the physical stability of protein formulations¹⁻³, where formulations showing higher T_m values are considered more stable. Many studies were performed in order to prove the predictive power of T_m ³⁻⁷ mainly by comparing the T_m of selected protein formulations with the results of traditional accelerated stress stability studies.

The degree of unfolding reversibility is a very important parameter that can be determined using μ DSC simply by considering the enthalpies of two subsequent μ DSC scans and can be calculated using the equation: % reversibility = $(\Delta H_2/\Delta H_1) \times 100$. So far, little attention was given to the use of unfolding reversibility in predicting protein formulations stability. However, the importance of the degree of unfolding reversibility in predicting the optimum pH of Flt3 Ligand formulations has been investigated⁸. In that study the prediction was based primarily on T_m in the whole pH range until the optimum T_m was reached. At a pH between 6.1 and 9.1 T_m didn't show any significant difference and the degree of unfolding reversibility declined over that pH range. It was found that using the degree of unfolding reversibility in the area where T_m is stable (T_m plateau) has improved the predictive power of μ DSC. The author has studied the predictive power of the unfolding reversibility only at the area of T_m plateau and only towards thermal stress.

In this chapter a critical evaluation of T_m and degree of unfolding reversibility in predicting the optimum pH value of Granulocyte colony stimulating factor (GCSF) was performed. The objective was not to find the optimum pH value for GCSF, but to test the predictive power in

a challenging set where both T_m and degree of reversibility are changing. Both T_m and degree of unfolding reversibility were determined for GCSF solutions in the pH range 2 – 7.

The ranking based on each parameter was compared with the ranking based on the results of an isothermal accelerated stability study. Furthermore, a mechanical stress study was also applied and the ranking based on which was compared with that based on both T_m and unfolding reversibility. The predictive power of T_m and the degree of unfolding reversibility over the whole pH range were evaluated.

2. Materials and methods:

2.1. Materials:

Granulocyte Colony stimulating factor (GCSF) was obtained as a gift from Roche Diagnostics GmbH (D-Penzberg). All other materials and solvent were of analytical grade. Deionized double-distilled water was used throughout the study.

2.2. Formulations:

GCSF bulk was obtained in Phosphate buffer 20 mM at pH 4 with a concentration of 4.2 mg/ml. The original solution was dialyzed using Slide-A-Lyzer^R Dialysis Cassette 2000 MWCO, 12-30 ml capacity (Pierce, Rockford, USA), to remove the buffer salt. After dialysis sample concentration was examined using an Uvikon 810 UV spectrophotometer (Tegimenta, Rotkreutz, Switzerland.) and the final concentration was adjusted to 0.2 mg/ml. The final pH of the sample was adjusted using 0.1N HCL as well as 0.1N NaOH to the following pH values: 2, 3, 3.5, 3.6, 3.7, 3.8, 3.9, 4, 4.5, 5, 6 and 7. This was performed using a Mettler Toledo MP220 pH meter (Mettler-Toledo GmbH, Schwezenbach, Switzerland). After preparation, all formulations were filtered using low protein binding syringe filters (25 mm, 0.2 μ m, polyvinylidene Fluoride (PVDF) membrane (Pall Corporation, MI, USA). For μ DSC measurements, a reference for each formulation was prepared by adjusting the pH of deionised water to the above mentioned values using 0.1N HCl and 0.1N NaOH. References were filtered using cellulose acetate disk filters, 0.2 μ m pore size (VWR international, USA). The same formulations were subjected to accelerated stress stability testing as well. In both μ DSC and stress studies, all formulations were kept at 2-8°C and the pH value was rechecked immediately before measurement.

2.3. Thermal stability using microcalorimetry (μ DSC):

All formulations were analyzed using a VP-DSC (Microcal Inc., MA). Samples, as well as the corresponding references were degassed for 5 min just before injection in the μ DSC cells using a Thermo vac pump (Microcal. Inc., MA). Both samples and references were loaded into cells using a gas tight Hamilton 2.5 ml glass syringe.

Each formulation was heated from 20°C to 80-90°C (depending on the formulation T_m) using 90K/hr heating rate. Thermal stability was determined 3 times for each formulation. The unfolding reversibility was investigated by temperature cycling using the upscan-upscan

method which employed two consecutive upscans. After the first upscan the device is programmed to cool the sample again and repeat the heating cycle immediately. In case of reversible formulations the reversibility was checked for all three heating replicates. The μ DSC cell was pressurized to prevent boiling of the sample during heating.

A base line run was performed before the sample run by loading both sample and reference cells with the corresponding reference. This base line was subtracted later from the protein thermal data and the excess heat capacity were normalized for protein concentration. For each formulation T_m and degree of reversibility were determined. The degree of unfolding reversibility is the percentage of the enthalpy of the second upscan (ΔH_2) in relation to the first upscan enthalpy (ΔH_1). Both ΔH_1 and ΔH_2 were the apparent calorimetric enthalpies calculated by the area under the unfolding endotherm. For data analysis ORIGIN DSC data analysis software was used.

2.4. Accelerated stress stability study:

All formulations were subjected to accelerated stress stability study in which the effects of mechanical and thermal stress were tested.

2.4.1. Mechanical stress:

10 ml of each formulation were filtered using 0.2 μ m low protein binding syringe filter (PALL 0.2 μ m PVDF Acrodisc LC 25 mm) into a 50 ml falcon tube. pH values were re-adjusted exactly to the desired value.

Figure 2.1 shows the setup for the vortex mixer (Heidolph REXA Top) used in the stress experiments. The tube was placed into the clamp in a way that allowed free movement of the tube. The vortex speed was fixed for all formulations. 3 ml samples were withdrawn at the beginning, after 15 min and 1 hr and analyzed.

2.4.2. Thermal stress:

20 ml of each formulation were rechecked for pH and filled into type I 20 ml sterile glass vials, stoppered, capped, and crimped. All filling procedures were performed under laminar flow.

All formulations were stored in a dark calibrated oven at 50°C. Samples were withdrawn at zero time, after one day, one week and two weeks time points.

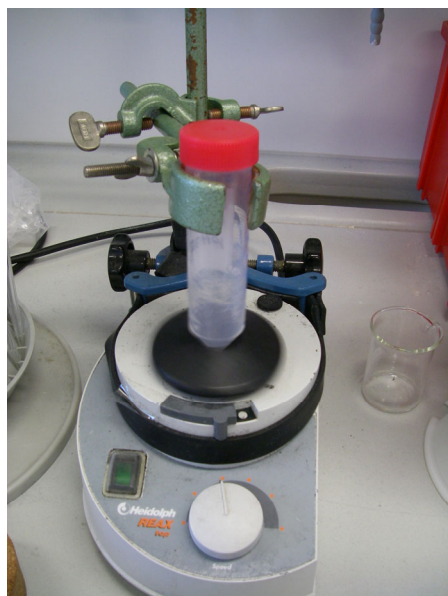


Figure 2. 1: The test set up for the mechanical stress.

2.5. Analytical methods:

2.5.1. Size-Exclusion high performance liquid chromatography (SE-HPLC):

Loss of GCSF monomer, due to aggregation or fragmentation, was monitored using SE-HPLC. The separation was achieved using Thermo separation system and a TSKgel G3000SWXL 7.8 mm ID x 30.0 cm L column (Tosoh Bioscience). Mobile phase consisted of 100 mM phosphate buffer pH 7. Flow rate of 0.6 ml/min was used and protein was detected at 215 nm. All samples were centrifuged before injection in the HPLC system. Reduction in the recovery of the whole protein content was noticed after stress, most probably, due to the formation of insoluble aggregates which are excluded from the formulation by centrifugation. Therefore, the method was not able to determine the percentage of such aggregates and as a result calculating the monomer content after stress may lead to misjudgements. Consequently, instead of calculating the monomer content, the percentage of monomer remaining in each formulation was determined after stress where the reduction in the monomer peak was calculated.

2.5.2. Light obscuration:

The insoluble aggregates (particle size > 1 μm) were determined in each formulation using light obscuration measurements (PAMAS SVSS-CTM (Rutesheim, Germany)), using a rinsing volume of 0.5 ml and a measuring volume of 0.3 ml and the number of measurements was set to 3 times. Before each measurement the device was rinsed with particle free water until less than 100 particles larger than 1 μm and no particles over 10 μm were counted.

2.5.3. Sodium dodecylsulphate polyacrylamide gel electrophoresis (SDS-PAGE):

SDS-PAGE was conducted under non-reducing conditions using XCell II mini cell system (Novex, Sand Diego, CA). The protein solutions were diluted in a pH 6.8 tris-buffer, containing 4% SDS and 20% glycerine. Samples were denatured at 95°C for 20 min and 10 μl were loaded into the gel wells (NuPage 10 % Bis-Tris Gel, Novex High performance pre-cast gels, Fa. Invitrogen, the Netherlands). Electrophoresis was performed in a constant current mode of 40mA in a MES SDS Running Buffer (NuPage MES SDS Running Buffer (20x), Fa. Invitrogen). Gel staining and drying were accomplished with a silver staining kit (SilverXpress) and a drying system (DryEase), both provided from Invitrogen, Groningen, the Netherlands.

2.6. Correlation:

To investigate the ability of μDSC parameters, unfolding temperature (T_m) and degree of unfolding reversibility, to predict the physical stability of unbuffered GCSF formulation, the correlation between the value of each parameter and the outcome of the accelerated stress stability studies was studied. The parameter values from each method were plotted on an X and Y axis and a linear fit was performed between the resulting curve points. For such a fitting a Pearson product moment correlation coefficient (R^2) could be calculated upon which the correlation is to be judged. Furthermore, rankings based on μDSC parameters and rankings based on accelerated stress studies were made and correlation between both rankings was studied as described above. For the ranking process it should be clear that the formulation ranked 1 is the best and the formulation ranked 12 is the worst.

Generally, the interpretation of such correlation coefficients depends mainly on context and purposes. A correlation of 0.9 may be considered very low if one is verifying a physical law using high quality instruments but may be regarded as very high in the social sciences where there may be a greater contribution from complicating factors. Guidelines for the

interpretation of a correlation coefficient were suggested⁹ where R^2 of 1 indicates that the two values are equally scaled, a value between 0.5 – 1 indicates strong correlation, 0.3 – 0.5 a medium correlation and a value of 0.1 – 0.3 indicates a weak correlation.

2.6.1. Ranking of formulations according to μ DSC:

Ranking was first made according to the apparent unfolding temperature (T_m) as a stability marker (R_{T_m}) and further optimized in a new ranking (R_{opT_m}) by considering the unfolding reversibility. Such procedure was suggested by Remmele⁸. In case formulations showed equal T_{ms} the formulation showing higher reversibility was ranked better (lower rank order). Furthermore, ranking based on degree of reversibility as a primary stability marker ($R_{Rev.}$) was performed and optimization was done by considering T_m ($R_{opRev.}$) in formulations showing no reversibility. In order to use both T_m and degree of reversibility equally a combined ranking was made by taking the average of the T_m based ranking and the reversibility based ranking ($R_{com.}$). In T_m ranking a minimum difference between formulations of 1°C was considered as significant.

2.6.2. Ranking of formulations according to stress stability studies::

Different rankings based on SE-HPLC and light obscuration data from stress stability study were performed according to the following steps:

- 1- 1st ranking (R_1): The formulations were ranked according to the percentage monomer remaining in each formulation at the end of the stress test.
- 2- 2nd ranking (R_2): The formulations were ranked according to their particle count at each time point. The USP requirements for light obscuration test <788> specifies that particles over 10 μ m size are controlled at or below 6000 particles / container and particles over 25 μ m are limited to or lower than 600 particles / container. No specifications were obtained for particles in the size range 1 – 10 μ m. In order to implicate the USP requirements in the ranking the following limits of particle counts were applied:

Formulation ranked 1: these are formulations which met the USP requirements and had less than 10,000 particles over 1 μ m.

Formulation ranked 2: these are formulations which met the USP requirements and had less than 100,000 particles over 1 μ m.

Formulation ranked 3: these are formulations which met the USP requirements and had more than 100,000 particles over 1 μ m.

Formulation ranked 4: all formulations showing a particle count exceeding the USP requirements.

3- Overall physical stability ranking (R_p): For each formulation the average of R_1 and R_2 was calculated as the overall physical stability ranking (R_p).

The previously described procedures were performed for both thermal and mechanical stress studies.

3. Results and discussion:

3.1. μ DSC measurements:

For each GCSF formulation both T_m and degree of reversibility were measured. Figure 2.2 shows a representative μ DSC scan for the formulation at pH 3. Figure 2.3 shows the values for T_m together with degree of reversibility for the whole pH range (2-7) of the tested formulations.

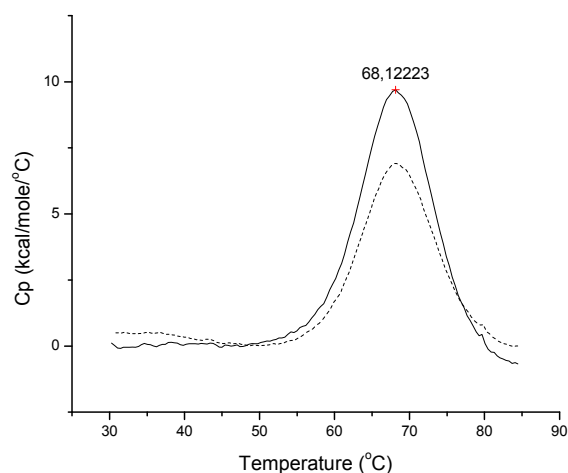


Figure 2. 2: A representative μ DSC scan for unbuffered GCSF formulation at pH 3 showing T_m (straight line) and a 2nd consecutive scan (dotted line).

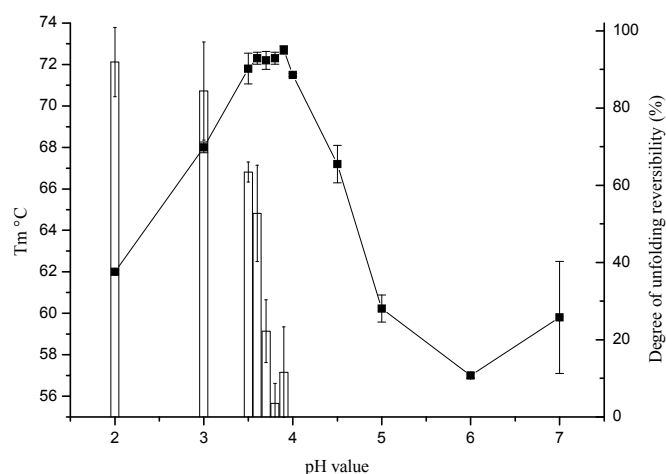


Figure 2. 3: Effect of pH value on T_m (—■—) and degree of unfolding reversibility (bars) of 12 unbuffered GCSF formulations. All errors are reported as standard deviation from the mean ($n=3$) and represented as error bars in the curve.

Figure 2.3 shows that the reversibility of GCSF decreased with increasing pH value whereas T_m increased till pH 3.5. From pH 3.5 – 4 no significant increase in T_m was found. At higher pH values T_m decreased again till pH 6 and 7. It should be mentioned that GCSF did not show any reversibility in buffered formulations and therefore all formulations were formulated in absence of buffer. Table 2.1 shows a list of T_m and the degree of reversibility of the 12 unbuffered GCSF formulations together with T_m based ranking (R_{Tm}) and “optimization” of the ranking using the degree of unfolding reversibility (R_{opTm}), unfolding reversibility based ranking ($R_{Rev.}$) and “optimization” using T_m ($R_{opRev.}$) and T_m – reversibility combined ranking ($R_{com.}$).

Table 2. 1: Values of T_m and degree of unfolding reversibility for the 12 unbuffered GCSF formulations together with the different predictive rankings.

Formulation	pH	T_m	Rev. ¹⁾	R_{Tm}	R_{opTm}	$R_{Rev.}$	$R_{opRev.}$	$R_{com.}$
GCSFun01	2	62	91,9	9	9	1	1	8
GCSFun02	3	68	84,4	7	7	2	2	6
GCSFun03	3.5	71,8	63,4	1	1	3	3	1
GCSFun04	3.6	72,3	52,7	1	2	4	4	2
GCSFun05	3.7	72,2	22,2	1	3	5	5	3
GCSFun06	3.8	72,3	3,5	1	5	7	7	5
GCSFun07	3.9	72,7	11,6	1	4	6	6	4
GCSFun08	4	71,5	0	1	6	8	8	6
GCSFun09	4.5	67,2	0	8	8	8	9	9
GCSFun10	5	60,23	0	10	10	8	10	10
GCSFun11	6	57	0	12	12	8	12	12
GCSFun12	7	59,8	0	11	11	8	11	11

1) Degree of unfolding reversibility

3.2. Accelerated stress stability studies:

In appendix 2.I all data from the accelerated stability studies are presented in tables 2.I.1 – 4.

3.2.1. Mechanical stress:

The samples were analyzed at 2 time intervals (15 and 60 min). The % monomer remaining at both time points is illustrated in figure 2.4 A. At pH 3.5 an extreme reduction in monomer content was noticed after 60 min which was not the case after 15 min and which might be caused by the nucleation of small aggregates to larger ones. Therefore, all formulations were

judged based on the results after 15 min. The extreme monomer loss was confirmed by the particle count results from the light obscuration measurements (figure 2.4 B).

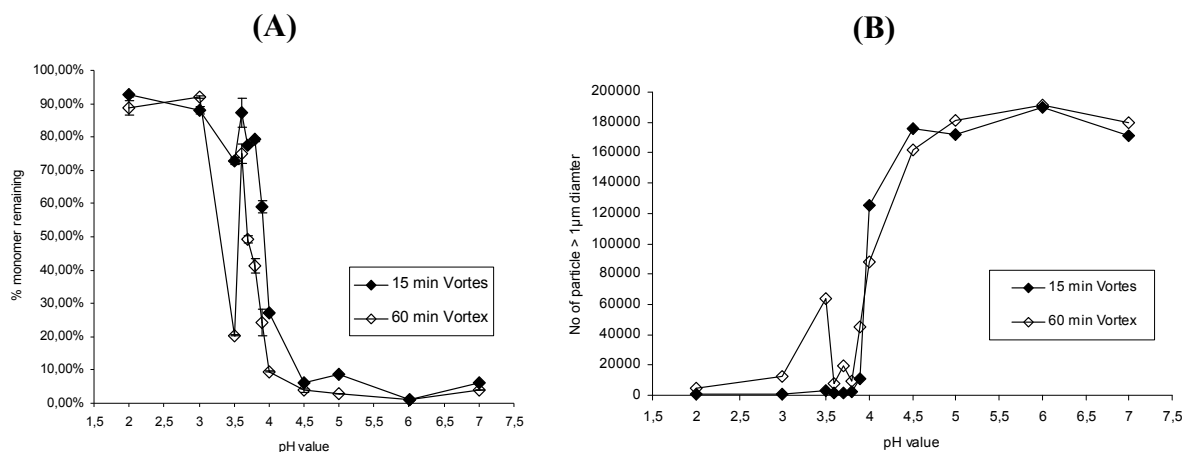


Figure 2. 4: Effect of mechanical stress on (A) monomer content and (B) the particle count over 1 µm particle diameter after 15 and 60 min. All errors are reported as standard deviation from the mean (n=3) and represented as error bars in the curve.

Increasing the pH value of GCSF formulations in absence of buffer salts from 2 to 7 reduced the physical stability of GCSF against mechanical stress. That was shown by a reduction in monomer content and an increase in particle count as the pH value was increased from 2 to 7.

3.2.2. Thermal stress:

Formulations were analyzed at the beginning and after storage at 50°C at three time points (after 1 day, 7 days and 14 days) and the monomer content as well as the particle count were determined. SDS-PAGE was performed at the beginning and at the end of the stress study. Figure 2.5 A shows the effect of thermal stress on the monomer content of each formulation at each time point. Formulations having pH values 5, 6 and 7 were analyzed only till 7 days as they were already completely destroyed after that time point. However, for these formulations only SDS-PAGE was done at 14 days time point. From the results it seems obvious that the physical stability of GCSF against thermal stress differs from its stability against mechanical stress. This difference is shown in the 1st part of the curve: The monomer content after 14 days thermal stress is highest at pH 3.5 and 3.6, whereas the highest monomer content after mechanical stress was at pH 2 (figure 2.4 A). This behaviour was also confirmed by SDS-

PAGE (figure 2.6) where pH 3.5 showed the lowest aggregation after 14 days storage at 50°C. Particle count measurements did not show any significant difference in the pH range 2 - 3.5 (figure 2.5 B). Otherwise the rest of formulations behaved similarly in both stresses at higher pH values except pH 7 which showed low particle count although very low monomer content was recovered after 7 days storage at 50°C. This is most probably due to the formation of smaller size aggregates which could be seen in SDS-PAGE (figure 2.6.)

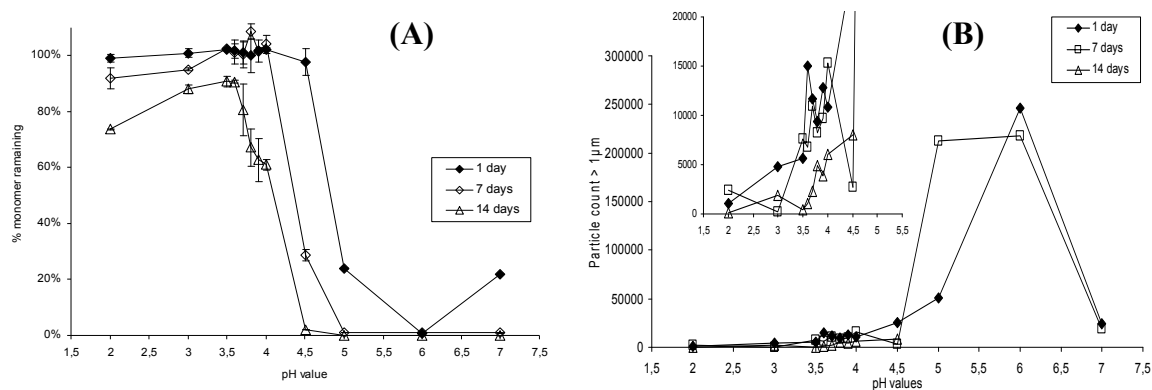


Figure 2. 5: Effect of Thermal stress on (A) monomer content and (B) the particle count over 1 μm particle diameter after 1, 7 and 14 days storage at 50°C. All errors are reported as standard deviation from the mean (n=3) and represented as error bars in the curve.

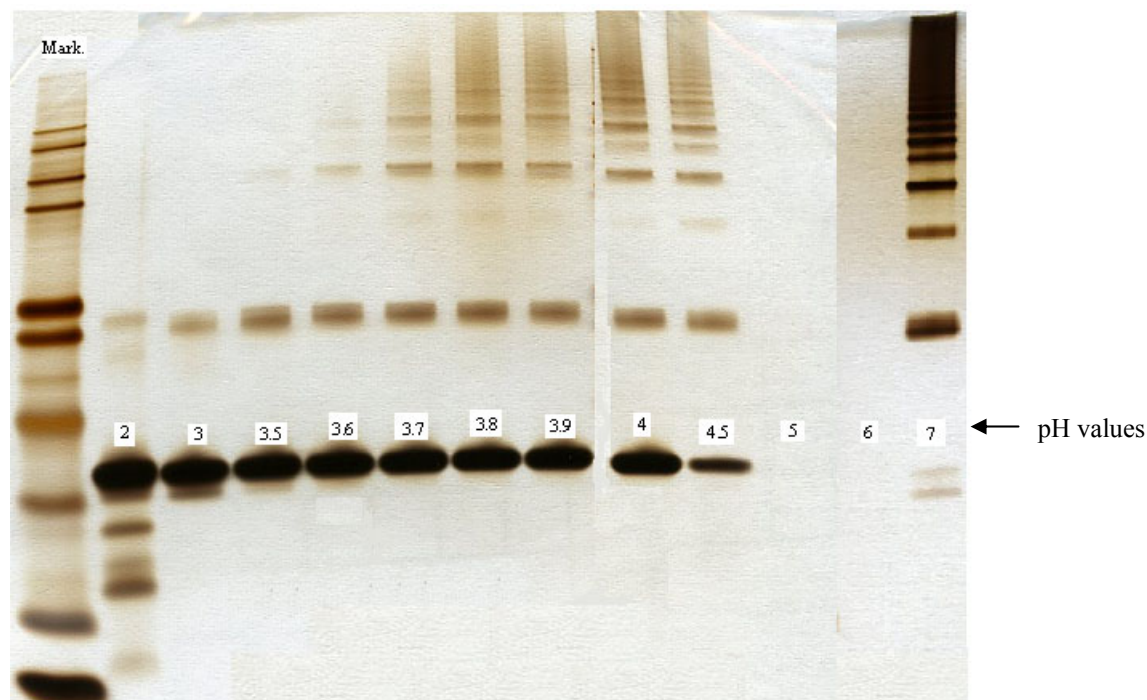


Figure 2. 6: SDS-PAGE for unbuffered GCSF formulations at different pH values after storage at 50°C for 14 days. The numbers on the graph are the corresponding pH values of each formulation.

3.3. Correlation:

A comparison between T_m values and the % of monomer remaining after both stress methods is illustrated in figure 2.7. A good correlation between T_m and the monomer content of GCSF especially after applying thermal stress was found. Considering the degree of unfolding reversibility at the pH range 3.5 – 4 (T_m plateau) the monomer content was better predicted. After applying mechanical stress GCSF showed at pH 2 the best monomer content although T_m was low. On the other hand the degree of unfolding reversibility showed the highest value at pH 2. Previous studies showed that pH range 3.5 – 4 is the best for GCSF stability^{10,11} due to hydrolysis of the protein at pH less than 3. During mechanical stress the chemical stability of the protein is not challenged as in thermal stress. In this case the degree of unfolding reversibility looked only for physical stability and T_m was better in predicting the best pH range for GCSF. Microcalorimetry as a predictive tool in protein formulation was judged by many authors by similar comparisons^{5,8,12}. However, the objective of this study is to evaluate whether T_m and/or unfolding reversibility are more precise to predict the stability ranking order and accordingly, the reliability of a μ DSC based decision is to be evaluated. Therefore, the correlation coefficients between the compared parameters and furthermore, between rankings were thought to be a reliable parameter which could be used in judging such a predictive method.

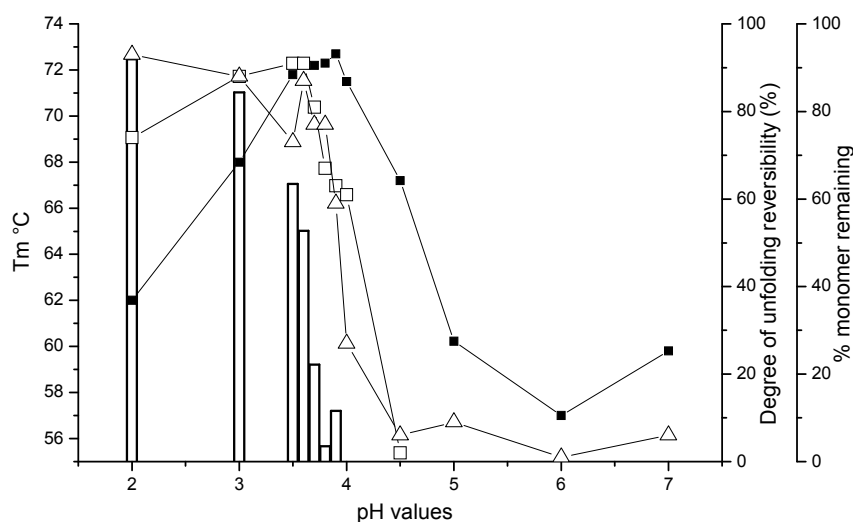


Figure 2. 7: Correlation between effects of thermal ($-\square-$) and mechanical ($-\triangle-$) stress on the monomer content of GCSF unbuffered formulations at different pH values and μ DSC parameters (T_m ($-\square-$) and unfolding reversibility (bars)).

3.3.1. Predictive power of the μ DSC parameters:

The 2 parameters obtained from the μ DSC study for each formulation are T_m and degree of unfolding reversibility. In addition, the % of monomer remaining after stress of each formulation as well as the particle count was measured. Each μ DSC parameter was compared with either % monomer remaining or particle count of the formulations. In appendix 2.II (figures 2.II.1 and 2.II.2) correlation curves are shown. One of these curves is presented here as an example and shows the correlation between T_m values and % monomer remaining after 14 days thermal stress (figure 2.8). The correlation coefficients resulting were compared with each other to evaluate the predictive power of the μ DSC parameters towards each stress test (figure 2.9). The negative correlation coefficients shown in figure 2.9 B indicate the inversed relation between T_m and degree of unfolding reversibility with the particle count after stress.

A correlation coefficient equal or even close to 1 or -1 was obtained in none of the correlation studies. The highest correlation coefficient was 0.714 obtained for the correlation of degree of unfolding reversibility with the particle count over 1 μ m after isothermal stress. Having a correlation coefficient less than 1 denies the scalability of either μ DSC parameters towards neither monomer content nor particle count after stress. However, this does not deny the strong correlation between them and the possibility of excellent prediction.

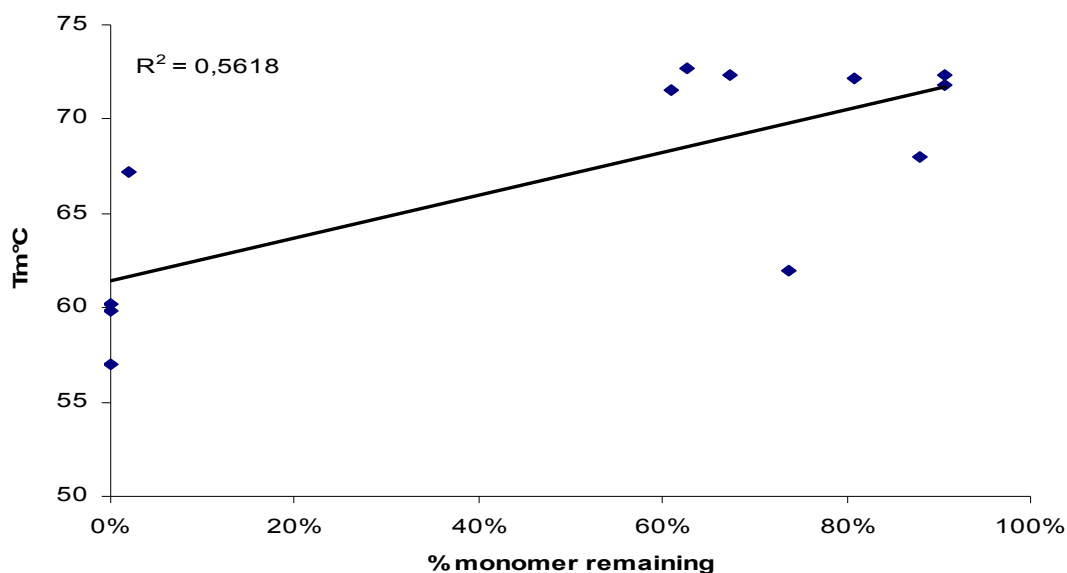


Figure 2. 8: Correlation between T_m values and % monomer remaining after 14 days storage at 50°C of 12 unbuffered GCSF formulations at different pH values

In most correlation curves (appendix 2.II, figures 2.II.1 and 2) the linear fit was made between two clusters of points (that can be noticed also in figure 2.8) which may cause over estimation

of the correlation coefficient as if it is made between 2 points only. The only exception is the correlation between the degree of unfolding reversibility and the particle count after thermal stress.

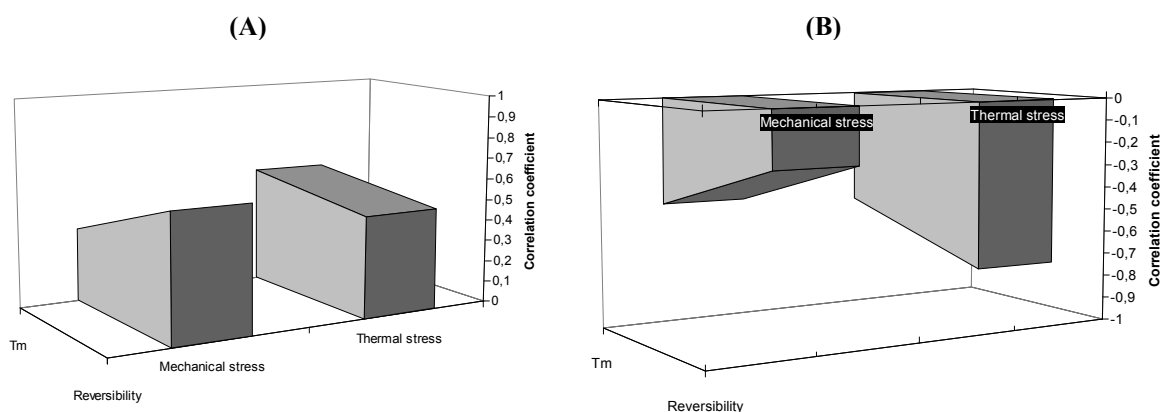


Figure 2. 9: Comparison between the resulted correlation coefficients from comparing μ DSC parameters with % monomer content (A) and particle count $> 1 \mu\text{m}$ (B) after thermal and mechanical stress.

3.3.2. Predictive power of μ DSC based rankings:

In table 2.1 the studied 12 unbuffered GCSF formulations were ranked based on μ DSC parameters. Tables 2.2 and 2.3 show the ranking of the same formulations based on the stress stability study using either mechanical or thermal stress, respectively.

Table 2. 2: Ranking of physical stability of GCSF formulations after vortex shaking for 15 min.

Formulation	pH	% Monomer remaining	$R_1^{1)}$	$R_2^{2)}$	Average ($R_1+R_2/2$)	$R_{pm}^{3)}$
GCSFun01	2	93%	1	1	1	1
GCSFun02	3	88%	2	1	1,5	2
GCSFun03	3.5	73%	6	1	3,5	6
GCSFun04	3.6	87%	2	1	1,5	2
GCSFun05	3.7	77%	4	1	2,5	4
GCSFun06	3.8	77%	4	1	2,5	4
GCSFun07	3.9	59%	7	2	4,5	7
GCSFun08	4	27%	8	3	5,5	8
GCSFun09	4.5	6%	9	3	6	9
GCSFun10	5	9%	9	3	6	9
GCSFun11	6	1%	12	4	8	12
GCSFun12	7	6%	9	3	6	9

1) Ranking of the 12 formulations according to the % monomer remaining after stress

2) Ranking based on light blockage measured particle count $>1 \mu\text{m}$ (appendix 2.I, table 2.1.3)

3) General physical stability ranking against mechanical stress based on the average of both R_1 and R_2

Table 2. 3: Ranking of physical stability of GCSF formulations after storing at 50°C for 14 days.

Formulation	pH	% Monomer remaining	R ₁	R ₂ ¹⁾	Average (R ₁ +R ₂ /2)	R _{pt} ²⁾
GCSFun01	2	74%	5	1	3	5
GCSFun02	3	88%	3	1	2	3
GCSFun03	3.5	91%	1	1	1	1
GCSFun04	3.6	91%	1	1	1	1
GCSFun05	3.7	81%	4	1	2,5	4
GCSFun06	3.8	67%	6	1	3,5	6
GCSFun07	3.9	63%	7	1	4	7
GCSFun08	4	61%	7	1	4	7
GCSFun09	4.5	2%	9	1	5	9
GCSFun10	5	0%	9	3	6	11
GCSFun11	6	0%	9	4	6,5	12
GCSFun12	7	0%	9	2	5,5	10

1) Ranking based on light blockage measured particle count >1 μm (appendix 2.I, table 2.I.4)

2) General physical stability ranking against thermal stress based on the average of both R₁ and R₂

Rankings from μDSC and stress stability studies were compared with each other and correlation coefficients were calculated. Correlation curves are presented in figures 2.10 and 2.11 for μDSC based ranking against mechanical and thermal stress based rankings, respectively. A comparison between the resulting correlation coefficients is presented in figure 2.12 showing approximately similar correlation of the thermal stability ranking to both T_m and reversibility based rankings. On the other hand, mechanical stress stability ranking correlated significantly better to the reversibility based ranking. Optimization of T_m based ranking using the degree of reversibility and vice versa did improve the correlation significantly in both stress studies. Furthermore, T_m- reversibility combined ranking (R_{com}) was the best predictive for the thermal stability of the group of GCSF formulations.

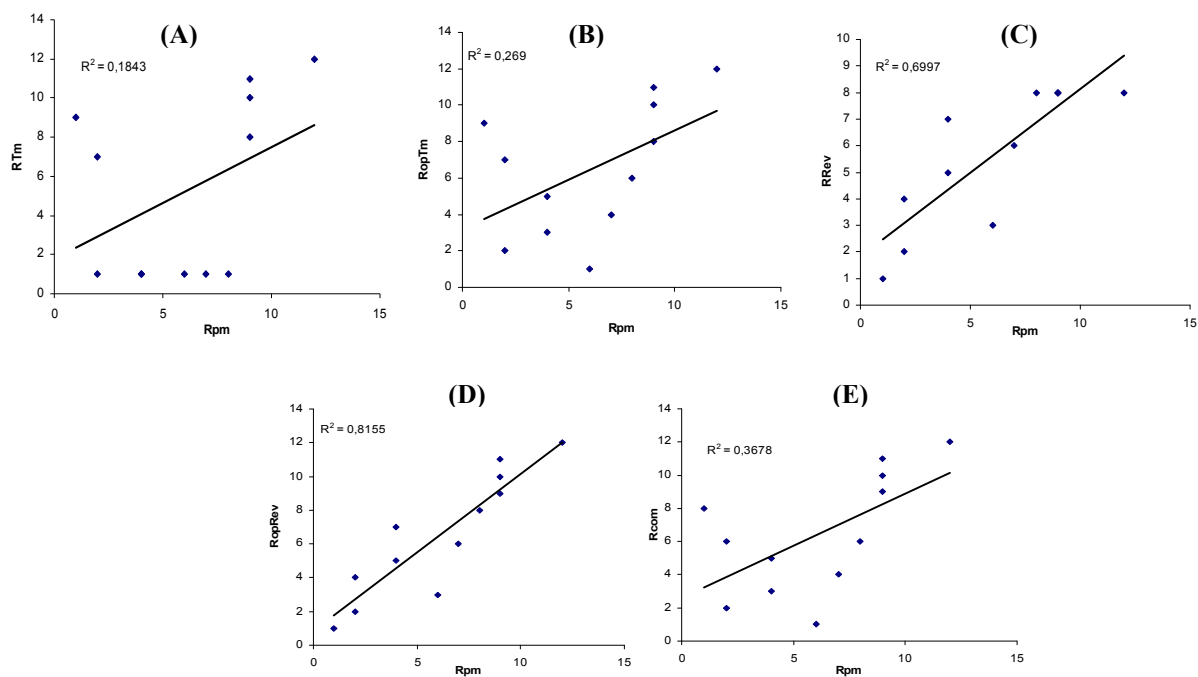


Figure 2. 10: Correlation curves between μ DSC based rankings and Physical stability based ranking after Mechanical stress (R_{pm}). (A) T_m based ranking (R_{Tm}), (B) T_m optimized ranking (R_{opTm}), (C) reversibility based ranking (R_{Rev}), (D) reversibility optimized ranking (R_{opRev}) and (E) T_m – Reversibility combined ranking (R_{com})

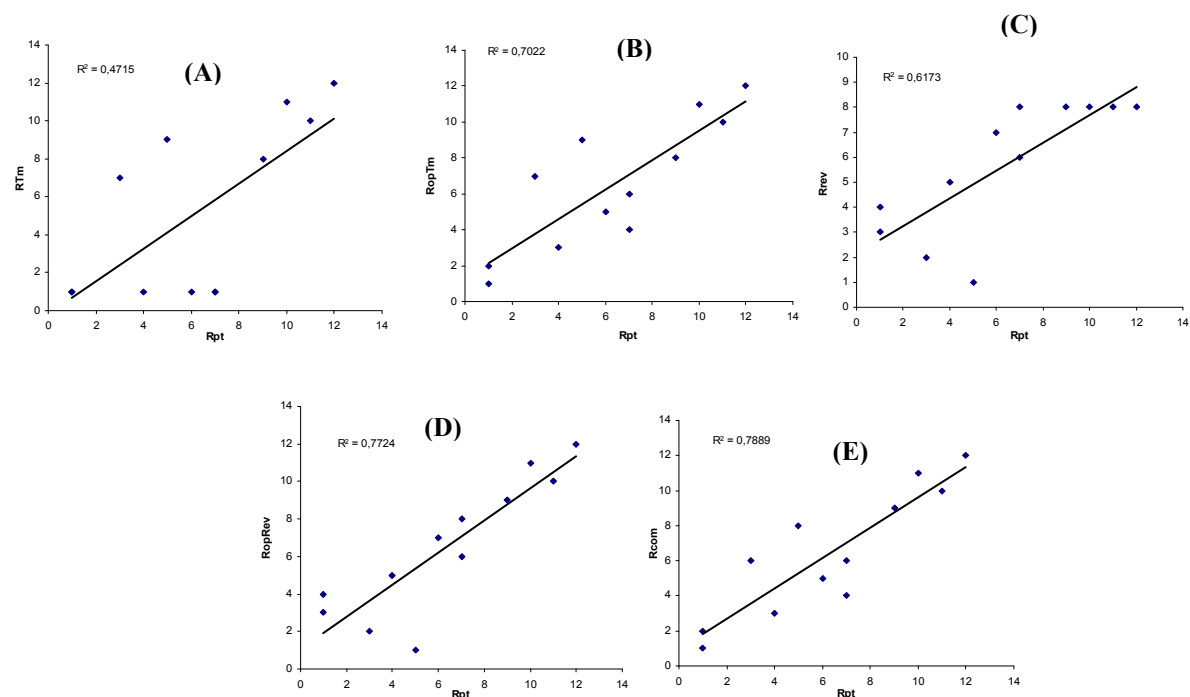


Figure 2. 11: Correlation curves between μ DSC based rankings and Physical stability based ranking after Thermal stress (R_{pt}). (A) T_m based ranking (R_{Tm}), (B) T_m optimized ranking (R_{opTm}), (C) reversibility based ranking (R_{Rev}), (D) reversibility optimized ranking (R_{opRev}) and (E) T_m – Reversibility combined ranking (R_{com})

Accordingly, the stability of GCSF in a pH row against different stresses can be predicted by different μ DSC based rankings. The stability against mechanical stress was predicted best when the degree of unfolding reversibility is considered as a primary ranking and when T_m is considered as an optimizing parameter (R_{opRev} , table 2.1). The stability against isothermal stress was predicted best when both parameters (T_m and unfolding reversibility) were equally considered in a combined ranking (R_{com} , table 2.1).

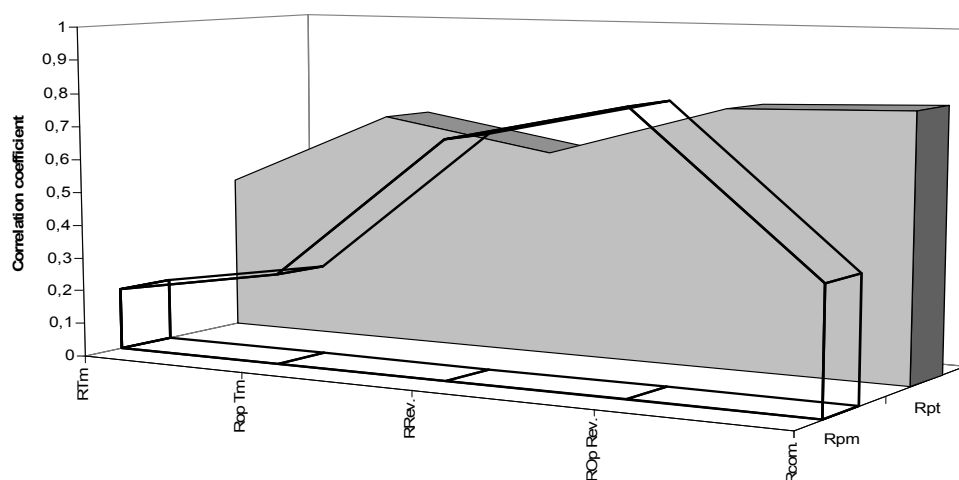


Figure 2. 12: Comparison between the correlation coefficient of different μ DSC based rankings and each of thermal and mechanical stability based rankings. On x axis: T_m based ranking (R_{Tm}), T_m optimized ranking (R_{opTm}), reversibility based ranking (R_{Rev}), reversibility optimized ranking (R_{opRev}) and T_m – Reversibility combined ranking (R_{com}). On Z-axis ranking based on the results of thermal stability (R_{pt}) and ranking based on mechanical stability (R_{pm})

4. Conclusion:

Absolute values of μ DSC parameters can not be used to predict certain monomer content or particle count after stress of protein formulations as these parameters are not scaled with either monomer remaining or particle count after stress. The stability of GCSF in a pH row against different stresses can be predicted by different μ DSC based rankings. These rankings are based on both T_m and the degree of unfolding reversibility and could be improved significantly through either optimized or combined rankings. Most interestingly, the degree of unfolding reversibility is powerful in predicting the effect of mechanical stress than the unfolding temperature (T_m).

5. References:

1. Lindman, S.; Xue, W. F.; Szczepankiewicz, O.; Bauer, M. C.; Nilsson, H.; Linse, S. Salting the charged surface: pH and salt dependence of protein G B1 stability. *Biophysical Journal* 90[8], 2911-2921. 2006.
2. Kang, F.; Jiang, G.; Hinderliter, A.; DeLuca, P. P.; Singh, J. Lysozyme Stability in Primary Emulsion for PLGA Microsphere Preparation: Effect of Recovery Methods and Stabilizing Excipients. *Pharmaceutical Research* 19[5], 629-633. 2002.
3. Singh, S.; Singh, J. Effect of polyols on the conformational stability and biological activity of a model protein lysozyme. *AAPS PharmSciTech* 4[3], 334-342. 2003.
4. Remmele, R. L., Jr.; Nightlinger, N. S.; Srinivasan, S.; Gombotz, W. R. Interleukin-1 receptor (IL-1R) liquid formulation development using differential scanning calorimetry. *Pharmaceutical Research* 15[2], 200-208. 1998.
5. Burton, L.; Gandhi, R.; Duke, G.; Paborji, M. Use of Microcalorimetry and Its Correlation with Size Exclusion Chromatography for Rapid Screening of the Physical Stability of Large Pharmaceutical Proteins in Solution. *Pharmaceutical Development and Technology* 12[3], 265-273. 2007.
6. Schrier, J. A.; Kenley, R. A.; Willians, R.; Corcoran, R. J.; Kim, Y.; Northey, R. P.; D'Augusta, D.; Huberty, M. Degradation pathways for recombinant human macrophage colony-stimulating factor in aqueous solution. *Pharmaceutical Research* 10[7], 933-944. 1993.
7. Remmele, R. L., Jr.; Gombotz, W. R. Differential scanning calorimetry: a practical tool for elucidating the stability of liquid biopharmaceuticals. *Biopharm Eur.* [June], 56, 58-60, 62. 2000.
8. Remmele, R. L., Jr.; Bhat, S. D.; Phan, D. H.; Gombotz, W. R. Minimization of Recombinant Human Flt3 Ligand Aggregation at the T_m Plateau: A Matter of Thermal Reversibility. *Biochemistry* 38[16], 5241-5247. 1999.
9. Cohen J. *Statistical power analysis for the behavioral sciences*; 02 ed.; Erlbaum, Lawrence & Associates: 1988.
10. Kueltoz, L. A.; Middaugh, C. R. Structural characterization of bovine granulocyte colony stimulating factor: Effect of temperature and pH. *Journal of Pharmaceutical Sciences* 92[9], 1793-1804. 2003.
11. Thirumangalathu, R.; Krishnan, S.; Brems, D. N.; Randolph, T. W.; Carpenter, J. F. Effects of pH, temperature, and sucrose on benzyl alcohol-induced aggregation of recombinant human granulocyte colony stimulating factor. *Journal of Pharmaceutical Sciences* 95[7], 1480-1497. 2006.
12. Huus, K.; Havelund, S.; Olsen, H. B.; Weert, M.; Frokjaer, S. Chemical and Thermal Stability of Insulin: Effects of Zinc and Ligand Binding to the Insulin Zinc-Hexamer. *Pharmaceutical Research* 23[11], 2611-2620. 2006.

6. Appendix 2.I:

Table 2.I. 1: Monomer remaining after mechanical stress of 12 unbuffered GCSF formulations at different pH values.

Formulations	pH values	15 min. Vortex (% monomer remaining)	60 min. Vortex (% monomer remaining)
GCSFun01	2	93%	90%
GCSFun02	3	88%	93%
GCSFun03	3.5	73%	21%
GCSFun04	3.6	87%	75%
GCSFun05	3.7	77%	49%
GCSFun06	3.8	77%	40%
GCSFun07	3.9	59%	24%
GCSFun08	4	27%	10%
GCSFun09	4.5	6%	4%
GCSFun10	5	9%	3%
GCSFun11	6	1%	1%
GCSFun12	7	6%	4%

Table 2.I. 2: Monomer remaining after thermal stress of 12 unbuffered GCSF formulations at different pH values.

Formulations	pH values	1 day at 50°C (% monomer remaining)	14 day at 50°C (% monomer remaining)	14 days at 50°C (% monomer remaining)
GCSFun01	2	99,19%	91,9%	73,7%
GCSFun02	3	100,84%	95,1%	88,1%
GCSFun03	3.5	102,31%	102,5%	90,7%
GCSFun04	3.6	101,68%	101,3%	90,7%
GCSFun05	3.7	101,01%	100,4%	80,7%
GCSFun06	3.8	99,95%	108,6%	67,3%
GCSFun07	3.9	101,93%	101,5%	62,7%
GCSFun08	4	102,20%	104,2%	61,0%
GCSFun09	4.5	97,75%	28,7%	2,1%
GCSFun10	5	23,90%	1,1%	N/A
GCSFun11	6	0,76%	1,1%	N/A
GCSFun12	7	21,92%	0,9%	N/A

Table 2.I. 3: Particle count after mechanical stress of 12 unbuffered GCSF formulations at different pH values measured by light obscuration.

Formulations	pH values	Particle range	T Zero	15 min	60 min	Ranking (15 min)
GCSFun01	2	> 1 μm	694	883	4699	1
		> 10 μm	12	8	31	
		> 25 μm	0	0	3	
GCSFun02	3	> 1 μm	2072	1093	12706	1
		> 10 μm	38	31	84	
		> 25 μm	1	2	3	
GCSFun03	3.5	> 1 μm	1890	3323	63967	1
		> 10 μm	128	21	181	
		> 25 μm	11	0	3	
GCSFun04	3.6	> 1 μm	1319	1353	8167	1
		> 10 μm	16	89	32	
		> 25 μm	0	6	2	
GCSFun05	3.7	> 1 μm	152	1293	19364	1
		> 10 μm	3	31	52	
		> 25 μm	0	0	0	
GCSFun06	3.8	> 1 μm	1672	2212	9640	1
		> 10 μm	50	32	37	
		> 25 μm	0	1	3	
GCSFun07	3.9	> 1 μm	1301	11080	45146	2
		> 10 μm	9	52	147	
		> 25 μm	0	8	2	
GCSFun08	4	> 1 μm	257	125146	87983	3
		> 10 μm	11	101	637	
		> 25 μm	6	4	0	
GCSFun09	4.5	> 1 μm	3768	175781	161772	3
		> 10 μm	44	967	1910	
		> 25 μm	6	6	7	
GCSFun10	5	> 1 μm	13117	172239	181356	3
		> 10 μm	70	1009	754	
		> 25 μm	10	19	11	
GCSFun11	6	> 1 μm	22563	189854	191818	4
		> 10 μm	292	23816	24146	
		> 25 μm	9	24	20	
GCSFun12	7	> 1 μm	8792	170827	179686	3
		> 10 μm	59	5907	4806	
		> 25 μm	6	19	8	

Table 2.I. 4: Particle count after thermal stress of 12 unbuffered GCSF formulations at different pH values measured by light obscuration.

Formulations	pH values	Particle range	T Zero	1 day	7 days	14 days	Ranking (14 days)
GCSFun01	2	> 1 μm	1419	1037	2411	152	1
		> 10 μm	8	9	11	7	
		> 25 μm	2	2	1	1	
GCSFun02	3	> 1 μm	5777	4743	227	1888	1
		> 10 μm	23	3	4	27	
		> 25 μm	1	0	3	7	
GCSFun03	3.5	> 1 μm	2584	5576	7570	388	1
		> 10 μm	12	12	12	2	
		> 25 μm	0	0	0	0	
GCSFun04	3.6	> 1 μm	888	15010	6750	1040	1
		> 10 μm	4	101	71	14	
		> 25 μm	0	0	1	1	
GCSFun05	3.7	> 1 μm	2568	11633	10900	2243	1
		> 10 μm	34	67	27	21	
		> 25 μm	0	0	0	1	
GCSFun06	3.8	> 1 μm	2798	9384	8179	4846	1
		> 10 μm	8	41	33	144	
		> 25 μm	0	0	1	7	
GCSFun07	3.9	> 1 μm	2317	12774	9738	3827	1
		> 10 μm	9	19	96	77	
		> 25 μm	0	0	3	1	
GCSFun08	4	> 1 μm	3391	10791	15328	6043	1
		> 10 μm	24	27	180	132	
		> 25 μm	4	1	10	7	
GCSFun09	4.5	> 1 μm	6044	25511	2683	8034	1
		> 10 μm	81	243	168	668	
		> 25 μm	4	8	22	67	
GCSFun10	5	> 1 μm	9951	50238	212078		3
		> 10 μm	106	461	168		
		> 25 μm	2	10	17		
GCSFun11	6	> 1 μm	11924	246400	217320		4
		> 10 μm	81	2020	24508		
		> 25 μm	1	22	76		
GCSFun12	7	> 1 μm	9141	24136	19243		2
		> 10 μm	31	703	411		
		> 25 μm	0	22	17		

7. Appendix 2.II:

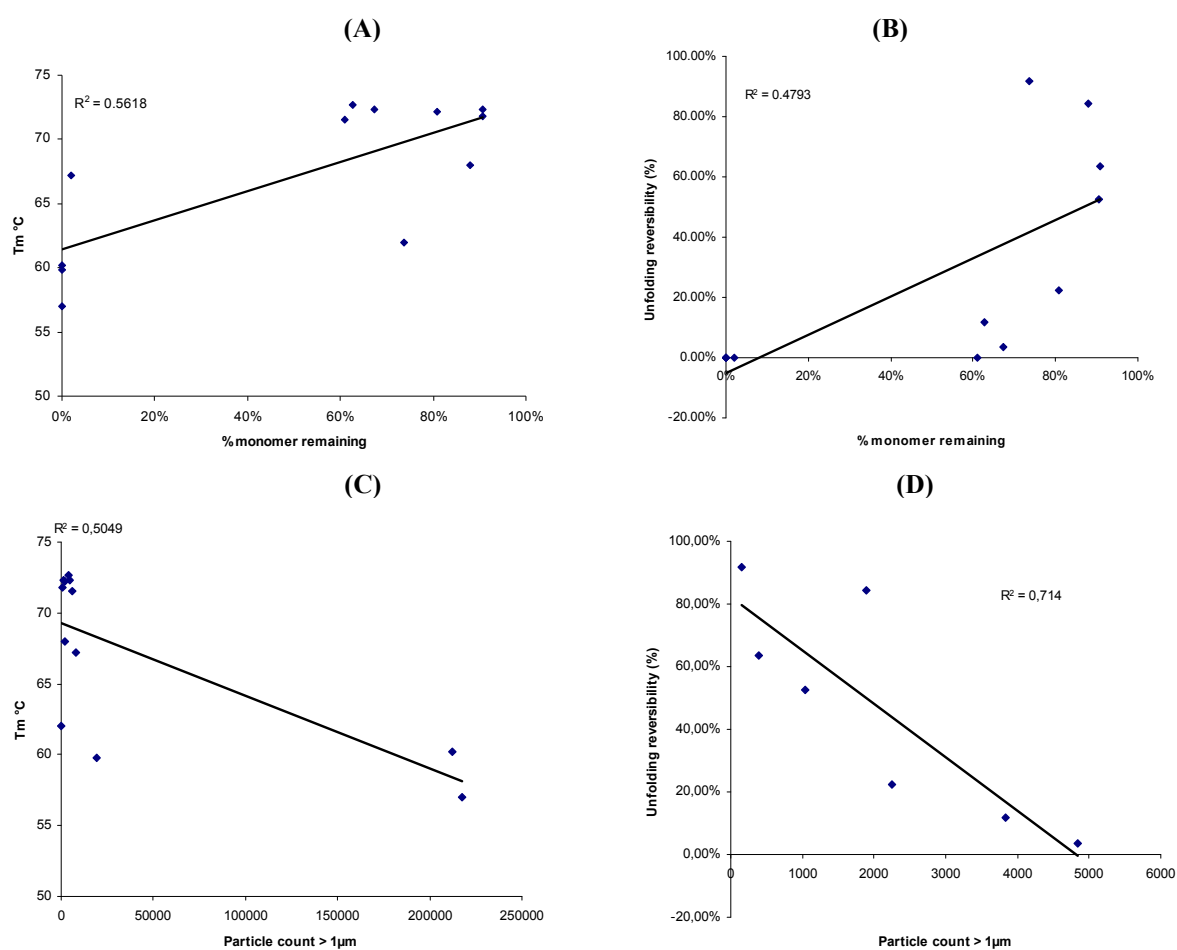


Figure 2.II. 1: Correlation curves between μDSC parameters and Physical stability after thermal stress. (A) Correlation between T_m and % monomer remaining, (B) Unfolding reversibility and % monomer remaining, (C) T_m and Particle count > 1 μm and (D) is the correlation between Unfolding reversibility and particle count > 1 μm .

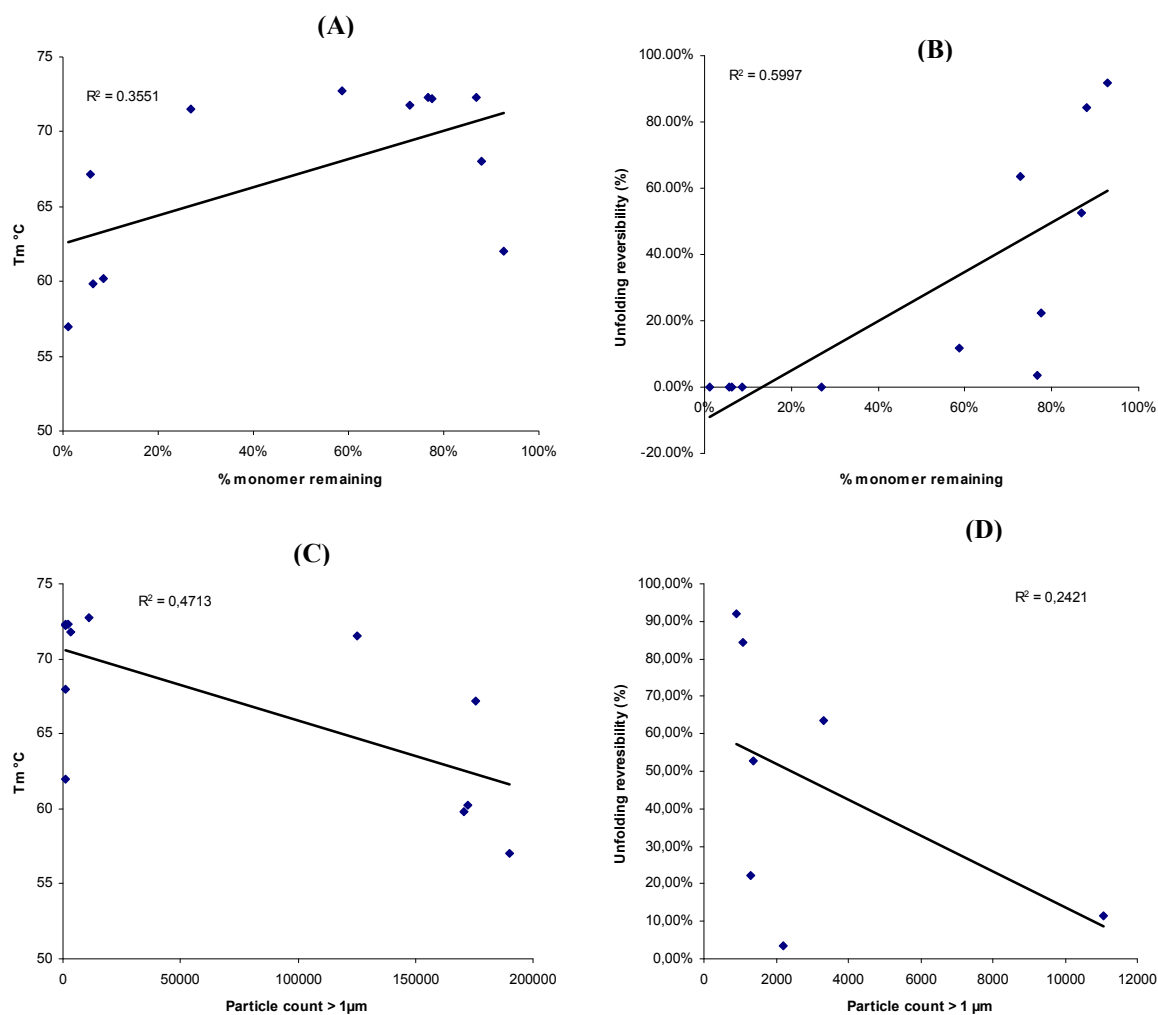


Figure 2.II. 2: Correlation curves between μDSC parameters and Physical stability after Mechanical stress. (A) Correlation between T_m and % monomer remaining, (B) Unfolding reversibility and % monomer remaining, (C) T_m and Particle count > 1 μm and (D) is the correlation between Unfolding reversibility and particle count > 1 μm .

Chapter 3

A critical evaluation of microcalorimetry as a predictive tool for long term stability of liquid protein formulations

1. Introduction:

In protein formulation development studies the best solution conditions and stabilizers needed to protect the protein from possible chemical or physical deteriorations are to be defined. In early phases many analytical methods are involved to provide better prediction of the long term stability where the main target is to prevent aggregation during long term storage and to prevent unexpected stability problem lately in clinical trials.

Differential scanning microcalorimetry (μ DSC) is one of the most common methods used in protein pre-formulation and formulation studies where many solution conditions as well as excipients can be screened^{1-3,3-5}

Several other techniques are available to determine T_m , monitoring either secondary or tertiary protein structure as a function of temperature. Rapid high throughput technologies are currently being applied to determine spectroscopy based T_m s. Such technologies are based mainly on measuring samples in multi-well plates using either fluorescence or UV spectroscopy to optimize formulation factors and to choose suitable stabilizers. Such screening was successfully performed for Respiratory Syncytial Virus (RSV)⁶ showing higher stability of RSV in formulations with sugars and polyols as indicated by an increase in T_m calculated from both secondary and tertiary structure loss.

The main concern against using T_m as a marker for protein stability, either obtained from μ DSC or other methods, is that the mechanism of protein denaturation under long term conditions at normal storage temperatures (2-8 °C) is not the same as at higher temperature (ca. 60 - 75°C).

Many studies^{3-5,7} proved correlation between T_m and protein physical stability where T_m was compared with data from accelerated stability studies, thereby comparing one surrogate study with another one instead of correlating real time stability studies at normal storage temperatures with T_m . There may be unpublished studies with predictive DSC studies in

industry, but comprehensive, systematic data from real time studies correlated with T_m determined by μ DSC have not been published yet.

In this chapter a systematic study on 3 different proteins, including 24 different Granulocyte Colony Stimulating Factor (GCSF), 15 Monoclonal antibody (MAB) and 14 Pegylated Interferon α 2a (PEG-INF) liquid formulations is presented. All formulations were included in a μ DSC study to determine T_m and unfolding reversibility, if applicable. The intention was to compare the stability prediction from the μ DSC, based on T_m determinations, with the data from IsoSS up to 24 months for GCSF and 12 months for both MAB and PEG-INF. In the IsoSS the most important analytical techniques to rate physical and/or chemical stabilities were involved including size exclusion high performance liquid chromatography (SE-HPLC), turbidimetry, light obscuration, gel electrophoresis and reversed phase-HPLC (RP-HPLC).

The stability of GCSF, MAB and PEG-INF formulations has been studied intensively before⁸⁻¹⁵. Also, many patents on stable formulations are available¹⁶⁻²¹. The long term stability of GCSF is determined by both chemical and physical effects where pH and salt content of the formulation determine the extent of aggregation and chemical degradation. MAB is a unique protein class where physical stability mainly determines its long term stability. PEG-INF is an example of a pegylated protein and expected to be stable in long term. Therefore, these three proteins were considered as interesting and relevant candidates for the purpose of the study.

It is essential to understand the study purpose which is not to find new or better formulations for the studied proteins, but to correlate long term stability data with predictive T_m measurements for a challenging set of formulation, i.e. formulations that are close to each other and difficult to rank from each other. For that reason formulations with obvious stability extremes were not included in the study. Thereby a challenging formulation grid including different buffer salts, excipients and different pH values was set up to evaluate the predictive power of μ DSC.

I. Granulocyte Colony Stimulating Factor (GCSF):

I.1. Materials and methods:

I.1.1. Materials:

Granulocyte Colony stimulating factor (GCSF) was obtained as a gift from Roche diagnostics GmbH (D-Penzberg, Germany). All other materials and solvent were of analytical grade. Deionized double-distilled water was used throughout the study.

I.1.2. Formulations:

GCSF was obtained in 20 mM Phosphate buffer at pH 4 with a concentration of 4.2 mg/ml. The original solution was dialyzed using Slide-A-Lyzer^R Dialysis Cassette 2000 MWCO, 12-30 ml Capacity (Pierce, Rockford, USA), to the required buffer. After dialysis the sample concentration was examined using an Uvikon 810 UV spectrophotometer (Tegimenta, Rotkreutz, Switzerland), and the final concentration was adjusted to 0.2 mg/ml. The final pH of the sample was determined with a Mettler Toledo MP220 pH meter (Mettler-Toledo GmbH, Schwezenbach, Switzerland). After preparation all formulations were filtered using low protein binding syringe filters (25 mm, 0.2 μ m, polyvinylidene fluoride (PVDF) membrane, Pall Corporation, MI, USA). A reference for each formulation containing the same buffer and the same excipients was also prepared and filtered using cellulose acetate disk filters, 0.2 μ m pore size (VWR international, USA).

For IsoSS the same formulations were prepared and filtered, filled into type I glass vials, stoppered, capped, and crimped under sterile conditions and then stored in the dark at ICH temperatures (4, 25, 40°C) in calibrated ovens. Each formulation was subjected to analysis at the beginning of the storage time (zero time) and in further time intervals.

The effect of three buffer systems (phosphate, acetate, and citrate) was studied. Furthermore, in order to have a more challenging formulation set, factorial experimental designs were used. The effect of acetate and citrate buffers, different buffer concentrations, different pH values, and the effect of different concentrations of Tween 80 and/or HP- β -CD was studied. The IsoSS at 40°C were terminated after 3 months, at 25°C were terminated after 10 months, and at 4°C after 20-24 months according to the stating point of the analysis.

The rationale behind using such an experimental design instead of using linear series with different pH values or excipient concentrations was to challenge the predictive power of T_m as

a marker for protein stability. Table 3.1 shows the 1st design of experiment (DOEa) which is a 2³ full factorial design. The effect of the studied factors was tested in the absence of any buffer system. Table 3.2 and 3.3 show the 2nd and the 3rd design of experiment (DOEb and DOEc) which are fractional factorial designs based on the partition of a 2⁴ full factorial design using the (-1) generator from the third order interaction (-ABCD) ²².

The effect of different factors on each DOE was calculated in the form of coefficients. Furthermore, to make these coefficients comparable when responses have different units, the coefficients were normalized, that is the coefficients were divided by the standard deviation of their respective response. All coefficient calculations as well as normalization were performed using MODDE8 software (Umetrics AB, Umea, Sweden).

I.1.3. Thermal stability using microcalorimetry (μ DSC):

All formulations were analyzed using a VP-DSC (Microcal Inc., MA). The sample as well as the corresponding reference was degassed for 5 min prior to injection in the μ DSC cells using a Thermo vac pump (Microcal. Inc., MA). Both sample and reference were loaded into cells using a gas tight Hamilton 2.5 ml glass syringe.

Each formulation with its corresponding reference was heated from 20°C to 80-90°C (depending on the formulation T_m) using a 90K/hr heating rate. Thermal stability was determined three times for each formulation.

Table 3. 1: GCSF formulation set of the 1st design of experiment (DOEa) (All T_m s values are the mean of triplicate μ DSC scans ($T_m \pm SD < 0.5^\circ C$))

Formulation	pH	Tween 80 (%)	HP- β -CD (%)	T_m	$R_{Tm}^{1)}$	Reversibility (%)	$R_{opTm}^{2)}$
GCSFDa1	4.2	0.0005	1	71,7	2	52,1	2
GCSFDa2	4.2	0.0005	10	69,4	5	32,8	6
GCSFDa3	4.2	0.05	1	70,5	4	21,1	4
GCSFDa4	4.2	0.05	10	66,9	8	62,7	8
GCSFDa5	4.8	0.0005	1	72,3	1	0	1
GCSFDa6	4.8	0.0005	10	69,4	5	55,5	5
GCSFDa7	4.8	0.05	1	71,8*	2	49,3	3
GCSFDa8	4.8	0.05	10	69*	7	32	7

1) Ranking based on T_m before optimization using reversibility.

2) Ranking based on T_m after optimization.

* $T_m \pm SD < 1^\circ C$

Table 3. 2: GCSF formulation set of the 2nd design of experiment (DOEb) (All T_ms values are the mean of triplicate μ DSC scans (T_m \pm SD < 0.5°C)

Formulation	Buffer	pH	Buffer Concentration	Tween 80 (%)	T _m	R _{Tm}	Reversibility (%)
GCSFDb1	No	4.5	No	0.05	69,5	4	N/A
GCSFDb2	No	4.5	No	0.005	69,9*	2	N/A
GCSFDb3	No	5	No	0.005	71,5*	1	N/A
GCSFDb4	No	5	No	0.05	69,6	3	N/A
GCSFDb5	Citrate	4.5	20	0.005	59	5	N/A
GCSFDb6	Citrate	4.5	50	0.05	57,3	7	N/A
GCSFDb7	Citrate	5	20	0.05	56,3	8	N/A
GCSFDb8	Citrate	5	50	0.005	57,5	6	N/A

* T_m \pm SD <1°C

Table 3. 3: GCSF formulation set of the 3rd design of experiment (DOEc) (All T_ms values are the mean of triplicate μ DSC scans (T_m \pm SD < 0.5°C)

Formulation	Buffer	pH	Buffer Concentration	HP- β -CD (%)	T _m	R _{Tm}	Rev. (%)	R _{opTm}
GCSFDc1	No	4	No	5	70,3	4	61,5	4
GCSFDc2	No	4	No	1	72,5	1	47,6	2
GCSFDc3	No	4.5	No	1	72,6	1	53,2	1
GCSFDc4	No	4.5	No	5	71,2*	3	45,2	3
GCSFDc5	Acetate	4	20	1	66,2	5	0	2
GCSFDc6	Acetate	4	100	5	61,7	7	0	7
GCSFDc7	Acetate	4.5	20	5	62,9	6	0	6
GCSFDc8	Acetate	4.5	100	1	60,5	8	0	8

* T_m \pm SD <1°C

The unfolding reversibility was investigated by temperature cycling using the upscan - upscan method which employed two consecutive upscans. After the first upscan the device is programmed to cool the sample again and repeat the heating cycle immediately. In case of reversible formulations, the reversibility was checked for all three heating replicates. The μ DSC cell was pressurized to prevent boiling of the sample during heating.

A base line run was performed before the sample run by loading both sample and reference cells with the corresponding reference. This base line was subtracted later from the protein thermal data and the excess heat capacity was normalized for protein concentration. For each formulation T_m and the degree of reversibility were determined. The degree of unfolding reversibility was the percentage of the enthalpy of the second upscan (ΔH_2) in relation to the

first one (ΔH_1). Both ΔH_1 and ΔH_2 were the apparent calorimetric enthalpies calculated by the area under the unfolding endotherm. For data analysis ORIGIN DSC data analysis software was used.

I.1.4. Isothermal stability study (IsoSS):

All formulations were stored under controlled conditions and analyzed immediately after sample withdrawal with the following methods.

I.1.4.1. Reversed-phase high performance liquid chromatography (RP-HPLC):

RP-HPLC was performed to study the chemical degradation of GCSF. The separation was achieved using a Thermo separation system with a Phenomenex (Jupiter 5 μ C18 300A 250 x 4.6 mm 5 micron) column. The flow rate of 1 ml/min was set and a detection wavelength of 215 nm was used. The mobile phase consisted of water with 60% acetonitril and 0.1% trifluoroacetic acid. A protein concentration of 0.2 mg/ml was used in the analysis. The injection volume was 100 μ l. All samples were filtered before injection using low protein binding syringe filters (4 mm, 0.2 μ m, polyvinylidene Fluoride (PVDF) membrane, Whatman International Ltd. Maidstone England). After storage the protein content was not completely recovered in all formulations, most probably, due to the formation of insoluble aggregates which are filtered out before injected in the HPLC system. Therefore, the % of intact GCSF remaining after stress was calculated from the intact GCSF in each formulation at zero time point. Due to the large number of formulations, the storage of all formulations could not be started at exactly the same time. Therefore, at the end of the storage period (especially at 4°C) some samples were slightly older than others. To avoid the confusion that may be caused due to slightly different storage periods, at each time point the %remaining of intact GCSF was calculated and a 1st order degradation kinetic curve was used in order to determine the degradation rate constant at each storage temperature for each formulation. These constants were used as a parameter for ranking the formulations.

I.1.4.2. Size-Exclusion-HPLC (SE-HPLC):

Loss of GCSF monomer, due to aggregation or fragmentation, was monitored using SE-HPLC. The separation was achieved using a Thermo separation system and a TSKgel G3000SWXL 7.8 mm ID x 30.0 cm L column (Tosoh Bioscience). A flow rate of 0.5 ml/min

was used, and the protein was detected at a wavelength of 215 nm. The mobile phase consisted of 31.7 g/L sodium hydrogen phosphate dibasic, and 1 g/L sodium dodecyl sulphate. The pH value was adjusted to 6.8 using 2N HCL. The injection volume was 20 µl. A protein concentration of 0.2 mg/ml was used in the analysis. All samples were filtered before injection using low protein binding filters (0.2 µm pore size). The % monomer remaining was calculated from the starting monomer content of each formulation at zero time point in order to overcome the incomplete protein recovery as in case of RP-HPLC. As mentioned above, in order to avoid confusion caused by slightly different storage periods, the monomer decline rate constant was calculated from the 1st order kinetic curves and used for ranking.

I.1.4.3. Turbidity measurements:

Turbidity was used as a simply but reliable value to determine the formation of insoluble aggregates of GCSF. At each time point the turbidity of each formulation was measured using a Dr. Lang Nephelometer (Dr. Bruno Lange GmbH, Berlin). 2 ml of each formulation were filled in a glass cuvette and the turbidity was measured in Formazin Nephelometric units (FNU). The FNU found for each formulation at the end of the storage period was used for ranking.

I.1.4.4. Light obscuration:

The insoluble aggregates were determined in each formulation by light obscuration measurements (PAMAS SVSS-CTM (Rutesheim, Germany)). Using a rinsing volume of 0.5 ml and a measuring volume of 0.3 ml and the number of measurements was set to three. Before each measurement the device was rinsed with particle free water until there were less than 100 particles larger than 1 µm counted and no particles over 10 µm present. In order to simplify the ranking process only the turbidity results were used for ranking. Light obscuration measurements were carried out only to double check with turbidity measurements for the level of insoluble aggregates in each formulation.

I.1.4.5. Sodium dodecyl sulphate polyacrylamide gel electrophoresis (SDS-PAGE)

SDS-PAGE was conducted under non-reducing conditions using XCell II mini cell system (Novex, Sand Diego, CA). The protein solutions were diluted in a pH 6.8 tris-buffer, containing 4% SDS and 20% glycerine. Samples were denatured at 95°C for 20 min and 10 µl

were loaded into the gel wells (NuPage 10 % Bis-Tris Gel, Novex High performance pre-cast gels, Fa. Invitrogen, the Netherlands). Electrophoresis was performed in a constant current mode of 40mA in a MES SDS Running Buffer (NuPage MES SDS Running Buffer (20x), Fa. Invitrogen, the Netherlands). Gel staining and drying was accomplished with a silver staining kit (SilverXpress) and a drying system (DryEase), both provided by Invitrogen, Groningen, Netherlands. From SDS-PAGE results, ranking was not possible. However, it was used as a confirmative method.

I.1.5. Correlation:

To correlate the results of μ DSC and the results of the IsoSS, formulations in each set as well as the whole 24 formulations were ranked according to T_m and separately according to their isothermal stability and then rank correlation was carried out. The ranking process was made in a way that for example in a 24 formulation set, the lower the ranking number the more stable is the formulation, i.e. the best formulation is ranked 1 and the worst is ranked 24.

The ranking methods for μ DSC as well as for the IsoSS results are described below.

I.1.5.1. Ranking of formulations according to μ DSC:

In chapter 2 up to 5 different rankings were possible as T_m and degree of unfolding reversibility showed significant differences over the whole formulations set. In this chapter the degree of reversibility was only observed in 12 out of 24 formulations. Moreover, in many reversible formulations a large deviation (in some formulations over 20%) was noticed. Therefore T_m based ranking was first made (R_{T_m}) which was further optimized by considering the degree of unfolding reversibility (R_{opT_m}). Only when T_m showed no difference the formulation showing higher reversibility was ranked better (lower rank number). In tables 3.1-3.3 the rankings are shown for DOEa, DOEb, and DOEc, respectively. In table 3.2 none of the formulations in DOEb showed reversibility, therefore optimization of R_{T_m} was not applicable.

I.1.5.2. Ranking of formulations according to IsoSS:

A different ranking had to be made based on IsoSS. An example of the ranking procedures based on IsoSS is illustrated in table 3.4 for DOEa formulations.

Table 3. 4: IsoSS ranking of GCSF formulations in DOEa after 20 months storage at 4°C

Formulations	$K_p4^{1)}$	R_{14}	$Tur.4^{2)}$	R_{24}	Avr. $(R_{14}+R_{24})/2$	R_p4	$K_c4^{3)}$	R_{c4}	Avr. $(R_p4+R_c4)/2$	R_s4
GCSFDa1	0,0027	1	0,8	1	1	1	0,0001	2	1,5	1
GCSFDa2*	-0,0447	6	0,62	1	3,5	5	0,0023	1	3	2
GCSFDa3**	-0,0085	4	0,96	1	2,5	4	-0,033	8	6	7
GCSFDa4	-0,0498	7	1,1	6	6,5	7	-0,0031	6	6,5	8
GCSFDa5*	0,002	2	0,98	1	1,5	2	-0,0003	4	3	2
GCSFDa6	-0,0574	8	2,6	8	8	8	0,0001	2	5	4
GCSFDa7	-0,0023	3	0,8	1	2	3	-0,0252	7	5	4
GCSFDa8*	-0,0381	5	1,47	6	5,5	6	-0,0018	5	5,5	6

*formulations were stored for 24 months.

** Formulation was not analyzed after 9 months

- 1) Monomer denaturation constant at 4°C according to SE-HPLC results.
- 2) Turbidity in FNU measured at the end of the IsoSS at 4°C.
- 3) Chemical degradation constant at 4°C according to RP-HPLC results.

I.1.5.2.1. Ranking based on physical stability (R_p):

This ranking was based on both SE-HPLC and turbidity data. The ranking process includes the following steps:

- 2- 1st ranking (R_1): The formulations were ranked according to the monomer loss rate constant.
- 3- 2nd ranking (R_2): The formulations were ranked according to their turbidity at the end of the storage period.
- 4- Overall physical stability ranking (R_p): For each formulation the average of R_1 and R_2 was calculated ($R_p = (R_1 + R_2)/2$).

These 3 rankings were done for each storage temperature to get R_{p4} , R_{p25} , and R_{p40} for the ranking at 4, 25 and 40°C, respectively.

I.1.5.2.2. Ranking based on chemical stability (R_c):

Ranking was based on RP-HPLC data and was done for all formulations at each storage temperature (R_{c4} , R_{c25} , and R_{c40}). Degradation rate constants, calculated from the 1st order degradation curve of each formulation, were used as the ranking parameter.

I.1.5.2.3. Ranking based on overall stability (R_s):

For each formulation the average of R_p and R_c was calculated ($R_s = (R_p + R_c)/2$), equally presenting both chemical and physical stabilities. This was calculated at each storage temperature (R_{s4} , R_{s25} , and R_{s40}).

The previously mentioned ranking steps were repeated for each DOE and again for the whole 24 formulations (handling the 3 DOEs as one formulation set).

I.1.6. Prediction quality:

In this study a new method for a formulator to make selection decisions based on predictive parameters was developed. After measuring T_m of 24 formulations, a formulator could make a decision and select the best 12 formulations and exclude the worst 12 based on T_m . To evaluate the reliability of such a decision, formulations that were selected either as the best or as the worst according to T_m and would also have been similarly selected in IsoSS at different storage temperatures (4, 25 and 40°C) were counted. This comparison was made regardless of the rank order of the formulations within the group of 12.

Figure 3.1 A represents an example of such a process where the correlation matrix between R_{T_m} and physical stability at 4°C (R_{p4}) for the all 24 formulations was divided into 4 areas. The white square represents the group of formulations that were predicted as the best and were then confirmed by reality (IsoSS) to be the best. The black frame (figure 3.1), in contrast, represents the group of formulations predicted to be the worst and confirmed by IsoSS. Both light and dark gray areas represent the number of formulations falsely selected by T_m as good and bad, respectively.

The number of points in each box is presented as a part of a histogram as shown later in the results and discussion section (page 70 figure 3.6 A) where each bar consists of 4 coloured areas representing those in figure 3.1 A. The white and black areas represent the number of formulations correctly selected and both gray areas in the histogram represent the number of formulations falsely selected. The gray area, consisting of both light and dark; in such histogram represents the quality of the previous decision, where the formulator selected 50% of the whole formulation set based on the corresponding ranking. A large gray area in the curve means a lower prediction quality and accordingly the decision is less reliable and vice versa. Furthermore, the reliability of a closer decision where the formulator would choose only 5 formulations (approximately 20%) from the whole 24 and exclude 19 formulations was also evaluated. Such a process is presented in figure 3.1 B.

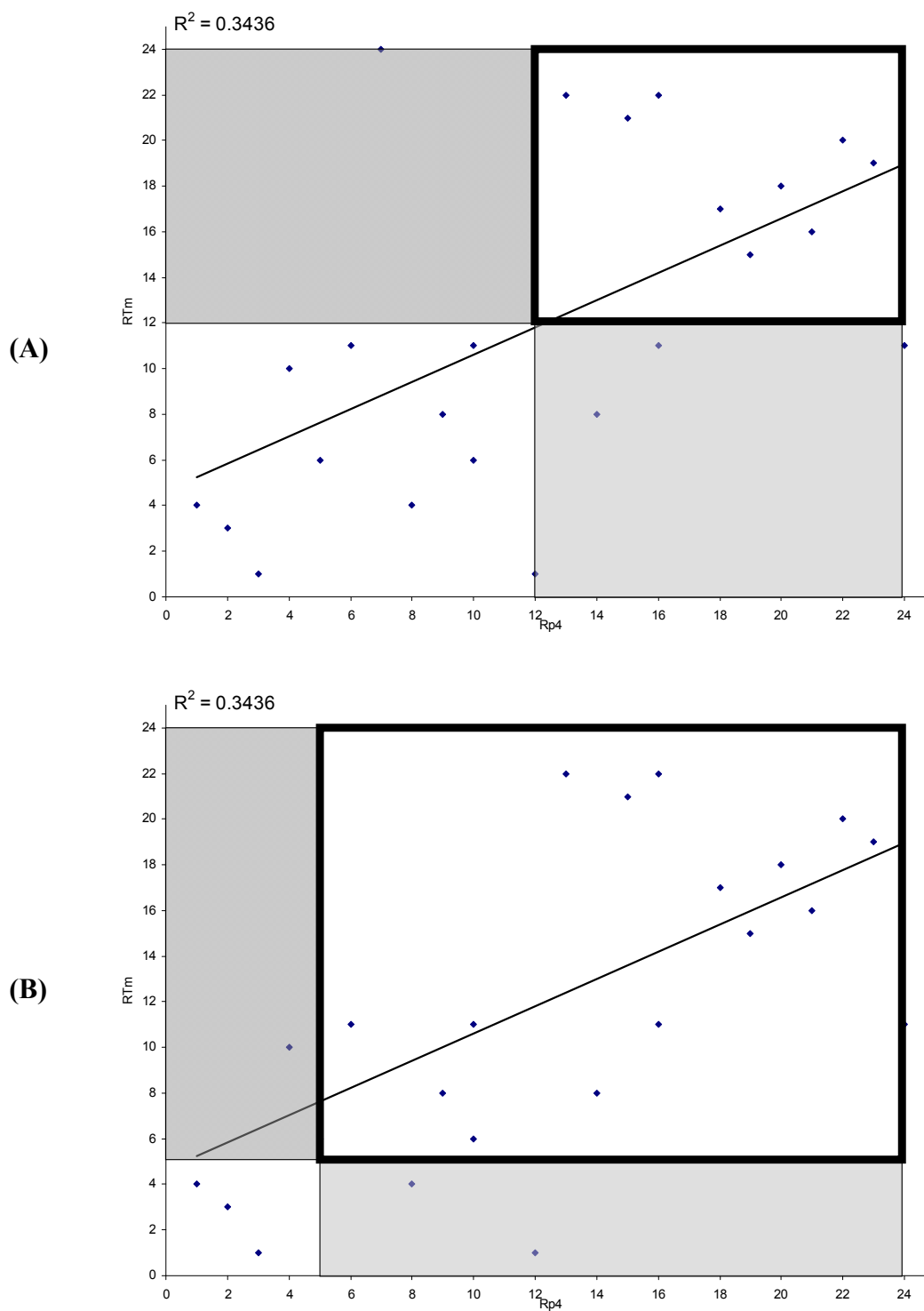


Figure 3. 1: Calculating the 50% (A) and 20% (B) prediction quality of T_m based ranking (R_{Tm}) for the physical stability at 4°C based ranking (R_{p4}) of 24 GCSF different formulations.

I.2. Results and discussion:

I.2.1. μ DSC measurements:

The μ DSC thermographs for three tested buffers salts (phosphate, acetate, and citrate) at pH 4 are shown in figure 3.2. In this short preliminary screening experiment the effect of three buffer salts was examined and judged from T_m values, acetate buffer is considered the favoured buffer whereas the citrate buffer exerted the lowest T_m .

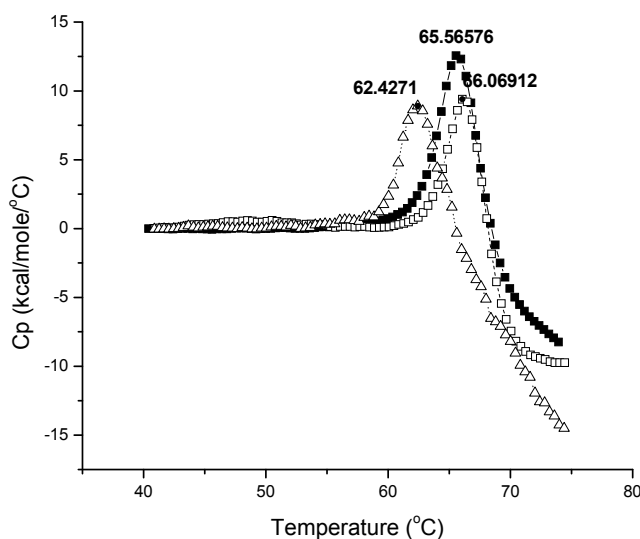


Figure 3. 2: T_m of three GCSF formulations (Δ) in citrate (\blacksquare) in phosphate and (\square) in acetate. All 20 mM buffer concentration and pH adjusted to 4

Tables 3.1 – 3.3 (pages 54 and 55) show the T_m and degree of unfolding reversibility as found for the full and two fractional factorial designs DOEa, DOEb, and DOEc, respectively. Tables 3.1 – 3.3 also display the formulation ranking as predicted from T_m (R_{Tm}). In formulations showing unfolding reversibility, optimization of R_{Tm} was considered only in case of formulations having equal T_m s.

The normalized coefficients of each DOE representing the effect of each factor on T_m and degree of unfolding reversibility are presented as bar charts in figure 3.3.

The most significant effect was the effect of using a buffer salt for GCSF liquid formulation which has a pronounced negative effect on both T_m and degree of reversibility. Increasing buffer concentration, however, showed a similar but less dramatic effect on T_m of GCSF liquid formulations. That correlates well with the teachings of patents in which GCSF was favourably formulated in the absence of buffer. However, in practice, buffer is needed and

therefore, in GCSF formulations buffers should be kept at the lowest possible concentration^{17,18,23}.

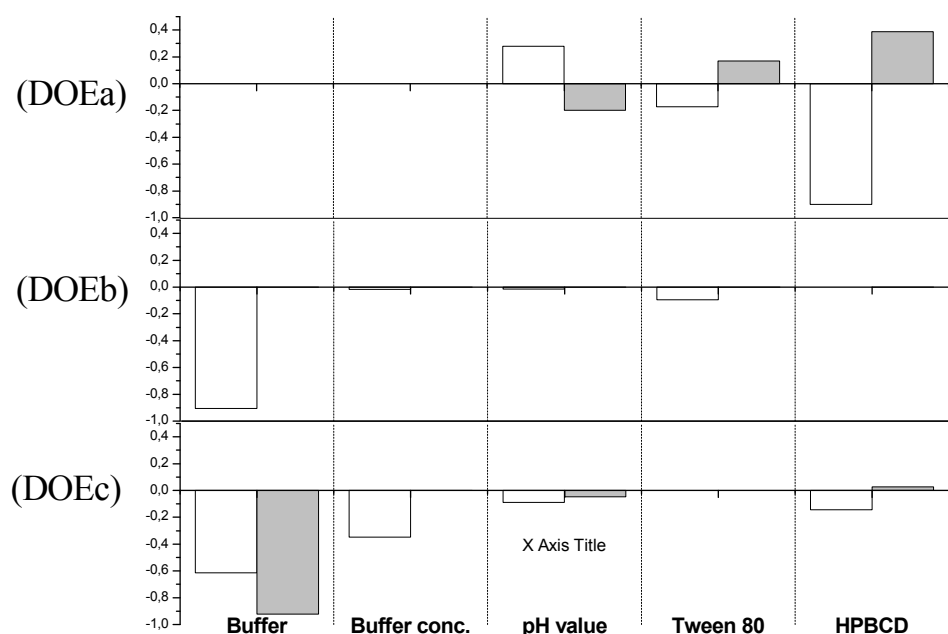


Figure 3. 3: Normalized coefficients for the effect of each factor on T_m (white bars) and unfolding reversibility (gray bars) of GCSF formulations of three studied DOEs.

Increasing the concentration of HP- β -CD in DOEa showed a strong negative effect on T_m and a weaker positive effect on the degree of reversibility (figure 3.3). This allows at least a qualitative conclusion to be drawn. Cyclodextrins in rather high concentrations reduce the T_m of a protein, but allow in general high reversibility. This could be explained by the potential interaction of the cyclodextrin cavity with hydrophobic amino acid chains during their exposure in the course of unfolding. Reduction of the intramolecular binding energies by competitive binding of cyclodextrins should lead to lower T_m s. On the other hand, cyclodextrin complexed hydrophobic amino acids could be protected from immediate interaction with other intra- or intermolecular hydrophobic species and reversibility is higher with cyclodextrins in place. Cyclodextrin may so interact with unfolded protein and acts as artificial chaperon^{24,25}.

The effect of pH value on the stability of GCSF is reported by many authors^{8,26} where the acidic pH is favoured. Therefore, increasing the pH value a reduction in T_m was expected. A significant effect of increasing the pH value was shown in none of the studied DOE (figure 3.3). In chapter 2 the effect of increasing the pH value was extensively studied showing a reduction in T_m by increasing the pH value in a pH rang from 4 to 5 (the pH range in all

DOE) and no reversibility was observed. A possible explanation to that is the interaction of different factors in one formulation set. Furthermore, DOEb and DOEc are composed of mixed buffered and un-buffered formulations. That represents qualitative difference which might have unexpected interaction with the other quantitative factors.

The stability of GCSF is already reported to be affected by adding tween80^{27,28}. Nevertheless, a significant effect neither on T_m nor on the degree of unfolding reversibility was obtained in each DOE. This behaviour is confirmed in another study where the effect of a surfactant on T_m of recombinant growth hormone studied by μ DSC didn't correlate with its physical stability²⁹. Surfactants mainly protect protein by preventing adsorption induced aggregation at interfaces³⁰. Such a protective mechanism is recognizable during isothermal storage of protein where aggregation might happen at the inner surface of a glass container as well as air-liquid interface. During a μ DSC experiment such mechanism might be not applicable. First, the affinity of a protein solution to adsorb on the inner surface of the sample cell is different than its affinity to adsorb on the surface of a glass vial. Second, the air space in a μ DSC sample cell is neglected. In addition the time of a μ DSC experiment might be very short, in comparison to isothermal stability study, for adsorption to take place. Therefore, in a μ DSC experiment a change in T_m might not be recognized.

I.2.2. Isothermal stability study (IsoSS):

24 GCSF liquid formulations were analyzed during isothermal storage at 4, 25 and 40°C over up to 24 months. At each time point the previously mentioned analytical methods were applied (section 1.4). In order to obtain comparable numbers for both SE-HPLC and RP-HPLC, the monomer loss rates as well as the chemical degradation rates were calculated according to 1st order kinetics for each formulation. Figure 3.4 represents an example of the degradation of one GCSF formulation in three different temperatures. This was obtained by SE-HPLC and RP-HPLC represented in Figure 3.4 A and B, respectively. At each temperature the degradation as well as the monomer loss rates was obtained from the slope of the curve.

Insoluble aggregates were determined in all formulations using both turbidity and light obscuration measurements. For ranking only the turbidity FNU measurements were considered as they are easier to rank compared to light obscuration measurements. In Appendix 3.I the light obscuration measurements for the 24 GCSF formulations at the end point were recorded and presented in table 3.I.1 – 3.I.3 for DOEa, DOEb and DOEc,

respectively. Turbidity measurements are recorded in the ranking tables in Appendix 3.I. (table 3.I.4 – 3.I.14)

SDS-PAGE was made for all formulations at the beginning of the storage time and after 20 - 24 months storage at 4°C. In Appendix 3.II all SDS gels are presented in figure 3.II.1.

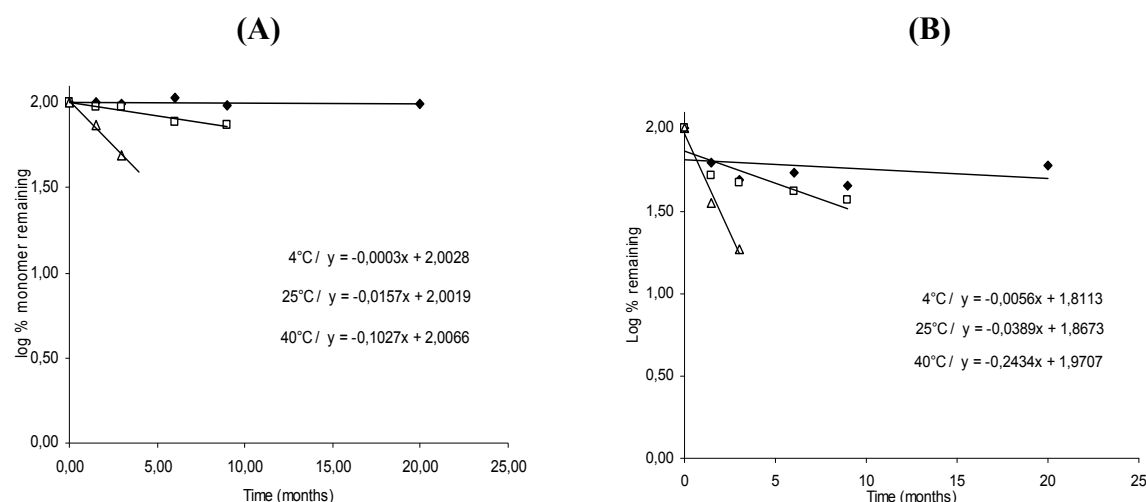


Figure 3. 4: Degradation of GCSFDb1 during isothermal stability study at 4°C (—■—), 25°C (—□—) and 40°C (—△—). (A) Monomer loss as measured by SE-HPLC. (B) Chemical degradation as measured by RP-HPLC.

1.2.3. μ DSC as a predictive tool for IsoSS:

Table 3.4 (Page 59) shows the IsoSS data after long term storage at 4°C as well as ranking of both physical and chemical stability for GCSF formulations of DOEa. The same rankings were made for 25°C and 40°C. The data collection and ranking were performed also for all other formulations in DOEb and DOEc and finally the ranking was done for the whole 24 formulations in one group (Appendix 3.I, tables 3.I.4 – 3.I.14).

The predictive power of μ DSC determined T_m s was judged in this chapter based on two main criteria. Primarily, the Pearson product moment correlation coefficient obtained from correlating predicted rankings against the IsoSS based ranking. Secondly, the prediction quality, explained above (section 1.6), to evaluate the selection decision based on μ DSC parameter.

I.2.3.1. Correlation coefficients:

In chapter 2 it was shown that T_m and the stability parameter are not scalable with each other and therefore the correlation between the rank orders was preferred. The Pearson product moment correlation coefficient was used as a judging parameter for the correlation. The correlation coefficients were studied in each DOE separately and finally the correlation was studied in the whole 24 formulations as one group.

In Appendix 3.II figures 3.II.2 – 13 (pages 133 – 143) all resulting correlation curves are presented. A list of correlation coefficients resulting from each correlation is shown in table 3.5. The data generated from such a high number of curves made it difficult to compare the correlation in each group of formulations. Accordingly, to allow such comparisons, an overview for all resulting correlation coefficients is presented in figure 3.5. Figure 3.5 A1 represents the correlation between a T_m based ranking (R_{T_m}) and all IsoSS based rankings (R_p for ranking based on physical stability, R_c for ranking based on chemical stability and R_s for the ranking based on the overall stability) for DOEa. Figure 3.5 A2 shows the correlation of the same group but versus the optimized based ranking (R_{opT_m}) where the degree of unfolding reversibility was considered in case of equal T_m values. Figure 3.5 B1 represents the correlation in DOEb with R_{T_m} (None of the formulations in this group showed reversibility and accordingly an optimized ranking (R_{opT_m}) was not possible). Figures 3.5 C1 and C2 represent the correlation of different IsoSS based rankings in DOEc with R_{T_m} and R_{opT_m} , respectively. Finally figures 3.5 D1 and D2 show the correlation coefficients when correlating the IsoSS based rankings of the whole 24 formulations (formulations of the three experimental designs DOEa, b and c) with R_{T_m} and R_{opT_m} , respectively.

All histograms in figure 3.5 were structured similarly where the correlation coefficients (R^2) are plotted on the y-axis, the different types of IsoSS ranking (R_p , R_c , and R_s) are plotted on the x-axis and the three different storage temperatures are plotted on the Z-axis.

This study was conducted to evaluate the predictive power of μ DSC for the long time storage stability of protein formulations. A protein formulator would expect from such work to answer some important questions: Can μ DSC analysis predict the overall long term stability of a protein drug in a certain formulation at its typical storage temperature of 4-8°C and 25°C? Would physical stability alone be better predicted? Is prediction of chemical stability possible via μ DSC at all? Furthermore, it is interesting to see whether prediction of storage stability via μ DSC correlates to storage data at elevated temperature 40°C. It should be emphasized, that storage stability at 40°C is usually not performed to allow later long term storage (e.g. over 3-6 months) at this temperature but to assess formulations for their tolerance towards higher

temperature and even more important to select the best formulation(s) from a group of candidates by studying them under stress conditions and to quantitative extrapolate to 4-8 °C. In that respect, 40°C storage can be considered also as a “predictive” method like μ DSC T_m analysis. The correlation coefficients shown in figure 3.5 can provide useful information to answer such questions.

Table 3. 5: Correlation coefficients resulting from correlating physical (R_p), chemical (R_c) and overall (R_s) stability based ranking at different temperatures with either T_m based ranking (R_{Tm}) or Optimized T_m based ranking (R_{opTm})

DOE	Temp	R_{Tm}			R_{opTm}		
		R_p	R_c	R_s	R_p	R_c	R_s
DOEa	4°C	0.7094	0.0053	0.5013	0.6944	0.0032	0.4401
	25°C	0.339	0.0022	0.0197	0.3023	0.0023	0.0204
	40°C	-0.0384	0.035	0.0088	-0.0292	0.0686	0.0204
DOEb	4°C	0.609	0.3543	0.9182			
	25°C	0.907	0.4768	0.7696			
	40°C	0.6553	0.5805	0.8278			
DOEc	4°C	0.8154	0.4328	0.8752	0.7719	0.3049	0.679
	25°C	0.5919	0.2174	0.7651	0.6553	0.1741	0.7372
	40°C	0.5384	0.4935	0.4922	0.8116	0.57	0.6753
All	4°C	0.3436	0.1134	0.4042	0.3308	0.1334	0.4178
	25°C	0.5076	0.0979	0.3626	0.5146	0.1197	0.392
	40°C	0.1544	0.2633	0.2164	0.177	0.3168	0.2585

None of the DOE data sets or the whole set of formulations showed a correlation coefficient of 1 to allow exact ranking prediction of IsoSS from μ DSC data. It is obvious from figure 3.5 that predictive power (especially for the IsoSS at 4°C) is lower in a larger group than in a smaller one. That was very clear when comparing the correlation coefficients of each design of experiment alone and for the whole 24 formulations as one set. Correlation trends are different for each experimental design as well, which proves an experimental design dependency of the prediction. R_{Tm} optimization using reversibility (R_{opTm}) didn't have a great effect on the predictive power of the method.

In all groups the physical stability ranking (R_p) is better predicted by μ DSC than the chemical stability ranking (R_c). Such a trend was expected as T_m is a measure of the physical strength of the protein integrity until unfolding occurs. But the overall stability ranking (R_s), based on the average ranking of physical and chemical stabilities, was predicted as good as the physical stability (R_p) in most cases.

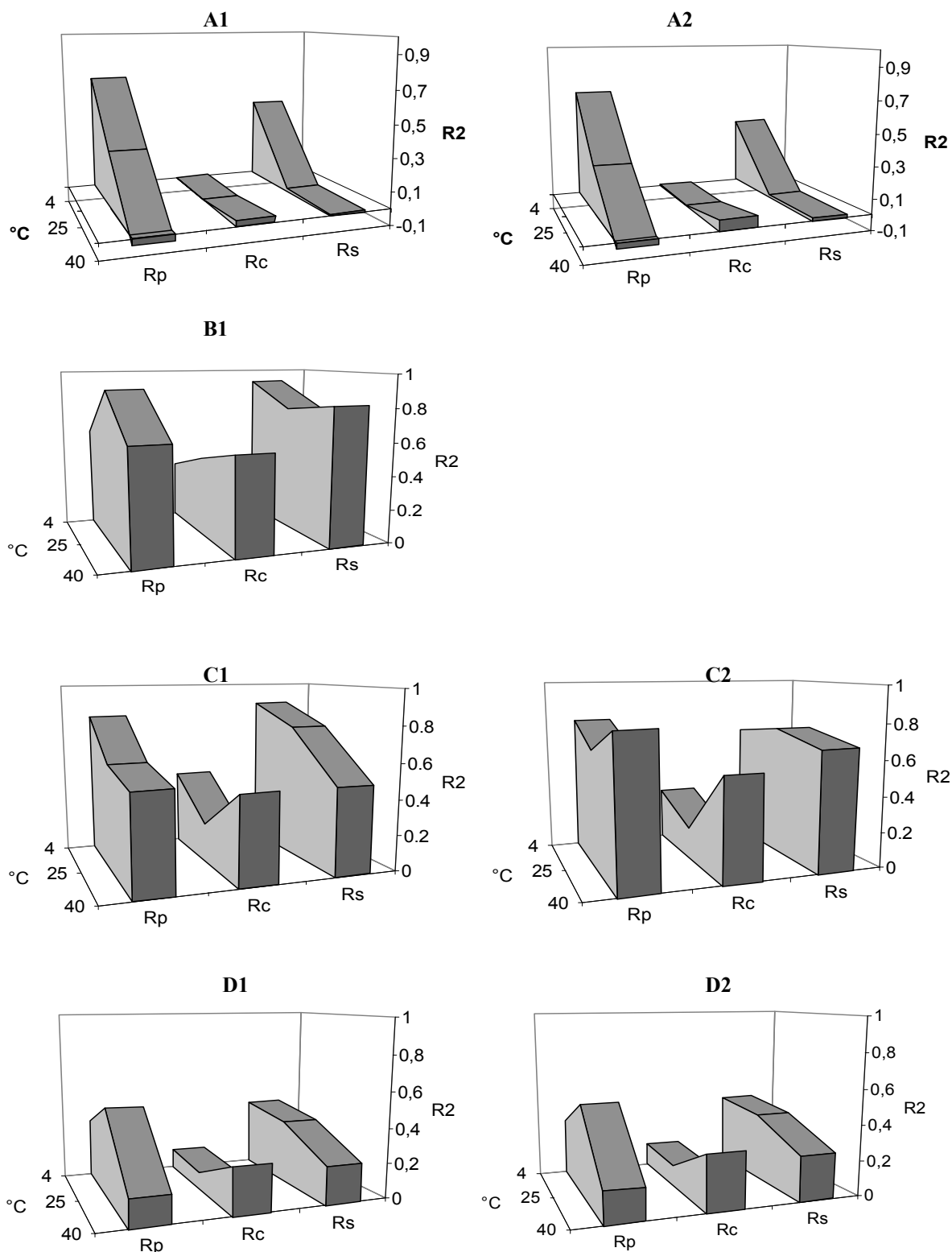


Figure 3. 5: An overview of the correlation coefficients (y-axis) resulting from correlating the ranking based on physical stability (R_p), ranking based on Chemical stability (R_c), and ranking based on the average of both chemical and physical stabilities (R_s) (x-axis) with either T_m (graphs A1 – D1) or opT_m (graphs A2 – D2) based rankings in the studied experimental designs. Graphs with the letter (A) show correlation for DOEa, (B) for DOEb, (C) for DOEc and (D) for the whole 24 formulations of the three designs together. The correlation was made at three different temperatures (z-axis)

For pure physical or chemical stabilities each design of experiment showed different trends with regards to the storage temperature. But surprisingly R_{T_m} was able to predict the overall stability ranking (R_s) best at 4°C in all experimental designs either separately or when combined in one set. Furthermore, R_{T_m} showed the lowest dependency on experimental design in predicting the overall stability.

I.2.3.2. Prediction quality:

Although it has to be accepted, that studying T_m alone does not allow predicting the absolute rank order of the stability of a wide range of different formulations, we had closer look on the reliability of T_m to exclude bad formulations and to pick the good ones. This was performed, as explained above, by monitoring the prediction quality for rankings based on μ DSC measurements. Figures 3.6 A and B represent the 50% and 20% prediction quality, respectively for rankings based on either T_m or opT_m of different kind of stability at different temperatures.

Comparing the prediction quality in figure 3.6, neither T_m nor opT_m were, of course, able to achieve complete selection certainty. Both rankings were more reliable in predicting physical stability than chemical stability. R_{T_m} showed higher 50% prediction quality in comparison with R_{opT_m} . However, both R_{T_m} and R_{opT_m} showed the highest 20% prediction quality towards predicting the overall stability at 4°C (figure 3.6 B) where 4 from 5 selected formulations based on T_m were selected in the best 5 by overall IsoSS ranking at 4°C. That supports the previously strong predictive power of T_m to IsoSS at 4°C compared with other temperatures.

Despite the importance of physical stability in determining the long term stability of protein pharmaceuticals, chemical stability has to be insured for a protein formulation as well. Therefore, an overall (physically and chemically) stable formulation is the main target in protein formulation development. Many authors have evaluated the physical degradation of GCSF^{9,31} which is affected greatly by the solution conditions like pH and buffer salts. On the other hand, the GCSF molecule contains 4 methionine residues³² which increase the sensitivity of the GCSF molecule for oxidation. The use of a mixed factorial experimental design in this study provided a great challenge for μ DSC predictive power due to the small changes in factor levels which makes formulation ranking, to some extent, difficult. Furthermore, the two main excipients included in the study affect the overall stability of GCSF through different mechanisms. HP- β -CD affects mainly the physical properties of the protein molecule and, according to our knowledge; no chemical effect of HP- β -CD on protein has been reported.

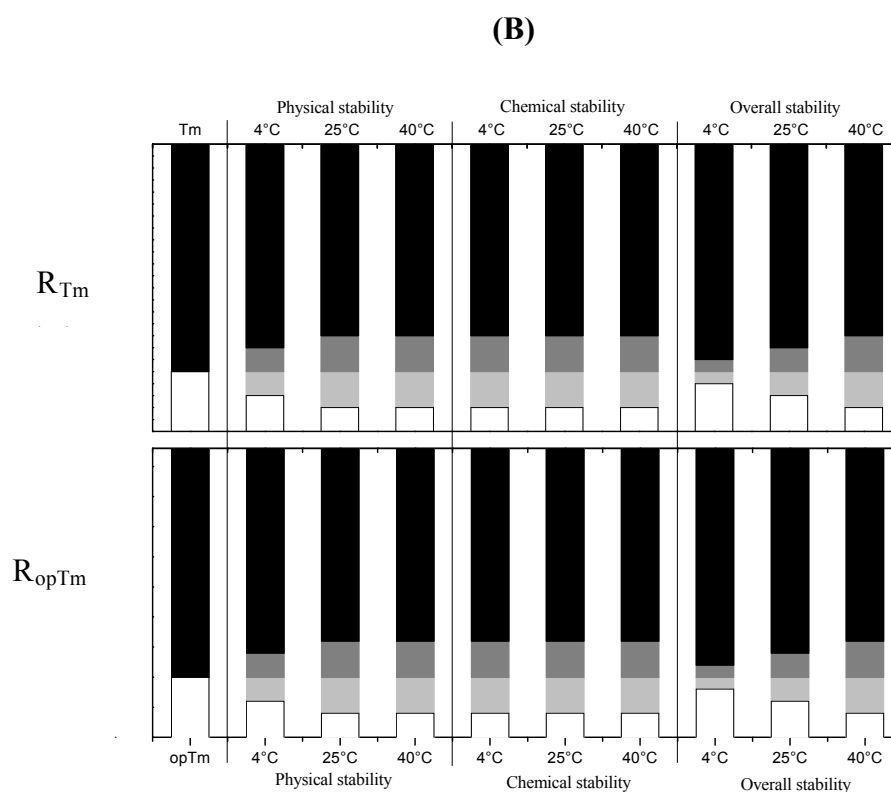
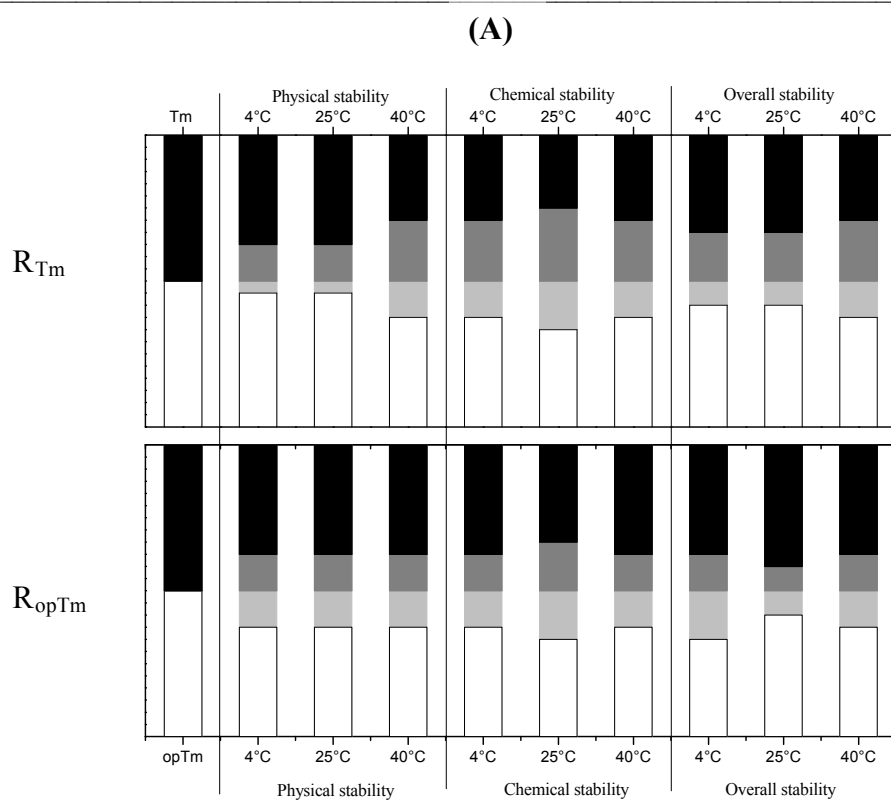


Figure 3. 6: Reliability of T_m and opT_m to pick the good 12 formulations and exclude the bad 12 (50% prediction quality (A)) and to pick up 5 and exclude 19 (20% prediction quality (B)) in a 24 GCSF formulation set. White and black bars represent the number of formulations predicted correctly and the gray area represents the number of formulation falsely predicted.

On the other hand, Tween 80 as a non-ionic surfactant affects protein physical stability^{29,30} and can contain peroxide residues which would cause oxidation of methionine residues in the GCSF molecule affecting its chemical stability as well²⁷. Therefore, different contributions of both physical and chemical stability in the overall stability ranking are expected which makes prediction of the overall stability ranking of GCSF using μ DSC a great challenge. This study showed that T_m was able to predict the overall stability ranking similarly or even better than physical stability especially at 4°C. Such conclusion was based not only on the higher correlation coefficients obtained from correlating R_{T_m} , but also on the higher 20% prediction quality obtained when selection was made based on R_{T_m} . That proves that T_m is not only able to predict physical stability as previously assumed, but also chemical stability is predicted to a certain extent. Doing so T_m showed even better predictive power for the overall stability ranking.

I.2.4. μ DSC in comparison with classical accelerated IsoSS:

In most protein formulation laboratories performing IsoSS at elevated temperatures (40 – 60°C) is a routine step upon which the decision for the best formulation(s) is mostly based. The predictive power of such strategies in comparison to other predictive strategies, for example μ DSC, has not yet been evaluated.

Which method is more predictive for the long term stability of protein formulations, μ DSC or routinely used accelerated IsoSS at elevated temperatures?

This section intends to answer this question by comparing the predictive powers of R_{T_m} and R_{opT_m} with that of ranking based on either IsoSS at 25°C or 40°C which are considered in this section as predictive methods. The ranking based on each was compared with that based on IsoSS at 4°C. The predictive powers of these two approaches (conformational stability and classical accelerated stability testing) were compared based primarily on the Pearson product moment correlation coefficients and secondarily on the prediction quality.

I.2.4.1. Correlation coefficients:

Figure 3.II.14 in Appendix 3.II shows the correlation curves between ranking based on IsoSS at elevated temperatures (R_{p25} , R_{p40} , R_{c25} , R_{c40} , R_{s25} , and R_{s40}) and the real IsoSS at 4°C (R_{p4} , R_{c4} , R_{s4}). An overview of the resulting correlation coefficients is presented in figure 3.7 to allow better comparison. Accordingly, the predictive powers of 2 μ DSC based rankings (ranking based on T_m (R_{T_m}) and optimized ranking by considering the degree of unfolding reversibility (R_{opT_m})) were compared with the predictive power of IsoSS at elevated

temperatures (25°C and 40°C), in predicting the real stability ranking (at 4°C). This comparison was made only for the whole 24 formulations.

IsoSS at 25°C obtained the highest correlation coefficient in predicting the physical stability and overall stability ranking at 4°C and together with IsoSS at 40°C in predicting the chemical stability.

Surprisingly, physical stability and overall stability ranking at real storage temperatures are significantly better predicted by just measuring T_m using μ DSC than the routinely more complicated IsoSS at 40°C. However, chemical stability is predicted significantly better by the accelerated IsoSS at elevated temperatures.

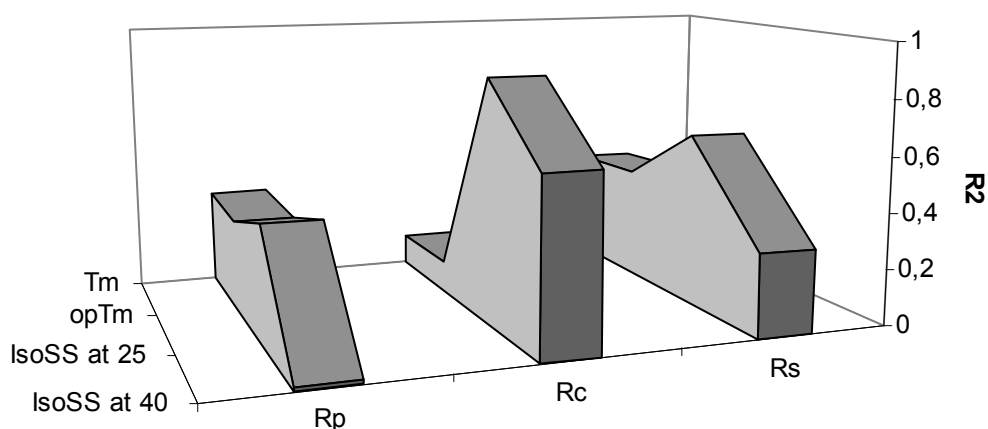


Figure 3. 7: An overview of the correlation coefficients (y-axis) resulting from correlating IsoSS based ranking at 4°C (x-axis) with either T_m , op T_m , IsoSS at 25°C or IsoSS at 40°C (z-axis) for the whole 24 formulations of three GCSF DOEs.

I.2.4.2. Prediction quality:

50% and 20% prediction qualities of R_{T_m} and R_{opT_m} in comparison with those of IsoSS at elevated temperature were evaluated and are presented in figures 3.8 A and B, respectively. For predicting physical stability, T_m and IsoSS at 25°C showed the highest 50% prediction quality, whereas IsoSS at 40°C showed the lowest. Chemical stability was predicted with higher 50% prediction quality by IsoSS at 25 and 40°C. Comparing the 20% prediction quality for both physical and chemical stability μ DSC parameters did not show great difference in comparison with IsoSS at elevated temperature but generally the superiority of T_m in predicting physical stability at 4°C to accelerated stability studies at 40°C is confirmed. On the other hand, IsoSS at 40°C had better predictive power with regards to chemical stability beside IsoSS at 25°C. The prediction of the overall stability based on T_m showed the highest 50% and 20% prediction quality and that support the higher correlation coefficient obtained in figure 3.7.

This study provides a critical evaluation of two commonly used predictive approaches for protein stability. Accelerated stability studies are commonly performed by observing the rate of monomer loss or chemical degradation. This is experimentally quantified in terms of the fraction of monomer as well as intact GCSF remains at a given time during isothermal stress at a given elevated temperature. In case of physical stability, the measured monomer loss rate represents, indirectly, the observed rate of aggregation which is, in contrast to chemical degradation kinetics, a complicated process. Such process is controlled by several coefficients including aggregation kinetics and two main thermodynamic contribution, the free energy of unfolding (ΔG_{unf}) and the osmotic second virial coefficient (B_{22})³³. Accelerated stability studies are commonly used in predicting real time physical stability based on the assumption that, as in chemical degradation, the observed rate of aggregation at elevated temperatures shows linear Arrhenius behaviour and therefore, extrapolation of such aggregation rates with respect to temperature should be able to predict the rate of aggregation at normal storage temperatures. Such approach would be true if all rate coefficients involved in determining the overall observed aggregation rate constant obey a linear Arrhenius temperature dependence. ΔG_{unf} , which is the most important factor involved in such process, is highly dependent on temperature (Equation 1) and this is one of many possible reasons, reviewed by Weiss et al³⁴, why such linear Arrhenius behaviour is not observed and accordingly predictions of protein physical stability based on IsoSS at elevated temperature is expected to fail as shown in this study. That in turn causes further failure in predicting the overall stability ranking where physical stability is highly weighed in the overall ranking.

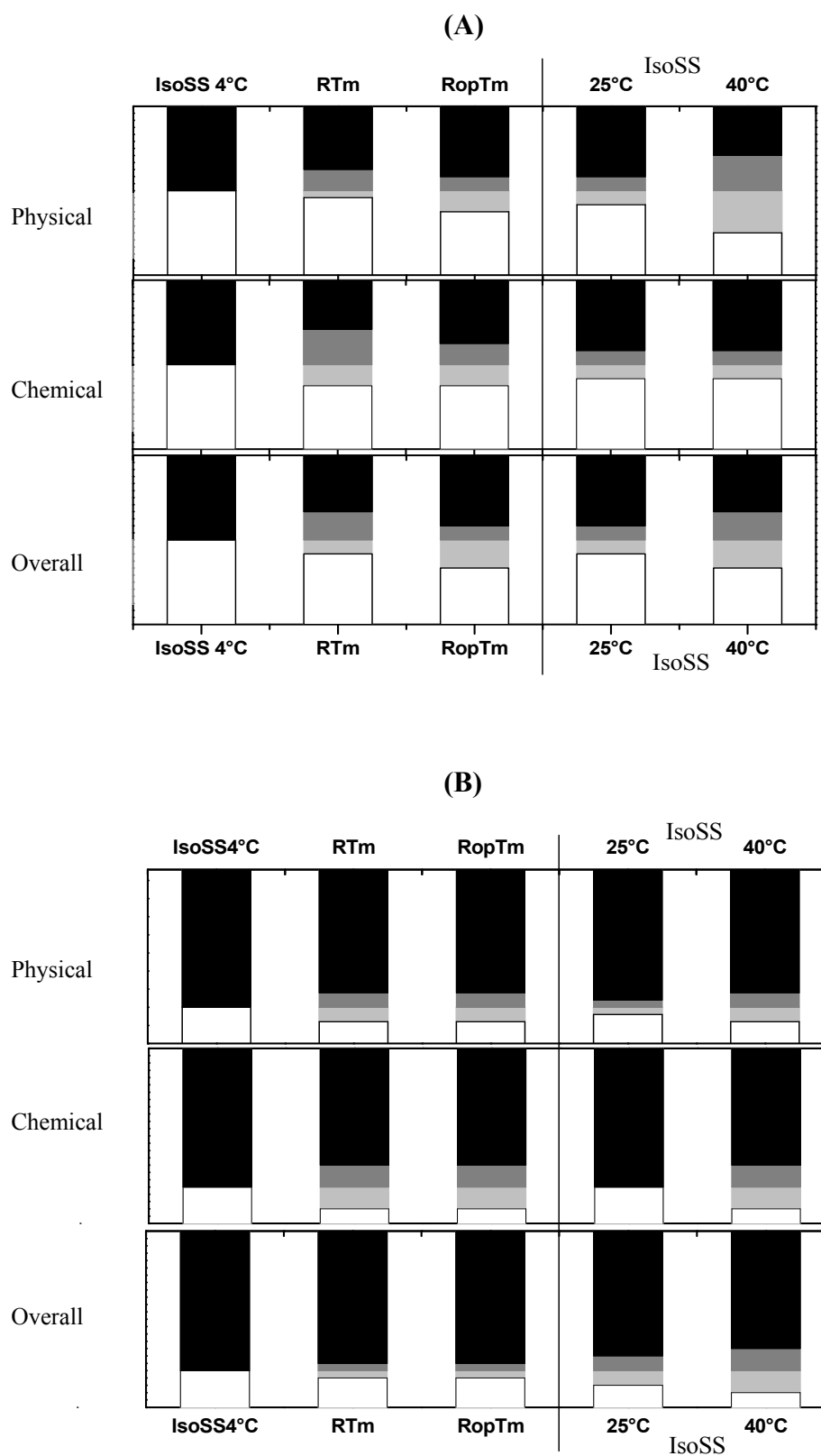


Figure 3. 8: 50% (A) and 20% (B) prediction quality of ranking based on T_m , opT_m , IsoSS at 25°C and IsoSS at 40°C in predicting the real stability at 4°C (rankings based on IsoSS at 4°C).

The second approach evaluated in this work was the prediction based on conformational stability which is typically quantified by the standard free energy of unfolding (ΔG_{unf}). This parameter is determined by performing chemical unfolding temperature experiments³⁵ or by using thermal scanning techniques such as μ DSC which has the advantage of being sensitive to conformational transitions that may be spectroscopically invisible if they don't cause strong changes in either 2^{ry} or 3^{ry} protein structure³⁴. ΔG_{unf} is calculated from Gibbs-Helmholtz equation³⁶.

$$\Delta G_{\text{unf}} = \Delta H_{\text{unf}} (1 - T/T_{\text{unf}}) + \Delta C_{p(\text{unf})} (T - T_{\text{unf}} - T (\ln (T / T_{\text{unf}}))) \quad (1)$$

Where T_{unf} is the unfolding temperature at which $\Delta G_{\text{unf}} = 0$, T is the temperature at which ΔG_{unf} is to be calculated, ΔH_{unf} the enthalpy change at unfolding and $\Delta C_{p(\text{unf})}$ is the difference in heat capacity between folded and unfolded states of protein.

In practice most proteins undergo formation of irreversible aggregates^{4,7,37,38}, which makes the extraction of accurate parameter to calculate ΔG_{unf} based on equation (1) impossible and it is only possible to determine T_m .

In comparison with the previously discussed Arrhenius extrapolation approach, measured T_m is a direct component of ΔG_{unf} , the most essential in aggregation thermodynamics, which may explain the significant higher predictive power of T_m compared to isothermal stability studies at 40°C. Of course this was not the case in predicting the chemical degradation rates where isothermal stability studies at elevated temperature are more successful.

II. Monoclonal Antibody (MAB):

II.1. Materials and methods:

II.1.1. Materials:

A monoclonal antibody (MAB) was obtained as a gift from Roche Diagnostics GmbH (D-Penzberg, Germany). All other materials and solvents were of analytical grade. Deionized double-distilled water was used throughout the study.

II.1.2. Formulations:

MAB was obtained in 10 mM Phosphate buffer pH 6.4 at a concentration of 13.8 mg/ml. The original solution was dialyzed using Slide-A-Lyzer^R Dialysis Cassette 10000 MWCO, (Pierce, Rockford, USA), to the required buffer. After dialysis MAB concentration was examined using Uvikon 810 UV spectrophotometer (Tegimenta, Rotkreutz, Switzerland.) and the final concentration was adjusted to 0.5 mg/ml for μ DSC measurements and 5 mg/ml for the long term stability study. The final pH of the sample was determined using a Mettler Toledo MP220 pH meter (Mettler-Toledo GmbH, Schwezenbach, Switzerland). After preparation all formulations were filtered using low protein binding syringe filters (25 mm, 0.2 μ m, polyvinylidene fluoride (PVDF) membrane, Pall Corporation, MI, USA). A reference for each formulation containing the same buffer and the same excipients was also prepared and filtered using cellulose acetate disk filters, 0.2 μ m pore size (VWR International, USA).

For IsoSS formulations were filled into type I glass vials, stoppered, capped, and crimped under sterile condition and then stored in the dark at ICH temperatures (4, 25, 40°C) in calibrated ovens. Each formulation was subjected to analysis at the beginning of the storage time (zero time) and at further time intervals.

A total of 15 different MAB liquid formulations were included in this study. The effects of 3 pH values (4.2, 5, and 6), three buffer systems (phosphate, histidine and succinate) and different excipients (tween 80, hydroxy propyl beta cyclodextrin (HP- β -CD), sorbitol, sucrose, glycerol and sodium chloride) were tested.

Table 3.6 shows the composition of the studied 15 MAB formulations.

Table 3. 6: Composition of 15 MAB formulations and the corresponding μ DSC parameters (All T_m s value and degree of unfolding reversibility are the mean of triplicate μ DSC scans ($T_m \pm SD < 0.5^\circ C$) (reversibility $\pm SD < 3\%$))

Formulation	Buffer ¹⁾	pH	Excipient	Conc.	T_{m1}	R_{Tm1}	T_{m2}	R_{Tm2}	T_{m3}	R_{Tm3}	Rev. ²⁾
MABF001	Pho.	4.2	No		60	15	73,9	15	79,3	14	48
MABF002	Pho.	5	No		66,1	14	76,6	13	82,2	2	24,6
MABF003	Pho.	6	No		71,3	7	77,2	7	81,4	4	0
MABF004	His	6	No		68,4	13	76,9	10	82,4	1	10
MABF005	Pho.	6	Tween 80	0,05 %	70,9*	10	77,27	3	81,4	4	0
MABF006	Pho.	6	Sorbitol	5%	72,2	1	77,9	1	82**	3	0
MABF007	Pho.	6	Sucrose	5%	72,1	2	77,7	2	81,2	6	0
MABF008	Pho.	6	Glycerol	2.5%	71,4	6	77,3	3	80,7	9	0
MABF009	Pho.	6	NaCl	150 mM	70,2	12	76,9	10	80,5	11	0
MABF010	Pho.	6	HP- β -CD	1%	71,5	4	77,2	7	80,9	8	0
MABF011	Pho.	6	HP- β -CD	10%	71,3	7	75,4	14	77	15	0
MABF012	Succ.	6	No		71,1	9	77,1	9	81,2	6	0
MABF013	Pho.	6	Tween 80	0,0005%	71,5	4	77,3	3	80,6	10	0
MABF014	Pho.	6	Sucrose	1%	70,9	3	77,27	3	81,4	12	0
MABF015	Pho.	6	NaCl	50 mM	72,2	11	77,9	10	82	13	0

1) Buffer concentration is 10 mM in all formulations. Abbreviations are: Pho. for Phosphate, His for Histidine and Succ. For Succinate.

2) Degree of unfolding reversibility. * $\pm SD = 0.5^\circ C$ ** $\pm SD = 0.6^\circ C$

II.1.3. Thermal stability using μ DSC:

All formulations were analyzed using a VP-DSC (Microcal Inc., MA). Samples, as well as the corresponding references were degassed for 5 min prior to injection in the μ DSC cells using a Thermo vac pump (Microcal. Inc., MA). Both sample and reference were loaded into cells using a gas tight Hamilton 2.5 ml glass syringe.

Each formulation with its corresponding reference was heated from $30^\circ C$ to $100^\circ C$ using a 60K/hr heating rate. The unfolding reversibility was investigated by temperature cycling using the upscan-upscan method which employed two consecutive upscans. After the first upscan the device is programmed to cool the sample again and repeat the heating cycle immediately. The μ DSC cell was pressurized to prevent boiling of the sample during heating.

A base line run was performed before the sample run by loading both sample and reference cells with the corresponding reference. This base line was subtracted later from the protein thermal data and the excess heat capacity was normalized for protein concentration. For each formulation T_m and degree of reversibility were determined. The degree of unfolding reversibility was the percentage of the enthalpy of the second upscan (ΔH_2) in relation to the first one (ΔH_1). Both ΔH_1 and ΔH_2 were the apparent calorimetric enthalpies calculated by

the area under the unfolding endotherm. For data analysis ORIGIN DSC data analysis software was used.

II.1.4. Isothermal stability study (IsoSS):

All formulations were stored under controlled conditions and analyzed immediately after sample withdrawal. The IsoSS of 11 from 15 MAB formulations was studied for a period of 12 months. Due to different starting time 4 formulations were studied only for 6 months. The following analytical methods were applied.

II.1.4.1. Size-exclusion HPLC (SE-HPLC):

Loss of MAB monomer, due to aggregation or fragmentation, was monitored using SE-HPLC. The separation was achieved using Dionex HPLC system (P680 pump, ASI 100 auto sampler, UVD170U) and two Superose 12 (10/300 GL) columns (Amersham Biosciences AB, Uppsala, Sweden). A flow rate of 0.5 ml/min was used, and the protein was detected at a wavelength of 280 nm. The mobile phase consisted of 200 mM Potassium phosphate, 150 mM potassium chloride, pH 6.9. A protein concentration of 1 mg/ml was used in the analysis. All samples were centrifuged before injection into the HPLC system. The % monomer remaining was calculated from the starting monomer content of each formulation at zero time point in order to overcome the incomplete protein recovery in some formulations. The monomer decline rate constant was calculated from the slope of the 1st order kinetic curves and used for ranking.

II.1.4.2. Light obscuration:

The insoluble aggregates were determined in each formulation by light obscuration measurements (PAMAS SVSS-CTM (Rutesheim, germany)). Using a rinsing volume of 0.5 ml and a measuring volume of 0.3 ml and the number of measurements was set to three. Before each measurement the device was rinsed with particle free water until there were less than 100 particles larger than 1 μm counted and no particles over 10 μm . Samples were diluted five times before measurements to 1 mg/ml using particle free water. The resulted particle count was multiplied by five and the final numbers were used in ranking.

II.1.4.3. Sodium dodecyl sulphate polyacrylamide gel electrophoresis (SDS-PAGE):

SDS-PAGE was conducted under non-reducing conditions using an XCell II mini cell system (Novex, Sand Diego, CA). Protein solutions were diluted in a pH 6.8 tris-buffer, containing 4% SDS and 20% glycerine. Samples were denatured at 95°C for 20 min and 10 µl were loaded into the gel wells (NuPage 7% Tris-Acetate Gel, Novex High performance pre-cast gels, Fa. Invitrogen, The Netherlands). Electrophoresis was performed in a constant current mode of 40mA in a Tris-Acetate SDS Running Buffer (Fa. Invitrogen). Gel staining and drying was accomplished with a Colloidal Coomassie blue stain (Fa. Novex) and a drying system (DryEase), both provided from Invetrogen, Groningen, Netherlands. SDS-PAGE was used as a confirmative method

II.1.4.4. Isoelectric focusing gel electrophoresis (IEF):

IEF is reported as a method to monitor chemical stability of monoclonal antibody formulations³⁹⁻⁴¹ and was used in this study for the same purpose. It was performed using Multiphor II electrophoresis system (GE healthcare bio-Sciences Ab, Uppsala, Sweden). Samples are diluted to 2 mg/ml using particle free water, centrifuged for 5 min and 5 µl were loaded into the gel (Servalyt Precotes, Range pH 6-9, Serva electrophoresis, Heidelberg, Germany). Electrophoresis was performed in constant current of 2000 volt. The duration of the electrophoresis was 150 min and was performed using Electrophoresis power supply, EPS3501XL (GE healthcare bio-Sciences Ab, Uppsala, Sweden). Gel staining was performed with Coomassie blue stain (Serva electrophoresis, Heidelberg, Germany).

II.1.5. Correlation:

The correlation was studied as explained in the GCSF section. The formulations were ranked according to T_m and separately according to their isothermal stability and then rank correlations were carried out. The ranking methods for µDSC as well as for the IsoSS results are described below.

II.1.5.1. Ranking of formulations according to µDSC:

The MAB molecule showed three different transitions and each of these transitions displayed different unfolding temperatures (as discussed later in the results section). Therefore, it was possible to perform three different rankings based on each T_m (R_{Tm1} , R_{Tm2} and R_{Tm3}). The unfolding reversibility was found for only three formulations. These were already

differentiated based on T_m values and therefore optimization was not possible. Rankings based on each T_m were correlated with ranking based on IsoSS. Table 3.6 (Page 77) shows different rankings for 15 MAB formulations where, R_{Tm1} , R_{Tm2} and R_{Tm3} are rankings based on T_{m1} , T_{m2} and T_{m3} respectively.

II.1.5.2. Ranking of formulations according to IsoSS:

IsoSS ranking was only possible for physical stability based on SE-HPLC and light obscuration measurements. The chemical stability was monitored using IEF which showed no difference between formulations and no acidic or basic species. Therefore, the chemical stability was considered equal for all formulations and thus was excluded from the ranking.

Accordingly the ranking process involved the following steps:

- 1- 1st ranking (R_1): The formulations were ranked according to the monomer loss rate constant.
- 2- 2nd ranking (R_2): The formulations were ranked according to their particle count at the end of the storage period. Ranking limits were as in chapter 2 (See chapter 2 section 2.6.2., Pages 31 and 32).
- 3- Overall physical stability ranking (R_p): For each formulation the average of R_1 and R_2 was calculated ($R_p = (R_1 + R_2)/2$).

These rankings were carried out for each storage temperature to obtain R_{p4} , R_{p25} , and R_{p40} for the ranking at 4, 25 and 40°C, respectively.

Ranking for the IsoSS at 4°C was done after 12 months for 11 formulations. This was repeated for the same formulation at 25 and 40°C. The other four formulations were studied for 6 months at 4°C and at 25°C no significant stability differences were noticed but they were included in a ranking for the whole 15 formulations for the IsoSS at 40°C. Table 3.7 shows an example for the ranking process of the 11 MAB formulations after 12 months at 4°C. It was obvious that the physical stability of the selected formulations very high as minor differences were obtained between formulations after 12 months storage at 4°C and only 4 from 11 formulations showed lower stability. In Appendix 3.I rankings for the 11 MAB formulations at 25 and 40°C are shown in tables 3.I.15 and 16. Ranking of the whole 15 MAB formulations based on IsoSS at 40°C after 6 months is represented in table 3.I.17.

Table 3. 7: Ranking procedures for 11 MAB formulations based on IsoSS at 4°C after 12 months

Formulation	$K_p4^{1)}$	R_{14}	$R_{24}^{2)}$	Avr. ($R_{14}+R_{24}$)/2	$R_p4^{3)}$
MABF001	-0.0015	10	1	5.5	10
MABF002	0.0001	1	1	1	1
MABF003	0.0001	1	1	1	1
MABF004	-0.0016	11	1	6	11
MABF005	0.0011	1	1	1	1
MABF006	0.0003	1	1	1	1
MABF007	0.0002	1	1	1	1
MABF008	-0.0001	9	1	5	9
MABF009	-0.00006	8	1	4.5	8
MABF010	0.0004	1	1	1	1
MABF011	0.0005	1	1	1	1

- 1) Monomer denaturation constant at 4°C according to SE-HPLC results.
- 2) Ranking based on light blockage measured particle count (table 3.I.18)
- 3) Ranking based on physical stability at 4°C

II.1.6. Prediction quality:

Both 50% and 20% prediction qualities were determined for the correlation of each T_m with physical stability ranking at different temperature.

Determining the prediction quality was discussed in details in section I.1.6 of this chapter (Pages 60, 61).

II.2. Results and discussion:

II.2.1. μ DSC measurements:

A representative μ DSC thermogram for the formulation MABF003 is shown in figure 3.9 where the MAB molecule showed two main transitions at approximately 71 and 77°C. Temperature induced unfolding of different monoclonal antibodies was extensively studied using μ DSC^{13,42-45} where similar two transitions were obtained. However, a thermogram of IgG of isotype 1, which showed only one transition peak, was reported⁴⁶. In these studies Fab and Fc fragments were studied separately from the intact antibody and in almost all cases 2 different transitions were obtained for Fc segments and only one strong transition was obtained for the Fab segment. It was shown that the experimental enthalpy of unfolding may be used to determine which transition represents the Fab fragment which unfold in a cooperative manner⁴⁵. Based on these finding it was suggested that the first transition in figure 3.9 should correspond to the Fc fragment and the second large transition correspond to the Fab fragment.

Using Origin software the deconvolutions of the transition envelope was possible to obtain the individual domain transitions. This results in three different T_m s as shown in the dotted lines in figure 3.9 including the two main transitions plus a small transition at about 81.4°C. This was applied for all MAB formulations included in this study and the resulted T_m s are recorded in table 3.6.

The unfolding temperature showed no concentration dependency for MAB (figure 3.10). Therefore, it was decided to use lower concentration for μ DSC scans (0.5 mg/ml) to avoid extreme aggregations in the μ DSC cell.

Reversibility was obtained in 3 formulations and recorded in table 3.6 as well.

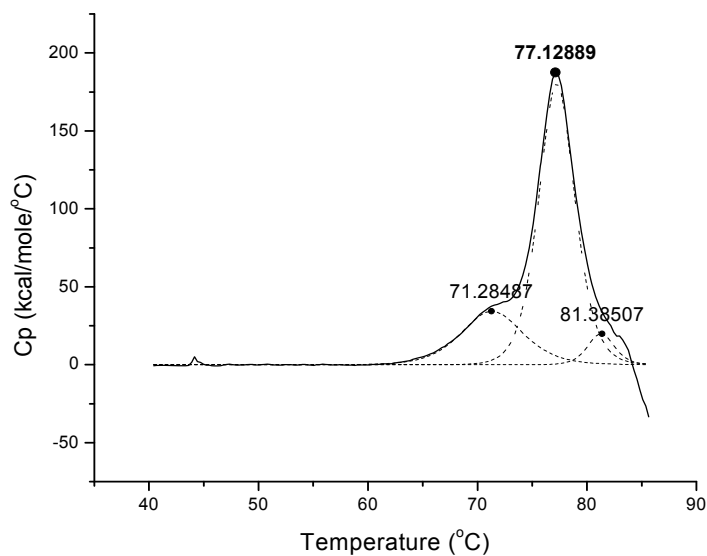


Figure 3. 9: Representative μ DSC thermogram for MABF003 showing three T_m s. The solid line illustrates the total transition envelope and dotted lines represent the deconvolutions carried out using Origin software.

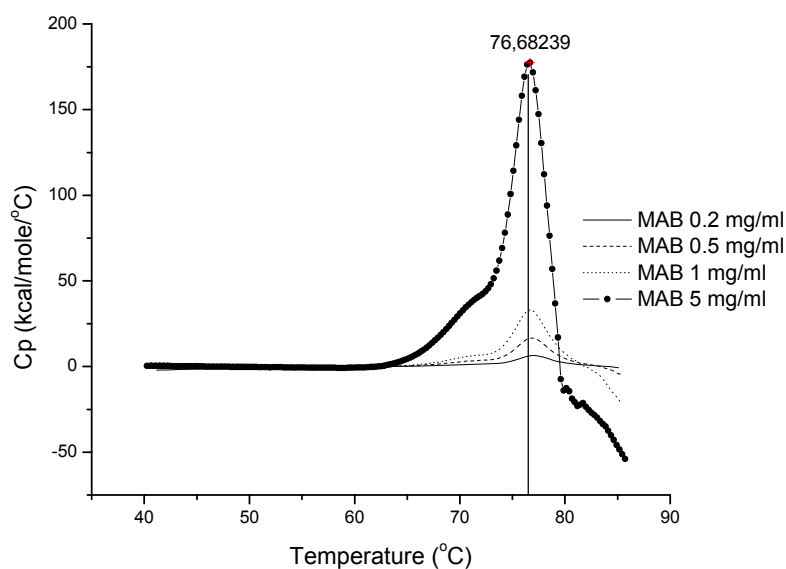


Figure 3. 10: Unfolding of MAB (in phosphate buffer 10 mM pH 6) at different concentrations (0.2, 0.5, 1 and 5 mg/ml).

II.2.2. Isothermal stability study (IsoSS):

MAB formulations were analyzed during isothermal storage at 4, 25 and 40°C according to a certain time table using different analytical methods. As previously done in the GCSF study the monomer loss rates were calculated according to 1st order kinetics for each formulation. Figure 3.11 represents an example of denaturation rate of MABF003 after 12 months storage obtained by SE-HPLC. The monomer loss rates at 3 different temperatures were obtained from the slope of each curve.

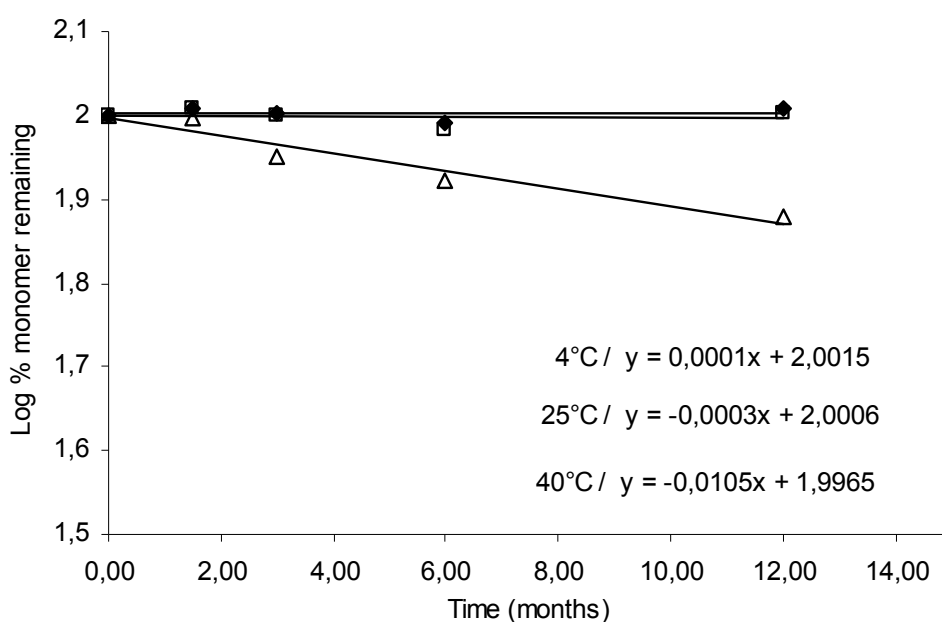


Figure 3. 11: Monomer loss of MABF003 during isothermal stability study at 4°C (—■—), 25°C (—□—) and 40°C (—△—).

Light obscuration measurements were used to determine insoluble aggregates in each formulation. In Appendix 3.I particle counts at the end of the stability study are listed in table 3.I.18.

SDS-PAGE and IEF were carried out for all formulations at zero time and after the last time point of the IsoSS. In appendix 3.II SDS-PAGE and IEF gels are presented in figures 3.II.15 and 16, respectively. The chemical stability of the MAB formulations included in this study seems not to be affected at 4°C as seen from the IEF gels. Furthermore at 40°C, where all formulation showed smearing, no specific ranking could be obtained. Therefore, all formulations were ranked equal with regard to chemical stability.

II.2.3. μ DSC as a predictive tool for IsoSS:

The predictive power of μ DSC was judged (as in GCSF study) primarily on the resulted Pearson product moment correlation coefficients from correlating the ranking based on μ DSC with those based on IsoSS. Secondly, the prediction quality (selection of best 50% or 20% formulations) was tested.

II.2.3.1. Correlation coefficients:

Correlation curves are presented in figures 3.12 – 3.14 for T_m based rankings and physical stability based ranking for 11 MAB formulations after 12 months storage at 4, 25, and 40°C. Figure 3.15 show the correlation curves for T_m based rankings and physical stability of 15 MAB formulations after 6 months storage at 40°C.

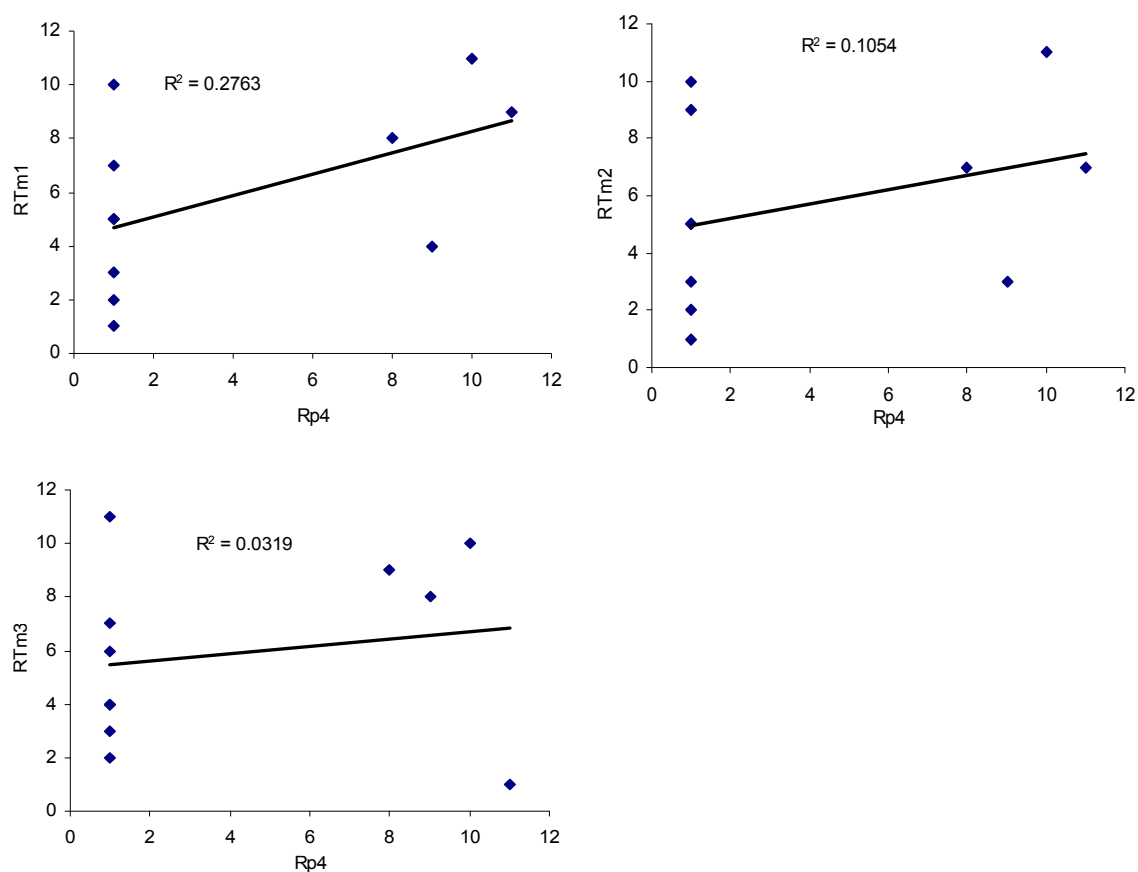


Figure 3. 12: Correlation curves of 11 MAB formulations. That includes correlation between T_m based rankings (R_{Tm1} , R_{Tm2} and R_{Tm3}) and ranking based on IsoSS at 4°C (R_p4) after 12 months.

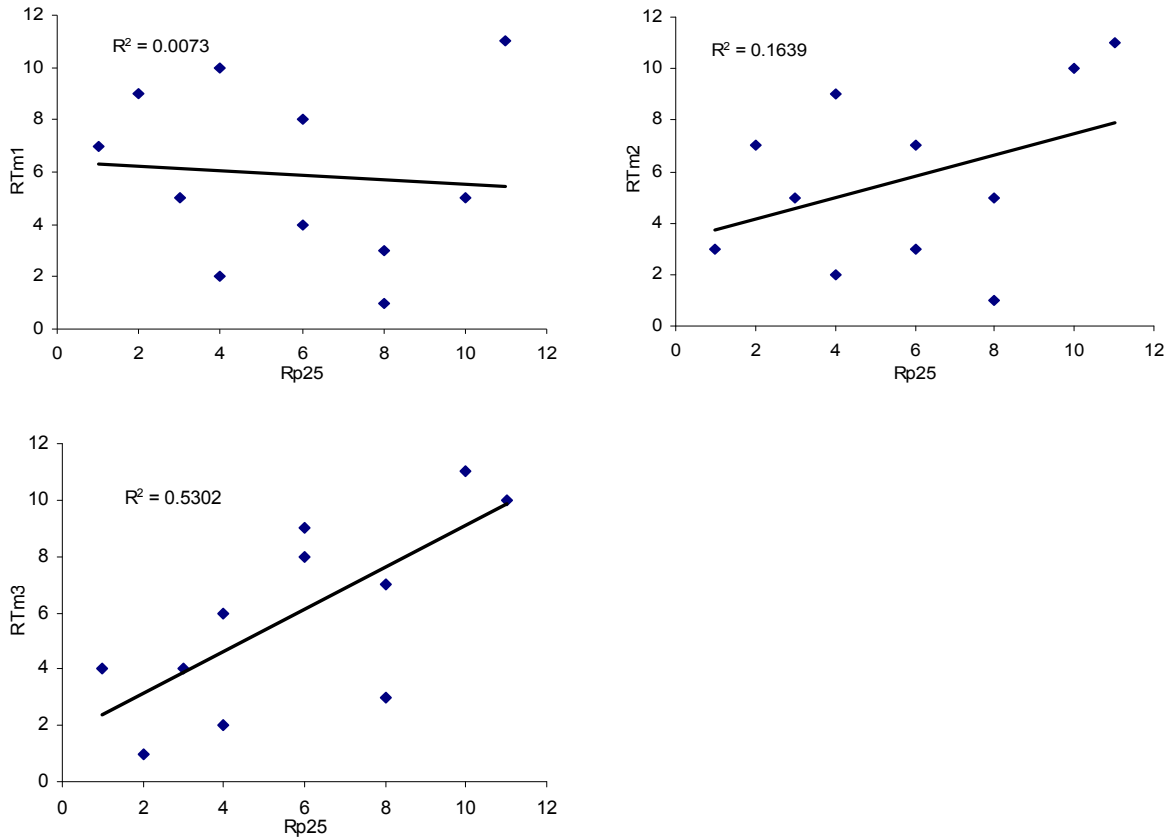


Figure 3. 13: Correlation curves of 11 MAB formulations. That includes correlation between T_m based rankings (R_{Tm1} , R_{Tm2} and R_{Tm3}) and ranking based on IsoSS at 25°C (R_{p25}) after 12 months.

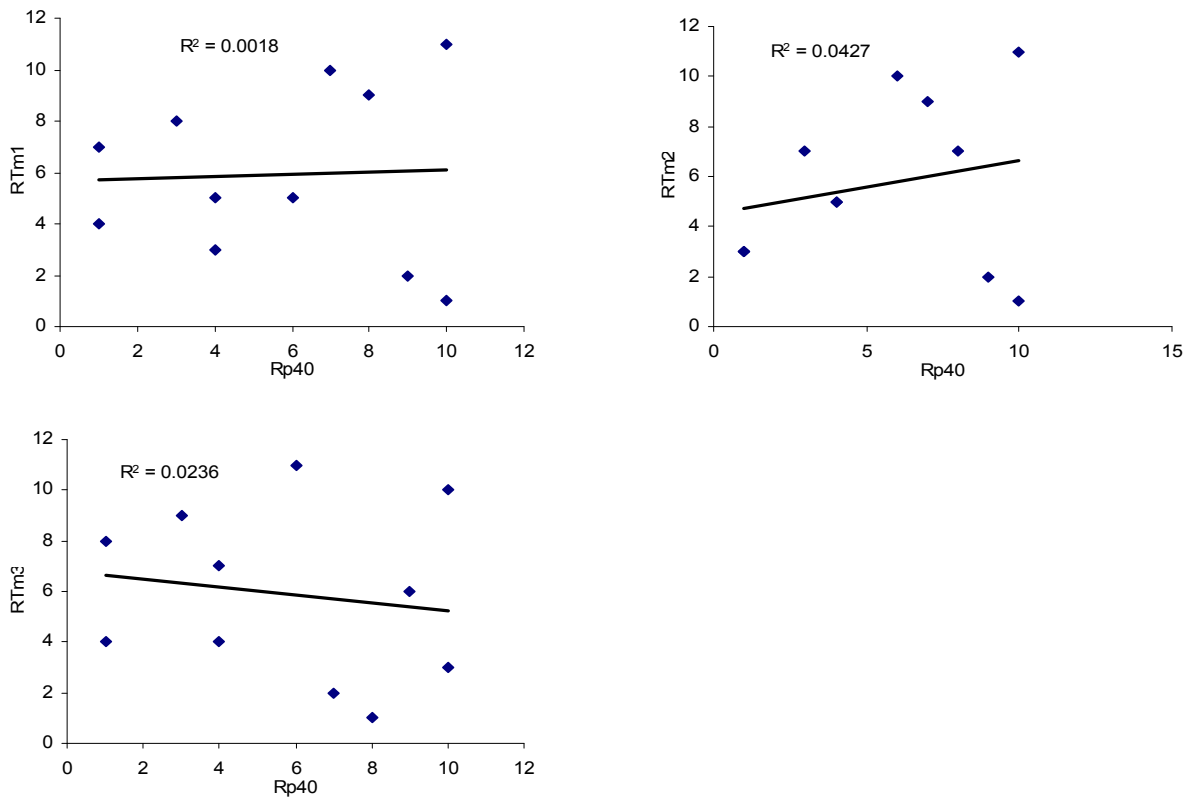


Figure 3. 14: Correlation curves of 11 MAB formulations. That includes correlation between T_m based rankings (R_{Tm1} , R_{Tm2} and R_{Tm3}) and ranking based on IsoSS at 40°C (R_{p40}) after 12 months.

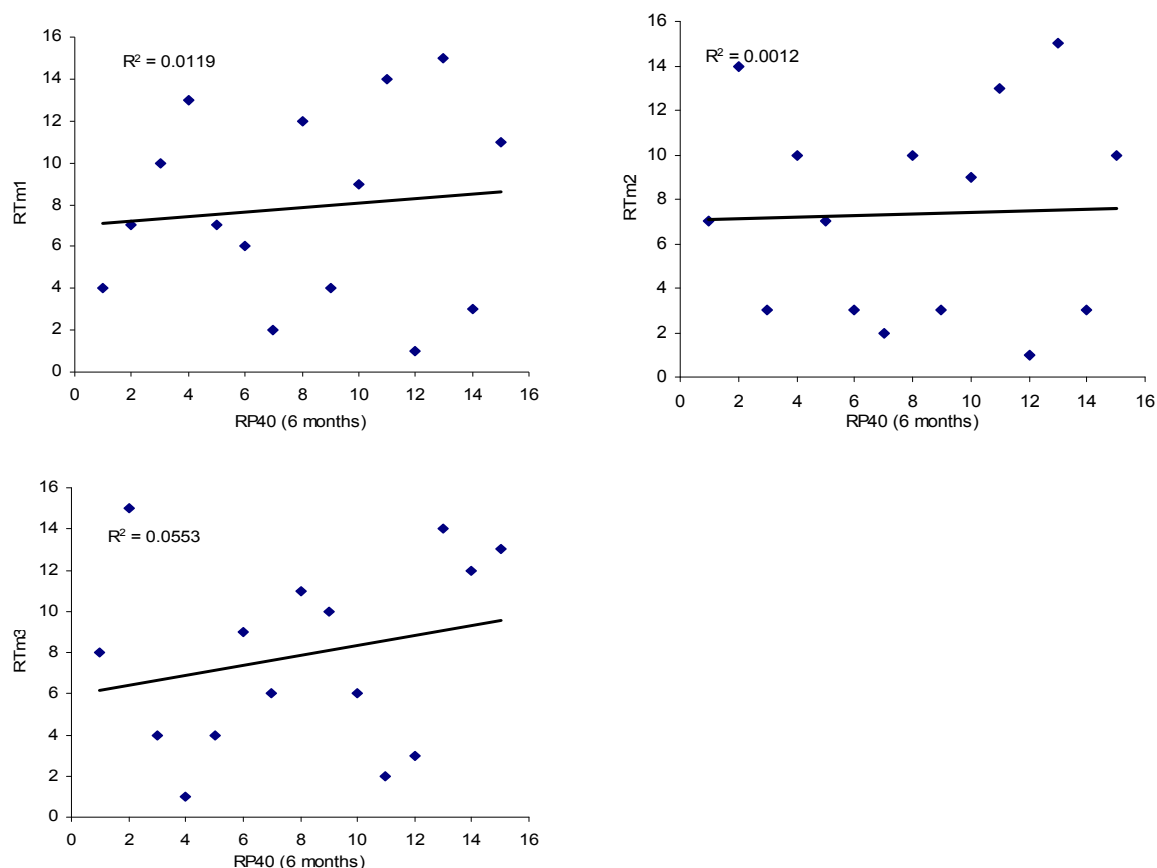


Figure 3. 15: Correlation curves of 15 MAB formulations. That includes correlation between T_m based rankings (R_{Tm1} , R_{Tm2} and R_{Tm3}) and ranking based on IsoSS at 40°C (R_{p40}) after 6 months.

An overview for all correlation coefficients is presented in figure 3.16 for 3 T_m based rankings (R_{Tm1} , R_{Tm2} and R_{Tm3}) and physical stability based rankings at different storage temperatures (R_{p4} , R_{p25} , and R_{p40}).

In this section the predictive power of μ DSC in formulation development of a monoclonal antibody was studied. Similar to GCSF study, in the first part of this chapter, an important question is to be answered. Can μ DSC analysis predict the overall long term physical stability of a monoclonal antibody in a certain formulation at its typical storage temperature of 4-8°C? Monoclonal antibodies usually show 3 T_m s in μ DSC experiments as mentioned in section II.2.1. A formulator will expect from such work to find out which is the most predictive T_m . Microcalorimetry T_m based ranking showed superior predictive power than routinely conducted IsoSS at elevated temperatures (40 – 60°C) in predicting the long term stability of GCSF formulations at 4°C. Will that be also the case with respect to monoclonal antibodies? Figure 3.16 showed that none of the T_m based rankings showed really high correlation coefficients with physical stability based rankings at different storage temperatures. At 4°C correlations were between 2 clusters of point (figure 3.12) and, except with T_{m1} based ranking, extremely weak correlations were obtained. However, this might be due to the small

differences in physical stability of the MAB formulations after 12 months storage at 4°C. In the ranking based on physical stability after 12 months storage at 4°C 7 formulations from 11 were stable through the study. Accordingly formulations ranked from 1 to 7 based on T_m are all ranked 1 based on physical stability at 4°C. At 25°C the formulations were easier to differentiate and a reasonable ranking based on physical stability was possible. Accordingly, the points in the correlation curve were better distributed (figure 3.13). The highest correlation coefficient was obtained from R_{Tm3} for the physical stability after 12 months storage at 25°C. After 12 as well as 6 months storage at 40°C (figures 3.14 and 3.15, respectively) all T_m based rankings showed very poor correlation to physical stability based ranking.

μ DSC could achieve a powerful prediction of the physical stability of MAB at 25°C using the T_{m3} based ranking. At 4°C MAB formulations didn't show significant differences in physical stability even after 12 months. Judging the predictive power of μ DSC based on the correlation coefficients, although R_{Tm1} showed relatively better correlation coefficient, is not enough and therefore, studying the prediction quality might be very useful in this case.

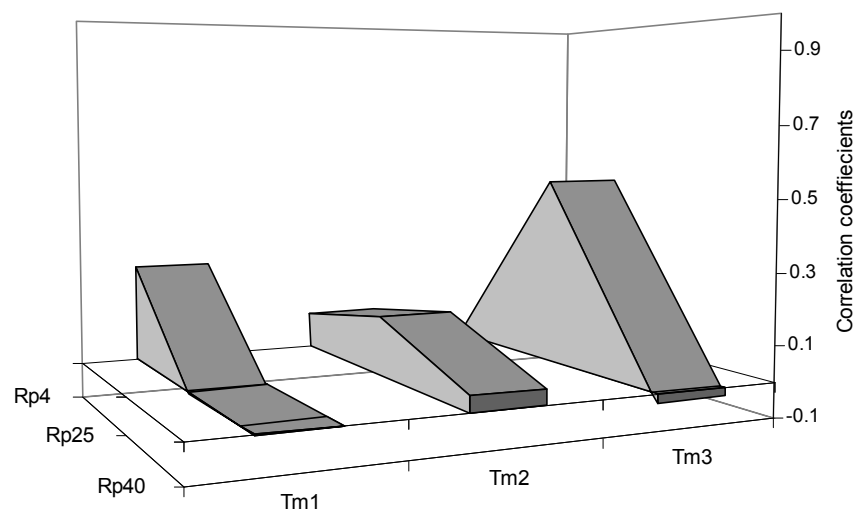


Figure 3. 16: An overview of the correlation coefficients (Y-axis) resulting from correlating the ranking based on physical stability (R_p) at different temperatures (R_{p4} , R_{p25} , and R_{p40}) (Z-axis) with ranking based on three different T_m s (R_{Tm1} , R_{Tm2} and R_{Tm3}) of 11 MAB formulation after 12 months IsoSS .

II.2.3.2. Prediction quality:

The prediction quality is studied in this chapter to evaluate how reliable a selection process based on T_m is. In such process a formulator will choose the formulations having the highest T_m and exclude those having the lowest. It is important to highlight that after selection the main focus is not on the excluded candidates but in fact the selected ones in order to go forward in clinical trials and parallel in long term stability studies. Consequently, in order to avoid unexpected failure in clinical studies due to instability issues false selection is not acceptable.

Figure 3.17 A and B show the 50% and 20% prediction quality, respectively, of three T_m based rankings (R_{T_m1} , R_{T_m2} and R_{T_m3}) in predicting the physical stability of 11 MAB formulations at three different temperatures (4, 25 and 40°C).

At 4°C T_m based rankings showed higher 50% quality in predicting the physical stability of MAB formulations in comparison with 25°C and 40°C. That was not clear from only comparing the correlation coefficients in section II.2.3.1. Most interestingly, the selected best 2 formulations based on T_{m1} or T_{m2} were included in the selected best stable formulations at 4°C (figure 3.17 B). However, as shown in figure 3.17 B, the 20% quality of physical stability prediction at 4°C showed larger gray area than at 25°C and 40°C which indicates lower prediction quality. But having a complete white bar indicates that the best 2 formulations based on T_m didn't fail in stability after 12 months storage at 4°C. The absent, or even incomplete, white bars as in case of the prediction quality of T_m based ranking at 25°C and 40°C means that all or at least part of the selected best formulations based on T_m didn't achieve good stability through the study period.

The predictive power of all T_m based rankings for the physical stability at 4°C showed similar 50% prediction quality (figure 3.17 A). On the other hand, T_{m1} and T_{m2} showed better 20% prediction quality than T_{m3} (figure 3.17 B). Using T_{m1} or T_{m2} as predictive tool for physical stability of MAB formulations at 4°C no false selection happened and the selected 2 best formulations showed no instability after 1 year at 4°C.

At 25°C T_{m3} showed the highest prediction quality (50% as well 20%) in comparison with T_{m1} and T_{m2} which was expected from the high correlation coefficient as shown in section II.2.3.1. However, a false selection could not be avoided as at least 1 of the 2 selected best formulations didn't achieve high physical stability after 1 year.

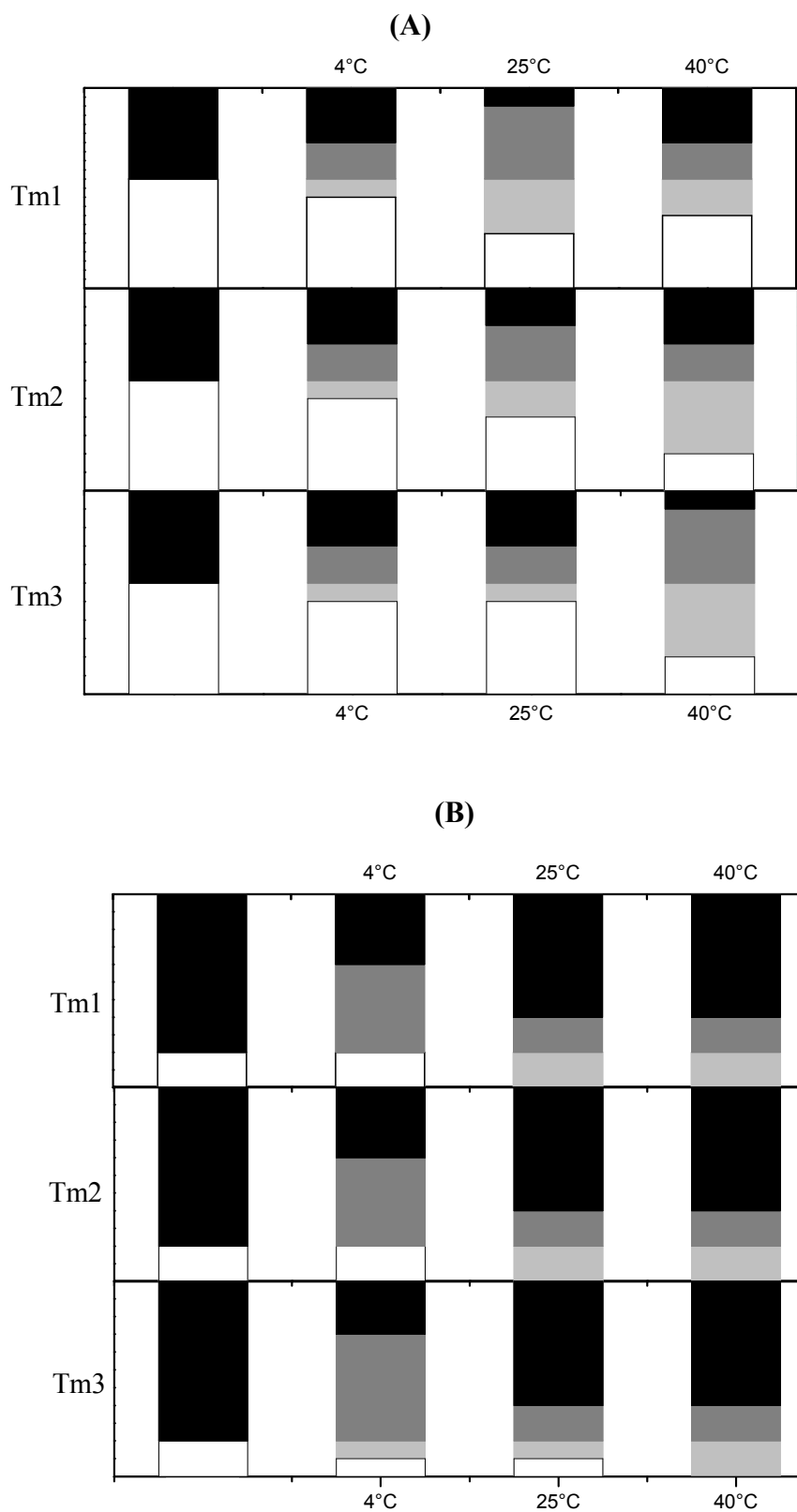


Figure 3. 17: prediction quality of three different T_m s to pick up the best 6 formulations and exclude the bad 5 (50% prediction quality (A)) and to pick up the best 2 and exclude the rest (20% prediction quality (B)) in 11 MAB formulation.

Prediction of the physical stability of MAB formulations at 40°C using T_m based rankings showed the highest 50 % quality with T_{m1} . On the other hand, all T_m based rankings showed bad 20% prediction quality for the physical stability at 40°C.

Despite the lower correlation coefficient, physical stability based ranking of 11 MAB formulations was best predicted at 4°C based on T_m . Using T_{m1} or T_{m2} in a predictive ranking, false prediction of the best 2 formulations was completely avoided. Moreover, T_{m1} showed higher correlation coefficient in predicting the physical stability at 4°C. Accordingly, using the 1st transition temperature (T_{m1}) as predictive parameter is recommended.

II.2.4. μ DSC in comparison with classical accelerated IsoSS:

Here isothermal stability studies at elevated temperatures (25°C and 40°C) are considered as “predictive” methods. The predictive power, of those accelerated stability studies, was compared with that of μ DSC T_{ms} . The IsoSS based ranking after 12 months storage at 25°C and after 3 months at 40°C, were compared with 3 T_m based rankings in predicting the stability of MAB formulations after 12 months storage at 4°C. The correlation curves of the 3 T_m based rankings were presented previously in figure 3.12 (page 85). Figure 3.18 shows the correlation curves between ranking based on IsoSS at 25°C and 40°C and the IsoSS at 4°C. Figure 3.19 shows an overview for all correlation coefficients.

In general all methods showed very low correlation coefficients. That is (as shown in correlation curves in figure 3.12 and 3.18) due to the insignificant differences between the MAB formulations after 12 months storage at 4°C. Therefore, the correlation is always between 2 clusters of points. T_{m1} based ranking showed a higher correlation coefficient in comparison with ranking based on T_{m2} and T_{m3} as well as those based on accelerated IsoSS at 25 and 40°C (figure 3.19). However, further evaluation of the prediction quality is needed for a meaningful evaluation of the predictive power of μ DSC measured T_{ms} in comparison with classical accelerated stability studies.

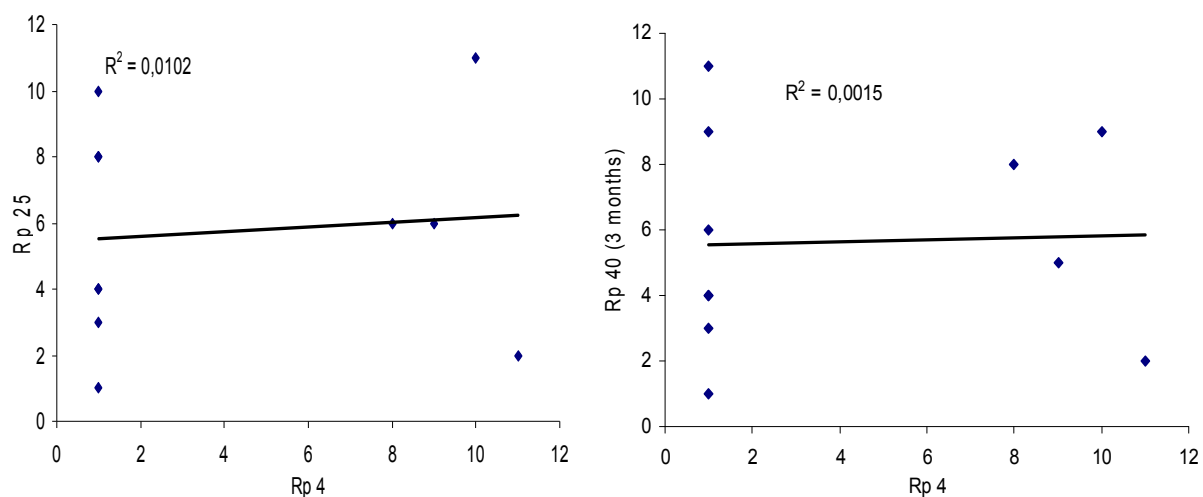


Figure 3.18: Correlation curves of 11 MAB formulations. That includes correlation between ranking based on IsoSS at 4°C ($R_p 4$) after 12 months, and ranking based on IsoSS at 25°C ($R_p 25$) after 12 months and at 40°C ($R_p 40$) after 3 months.

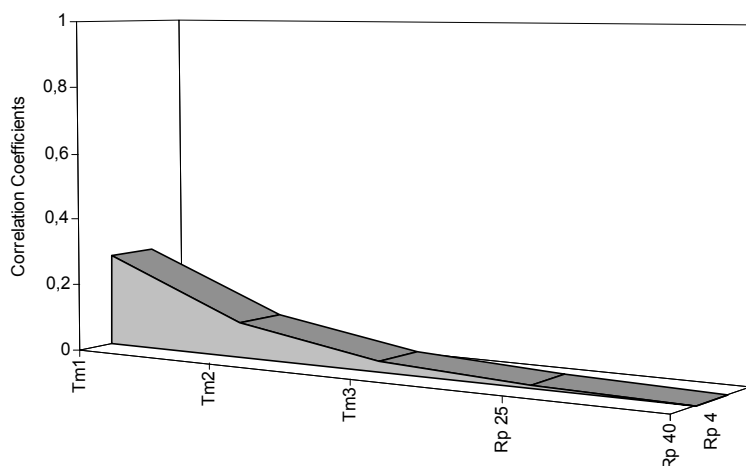


Figure 3. 19: An overview of the correlation coefficients resulting from correlating the IsoSS based ranking at 4°C ($R_p 4$) (Z-axis) with rankings based on either μ DSC determined T_m s ($R_{T_{m1}}$, $R_{T_{m2}}$, and $R_{T_{m3}}$) or accelerated stability studies at 25 and 40°C ($R_p 25$ and $R_p 40$).

The 3 T_m based rankings showed significantly higher 50% prediction quality than that of classical accelerated stability studies (figure 3.20 A). Furthermore, studying the 20% prediction qualities (figure 3.20 B) T_{m1} and T_{m2} based rankings were able to achieve the best

prediction quality and no false selection of the best 2 formulations. Neither ranking based on T_m3 nor those based on classical accelerated stability studies could achieve the same quality.

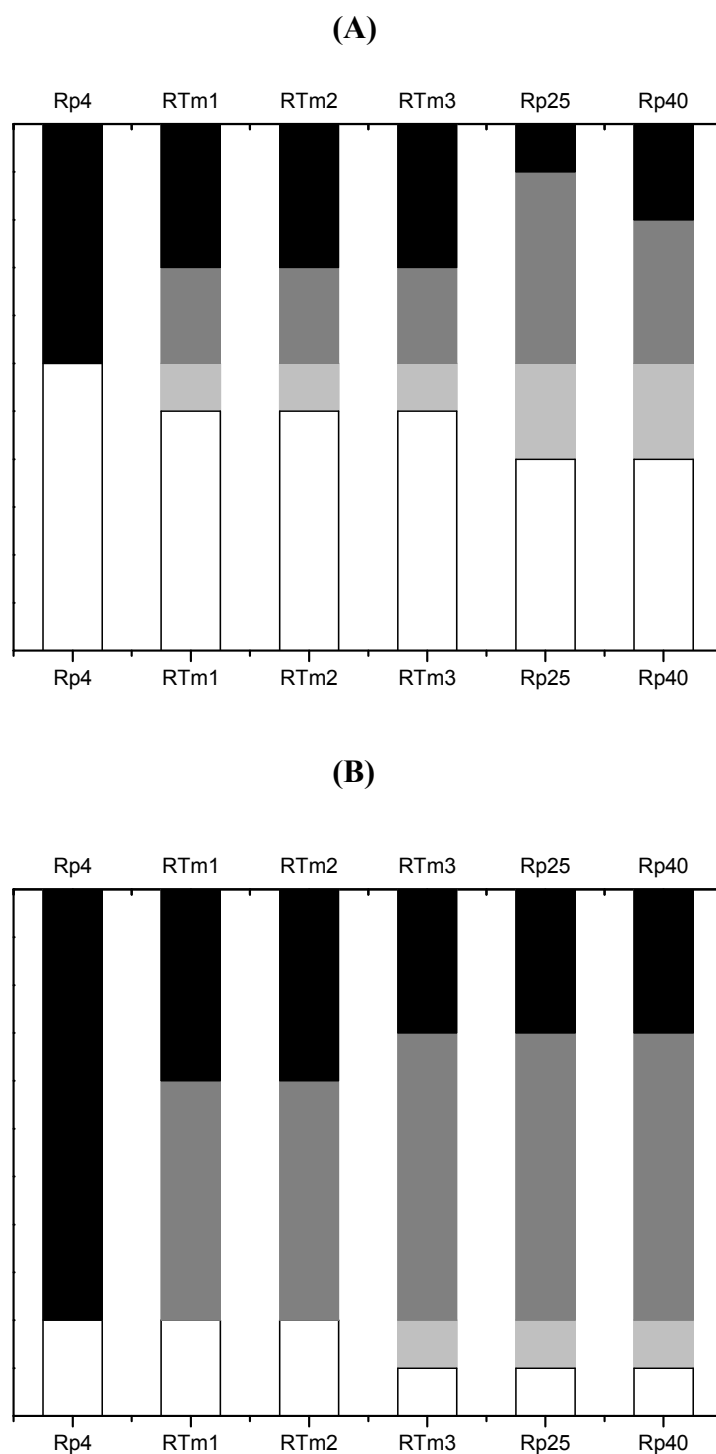


Figure 3. 20: 50% (A) and 20% (B) prediction quality of three μ DSC measured T_m s and IsoSS at 25°C and 40°C in predicting IsoSS at 4°C.

III. Pegylated Interferon α 2a (PEG-INF):

III.1. Materials and methods:

III.1.1. Materials:

Pegylated Interferon α 2a (PEG-INF) was obtained as a gift from Roche Diagnostics GmbH (D-Penzberg, Germany). All other materials and solvents were of analytical grade. Deionized double-distilled water was used throughout the study.

III.1.2. Formulations:

PEG-INF was obtained in 20 mM Sodium acetate buffer pH 6.0 with 50 mM NaCl. Protein concentration of the bulk solution was determined to be approximately 1.4 mg/ml. The original solution was dialyzed using Slide-A-Lyzer^R Dialysis Cassette 2000 MWCO, (Pierce, Rockford, USA), to the required buffer. After dialysis the sample concentration was examined using an Uvikon 810 UV spectrophotometer (Tegimenta, Rotkreutz, Switzerland.). The final concentration was adjusted to 0.4 mg/ml for both μ DSC measurements and the isothermal stability study (IsoSS). The final pH of the sample was determined using a Mettler Toledo MP220 pH meter (Mettler-Toledo GmbH, Schwezenbach, Switzerland). After preparation all formulations were filtered using low protein binding syringe filters (25 mm, 0.2 μ m, polyvinylidene fluoride (PVDF) membrane, Pall Corporation, MI, USA). A reference for each formulation containing the same buffer and the same excipients was also prepared and filtered using cellulose acetate disk filters, 0.2 μ m pore size (VWR International, USA).

For IsoSS formulations were filled into type I glass vials, stoppered, capped, and crimped under sterile condition and then stored in the dark at ICH temperatures (4, 25, 40°C) in calibrated ovens. Formulations were subjected to analysis at the beginning of the storage time (zero time) and at further time intervals.

A total of 14 different PEG-INF liquid formulations were included in this study. The effects of 4 pH values (4, 5, 6 and 7.4), three buffer systems (acetate, phosphate and citrate) and different excipients (tween 80, hydroxy propyl beta cyclodextrin (HP- β -CD), sucrose, and sodium chloride) were tested.

Table 3.8 shows the composition of the studied PEG-INF formulations.

Table 3. 8: Composition of 14 PEG-INF formulations and the corresponding T_m (All T_m s value are the mean of triplicate μ DSC scans ($T_m \pm SD < 0.25^\circ\text{C}$))

Formulation	Buffer ¹⁾	pH	Excipient	Conc.	T_m	R_{T_m}
P-INFF001	Acet.	4	No	-	64,1*	14
P-INFF002	Acet.	5	No	-	68,7	8
P-INFF003	Acet.	6	No	-	68,8*	5
P-INFF004	Acet.	7.4	No	-	67,8	13
P-INFF005	Pho.	6	No	-	68,8	5
P-INFF006	Cit.	6	No	-	69,1	2
P-INFF007	Acet.	6	NaCl	50 mM	69,1	2
P-INFF008	Acet.	6	NaCl	200 mM	69,8	1
P-INFF009	Acet.	6	HP- β -CD	1%	68,8	5
P-INFF010	Acet.	6	HP- β -CD	10%	68,6	9
P-INFF011	Acet.	6	Tween 80	0,0005%	68,5	10
P-INFF012	Acet.	6	Tween 80	0,05%	68,1	12
P-INFF013	Acet.	6	Sucrose	50 mM	68,5	10
P-INFF014	Acet.	6	Sucrose	200 mM	68,9	4

1) Buffer concentration was 20 mM in all formulations. Abbreviations are: Acet for Acetate, Pho. for Phosphate and Cit. for Citrate.

* $\pm SD < 0.6^\circ\text{C}$

III.1.3. Thermal stability using μ DSC:

All formulations were analyzed using a VP-DSC (Microcal Inc., MA). Samples as well as corresponding references were degassed for 5 min prior to injection into the μ DSC cells using a Thermo vac pump (Microcal. Inc., MA). Both sample and reference were loaded into cells using a gas tight Hamilton 2.5 ml glass syringe.

Each formulation with its corresponding reference was heated from 30°C to 80°C using a 60K/hr heating rate. The unfolding reversibility was investigated by temperature cycling using the upscan-upscan method. The μ DSC cell was pressurized to prevent boiling of the sample during heating.

A base line run was performed before the sample run by loading both sample and reference cells with the corresponding reference. This baseline was subtracted later from the protein thermal data and excess heat capacities were normalized for protein concentration.

III.1.4. Isothermal stability study (IsoSS):

All formulations were stored under controlled conditions and analyzed immediately after sample withdrawal. Isothermal stabilities of 11 PEG-INF formulations were studied for a

period of 12 months. Due to different starting time the remaining three formulations were studied only for 6 months. The following analytical methods were applied.

III.1.4.1. Size-exclusion-high performance liquid chromatography (SE-HPLC):

Loss of PEG-INF monomer, due to aggregation or fragmentation, was monitored using SE-HPLC. The separation was achieved using Dionex HPLC system (P680 pump, ASI 100 auto sampler, UVD170U) and a Superose 6 (10/300 GL) column (Amersham Biosciences AB, Uppsala, Sweden). A flow rate of 0.4 ml/min was used, and the protein was detected at a wavelength of 210 nm. The mobile phase consisted of 20 mM sodium phosphate, 150 mM sodium chloride, 1% diethyleneglycol and 10% ethanol. The pH of the mobile phase was adjusted to 6.8. A protein concentration of 0.4 mg/ml was used in the analysis. All samples were centrifuged before injected in the HPLC system. The % monomer remaining was calculated from the starting monomer content of each formulation at zero time point in order to overcome the incomplete protein recovery in some formulations. The monomer decline rate constant was calculated, over 12 months, from the slope of the 1st order kinetic curves and used for ranking.

III.1.4.2. Reversed phase – HPLC (RP-HPLC):

RP-HPLC was performed to study the chemical degradation of PEG-INF. The separation was achieved using Dionex HPLC system (P680 pump, ASI 100 auto sampler, UVD170U) using a Hypersil BDS-C18 4 x 125 mm, 5 µm (Agilent Technologies). As a mobile phase a gradient flow from solution A (30% acetonitril, 0.2% trifluoroacetic acid (TFA)) and solution B (80% acetonitril, 0.2% TFA) was used. A flow rate of 0.4 ml/min was set and a detection wavelength of 215 nm was used. A protein concentration of 0.4 mg/ml was used in the analysis. The injection volume was 50 µl. All samples were centrifuged before injected into the HPLC system. The % of intact PEG-INF remaining after stress was calculated from the intact PEG-INF in each formulation at zero time point and the degradation rate constant was calculated, over 6 months, from the slope of the 1st order kinetic curves and used for ranking.

III.1.4.3. Light obscuration:

The insoluble aggregates were determined in each formulation by light obscuration measurements (PAMAS SVSS-CTM (Rutesheim, germany)). Using a rinsing volume of 0.5 ml and a measuring volume of 0.3 ml and the number of measurements was set to three.

Before each measurement the device was rinsed with particle free water until there were less than 100 particles larger than 1 μm counted and no particles over 10 μm . The resulting particle counts at the end point of the stability study were used in ranking.

III.1.4.4. Sodium dodecyl sulphate polyacrylamide gel electrophoresis (SDS-PAGE):

SDS-PAGE was conducted under non-reducing conditions using XCell II mini cell system (Novex, Sand Diego, CA). Protein solutions were diluted in a pH 6.8 tris-buffer, containing 4% SDS and 20% glycerine. Samples were denatured at 95°C for 20 min and 10 μl were loaded into the gel wells (NuPage 7% Tris-Acetate Gel, Novex High performance pre-cast gels, Fa. Invitrogen, The Netherlands). Electrophoresis was performed in a constant current mode of 40mA in a Tris-Acetate SDS Running Buffer (Fa. Invitrogen). Gel staining and drying was accomplished with a silver staining kit (SilverXpress) and a drying system (DryEase), both provided from Invitrogen, Groningen, Netherlands. Based on SDS-PAGE no ranking was possible but it was used as a confirmative method.

III.1.5. Correlation:

All formulations were ranked according to T_m and separately according to their isothermal stability and then rank correlations were carried out. The ranking methods for μDSC as well as for the IsoSS results are described below.

III.1.5.1. Ranking of formulations according to μDSC :

The PEG-INF molecule showed no unfolding reversibility in all formulations. Therefore ranking was made only based on T_m (R_{T_m} for PEG-INF formulations is shown in table 3.8).

III.1.5.2. Ranking of formulations according to IsoSS:

III.1.5.2.1. Ranking based on physical stability (R_p):

This ranking was based on both SE-HPLC and light obscuration data. The ranking process has the following steps:

- 1- 1st ranking (R_1): The formulations were ranked according to the monomer loss rate constant.
- 2- 2nd ranking (R_2): The formulations were ranked according to their particle count at the end of the storage period. Ranking limits were the same used in chapter 2 (See chapter 2 section 2.6.2.)

3- Overall physical stability ranking (R_p): For each formulation the average of R_1 and R_2 was calculated ($R_p = (R_1 + R_2)/2$).

These 3 rankings were done for each storage temperature to get R_{p4} , R_{p25} , and R_{p40} for the ranking at 4, 25 and 40°C, respectively.

III.1.5.2.2. Ranking based on chemical stability (R_c):

Ranking was based on RP-HPLC data and was done for all formulations at each storage temperature (R_{c4} , R_{c25} , and R_{c40}). Degradation rate constants, calculated from the 1st order degradation curve of each formulation, were used in ranking.

III.1.5.2.3. Ranking based on overall stability (R_s):

For each formulation the average of R_p and R_c was calculated ($R_s = (R_p + R_c)/2$), equally presenting both chemical and physical stabilities. This was calculated at each storage temperature (R_{s4} , R_{s25} , and R_{s40}).

Ranking procedures were carried out after 12 months for only 11 formulations at 4°C, 25°C and 40°C. The remaining three formulations were studied for 6 months and therefore at 4°C and at 25°C no significant stability differences were noticed but they were included in a separate ranking for the whole 14 formulations for the IsoSS at 40°C. Table 3.9 shows an example for the ranking process of the 11 PEG-INF formulations after 12 months at 4°C. In Appendix 3.I rankings for the 11 PEG-INF formulations at 25 and 40°C are shown in tables 3.I.19 and 20. Ranking of the whole 14 PEG-INF formulations based on IsoSS at 40°C after 6 months is represented in table 3.I.21.

III.1.6. Prediction quality:

Both 50% and 20% prediction qualities were determined for the correlation of T_m with stability rankings at different temperatures.

Determining the prediction quality was discussed in details in section I.1.6 of this chapter (Pages 60, 61).

Table 3. 9: Ranking procedures for 11 PEG-INF formulations based on IsoSS at 4°C after 12 months

Formulation	$K_p4^{1)}$	R_{14}	$R_{24}^{2)}$	Avr. ($R_{14}+R_{24}$)/2	R_p4	$K_c4^{3)}$	R_c4	Avr. (R_p4+R_c4)/2	R_s4
P-INFF001	0,002	1	1	1	1	0,0074	1	1	1
P-INFF002	-0,0035	10	1	5,5	10	0,0068	1	5,5	5
P-INFF003	0,0004	1	1	1	1	0,003	7	4	3
P-INFF004	-0,0025	8	1	4,5	8	0,0047	4	6	6
P-INFF006	-0,0064	11	1	6	11	0,0048	4	7,5	10
P-INFF007	0,001	1	1	1	1	0,0047	4	2,5	2
P-INFF008	-0,0024	7	1	4	7	0,0063	1	4	3
P-INFF009	-0,0003	4	1	2,5	4	-0,0002	10	7	8
P-INFF010	-0,0029	9	1	5	9	-0,0016	11	10	11
P-INFF012	-0,0008	5	1	3	5	0,0008	8	6,5	7
P-INFF014	-0,0017	6	1	3,5	6	0,0008	8	7	8

1) Monomer denaturation constant at 4°C according to SE-HPLC results.

2) Ranking based on light blockage measured particle count (table 3.I.22)

3) Chemical degradation rate constant at 4°C after 6 months IsoSS according to RP-HPLC results

III.2. Results and discussion:

III.2.1. μ DSC measurements:

A representative μ DSC thermogram for P-INFF003 is shown in figure 3.21 where the PEG-INF molecule showed only one transition at approximately 68.8°C. This was applied for all PEG-INF formulations included in this study and the resulted T_m s are listed in table 3.8.

None of the studied PEG-INF formulations showed reversibility.

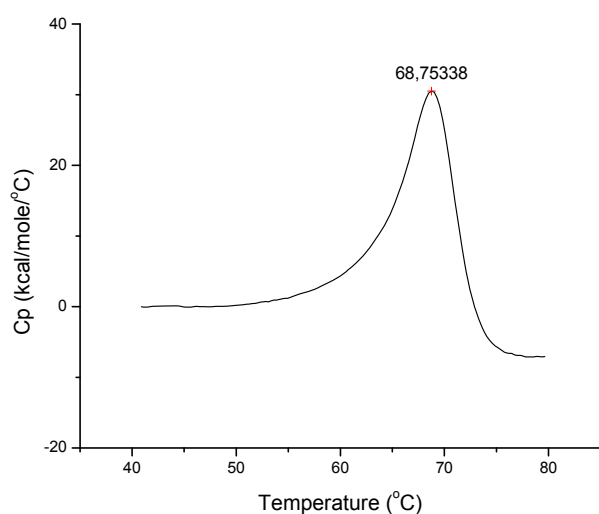


Figure 3. 21: P-INFF003 μ DSC thermogram showing unfolding transition temperature at 68.8°C. PEG-INF was formulated in 20 mM acetate buffer pH 6.

III.2.2. Isothermal stability study (IsoSS):

PEG-INF formulations were analyzed during isothermal storage at 4, 25 and 40°C according to certain time table using different analytical methods. The monomer loss rate was calculated according to 1st order kinetics for each formulation. Figure 3.22 represents an example of denaturation rate of P-INFF003 after 12 months storage obtained by SE-HPLC (A) and RP-HPLC (B).

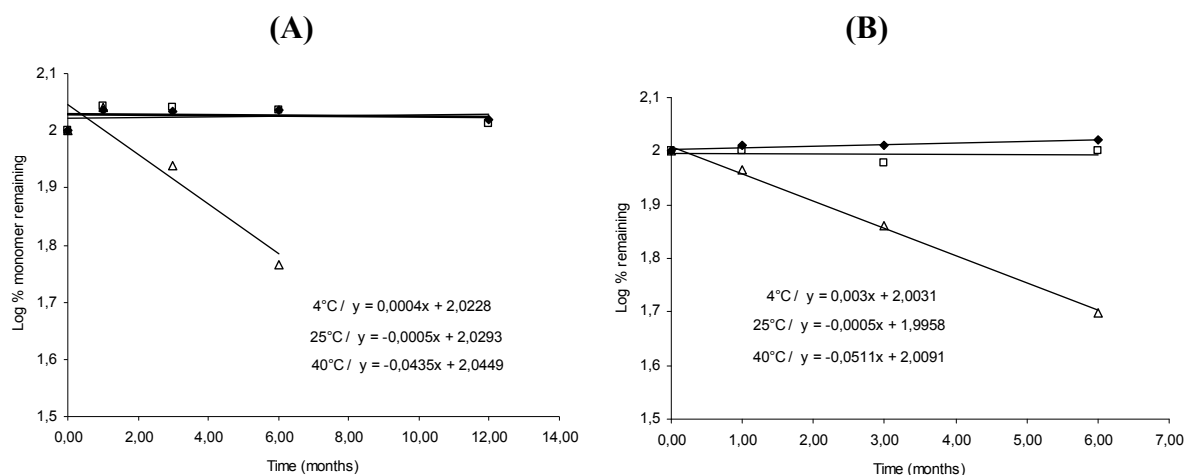


Figure 3. 22: Degradation of P-INFF003 during isothermal stability study at 4°C (–■–), 25°C (–□–) and 40°C (–Δ–). (A) Monomer loss as measured by SE-HPLC over 12 months. (B) Chemical degradation as measured by RP-HPLC.

Light obscuration measurements were used to determine insoluble aggregates in each formulation. In Appendix 3.I particle counts at the end point are listed in table 3.I.22.

SDS-PAGE was carried out for all formulations at zero time and after 6 months of the IsoSS. SDS-PAGE gels are presented in figures 3.23. The bands showed broadening and after stress some formulations showed smearing. Such behaviour was reported for pegylated proteins when analyzed by SDS-PAGE⁴⁷⁻⁴⁹ where such effects increased with increasing either PEG or SDS concentrations. An explanation for that might be the complex interaction between PEG chains and SDS micelles⁵⁰. After 6 months storage at 40°C many PEG-INF formulations showed smearing indicating increased concentrations of free poly ethylene glycol (PEG) in the formulation.

III.2.3. μ DSC as a predictive tool for IsoSS of PEG-INF:

The predictive power of μ DSC was judged primarily on the resulted Pearson product moment correlation coefficients from correlating the ranking based on μ DSC with those based on IsoSS. Secondary, the predictive power was tested with regards to the prediction quality.

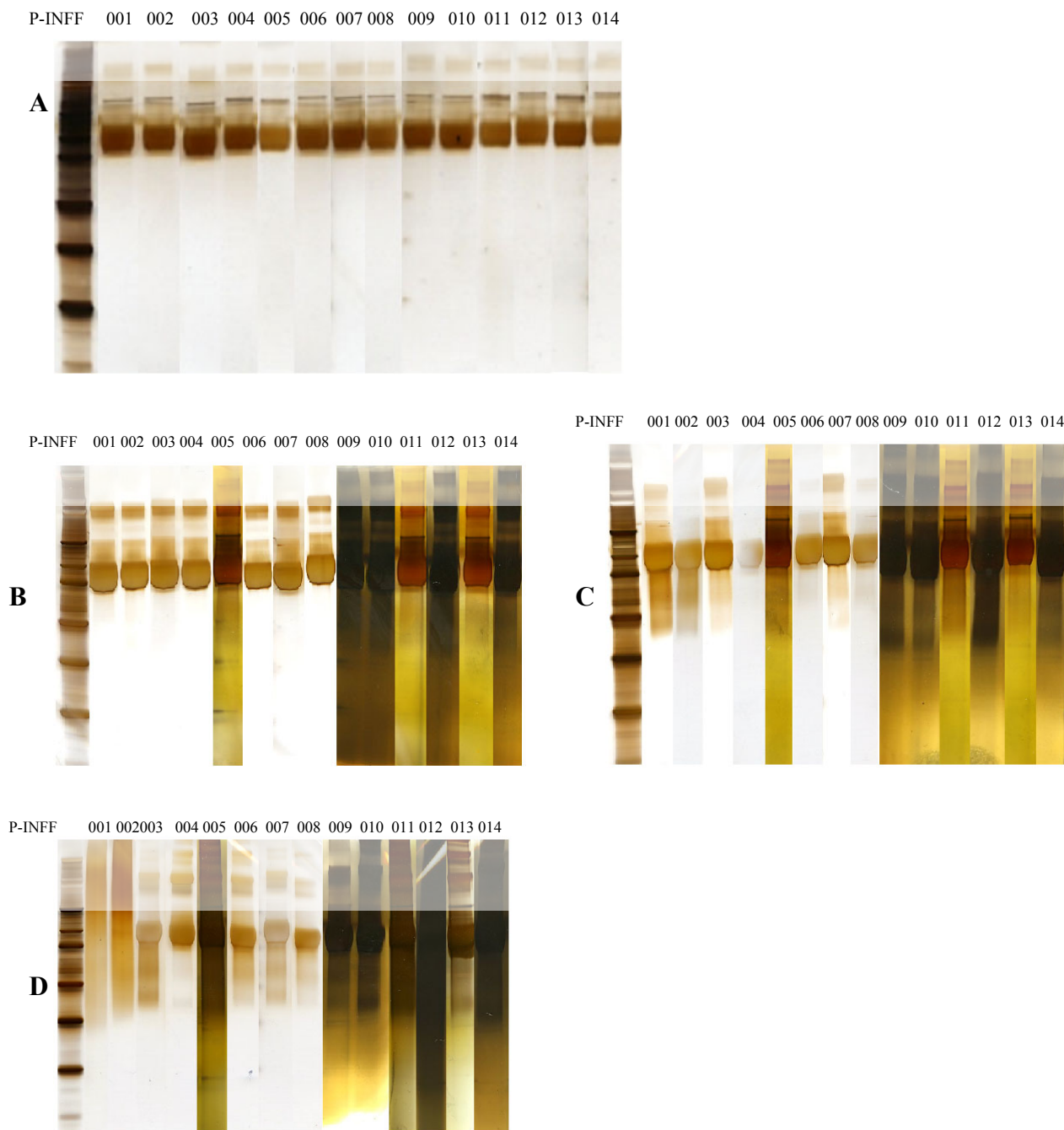


Figure 3. 23: SDS-PAGE for 14 PEG-INF formulations at the beginning (A) of the IsoSS and after 6 months storage at 4°C (B) and 25°C (C) and 40°C (D). Composition of formulations P-INFF001 – P-INFF014 (see table 3.8)

III.2.3.1. Correlation coefficients:

All correlation curves are presented in appendix 3.II figures 3.II.17 – 20. An overview for the resulting correlation coefficients is presented in figure 3.24. Figure 3.24 A shows the correlation coefficients (presented on the y-axis) of T_m based ranking and physical, chemical, and overall stability ranking (R_p , R_c , and R_s , respectively and presented on the z-axis) after 12 months storage at 4 and 25 °C and 6 months storage at 40°C (temperatures are presented on

the x-axis) for the 11 PEG-INF formulations. Figure 3.24 B is similarly constructed and presenting the correlation coefficients resulting from correlating the T_m based ranking with the physical chemical and overall stability after 6 months storage at 40°C but for the whole 14 PEG-INF formulations.

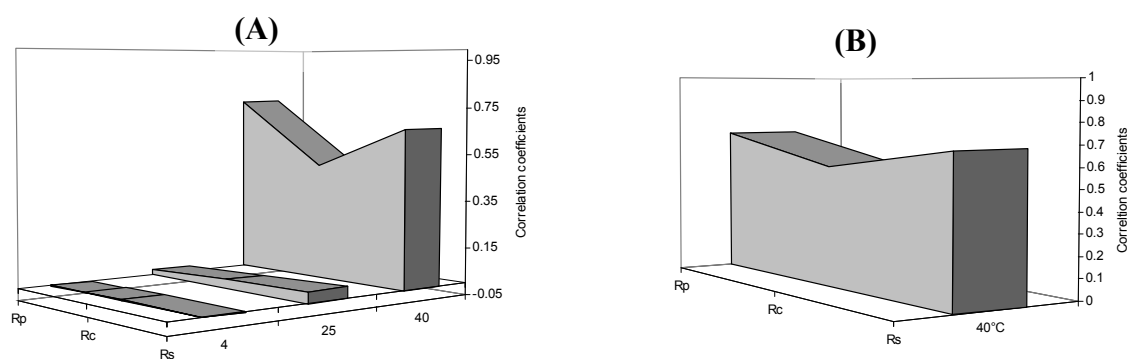


Figure 3. 24: An overview for the correlation coefficients (y-axis) resulting from correlating the ranking based on physical stability (R_p), chemical stability (R_c) and overall stability ranking (R_s) (z-axis) at different temperatures (4, 25, and 40°C) (x-axis) with ranking based on T_m (R_{Tm}) of 11 PEG-INF formulations after 12 months IsoSS (A) and for the whole 14 PEG-INF formulations at 40°C after 6 months IsoSS (B).

From the correlation coefficients represented in figure 3.24 and similar to the correlation found for GCSF and MAB in the 1st and 2nd part of this chapter, T_m was not able to predict the exact rank order of the formulations after 12 months isothermal stability study. Surprisingly and in contrast to GCSF and MAB, the higher correlation coefficients were obtained for IsoSS at 40°C. On the other hand at 4 and 25°C very weak predictions were observed. This behavior was also seen in predicting the IsoSS stability of the whole 14 PEG-INF formulations at 40°C. As shown from the correlation coefficients the prediction of chemical stability is weaker than predicting both physical and overall stability of the PEG-INF formulations.

Pegylation of therapeutic proteins is performed in order to improve molecule life time in blood and reduce immune responses^{51,52}. In such process one or more PEG molecules are covalently attached to the protein. Pegylation of Interferon α 2a caused an increase in T_m indicating higher conformation stability¹⁴. The same was reported for many other proteins molecule where T_m showed higher values due to pegylation^{53,54}. In literature the main hypothesis describing the molecular mechanism by which pegylation increases the thermodynamic stability is that the protein structure becomes more rigid^{53,55}. During storage of PEG-INF formulation chemical dissociation of the PEG molecule from the protein (de-

pegylation) may take place. Once that happens the protein molecule would not be protected any more and therefore will denature faster. That would explain the degradation profile of some PEG-INF formulations involved in this study. Figure 3.25 shows the monomer loss of P-INFF001, as an example of such behaviour, at three different temperatures. At 25°C the monomer loss was very slow during the first 6 months and faster during the last 6 months. This biphasic denaturation behaviour could be explained by the first de-pegylation step and once it happens fast monomer loss takes place. Such behaviour seems to be temperature dependent (figure 3.25) seeing that at 4°C approximately no reduction in monomer content is noticed where the de-pegylation is not happening or very slow. Increasing the temperature to 25°C the first step was faster and the second step begun somewhere in the last 6 months while at 40°C the first step is very fast and was not detected by the used sampling intervals. The suggestion that the first slow step is de-pegylation is supported by the results of SDS-PAGE shown above and represented in figure 3.23 where at 40°C formulations showed smearing which indicates the presence of free PEG molecule. This smearing was weaker at 25°C and almost absent at 4°C proving that de-pegylation is a temperature dependent process in these formulations.

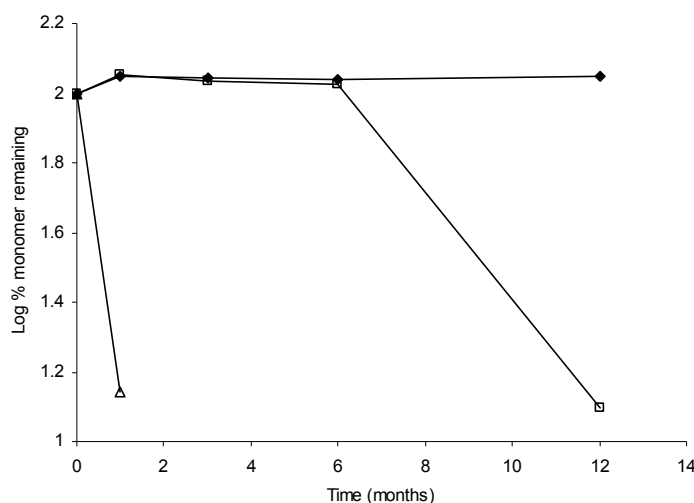


Figure 3. 25: Monomer loss of P-INFF001 during isothermal stability study at 4°C (—■—), 25°C (—□—) and 40°C (—△—).

During a μ DSC measurement samples were heated from room temperature to 80°C. Assuming that the theory of de-pegylation is true and that it is a temperature dependent process, then it is expected that it will happen during the temperature ramp in the μ DSC. This means that during the measurement the pegylated protein will be de-pegylated somewhere, most probably, before reaching T_m . Accordingly the resulting T_m might come later but the unfolding is happening to the naked INF molecule without pegylation. On the other hand, if the de-pegylation theory were true, then the denaturation of the PEG-INF molecule at 40°C

would be also a denaturation of a naked INF without pegylation and therefore excellently predicted with T_m . In contrast, that would not be the case at 4°C where de-pegylation either very slow or never takes place. Therefore, predicting the stability of the PEG-INF formulations at 4°C was not successful using T_m .

III.2.3.2. Prediction quality:

Figure 3.26 A and B represent the 50% and 20% prediction, respectively for T_m based ranking in predicting physical, chemical and overall stability of 11 PEG-INF formulations at three different temperatures (4, 25 and 40°C). T_m was able to predict the stability of PEG-INF formulation with higher 50% prediction quality at 40°C regarding all stability rankings (figure 3.26 A). 20% prediction quality showed that T_m is still able to predict one of the best 2 formulations in IsoSS at 4°C.

Based on both correlation coefficients and the “prediction quality” tool T_m was not able to predict well the long term stability at 4°C but, in contrast to GCSF and MAB studies, the best prediction was to the stability of the PEG-INF at 40°C.

III.2.4. μ DSC in comparison with classical accelerated IsoSS:

Although predicting the long term stability of PEG-INF formulations at 4°C was not possible using T_m based ranking, but selecting the best formulations and excluding the bad ones was still possible (figure 3.26) even for the stability at 4°C.

Therefore, it still makes sense to compare T_m with classical accelerated stability studies in predicting the long term stability of PEG-INF at 4°C. Such information is very useful especially when a formulator has only few methods to predict the stability of a pegylated protein. With this respect, the predictive power of μ DSC T_m against classical accelerated stability studies was investigated. The IsoSS based rankings after 12 months storage at 25°C and after 6 months at 40°C were correlated with the IsoSS based ranking after 12 months at 4°C and correlation curves are presented in figure 3.27. The predictive power of those accelerated stability studies were compared with that of μ DSC. Figure 3.28 shows an overview of the resulting correlation coefficients. The comparison showed stronger correlation with IsoSS at 25°C than both T_m and IsoSS at 40°C. Such behaviour would fit with the correlation discussed in the last section as the 1st de-pegylation step at 25°C has the closest rate to that at 4°C and both fast T_m determination and higher temperature IsoSS are completely uncorrelated with the ranking based on IsoSS at 4°C.

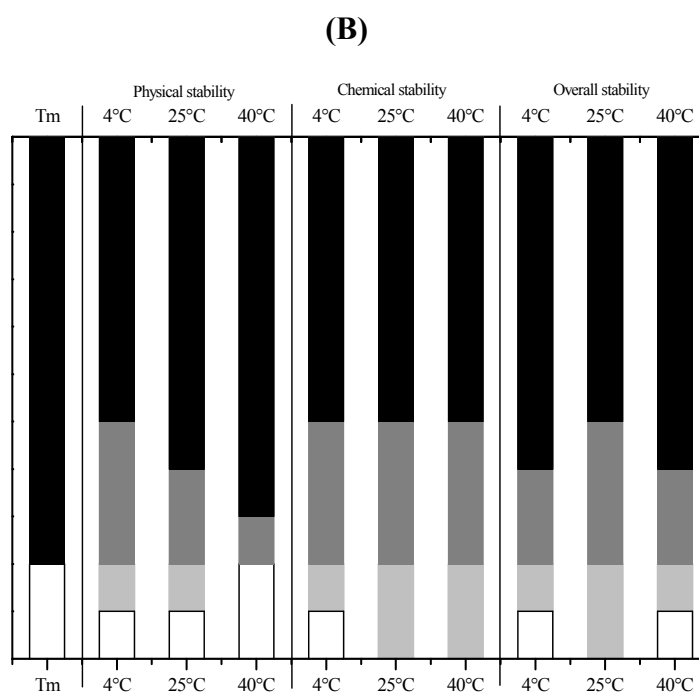
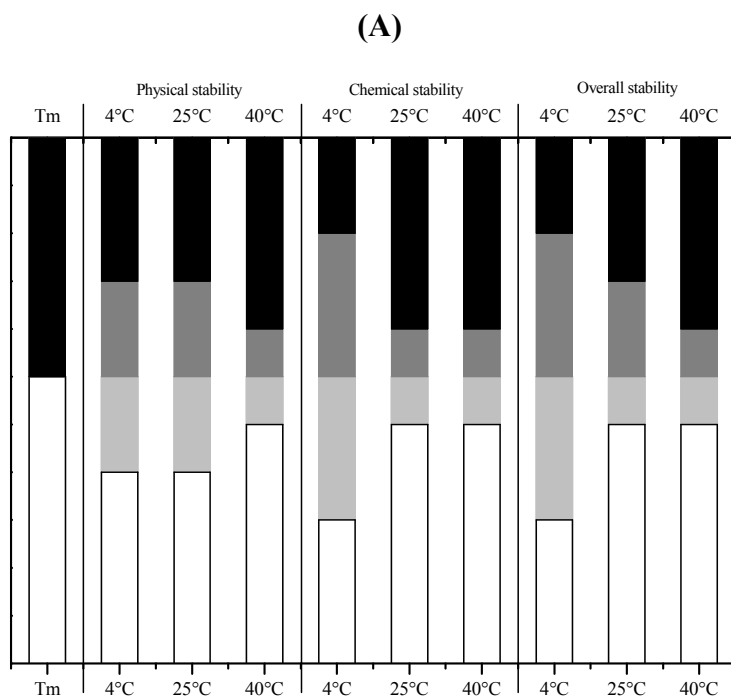


Figure 3. 26: Reliability of T_m based ranking to pick up the best 6 formulations and exclude the bad 5 (50% prediction quality (A)) and to pick up the best 2 and exclude the rest (20% prediction quality (B)) in an 11 PEG-INF formulation set.

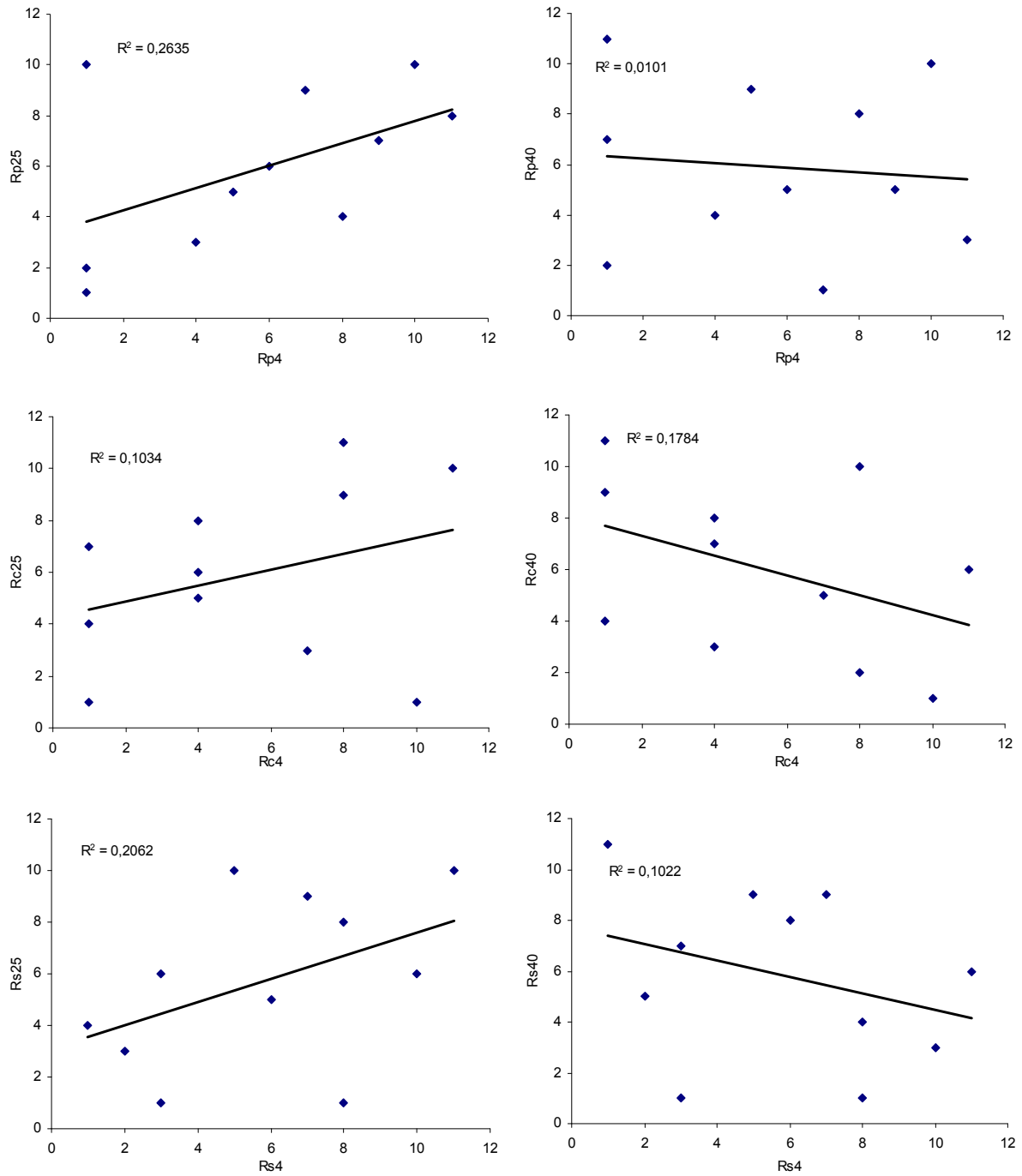


Figure 3.27: Correlation curves of 11 PEG-INF formulations. That includes correlation between rankings based on IsoSS at 4°C (R_{p4} , R_{c4} and R_{s4}) after 12 months, and ranking based on IsoSS at elevated temperatures (25 and 40°C)

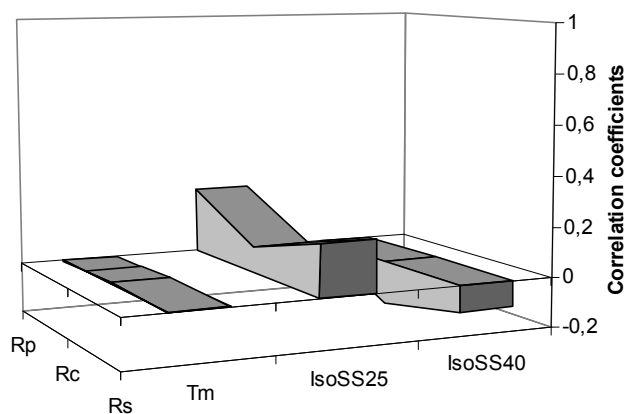


Figure 3. 28: An overview for the correlation coefficients resulting from correlating the IsoSS based rankings at 4°C (R_p , R_c and R_s) (z-axis) with rankings based on either μ DSC determined T_m (R_{T_m}) or accelerated stability studies at elevated temperatures (25 and 40°C).

Studying the 50% and 20% prediction quality in figures 3.29 A and B, respectively, the selection was best made based on IsoSS at 25°C too. But despite the very weak correlation coefficients the prediction quality showed the possibility of selecting the best formulations based on T_m . Such selection proved to be more successful than a selection based on IsoSS at 40°C.

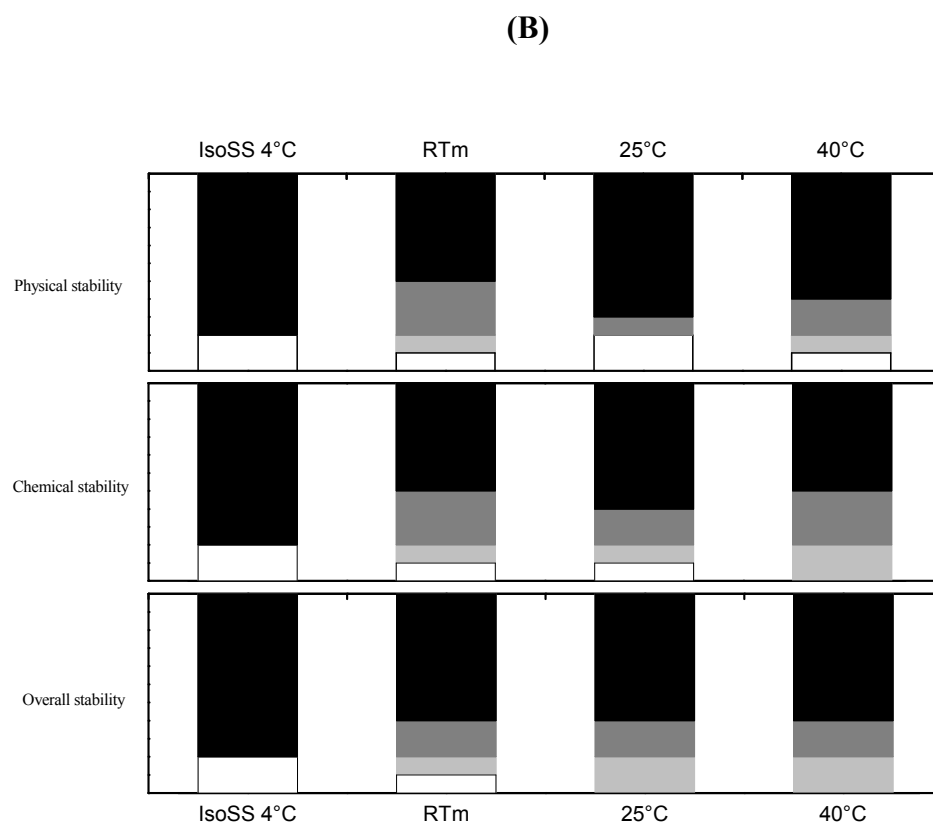
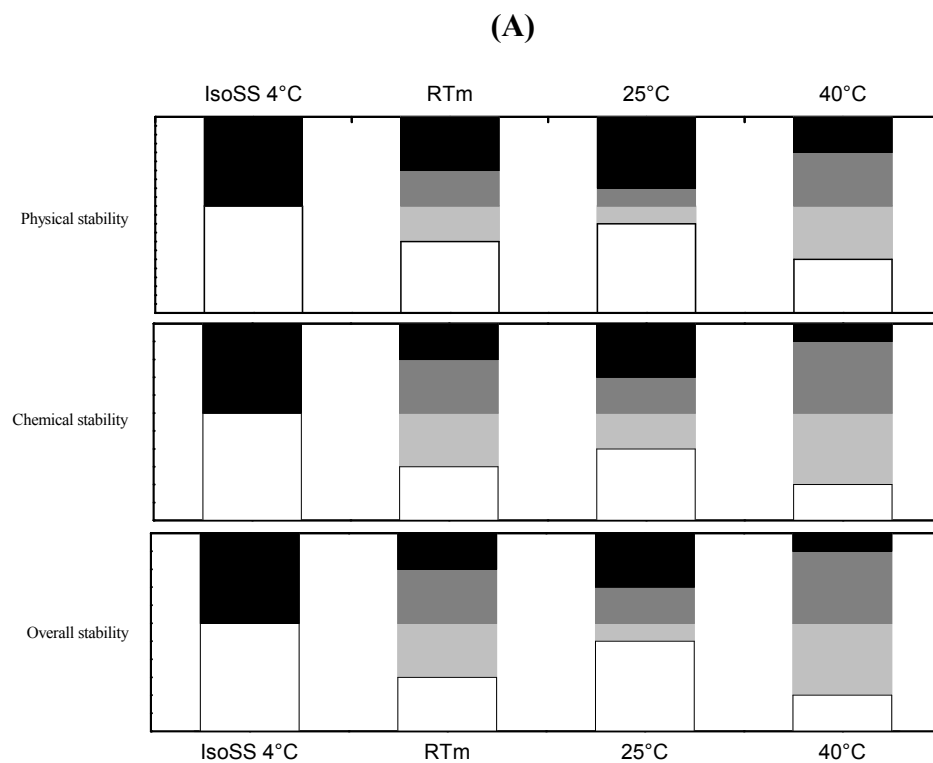


Figure 3. 29: 50% (A) and 20% (B) prediction quality of μ DSC measured T_m and IsoSS at 25°C and 40°C in predicting IsoSS at 4°C

2. Conclusion:

μ DSC determined T_m was critically evaluated with regards to its predictive power of long term stability of three different protein molecules. Those three proteins were considered as interesting and relevant candidates for the purpose of the study as each protein represents a unique class and shows different stability behaviour. The long term stability of GCSF is determined by both chemical and physical effects where pH and salt content of the formulation determine the extent of aggregation and chemical degradation. MAB is a protein class where physical stability mainly determines its long term stability. PEG-INF is an example of a pegylated protein and expected to be stable on long term.

Even in large groups of formulations, where T_m was not able to predict the exact rank order, selecting the good formulations and excluding the bad ones was an excellent approach to reduce the work load in long term stability studies. Surprisingly, T_m showed stronger correlation and more reliability than routinely applied accelerated stability studies (at 40°C). This was even true in the case of PEG-INF where accelerated prediction is generally not successful.

μ DSC provided different information about the protein conformational stability. In this study each protein showed a different μ DSC profile and thus the predictive power was not the same for the 3 studied proteins.

In 24 GCSF formulations, where T_m and unfolding reversibility could be determined, further optimization of T_m based ranking by considering the degree of unfolding reversibility did not show any significant benefit on predictions. T_m showed superior predictive power, in predicting the overall stability ranking especially at 4°C. Moreover, predictive studies based on T_m measurements had proved superiority in predicting physical and accordingly overall stability ranking to the routinely performed accelerated isothermal stability studies at 40°C. Although ranking based on IsoSS at 25°C showed higher correlation coefficients and higher prediction quality toward real time stability at 4°C, 9 to 12 months are needed to reach predictive results. Predictive studies using μ DSC for 24 formulations can be carried out in an experimental plan which needs maximum 4 weeks to be done and delivers approximately similar correlation coefficients and equal prediction quality compared to IsoSS at 25°C. Concerning chemical stability, IsoSS at elevated temperatures (e.g. 40°C) showed significantly higher correlation coefficients and higher prediction quality.

In a μ DSC study of 15 MAB formulations three different transitions were determined. Selecting the good formulations and excluding the bad ones was very successful based on the earliest transition (T_{m1}) especially for long term stability at 4°C. Predictive studies based on

T_m 1 measurements had proved superiority in predicting physical stability ranking to the routinely performed accelerated isothermal stability studies at elevated temperatures.

For PEG-INF formulations T_m based ranking was not able to predict the long term stability at 4°C but selecting the good formulations and excluding the bad ones still did work. Pegylation of a protein molecule makes the prediction process much more complicated. This might be due to a complex degradation biphasic process where an assumed “de-pegylation” process might happen prior to the expected physical denaturation. On the other hand, prediction of the accelerated stability at 40°C was excellent using T_m .

3. References:

1. Lindman, S.; Xue, W. F.; Szczepankiewicz, O.; Bauer, M. C.; Nilsson, H.; Linse, S. Salting the charged surface: pH and salt dependence of protein G B1 stability. *Biophysical Journal* 90[8], 2911-2921. 2006.
2. Kang, F.; Jiang, G.; Hinderliter, A.; DeLuca, P. P.; Singh, J. Lysozyme Stability in Primary Emulsion for PLGA Microsphere Preparation: Effect of Recovery Methods and Stabilizing Excipients. *Pharmaceutical Research* 19[5], 629-633. 2002.
3. Singh, S.; Singh, J. Effect of polyols on the conformational stability and biological activity of a model protein lysozyme. *AAPS PharmSciTech* 4[3], 334-342. 2003.
4. Remmele, R. L., Jr.; Nightlinger, N. S.; Srinivasan, S.; Gombotz, W. R. Interleukin-1 receptor (IL-1R) liquid formulation development using differential scanning calorimetry. *Pharmaceutical Research* 15[2], 200-208. 1998.
5. Burton, L.; Gandhi, R.; Duke, G.; Paborji, M. Use of Microcalorimetry and Its Correlation with Size Exclusion Chromatography for Rapid Screening of the Physical Stability of Large Pharmaceutical Proteins in Solution. *Pharmaceutical Development and Technology* 12[3], 265-273. 2007.
6. Ausar, S. F.; Espina, M.; Brock, J.; Thyagarayapuram, N.; Repetto, R.; Khandke, L.; Middaugh, C. R. High-throughput screening of stabilizers for respiratory syncytial virus: identification of stabilizers and their effects on the conformational thermostability of viral particles. *Human Vaccines* 3[3], 94-103. 2007.
7. Remmele, R. L., Jr.; Bhat, S. D.; Phan, D. H.; Gombotz, W. R. Minimization of Recombinant Human Flt3 Ligand Aggregation at the T_m Plateau: A Matter of Thermal Reversibility. *Biochemistry* 38[16], 5241-5247. 1999.
8. Kuelto, L. A.; Middaugh, C. R. Structural characterization of bovine granulocyte colony stimulating factor: Effect of temperature and pH. *Journal of Pharmaceutical Sciences* 92[9], 1793-1804. 2003.
9. Chi, E. Y.; Krishnan, S.; Kendrick, B. S.; Chang, B. S.; Carpenter, J. F.; Randolph, T. W. Roles of conformational stability and colloidal stability in the aggregation of recombinant human granulocyte colony-stimulating factor. *Protein Science* 12[5], 903-913. 2003.
10. Yin, J.; Chu, J. W.; Ricci, M. S.; Brems, D. N.; Wang, D. I. C.; Trout, B. L. Effects of Excipients on the Hydrogen Peroxide-Induced Oxidation of Methionine Residues in Granulocyte Colony-Stimulating Factor. *Pharmaceutical Research* 22[1], 141-147. 2005.
11. Thirumangalathu, R.; Krishnan, S.; Brems, D. N.; Randolph, T. W.; Carpenter, J. F. Effects of pH, temperature, and sucrose on benzyl alcohol-induced aggregation of recombinant human granulocyte colony stimulating factor. *Journal of Pharmaceutical Sciences* 95[7], 1480-1497. 2006.
12. Park, S. S.; Kim, J.; Brandts, J. F.; Hong, H. J. Stability of murine, chimeric and humanized antibodies against pre-S2 surface antigen of hepatitis B virus. *Biologicals* 31[4], 295-302. 2003.

13. Welfle, K.; Misselwitz, R.; Hausdorf, G.; Hohne, W.; Welfle, H. Conformation, pH-induced conformational changes, and thermal unfolding of anti-p24 (HIV-1) monoclonal antibody CB4-1 and its Fab and Fc fragments. *Biochimica et Biophysica Acta, Protein Structure and Molecular Enzymology* 1431[1], 120-131. 1999.
14. Dhalluin, C.; Ross, A.; Leuthold, L. A.; Foser, S.; Gsell, B.; Mueller, F.; Senn, H. Structural and Biophysical Characterization of the 40 kDa PEG-Interferon- α 2a and Its Individual Positional Isomers. *Bioconjugate Chemistry* 16[3], 504-517. 2005.
15. Bailon, P.; Palleroni, A.; Schaffer, C. A.; Spence, C. L.; Fung, W. J.; Porter, J. E.; Ehrlich, G. K.; Pan, W.; Xu, Z. X.; Modi, M. W.; Farid, A.; Berthold, W.; Graves, M. Rational Design of a Potent, Long-Lasting Form of Interferon: A 40 kDa Branched Polyethylene Glycol-Conjugated Interferon α -2a for the Treatment of Hepatitis C. *Bioconjugate Chemistry* 12[2], 195-202. 2001.
16. Machida, M. Pharmaceutical containing stabilized granulocyte colony-stimulating factor. DE A1 3723781, Jul 17, 1987.
17. Boone, T. C. Stabilized hydrophobic protein formulations. EP A2 373679, 1991.
18. Michaelis, U.; Rudolph, R.; Winter, G.; Woog, H. Buffers for stabilization of aqueous pharmaceutical preparations of G-CSF. DE A1 4242919, 1994.
19. Baumann, M.; Beck, W.; Marschner, J.-P.; Naoumov, N. Combined pharmaceutical preparations containing human monoclonal antibodies for treating chronic hepatitis B. WO A1 9904814, Feb 4, 1999.
20. Kallmeyer, G.; Winter, G.; Klessen, C.; Woog, H. Stable lyophilized pharmaceutical substances from monoclonal or polyclonal antibodies. WO A2 9822136, 19980528.
21. Gross, G.; Del Terzo, S.; Kumar, S. K. Interferon solution for parenteral administration. EP A2 736303, 1996.
22. Gareth A. Lewis; Didier Mathieu; Roger Phan-Tan-Luu . Pharmaceutical Experimental Design. 23-150. 1999. Marcel Dekker, Inc.
23. Podobnik, B.; Gaberc Porekar, V.; Menart, V. Stable pharmaceutical composition comprising granulocyte-colony stimulating factor. WO A1 2005042024, May 12, 5 A.D.
24. Lovatt, M.; Cooper, A.; Camilleri, P. Energetics of cyclodextrin-induced dissociation of insulin. *Journal of Inclusion Phenomena and Molecular Recognition in Chemistry* 25[1-3], 169-172. 1996.
25. Irie, T.; Uekama, K. Cyclodextrins in peptide and protein delivery. *Advanced Drug Delivery Reviews* 36[1], 101-123. 1999.
26. Ricci, M. S.; Sarkar, C. A.; Fallon, E. M.; Lauffenburger, D. A.; Brems, D. N. pH Dependence of structural stability of interleukin-2 and granulocyte colony-stimulating factor. *Protein Sci* 12[5], 1030-1038. 2003.

27. Herman, A. C.; Boone, T. C.; Lu, H. S. Characterization, formulation, and stability of Neupogen (Filgrastim), a recombinant human granulocyte-colony stimulating factor. *Pharmaceutical Biotechnology* 9, 303-328. 1996.
28. Johnston, T. P. Adsorption of recombinant human granulocyte colony stimulating factor (rhG-CSF) to polyvinyl chloride, polypropylene, and glass: Effect of solvent additives. *PDA Journal of Pharmaceutical Science and Technology* 50[4], 238-245. 1996.
29. Bam, N. B.; CLeland, J. L.; Yang, J.; Manning, M. C.; Carpenter, J. F.; Kelley, R. F.; Randolph, T. W. Tween Protects Recombinant Human Growth Hormone against Agitation-Induced Damage via Hydrophobic Interactions. *Journal of Pharmaceutical Sciences* 87[12], 1554-1559. 1998.
30. Randolph, T. W.; Jones, L. S. Surfactant-protein interactions. *Pharmaceutical Biotechnology* 13[Rational Design of Stable Protein Formulations], 159-175. 2002.
31. Krishnan, S.; Chi, E. Y.; Webb, J. N.; Chang, B. S.; Shan, D.; Goldenberg, M.; Manning, M. C.; Randolph, T. W.; Carpenter, J. F. Aggregation of Granulocyte Colony Stimulating Factor under Physiological Conditions: Characterization and Thermodynamic Inhibition. *Biochemistry* 41[20], 6422-6431. 2002.
32. Pan, B.; Abel, J.; Ricci, M. S.; Brems, D. N.; Wang, D. I. C.; Trout, B. L. Comparative Oxidation Studies of Methionine Residues Reflect a Structural Effect on Chemical Kinetics in rhG-CSF. *Biochemistry* 45[51], 15430-15443. 2006.
33. Chi, E. Y.; Krishnan, S.; Randolph, T. W.; Carpenter, J. F. Physical Stability of Proteins in Aqueous Solution: Mechanism and Driving Forces in Nonnative Protein Aggregation. *Pharmaceutical Research* 20[9], 1325-1336. 2003.
34. Weiss, W. F., IV; Young, T. M.; Roberts, C. J. Principles, approaches, and challenges for predicting protein aggregation rates and shelf life. *J.Pharm.Sci.* 98[4], 1246-1277. 2009.
35. Ijeoma, O.; Hollowell, H. N.; Bodnar, M. A.; Britt, B. M. Thermodynamic analysis of the nondenaturational conformational change of baker's yeast phosphoglycerate kinase at 24 DegC. *Arch.Biochem.Biophys.* 478[2], 206-211. 2008.
36. Bechtel, W. J.; Schellman, J. A. Protein stability curves. *Biopolymers* 26[11], 1859-1877. 1987.
37. Sanchez-Ruiz, J. M.; Lopez-Lacomba, J. L.; Cortijo, M.; Mateo, P. L. Differential scanning calorimetry of the irreversible thermal denaturation of thermolysin. *Biochemistry* 27[5], 1648-1652. 1988.
38. Remmele, R. L., Jr.; Zhang-van Enk, J.; Dharmavaram, V.; Balaban, D.; Durst, M.; Shoshitaishvili, A.; Rand, H. Scan-Rate-Dependent Melting Transitions of Interleukin-1 Receptor (Type II): Elucidation of Meaningful Thermodynamic and Kinetic Parameters of Aggregation Acquired from DSC Simulations. *Journal of the American Chemical Society* 127[23], 8328-8339. 2005.

39. Kroon, D. J.; Baldwin-Ferro, A.; Lalan, P. Identification of sites of degradation in a therapeutic monoclonal antibody by peptide mapping. *Pharm.Res.* 9[11], 1386-1393. 1992.
40. Johnson, R. E. Stable pH optimized formulation of a modified antibody, TNFalpha specific humanized antibody CDP870. WO A2 2004019861, Mar 11, 2004.
41. Usami, A.; Ohtsu, A.; Takahama, S.; Fujii, T. The effect of pH, hydrogen peroxide and temperature on the stability of human monoclonal antibody. *J.Pharm.Biomed.Anal.* 14[8-10], 1133-1140. 1996.
42. Vermeer, A. W. P.; Norde, W. The thermal stability of immunoglobulin: unfolding and aggregation of a multi-domain protein. *Biophysical Journal* 78[1], 394-404. 2000.
43. Tischenko, V. M.; Zav'yalov, V. P.; Medgyesi, G. A.; Potekhin, S. A.; Privalov, P. L. A thermodynamic study of cooperative structures in rabbit immunoglobulin G. *Eur J Biochem* 126[3], 517-521. 1982.
44. Tischenko, V. M.; Abramo, V. M.; Zavyalov, V. P. Investigation of the Cooperative Structure of Fc Fragments from Myeloma Immunoglobulin G. *Biochemistry* 37[16], 5576-5581. 1998.
45. Ionescu, R. M.; Vlasak, J.; Price, C.; Kirchmeier, M. Contribution of variable domains to the stability of humanized IgG1 monoclonal antibodies. *Journal of Pharmaceutical Sciences* 97[4], 1414-1426. 2008.
46. Vermeer, A. W. P.; Bremer, M. G. E. G.; Norde, W. Structural changes of IgG induced by heat treatment and by adsorption onto a hydrophobic Teflon surface studied by circular dichroism spectroscopy. *Biochim.Biophys.Acta, Gen.Subj.* 1425[1], 1-12. 1998.
47. Zheng, C. Y.; Ma, G.; Su, Z. Native PAGE eliminates the problem of PEG-SDS interaction in SDS-PAGE and provides an alternative to HPLC in characterization of protein PEGylation. *Electrophoresis* 28[16], 2801-2807. 2007.
48. Yun, Q.; Xing, W.; Ma, G.; Su, Z. Preparation and characterization of mono-PEGylated consensus interferon by a novel polyethylene glycol derivative. *J.Chem.Technol.Biotechnol.* 81[5], 776-781. 2006.
49. Odom, O. W.; Kudlicki, W.; Kramer, G.; Hardesty, B. An effect of polyethylene glycol 8000 on protein mobility in sodium dodecyl sulfate-polyacrylamide gel electrophoresis and a method for eliminating this effect. *Anal.Biochem.* 245[2], 249-252. 1997.
50. Bernazzani, L.; Borsacchi, S.; Catalano, D.; Gianni, P.; Mollica, V.; Vitelli, M.; Asaro, F.; Feruglio, L. On the Interaction of Sodium Dodecyl Sulfate with Oligomers of Poly(Ethylene Glycol) in Aqueous Solution. *J.Phys.Chem.B* 108[26], 8960-8969. 2004.
51. Abuchowski, A.; McCoy, J. R.; Palczuk, N. C.; Van Es, T.; Davis, F. F. Effect of covalent attachment of polyethylene glycol on immunogenicity and circulating life of bovine liver catalase. *J.Biol.Chem.* 252[11], 3582-3586. 1977.

52. Abuchowski, A.; Van Es, T.; Palczuk, N. C.; Davis, F. F. Alteration of immunological properties of bovine serum albumin by covalent attachment of polyethylene glycol. *J.Biol.Chem.* 252[11], 3578-3581. 1977.
53. Lopez-Cruz, J. I.; Viniegra-Gonzalez, G.; Hernandez-Arana, A. Thermostability of Native and Pegylated *Myceliophthora thermophila* Laccase in Aqueous and Mixed Solvents. *Bioconjugate Chem.* 17[4], 1093-1098. 2006.
54. Nie, Y.; Zhang, X.; Wang, X.; Chen, J. Preparation and Stability of N-Terminal Mono-PEGylated Recombinant Human Endostatin. *Bioconjugate Chem.* 17[4], 995-999. 2006.
55. Rodriguez-Martinez, J. A.; Sola, R. J.; Castillo, B.; Cintron-Colon, H. R.; Rivera-Rivera, I.; Barletta, G.; Griebenow, K. Stabilization of alpha -chymotrypsin upon PEGylation correlates with reduced structural dynamics. *Biotechnol.Bioeng.* 101[6], 1142-1149. 2008.

4. Appendix 3.I:

Table 3.I. 1: Particle count after isothermal storage of GCSF liquid formulation of DOEa at 4, 25 and 40°C.

Formulations	Particle range	4°C	25°C	40°C
		(20 - 24 months)	(10 months)	(3 months)
GCSFDa1	> 1 µm	53	200	463
	> 10 µm	0	4	0
	> 25 µm	0	1	0
GCSFDa2	> 1 µm	271	682	9493
	> 10 µm	11	36	144
	> 25 µm	2	2	10
GCSFDa3	> 1 µm	214	340	1078
	> 10 µm	16	29	24
	> 25 µm	0	0	3
GCSFDa4	> 1 µm	211	227	4778
	> 10 µm	8	3	22
	> 25 µm	3	1	0
GCSFDa5	> 1 µm	1848	14179	15929
	> 10 µm	6	10	263
	> 25 µm	3	1	10
GCSFDa6	> 1 µm	448	7811	3156
	> 10 µm	8	511	100
	> 25 µm	3	78	0
GCSFDa7	> 1 µm	96	292	2477
	> 10 µm	0	11	4
	> 25 µm	0	1	0
GCSFDa8	> 1 µm	238	299	1234
	> 10 µm	16	3	20
	> 25 µm	6	1	2

Table 3.I. 2: Particle count after isothermal storage of GCSF liquid formulation of DOEb at 4, 25 and 40°C.

Formulations	Particle range	4°C	25°C	40°C
		(20 months)	(10 months)	(3 months)
GCSFDb1	> 1 µm	52	99	56
	> 10 µm	2	2	1
	> 25 µm	2	1	0
GCSFDb2	> 1 µm	49	158	137
	> 10 µm	4	3	2
	> 25 µm	2	1	1
GCSFDb3	> 1 µm	183	273	1044
	> 10 µm	3	2	14
	> 25 µm	0	0	1
GCSFDb4	> 1 µm	91	312	350
	> 10 µm	9	18	6
	> 25 µm	1	1	2
GCSFDb5	> 1 µm	19910	14704	12009
	> 10 µm	166	320	328
	> 25 µm	12	26	168
GCSFDb6	> 1 µm	3991	2002	11750
	> 10 µm	169	344	3499
	> 25 µm	17	94	2011
GCSFDb7	> 1 µm	3041	15871	389
	> 10 µm	12	40	18
	> 25 µm	3	3	11
GCSFDb8	> 1 µm	14049	9076	6652
	> 10 µm	289	946	57
	> 25 µm	12	103	2

Table 3.I. 3: Particle count after isothermal storage of GCSF liquid formulation of DOEc at 4, 25 and 40°C.

Formulations	Particle range	4°C	25°C	40°C
		(20 months)	(10 months)	(3 months)
GCSFDc1	> 1 µm	699	568	1451
	> 10 µm	6	20	14
	> 25 µm	2	7	1
GCSFDc2	> 1 µm	826	731	1300
	> 10 µm	8	3	4
	> 25 µm	1	1	0
GCSFDc3	> 1 µm	1007	857	1836
	> 10 µm	13	18	12
	> 25 µm	3	2	0
GCSFDc4	> 1 µm	786	1214	989
	> 10 µm	7	10	12
	> 25 µm	0	2	0
GCSFDc5	> 1 µm	850	373	260
	> 10 µm	63	10	9
	> 25 µm	10	3	0
GCSFDc6	> 1 µm	4910	2554	8401
	> 10 µm	101	90	119
	> 25 µm	10	10	26
GCSFDc7	> 1 µm	3232	4554	1599
	> 10 µm	37	47	29
	> 25 µm	8	12	7
GCSFDc8	> 1 µm	11831	3539	4713
	> 10 µm	266	442	93
	> 25 µm	23	28	12

Table 3.I. 4: IsoSS ranking of GCSF formulations in DOEa after 10 months storage at 25°C

Formulations	K _p 25	R ₁ 25	Tur. ₂₅ ¹⁾	R ₂ 25	Avr. (R ₁ 25+R ₂ 25)/2	R _p 25	K _c 25	R _c 25	Avr. (R _p 25+R _c 25)/2	R _s 25
GCSFDa1	-0,0019	1	0.82	1	1	1	-0,0017	2	1,5	1
GCSFDa2	-0,0388	7	0.7	1	4	4	0,0008	1	2,5	2
GCSFDa3	-0,0139	4	1.1	6	5	7	-0,0262	7	7	8
GCSFDa4	-0,0134	3	1.34	6	4.5	5	-0,0236	6	5,5	5
GCSFDa5	-0,0097	2	0.73	1	1.5	2	-0,0051	4	3	3
GCSFDa6	-0,0141	5	1.18	6	5.5	8	-0,0026	3	5,5	6
GCSFDa7	-0,0194	6	0.71	1	3.5	3	-0,0652	8	5,5	7
GCSFDa8	-0,0393	8	0.95	1	4.5	5	-0,0146	5	5	4

1) Turbidity in FNU measured at the end of the IsoSS at 25°C

Table 3.I. 5: IsoSS ranking of GCSF formulations in DOEa after 3 months storage at 40°C

Formulations	K _p 40	R ₁ 40	Tur. ₄₀ ¹⁾	R ₂ 40	Avr. (R ₁ 40+R ₂ 40)/2	R _p 40	K _c 40	R _c 40	Avr. (R _p 40+R _c 40)/2	R _s 40
GCSFDa1	-0,0088	1	0.58	1	1	1	-0,0011	1	1	1
GCSFDa2	-0,0175	2	1.66	3	2.5	2	-0,0331	4	3	3
GCSFDa3	-0,0764	5	3.24	7	6	7	-0,1593	7	7	7
GCSFDa4	-0,1081	7	1.6	3	5	5	-0,087	5	5	5
GCSFDa5	-0,502	8	1.86	3	5.5	6	-0,0318	3	4,5	4
GCSFDa6	-0,0514	4	0.89	1	2.5	2	-0,0118	2	2	2
GCSFDa7	-0,1001	6	4.22	8	7	8	-0,1766	8	8	8
GCSFDa8	-0,0251	3	1.75	3	3	4	-0,1012	6	5	6

1) Turbidity in FNU measured at the end of the IsoSS at 40°C

Table 3.I. 6: IsoSS ranking of GCSF formulations in DOEb after 20 months storage at 4°C

Formulations	K _p 4	R ₁ 4	Tur. ₄ ¹⁾	R ₂ 4	Avr. (R ₁ 4+R ₂ 4)/2	R _p 4	K _c 4	R _c 4	Avr. (R _p 4+R _c 4)/2	R _s 4
GCSFDb1	-0.0003	2	1	5	3.5	3	-0.0056	5	4	3
GCSFDb2	-0.0001	1	0.7	1	1	1	-0.0012	4	2.5	2
GCSFDb3	-0.0007	4	0.6	1	2.5	2	-0.00005	1	1.5	1
GCSFDb4	-0.0011	6	0.8	1	3.5	3	-0.0066	6	4.5	4
GCSFDb5	-0.0009	5	1.6	5	5	7	-0.0005	2	4.5	4
GCSFDb6	-0.0006	3	1	5	4	5	-0.0119	8	6.5	7
GCSFDb7	-0.0017	8	0.8	1	4.5	6	-0.0101	7	6.5	7
GCSFDb8	-0.0011	6	1.2	5	5.5	8	-0.0011	3	5.5	6

1) Turbidity in FNU measured at the end of the IsoSS at 4°C

Table 3.I. 7: IsoSS ranking of GCSF formulations in DOEb after 10 months storage at 25°C

Formulations	K _p 25	R ₁ 25	Tur. ₂₅ ¹⁾	R ₂ 25	Avr. (R ₁ 25+R ₂ 25)/2	R _p 25	K _c 25	R _c 25	Avr. (R _p 25+R _c 25)/2	R _s 25
GCSFDb1	-0.016	6	0.48	1	3.5	4	-0.039	7	5.5	6
GCSFDb2	0.001	1	0.55	1	1	1	-0.006	2	1.5	1
GCSFDb3	-0.005	4	0.52	1	2.5	2	-0.004	1	1.5	1
GCSFDb4	-0.015	5	0.49	1	3	3	-0.030	5	4	3
GCSFDb5	-0.003	2	2.94	7	4.5	5	-0.007	3	4	3
GCSFDb6	-0.027	8	1.28	5	6.5	8	-0.048	8	8	8
GCSFDb7	-0.017	7	1.28	5	6	7	-0.033	6	6.5	7
GCSFDb8	-0.003	3	2.92	7	5	6	-0.008	4	5	5

1) Turbidity in FNU measured at the end of the IsoSS at 25°C

Table 3.I. 8: IsoSS ranking of GCSF formulations in DOEb after 3 months storage at 40°C

Formulations	K _p 40	R ₁ 40	Tur. ₄₀ ¹⁾	R ₂ 40	Avr. (R ₁ 40+R ₂ 40)/2	R _p 40	K _c 40	R _c 40	Avr. (R _p 40+R _c 40)/2	R _s 40
GCSFDb1	-0.103	3	1.87	3	3	3	-0.243	6	4.5	3
GCSFDb2	-0.021	1	0.61	1	1	1	-0.030	1	1	1
GCSFDb3	-0.040	2	1.17	3	2.5	2	-0.038	2	2	2
GCSFDb4	-0.136	4	1.19	3	3.5	4	-0.239	5	4.5	3
GCSFDb5	-0.163	6	1.79	3	4.5	6	-0.167	3	4.5	3
GCSFDb6	-0.718	8	14.25	8	8	8	-0.610	8	8	8
GCSFDb7	-0.608	7	0.61	1	4	5	-0.540	7	6	7
GCSFDb8	-0.156	5	3.71	7	6	7	-0.168	4	5.5	6

1) Turbidity in FNU measured at the end of the IsoSS at 40°C

Table 3.I. 9: IsoSS ranking of GCSF formulations in DOEc after 20 months storage at 4°C

Formulations	K _p 4	R ₁ 4	Tur. ₄ ¹⁾	R ₂ 4	Avr. (R ₁ 4+R ₂ 4)/2	R _p 4	K _c 4	R _c 4	Avr. (R _p 4+R _c 4)/2	R _s 4
GCSFDc1	-0.0387	7	0.7	1	4	5	0.0003	2	3.5	3
GCSFDc2	-0.0005	2	1.1	4	3	2	0.0004	1	1.5	1
GCSFDc3	0.00004	1	0.9	1	1	1	-0.0002	4	2.5	2
GCSFDc4	-0.0377	5	0.7	1	3	2	-0.0005	6	4	4
GCSFDc5	-0.0011	3	1.1	4	3.5	4	-0.0004	5	4.5	5
GCSFDc6	-0.0383	6	2.9	7	6.5	8	-0.0005	7	7.5	8
GCSFDc7	-0.0398	8	1.6	4	6	6	0.0003	3	4.5	5
GCSFDc8	-0.0021	4	5.2	8	6	6	-0.0006	8	7	7

1) Turbidity in FNU measured at the end of the IsoSS at 4°C

Table 3.I. 10: IsoSS ranking of GCSF formulations in DOEc after 10 months storage at 25°C

Formulations	K _p 25	R ₁ 25	Tur. ₂₅ ¹⁾	R ₂ 25	Avr. (R ₁ 25+R ₂ 25)/2	R _p 25	K _c 25	R _c 25	Avr. (R _p 25+R _c 25)/2	R _s 25
GCSFDc1	-0.015	7	0.65	1	4	5	0.000	2	3.5	3
GCSFDc2	-0.011	4	0.62	1	2.5	4	0.001	1	2.5	1
GCSFDc3	-0.003	1	0.52	1	1	1	-0.002	4	2.5	1
GCSFDc4	-0.009	3	0.76	1	2	3	-0.003	7	5	6
GCSFDc5	-0.006	2	0.51	1	1.5	2	-0.002	6	4	4
GCSFDc6	-0.018	8	1.17	6	7	8	-0.002	4	6	7
GCSFDc7	-0.014	5	1.8	6	5.5	6	0.000	3	4.5	5
GCSFDc8	-0.014	5	3.32	8	6.5	7	-0.004	8	7.5	8

1) Turbidity in FNU measured at the end of the IsoSS at 25°C

Table 3.I. 11: IsoSS ranking of GCSF formulations in DOEc after 3 months storage at 40°C

Formulations	K _p 40	R ₁ 40	Tur. ₄₀ ¹⁾	R ₂ 40	Avr. (R ₁ 40+R ₂ 40)/2	R _p 40	K _c 40	R _c 40	Avr. (R _p 40+R _c 40)/2	R _s 40
GCSFDc1	-0.038	5	0.69	1	3	3	-0.011	1	2	2
GCSFDc2	-0.035	3	1.04	4	3.5	4	-0.020	5	4.5	5
GCSFDc3	-0.028	2	0.94	1	1.5	1	-0.013	2	1.5	1
GCSFDc4	-0.039	6	0.82	1	3.5	4	-0.014	3	3.5	4
GCSFDc5	-0.020	1	1.53	4	2.5	2	-0.016	4	3	3
GCSFDc6	-0.045	7	1.23	4	5.5	6	-0.036	7	6.5	6
GCSFDc7	-0.037	4	9.91	8	6	7	-0.029	6	6.5	6
GCSFDc8	-0.069	8	1.04	4	6	7	-0.059	8	7.5	8

1) Turbidity in FNU measured at the end of the IsoSS at 40°C

Table 3.I. 12: IsoSS ranking of 24 GCSF formulations (DOEa, DOEb and DOEc) after 20 months storage at 4°C

Formulations	K _{p4}	R ₁₄	Tur. ₄ ¹⁾	R ₂₄	Avr. (R ₁₄ +R ₂₄)/2	R _{p4}	K _{c4}	R _{c4}	Avr. (R _{p4} +R _{c4})/2	R _{s4}
GCSFDa1	0.0027	1	0.8	1	1	1	0.0001	5	3	1
GCSFDa2	-0.0447	22	0.62	1	11.5	16	0.0023	1	8.5	6
GCSFDa3	-0.0125	16	0.96	1	8.5	9	-0.033	24	16.5	19
GCSFDa4	-0.0498	23	1.1	13	18	21	-0.0031	18	19.5	24
GCSFDa5	0.002	2	0.98	1	1.5	2	-0.0003	9	5.5	2
GCSFDa6	-0.0574	24	2.6	22	23	24	0.0001	6	15	16
GCSFDa7	-0.0023	15	0.8	1	8	8	-0.0252	23	15.5	17
GCSFDa8	-0.0381	18	1.47	13	15.5	19	-0.0018	17	18	21
GCSFDb1	-0.0003	5	1	13	9	10	-0.0056	19	14.5	15
GCSFDb2	-0.0001	4	0.7	1	2.5	4	-0.0012	16	10	8
GCSFDb3	-0.0007	8	0.6	1	4.5	5	-0.00005	7	6	4
GCSFDb4	-0.0011	10	0.8	1	5.5	6	-0.0066	20	13	11
GCSFDb5	-0.0009	9	1.6	13	11	15	-0.0005	11	13	11
GCSFDb6	-0.0006	7	1	13	10	13	-0.0119	22	17.5	20
GCSFDb7	-0.0017	13	0.8	1	7	7	-0.0101	21	14	13
GCSFDb8	-0.0011	10	1.2	13	11.5	16	-0.0011	15	15.5	17
GCSFDc1	-0.0387	20	0.7	1	10.5	14	0.0003	3	8.5	6
GCSFDc2	-0.0005	6	1.1	13	9.5	12	0.0004	2	7	5
GCSFDc3	0.00004	3	0.9	1	2	3	-0.0002	8	5.5	2
GCSFDc4	-0.0377	17	0.7	1	9	10	-0.0005	12	11	9
GCSFDc5	-0.0011	12	1.1	13	12.5	18	-0.0004	10	14	13
GCSFDc6	-0.0383	19	2.9	22	20.5	23	-0.0005	13	18	21
GCSFDc7	-0.0398	21	1.6	13	17	20	0.0003	4	12	10
GCSFDc8	-0.0021	14	5.2	24	19	22	-0.0006	14	18	21

1) Turbidity in FNU measured at the end of the IsoSS at 4°C

Table 3.I. 13: IsoSS ranking of 24 GCSF formulations (DOEa, DOEb and DOEc) after 10 months storage at 25°C

Formulations	K _p 25	R ₁ 25	Tur. ₂₅ ¹⁾	R ₂ 25	Avr. (R ₁ 25+R ₂ 25)/2	R _p 25	K _c 25	R _c 25	Avr. (R _p 25+R _c 25)/2	R _s 25
GCSFDa1	-0.0019	2	0.82	1	1.5	2	-0,0017	5	3,5	1
GCSFDa2	-0.0388	23	0.7	1	12	13	0,0008	1	7	6
GCSFDa3	-0.0139	14	1.1	15	14.5	19	-0,0262	19	19	22
GCSFDa4	-0.0134	11	1.34	15	13	15	-0,0236	18	16,5	17
GCSFDa5	-0.0097	9	0.73	1	5	7	-0,0051	13	10	10
GCSFDa6	-0.0141	15	1.18	15	15	20	-0,0026	9	14,5	12
GCSFDa7	-0.0194	21	0.71	1	11	12	-0,0652	24	18	21
GCSFDa8	-0.0393	24	0.95	1	12.5	14	-0,0146	17	15,5	16
GCSFDb1	-0.016	18	0.48	1	9.5	11	-0,0389	22	16,5	18
GCSFDb2	0.0014	1	0.55	1	1	1	-0,0056	14	7,5	7
GCSFDb3	-0.0049	6	0.52	1	3.5	4	-0,004	11	7,5	8
GCSFDb4	-0.0147	16	0.49	1	8.5	9	-0,0298	20	14,5	13
GCSFDb5	-0.0031	4	2.94	22	13	15	-0,0069	15	15	15
GCSFDb6	-0.0272	22	1.28	15	18.5	24	-0,0476	23	23,5	24
GCSFDb7	-0.0166	19	1.28	15	17	21	-0,0328	21	21	23
GCSFDb8	-0.0032	5	2.92	22	13.5	17	-0,0081	16	16,5	19
GCSFDc1	-0.0147	16	0.65	1	8.5	9	0,00008	3	6	4
GCSFDc2	-0.0109	10	0.62	1	5.5	8	0,0005	2	5	3
GCSFDc3	-0.0025	3	0.52	1	2	3	-0,0017	6	4,5	2
GCSFDc4	-0.0088	8	0.76	1	4.5	6	-0,0026	10	8	9
GCSFDc5	-0.0059	7	0.51	1	4	5	-0,0023	8	6,5	5
GCSFDc6	-0.018	20	1.17	15	17.5	22	-0,0017	7	14,5	14
GCSFDc7	-0.0138	12	1.8	15	13.5	17	-0,0003	4	10,5	11
GCSFDc8	-0.0138	12	3.32	24	18	23	-0,004	12	17,5	20

1) Turbidity in FNU measured at the end of the IsoSS at 25°C

Table 3.I. 14: IsoSS ranking of 24 GCSF formulations (DOEa, DOEb and DOEc) after 3 months storage at 40°C

Formulations	K _p 40	R ₁ 40	Tur. ₄₀ ¹⁾	R ₂ 40	Avr. (R ₁ 40+R ₂ 40)/2	R _p 40	K _c 40	R _c 40	Avr. (R _p 40+R _c 40)/2	R _s 40
GCSFDa1	-0.0088	1	0.58	1	1	1	-0,0011	1	1	1
GCSFDa2	-0.0175	2	1.66	8	5	4	-0,0331	11	7,5	8
GCSFDa3	-0.0764	15	3.24	20	17.5	21	-0,1593	17	19	20
GCSFDa4	-0.1081	18	1.6	8	13	16	-0,087	15	15,5	16
GCSFDa5	-0.502	22	1.86	8	15	19	-0,0318	10	14,5	15
GCSFDa6	-0.0514	13	0.89	1	7	9	-0,0118	3	6	6
GCSFDa7	-0.1001	16	4.22	22	19	22	-0,1766	20	21	22
GCSFDa8	-0.0251	5	1.75	8	6.5	8	-0,1012	16	12	10
GCSFDb1	-0.1027	17	1.87	8	12.5	15	-0,2434	22	18,5	18
GCSFDb2	-0.0205	4	0.61	1	2.5	2	-0,0303	9	5,5	4
GCSFDb3	-0.0399	11	1.17	8	9.5	11	-0,0384	13	12	11
GCSFDb4	-0.1359	19	1.19	8	13.5	17	-0,2393	21	19	21
GCSFDb5	-0.1627	21	1.79	8	14.5	18	-0,1672	18	18	17
GCSFDb6	-0.7183	24	14.25	24	24	24	-0,6095	24	24	24
GCSFDb7	-0.608	23	0.61	1	12	14	-0,5401	23	18,5	19
GCSFDb8	-0.1562	20	3.71	20	20	23	-0,1681	19	21	23
GCSFDc1	-0.0378	9	0.69	1	5	4	-0,011	2	3	2
GCSFDc2	-0.035	7	1.04	8	7.5	10	-0,01996	7	8,5	9
GCSFDc3	-0.0277	6	0.94	1	3.5	3	-0,0131	4	3,5	3
GCSFDc4	-0.0393	10	0.82	1	5.5	6	-0,0138	5	5,5	5
GCSFDc5	-0.0197	3	1.53	8	5.5	6	-0,0155	6	6	7
GCSFDc6	-0.0446	12	1.23	8	10	12	-0,0355	12	12	12
GCSFDc7	-0.0369	8	9.91	23	15.5	20	-0,0293	8	14	14
GCSFDc8	-0.0692	14	1.04	8	11	13	-0,0586	14	13,5	13

1) Turbidity in FNU measured at the end of the IsoSS at 40°C

Table 3.I. 15: Ranking procedures for 11 MAB formulation based on IsoSS at 25°C after 12 months

Formulation	K _p 25	R ₁ 25	R ₂ 25 ¹⁾	Avr. (R ₁ 4+R ₂ 4)/2	R _p 25
MABF001	-0.0041	11	1	6	11
MABF002	-0.0005	4	1	2.5	4
MABF003	-0.0003	3	1	2	3
MABF004	-0.00003	2	1	1.5	2
MABF005	0.0003	1	1	1	1
MABF006	-0.0013	8	1	4.5	8
MABF007	-0.0005	4	1	2.5	4
MABF008	-0.0007	7	1	4	6
MABF009	-0.0006	6	2	4	6
MABF010	-0.0013	8	1	4.5	8
MABF011	-0.0014	10	1	5.5	10

1) Ranking based on light blockage measured particle count (table 3.I.18)

Table 3.I. 16: Ranking procedures for 11 MAB formulation based on IsoSS at 40°C after 12 months

Formulation	K _p 40	R ₁ 40	R ₂ 40 ¹⁾	Avr. (R ₁ 4+R ₂ 4)/2	R _p 40
MABF001	-0.0214	11	1	6	10
MABF002	-0.0121	7	1	4	7
MABF003	-0.0105	4	2	3	4
MABF004	-0.0128	8	1	4.5	8
MABF005	-0.0099	2	1	1.5	1
MABF006	-0.0178	10	2	6	10
MABF007	-0.0134	9	2	5.5	9
MABF008	-0.0093	1	2	1.5	1
MABF009	-0.0102	3	2	2.5	3
MABF010	-0.0113	5	1	3	4
MABF011	-0.0115	6	1	3.5	6

1) Ranking based on light blockage measured particle count (table 3.I.18)

Table 3.I. 17: Ranking procedures for 15 MAB formulation based on IsoSS at 40°C after 6 months

Formulation	K _p 40	R ₁ 40	R ₂ 40 ¹⁾	Avr. (R ₁ 4+R ₂ 4)/2	R _p 40
MABF001	-0.0316	14	1	7.5	13
MABF002	-0.0178	12	2	7	11
MABF003	-0.0143	5	1	3	5
MABF004	-0.0128	4	1	2.5	4
MABF005	-0.0127	3	1	2	3
MABF006	-0.0226	13	1	7	12
MABF007	-0.0161	8	1	4.5	7
MABF008	-0.015	6	2	4	6
MABF009	-0.0155	7	2	4.5	8
MABF010	-0.0101	2	1	1.5	1
MABF011	-0.0089	1	2	1.5	2
MABF012	-0.0171	10	2	6	10
MABF013	-0.0168	9	2	5.5	9
MABF014	-0.0174	11	4	7.5	14
MABF015	-0.163	15	3	9	15

1) Ranking based on light blockage measured particle count (table 3.I.18)

Table 3.I. 18: Particle count for 15 MAB formulations after isothermal storage at 4, 25 and 40°C

Formulations	Particle range	4°C (12 mon.)	R ₂ 4	25°C (12mon.)	R ₂ 25	40°C (12 mon.)	R ₂ 40	40°C (6 mon.)	R ₂ 40 (6mon.)
MABF001	> 1 µm	1080	1	1870	1	2935	1	1950	1
	> 10 µm	50		110		80		5	
	> 25 µm	50		90		55		0	
MABF002	> 1 µm	6390	1	2310	1	7060	1	13810	2
	> 10 µm	220		290		385		220	
	> 25 µm	80		250		255		10	
MABF003	> 1 µm	3680	1	6380	1	16180	2	8620	1
	> 10 µm	105		380		1095		220	
	> 25 µm	95		300		490		10	
MABF004	> 1 µm	1765	1	630	1	2100	1	785	1
	> 10 µm	150		50		230		5	
	> 25 µm	110		35		130		0	
MABF005	> 1 µm	1720	1	2510	1	5770	1	2350	1
	> 10 µm	50		40		215		15	
	> 25 µm	5		15		90		0	
MABF006	> 1 µm	2960	1	3570	1	15220	2	5230	1
	> 10 µm	70		80		540		15	
	> 25 µm	35		20		285		5	
MABF007	> 1 µm	4855	1	3780	1	12590	2	5045	1
	> 10 µm	90		160		405		65	
	> 25 µm	35		60		255		0	
MABF008	> 1 µm	6845	1	2770	1	16200	2	10255	2
	> 10 µm	205		155		210		160	
	> 25 µm	110		95		50		10	
MABF009	> 1 µm	2065	1	25445	2	91480	2	46430	2
	> 10 µm	120		240		465		380	
	> 25 µm	60		85		110		15	
MABF010	> 1 µm	3785	1	5600	1	4955	1	9160	1
	> 10 µm	10		10		650		70	
	> 25 µm	0		0		35		15	
MABF011	> 1 µm	805	1	4000	1	6690	1	11910	2
	> 10 µm	30		20		195		250	
	> 25 µm	5		0		35		145	
MABF012	> 1 µm							92055	2
	> 10 µm							390	
	> 25 µm							0	
MABF013	> 1 µm							80335	2
	> 10 µm							280	
	> 25 µm							55	
MABF014	> 1 µm							565055	4
	> 10 µm							9390	
	> 25 µm							780	
MABF015	> 1 µm							173055	3
	> 10 µm							4500	
	> 25 µm							335	

Table 3.I. 19: Ranking procedures for 11 PEG-INF formulations based on IsoSS at 25°C after 12 months

Formulation	K _p 25	R ₁ 25	R ₂ 25 ¹⁾	Avr. (R ₁ 25+R ₂ 25)/2	R _p 25	K _c 25	R _c 25	Avr. (R _p 25+R _c 25)/2	R _s 25
P-INFF001	-0,0757	11	1	6	10	0,0039	1	5,5	4
P-INFF002	-0,0432	10	2	6	10	-0,0032	7	8,5	10
P-INFF003	-0,0005	1	1	1	1	-0,0005	3	2	1
P-INFF004	-0,0032	4	1	2,5	4	-0,0045	8	6	5
P-INFF006	-0,0087	8	1	4,5	8	-0,0016	5	6,5	6
P-INFF007	-0,0022	2	1	1,5	2	-0,0031	6	4	3
P-INFF008	-0,0185	9	1	5	9	-0,0008	4	6,5	6
P-INFF009	-0,0031	3	1	2	3	0,0032	1	2	1
P-INFF010	-0,0057	7	1	4	7	-0,0112	10	8,5	10
P-INFF012	-0,0037	5	1	3	5	-0,0161	11	8	9
P-INFF014	-0,0043	6	1	3,5	6	-0,0089	9	7,5	8

1) Ranking based on light blockage measured particle count (table 3.I.22)

Table 3.I. 20: Ranking procedures for 11 PEG-INF formulations based on IsoSS at 40°C after 6 months

Formulation	K _p 40	R ₁ 40	R ₂ 40 ¹⁾	Avr. (R ₁ 40+R ₂ 40)/2	R _p 40	K _c 40	R _c 40	Avr. (R _p 40+R _c 40)/2	R _s 40
P-INFF001	-0,8582	11	2	6,5	11	-2	11	11	11
P-INFF002	-0,1245	10	1	5,5	9	-0,1456	9	9	9
P-INFF003	-0,0435	7	2	4,5	7	-0,0511	5	6	7
P-INFF004	-0,06	8	2	5	8	-0,0686	8	8	8
P-INFF006	-0,0392	3	1	2	3	-0,0489	3	3	3
P-INFF007	-0,0341	2	1	1,5	1	-0,0531	7	4	4
P-INFF008	-0,0324	1	2	1,5	1	-0,0496	4	2,5	1
P-INFF009	-0,0394	4	2	3	4	-0,0456	1	2,5	1
P-INFF010	-0,0412	5	1	3	4	-0,0529	6	5	6
P-INFF012	-0,111	9	2	5,5	9	-0,1514	10	9,5	10
P-INFF014	-0,0412	5	2	3,5	6	-0,0486	2	4	4

1) Ranking based on light blockage measured particle count (table 3.I.22)

Table 3.I. 21: Ranking procedures for 14 PEG-INF formulations based on IsoSS at 40°C after 6 months

Formulation	K_p40	R_140	$R_240^{1)}$	Avr. $(R_140+R_240)/2$	R_p40	K_c40	R_c40	Avr. $(R_p40+R_c40)/2$	R_s40
P-INFF001	-0,8582	14	1	7,5	14	-2	14	14	14
P-INFF002	-0,1245	13	1	7	13	-0,1456	12	12,5	12
P-INFF003	-0,0435	7	1	4	7	-0,0511	5	6	7
P-INFF004	-0,06	9	1	5	9	-0,0686	11	10	10
P-INFF005	-0,0572	8	1	4,5	8	-0,0672	10	9	8
P-INFF006	-0,0392	3	1	2	3	-0,0489	3	3	3
P-INFF007	-0,0341	2	1	1,5	2	-0,0531	7	4,5	5
P-INFF008	-0,0324	1	1	1	1	-0,0496	4	2,5	1
P-INFF009	-0,0394	4	1	2,5	4	-0,0456	1	2,5	1
P-INFF010	-0,0412	5	1	3	5	-0,0529	6	5,5	6
P-INFF011	-0,0628	10	1	5,5	10	-0,0599	8	9	8
P-INFF012	-0,111	12	1	6,5	12	-0,1514	13	12,5	12
P-INFF013	-0,0633	11	1	6	11	-0,0629	9	10	10
P-INFF014	-0,0412	6	1	3,5	6	-0,0486	2	4	4

1) Ranking based on light blockage measured particle count (table 3.I.22)

Table 3.I. 22: Particle count for 14 PEG-INF formulations after isothermal storage at 4, 25 and 40°C

Formulations	Particle range	4°C (12 mon.)	R ₂₄	25°C (12mon.)	R ₂₅	40°C (6 mon.)	R ₂₄₀
P-INFF001	> 1 µm	1333	1	9178	1	203	1
	> 10 µm	33		89		8	
	> 25 µm	11		22		1	
P-INFF002	> 1 µm	1233	1	17144	2	152	1
	> 10 µm	44		78		4	
	> 25 µm	11		0		0	
P-INFF003	> 1 µm	4156	1	2378	1	288	1
	> 10 µm	44		367		7	
	> 25 µm	0		33		2	
P-INFF004	> 1 µm	2044	1	1311	1	310	1
	> 10 µm	44		22		6	
	> 25 µm	0		11		1	
P-INFF005	> 1 µm					4700	1
	> 10 µm					22	
	> 25 µm					11	
P-INFF006	> 1 µm	722	1	544	1	378	1
	> 10 µm	22		33		4	
	> 25 µm	0		0		0	
P-INFF007	> 1 µm	1189	1	2756	1	204	1
	> 10 µm	44		56		2	
	> 25 µm	11		0		0	
P-INFF008	> 1 µm	1744	1	2933	1	773	1
	> 10 µm	33		22		8	
	> 25 µm	11		11		2	
P-INFF009	> 1 µm	2056	1	1933	1	311	1
	> 10 µm	33		44		6	
	> 25 µm	0		0		2	
P-INFF010	> 1 µm	2222	1	2344	1	358	1
	> 10 µm	111		144		6	
	> 25 µm	11		22		0	
P-INFF011	> 1 µm					3044	1
	> 10 µm					33	
	> 25 µm					0	
P-INFF012	> 1 µm	3011	1	1400	1	221	1
	> 10 µm	22		11		2	
	> 25 µm	0		0		1	
P-INFF013	> 1 µm					7422	1
	> 10 µm					22	
	> 25 µm					0	
P-INFF014	> 1 µm	4111	1	3156	1	997	1
	> 10 µm	233		44		12	
	> 25 µm	11		11		7	

5. Appendix 3.II:

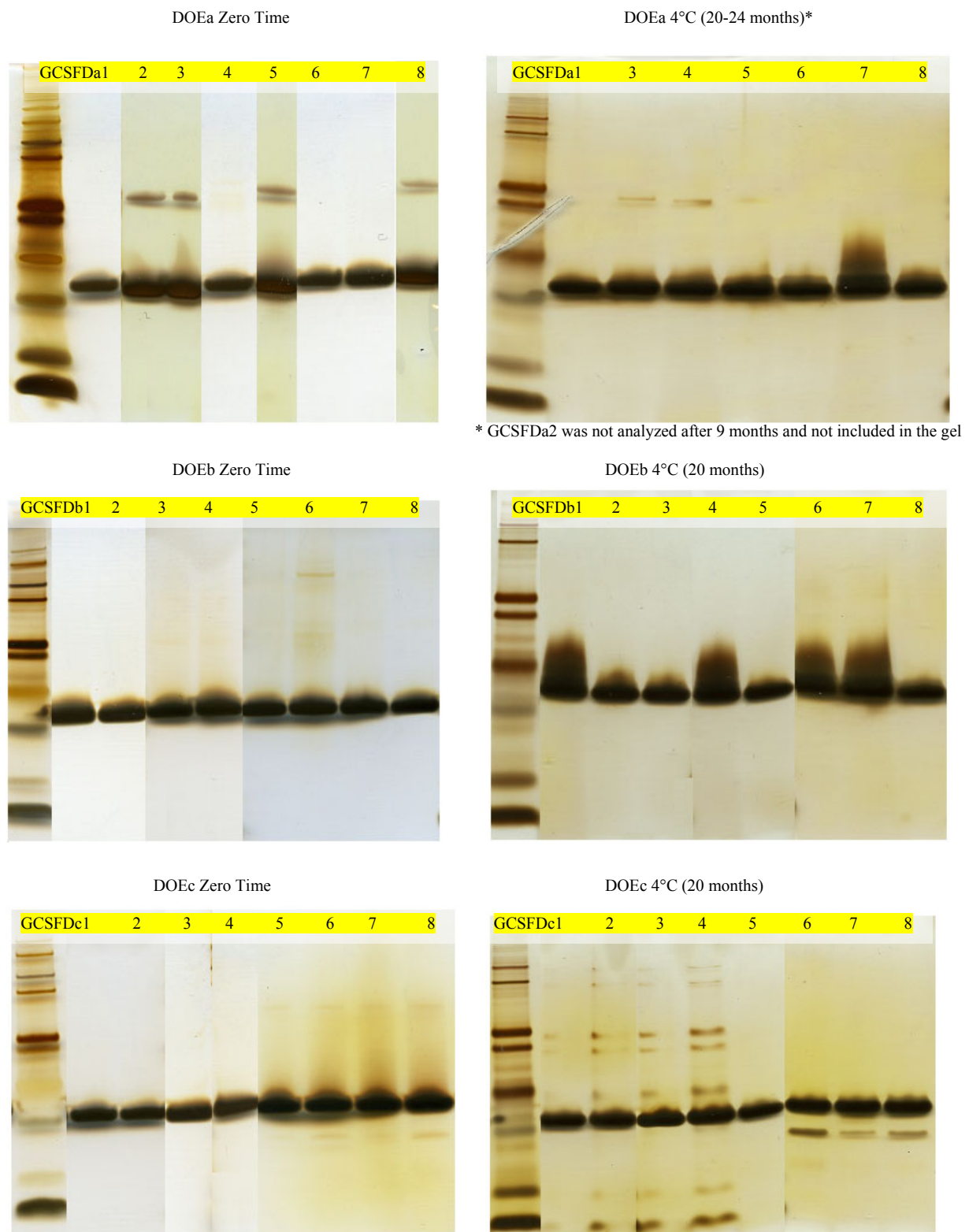


Figure 3.II. 1: SDS-PAGE for GCSF formulations of DOEa, DOEb and DOEc before and after storage at 4 °C for 20 – 24 months.

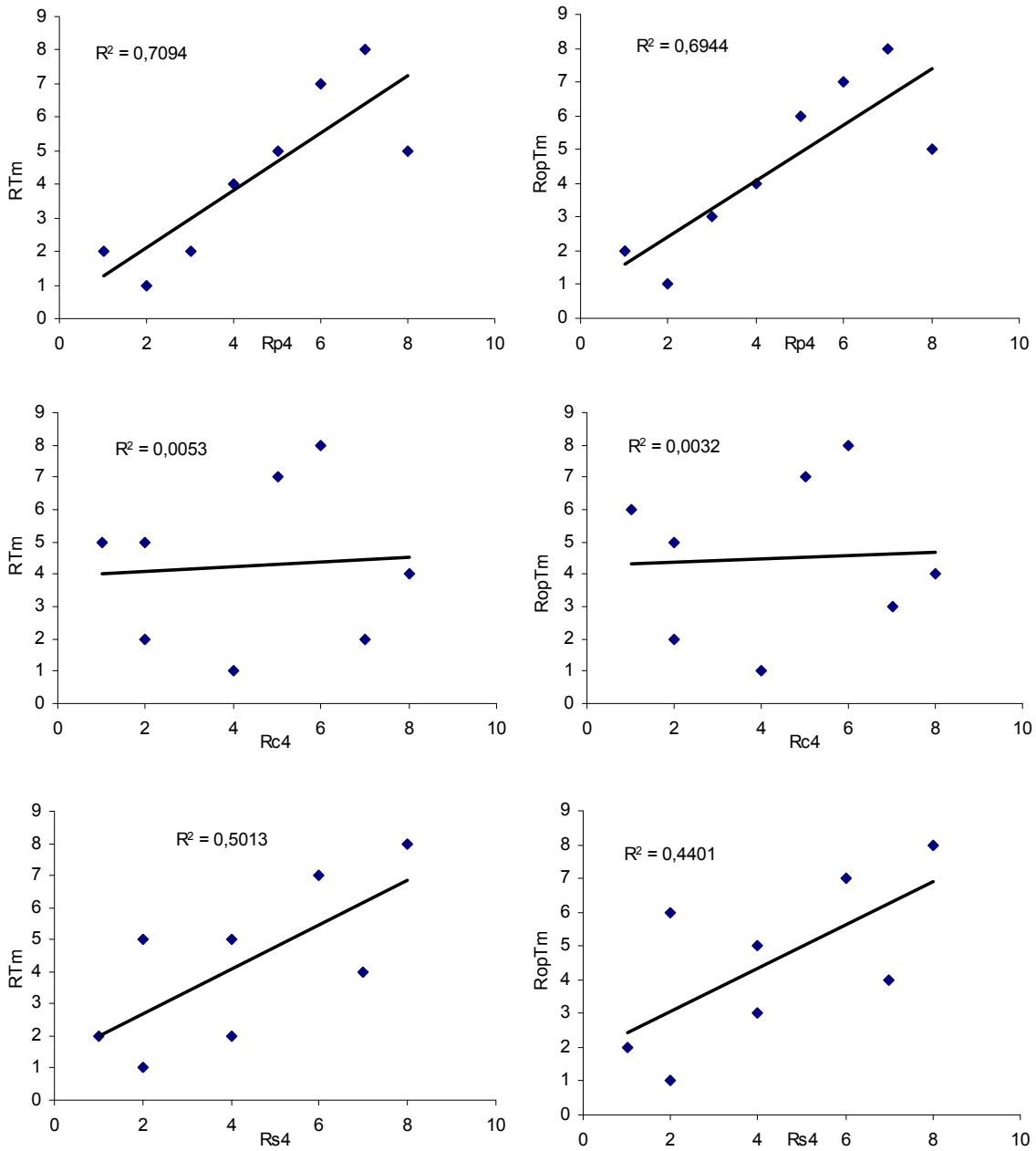


Figure 3.II. 2: Correlation curves of GCSF formulations in DOEa. That includes correlation between R_{Tm} (ranking based on T_m) or R_{opTm} (ranking after optimization of R_{Tm} using the degree of unfolding reversibility), and physical, chemical or overall stabilities (R_p , R_c and R_s , respectively) of the formulations at 4°C.

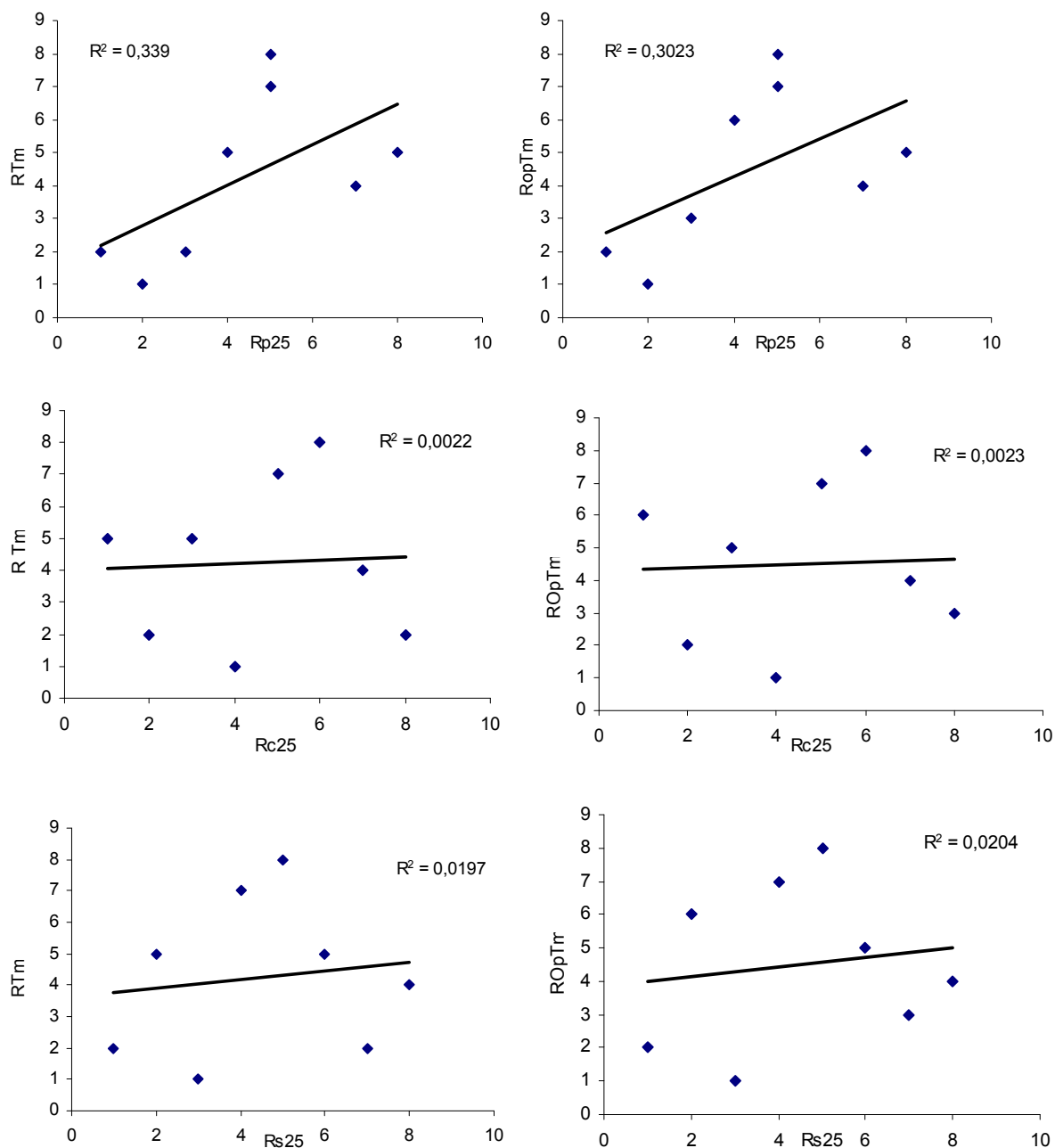


Figure 3.II. 3: Correlation curves of GCSF formulations in DOEa. That includes correlation between R_{Tm} (ranking based on T_m) or R_{OpTm} (ranking after optimization of R_{Tm} using the degree of unfolding reversibility), and physical, chemical or overall stabilities (R_p , R_c and R_s , respectively) of the formulations at 25°C.

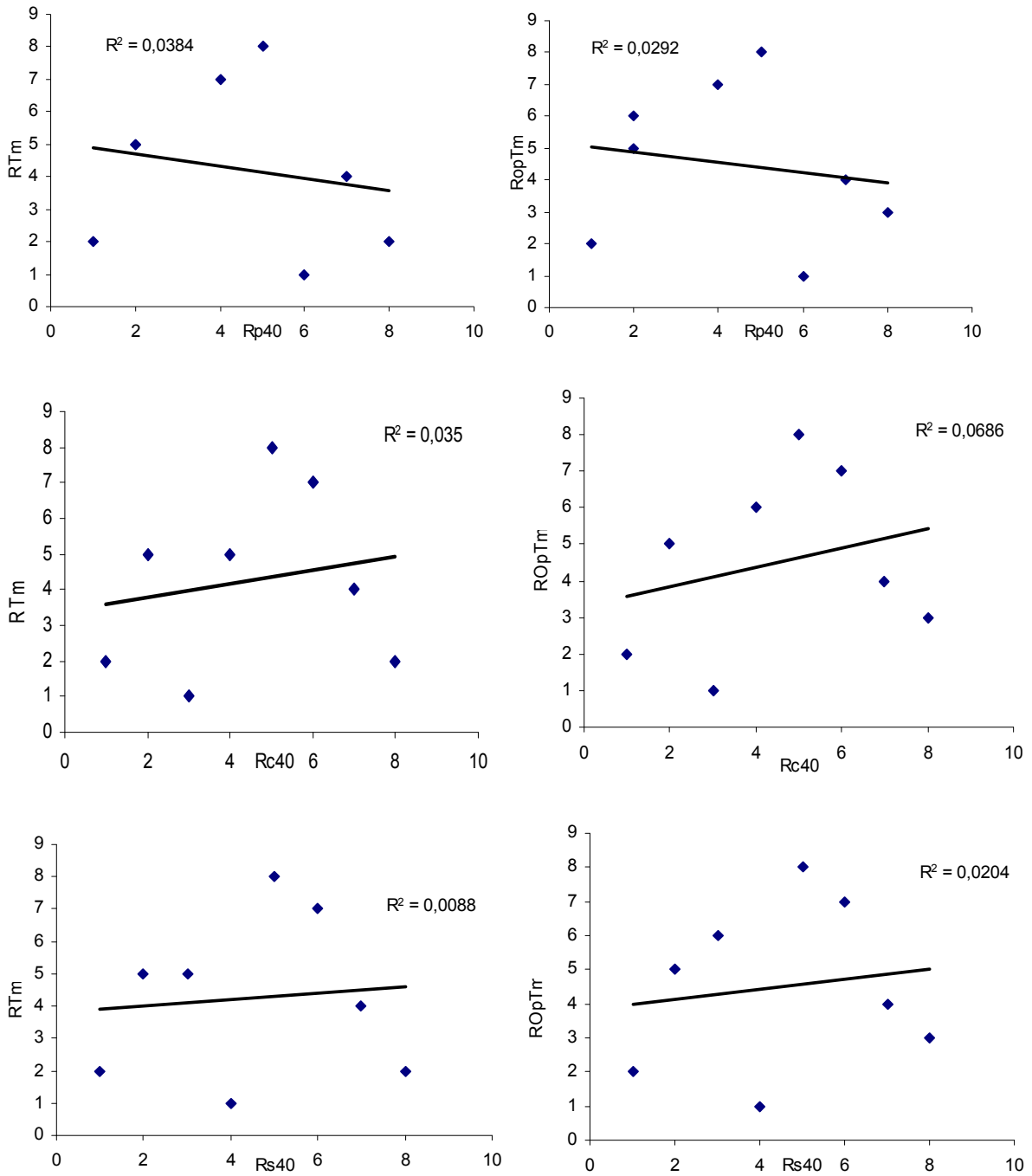


Figure 3.II. 4: Correlation curves of GCSF formulations in DOEa. That includes correlation between R_{Tm} (ranking based on T_m) or R_{opTm} (ranking after optimization of R_{Tm} using the degree of unfolding reversibility), and physical, chemical or overall stabilities (R_p , R_c and R_s , respectively) of the formulations at 40°C.

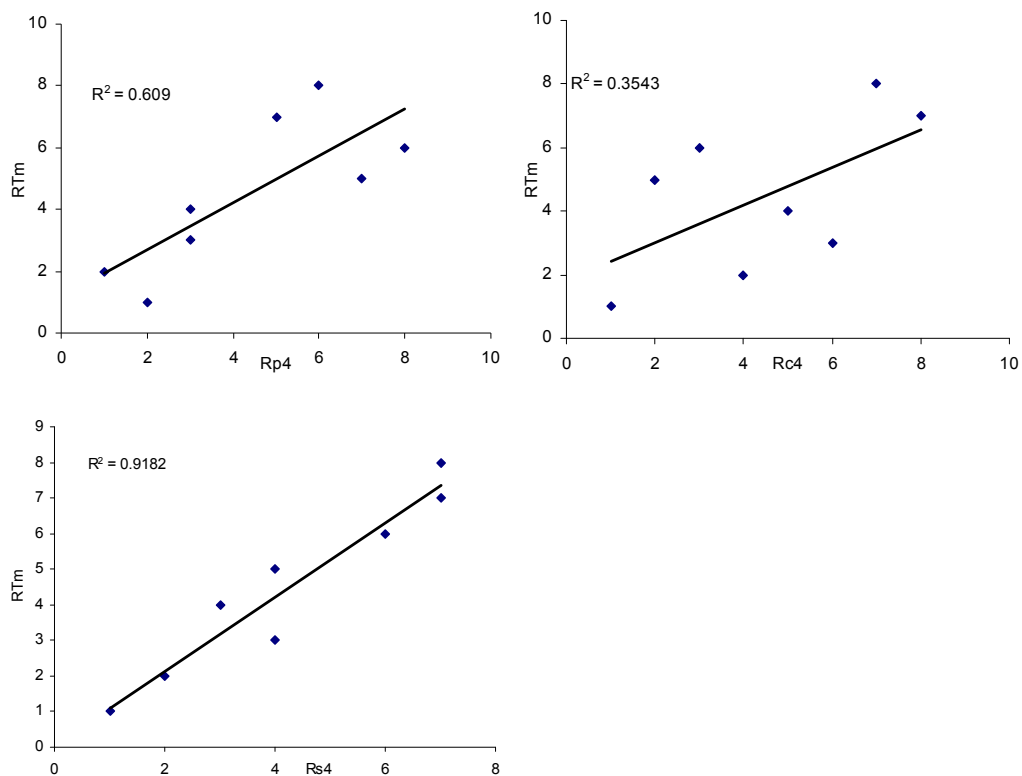


Figure 3.II. 5: Correlation curves of GCSF formulations in DOEb. That includes correlation between R_{Tm} (ranking based on T_m) and physical, chemical or overall stabilities (R_p , R_c and R_s , respectively) of the formulations at 4°C.

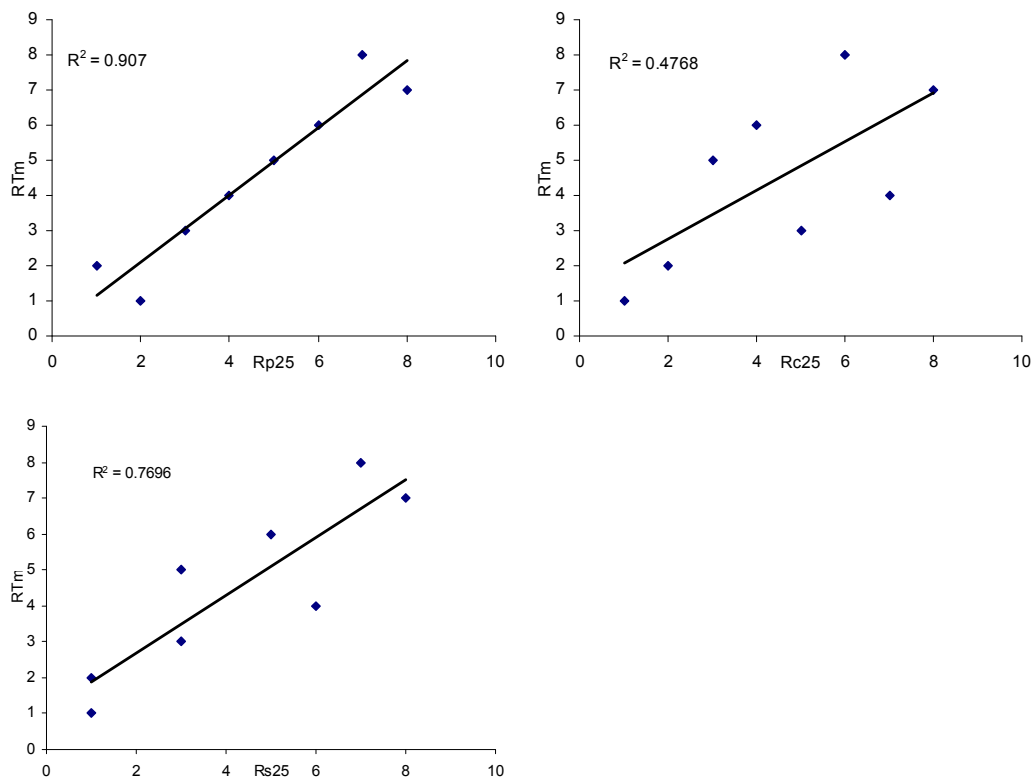


Figure 3.II. 6: Correlation curves of GCSF formulations in DOEb. That includes correlation between R_{Tm} (ranking based on T_m) and physical, chemical or overall stabilities (R_p , R_c and R_s , respectively) of the formulations at 25°C.

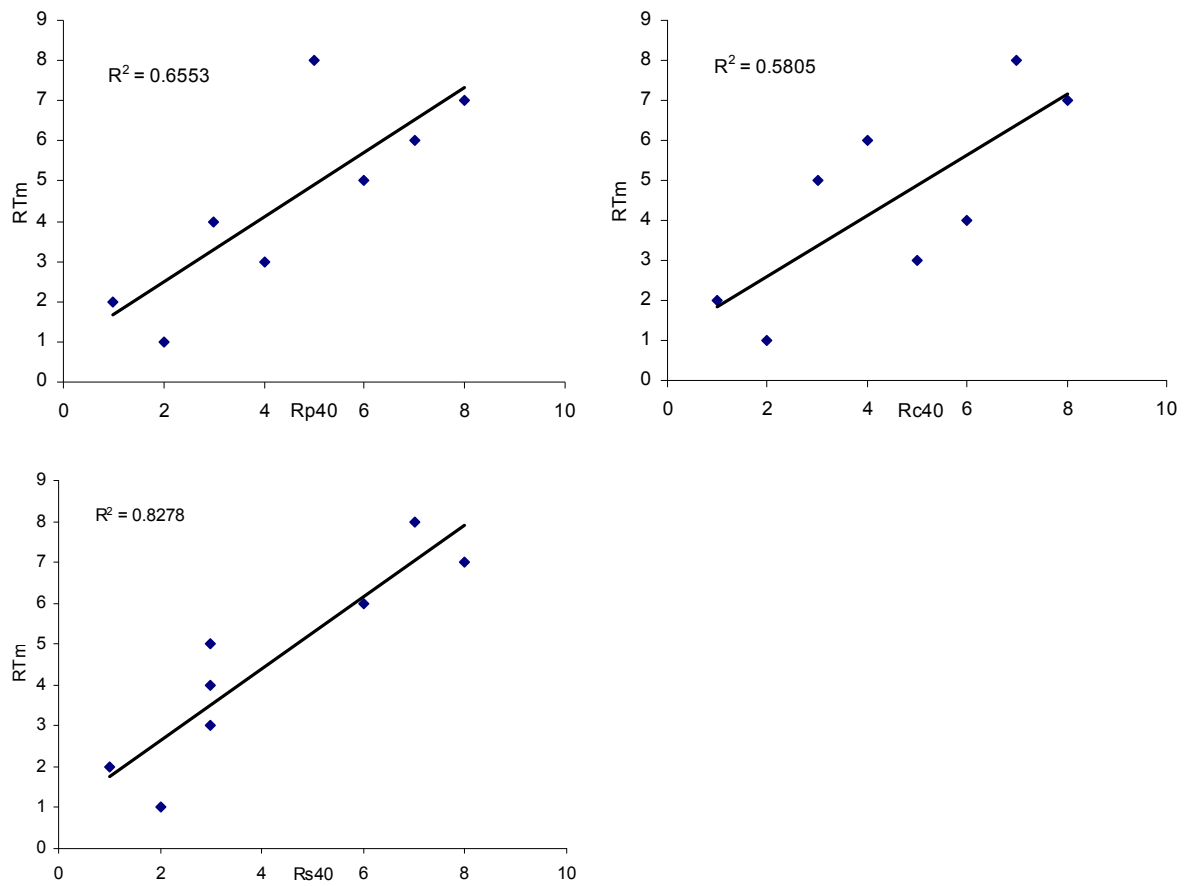


Figure 3.II. 7: Correlation curves of GCSF formulations in DOEb. That includes correlation between R_{Tm} (ranking based on T_m) and physical, chemical or overall stabilities (R_p , R_c and R_s , respectively) of the formulations at 40°C.

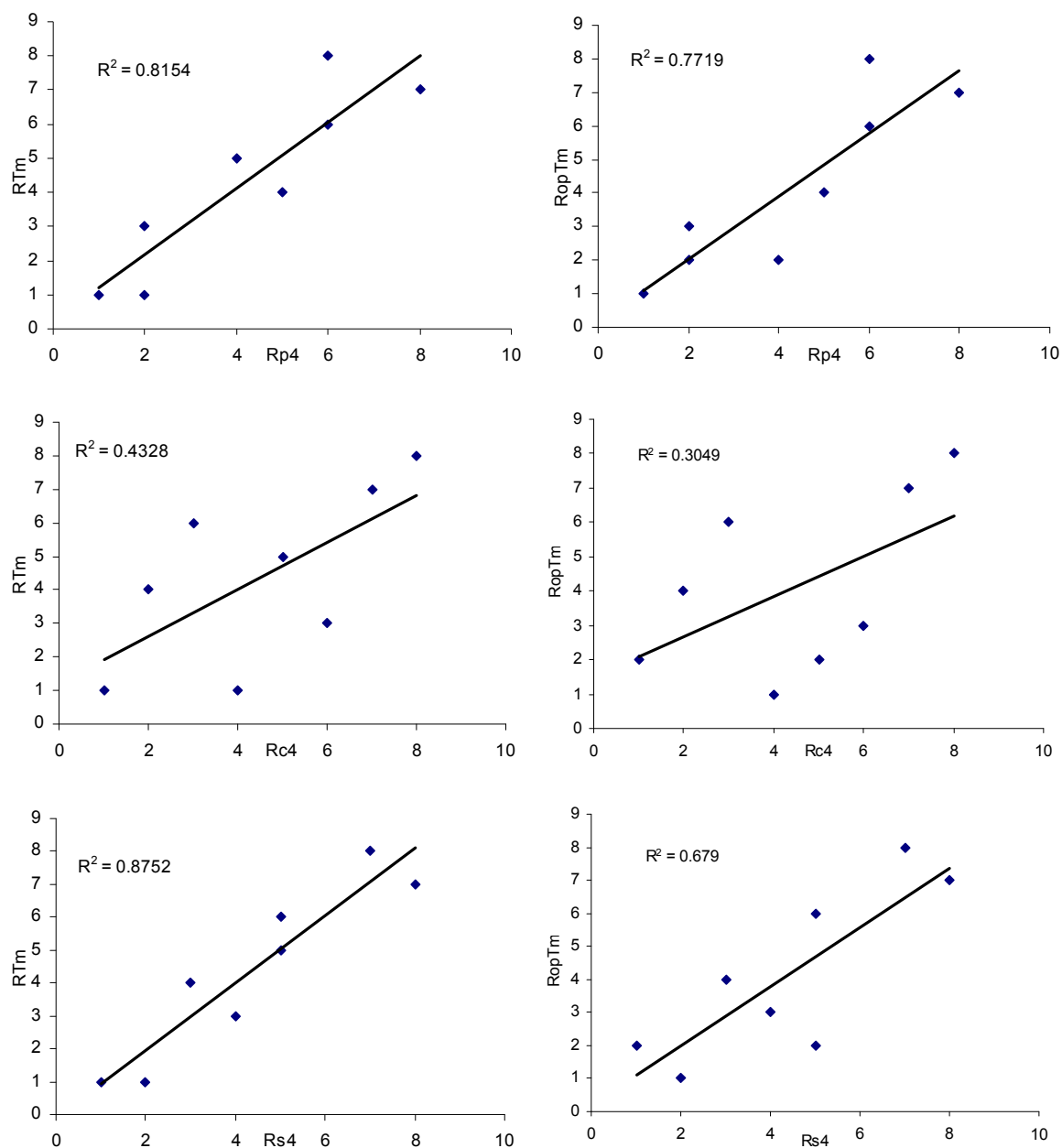


Figure 3.II. 8: Correlation curves of GCSF formulations in DOEc. That includes correlation between R_{Tm} (ranking based on T_m) or R_{opTm} (ranking after optimization of R_{Tm} using the degree of unfolding reversibility), and physical, chemical or overall stabilities (R_p , R_c and R_s , respectively) of the formulations at 4°C.

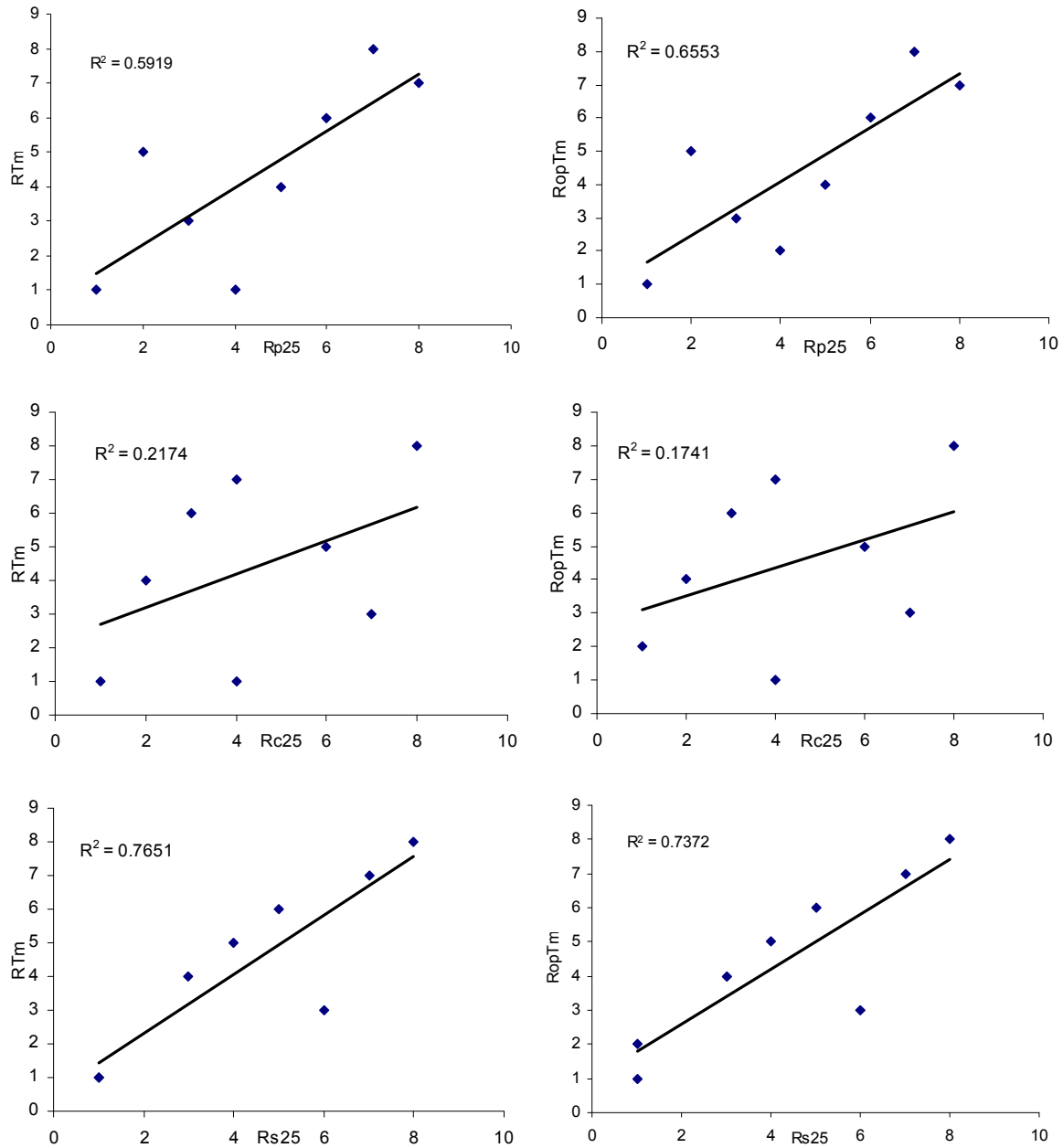


Figure 3.II. 9: Correlation curves of GCSF formulations in DOEc. That includes correlation between R_{Tm} (ranking based on T_m) or R_{opTm} (ranking after optimization of R_{Tm} using the degree of unfolding reversibility), and physical, chemical or overall stabilities (R_p , R_c and R_s , respectively) of the formulations at 25°C.

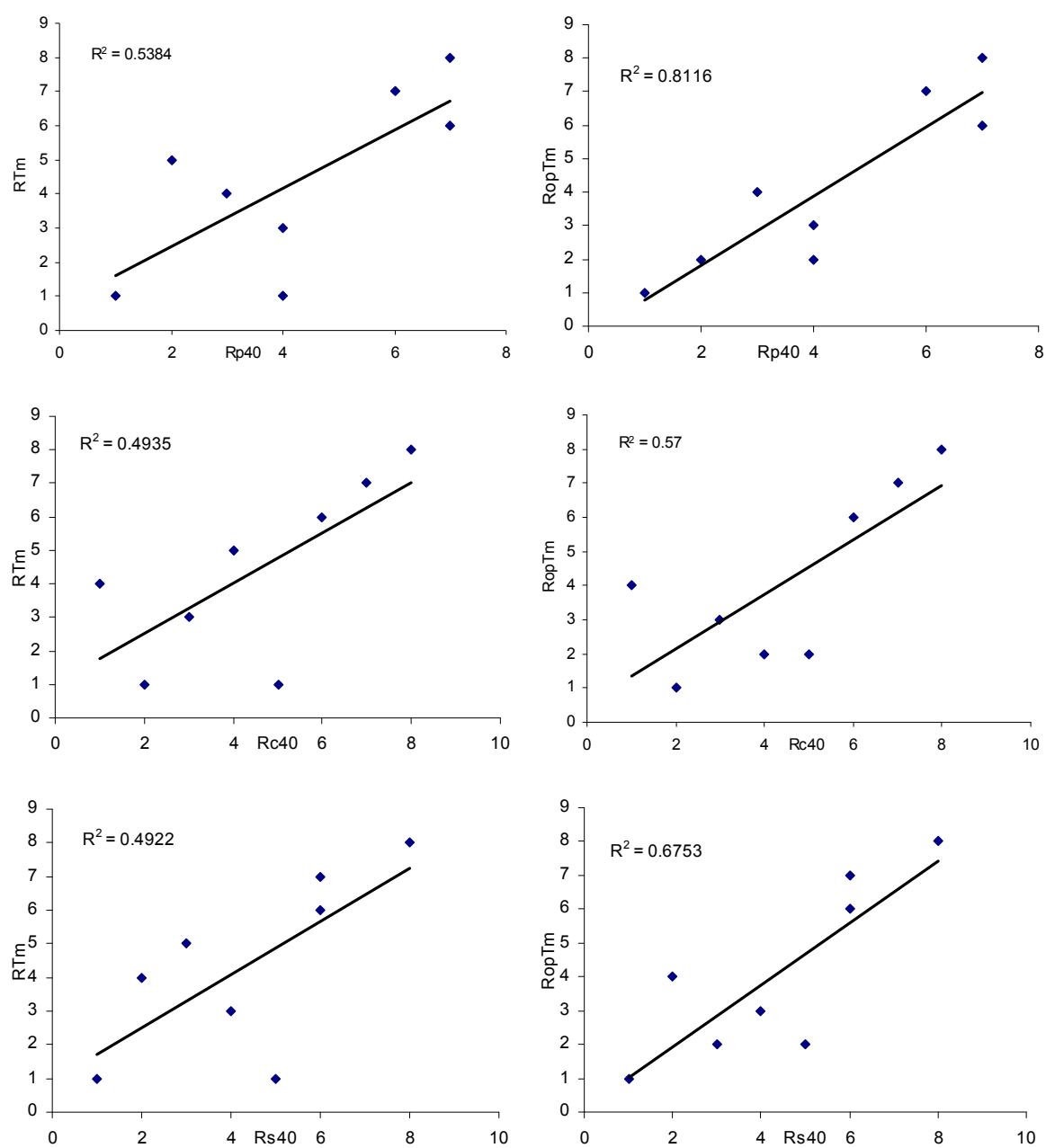


Figure 3.II. 10: Correlation curves of GCSF formulations in DOEc. That includes correlation between R_{Tm} (ranking based on T_m) or R_{opTm} (ranking after optimization of R_{Tm} using the degree of unfolding reversibility), and physical, chemical or overall stabilities (R_p , R_c and R_s , respectively) of the formulations at 40°C.

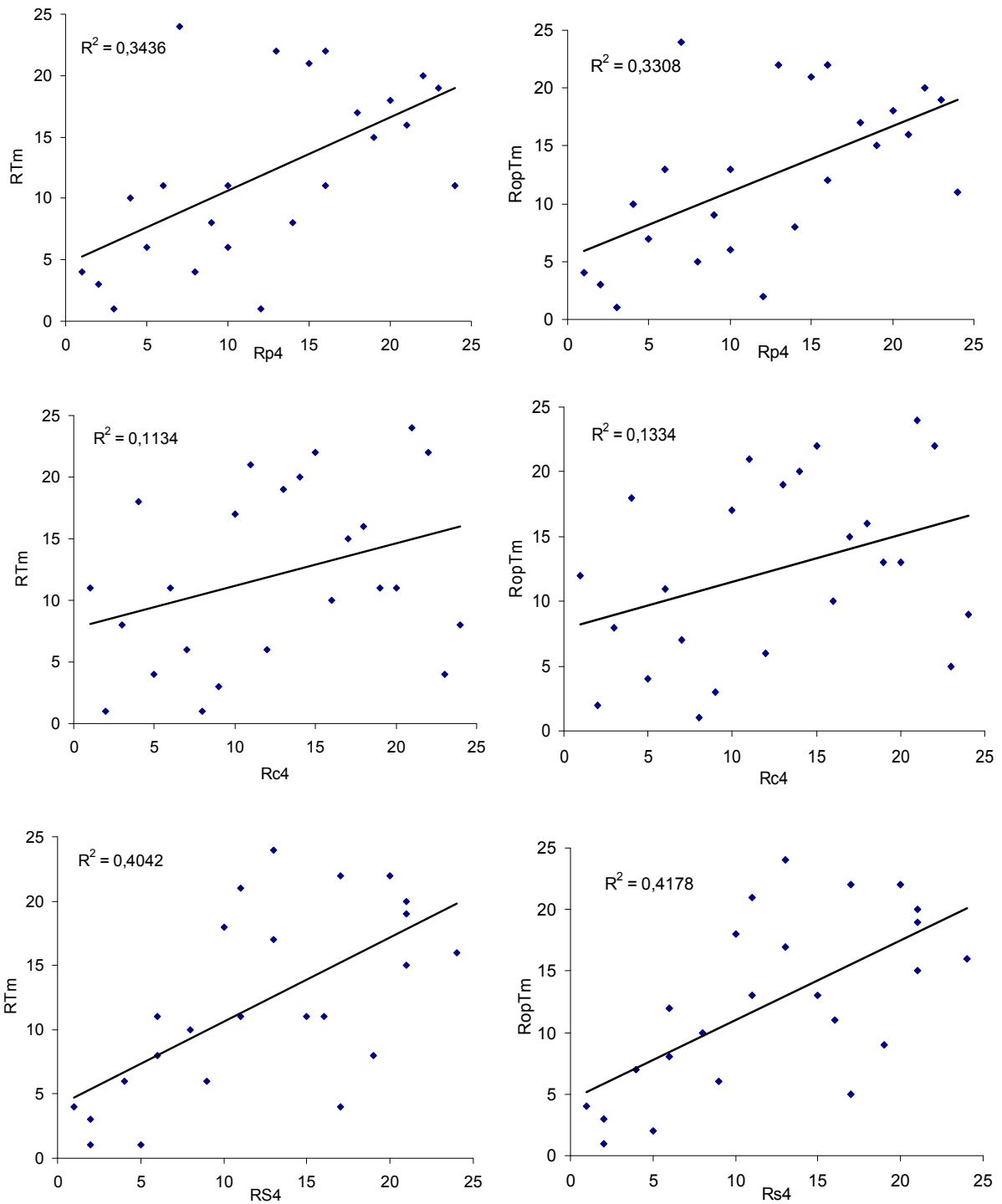


Figure 3.II. 11: Correlation curves of 24 GCSF formulations in DOEa, DOEb and DOEc. That includes correlation between R_{Tm} (ranking based on T_m) or R_{opTm} (ranking after optimization of R_{Tm} using the degree of unfolding reversibility), and physical, chemical or overall stabilities (R_p , R_c and R_s , respectively) of the formulations at 4°C.

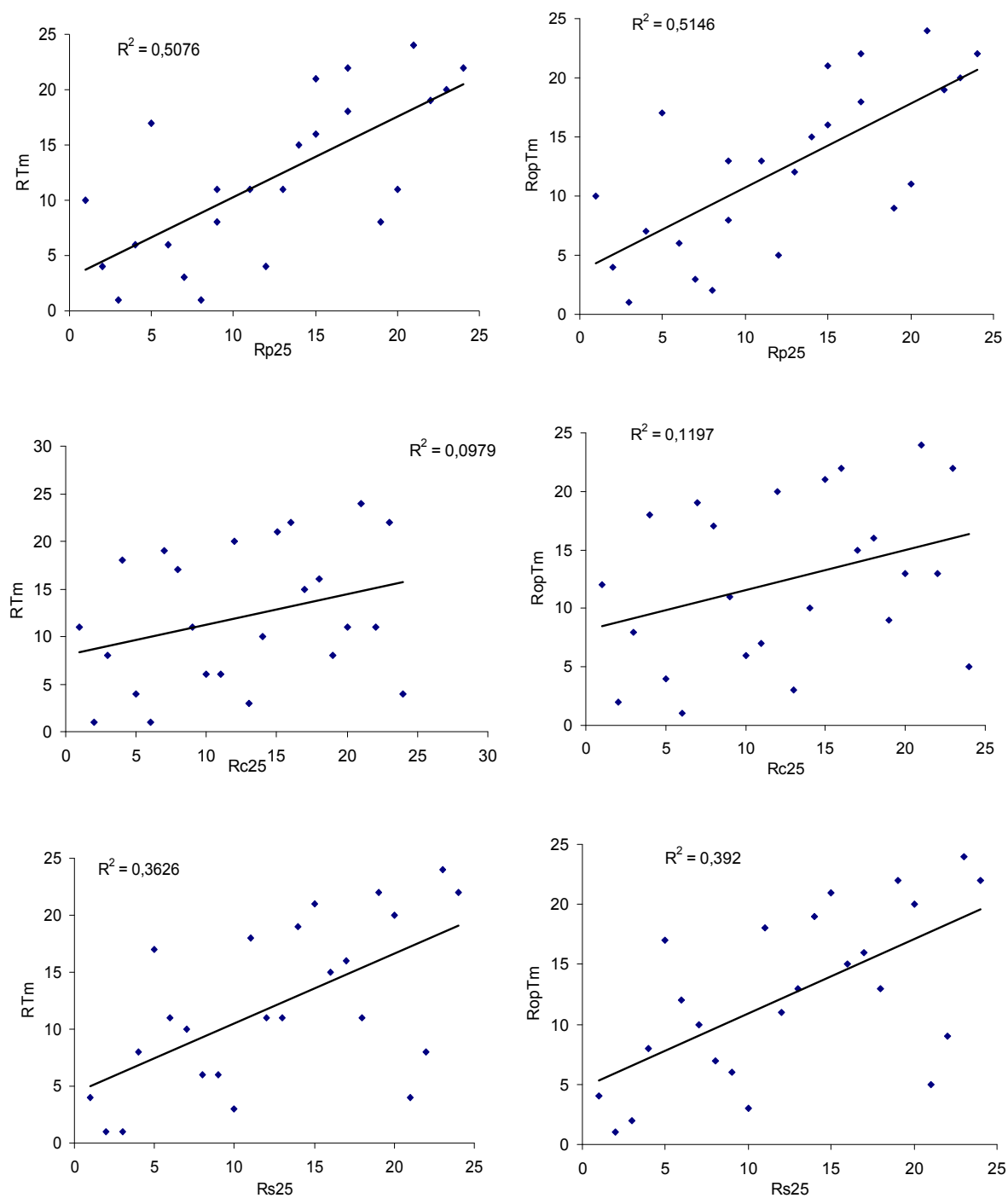


Figure 3.II. 12: Correlation curves of 24 GCSF formulations in DOEa, DOEb and DOEc. That includes correlation between R_{Tm} (ranking based on T_m) or R_{opTm} (ranking after optimization of R_{Tm} using the degree of unfolding reversibility), and physical, chemical or overall stabilities (R_p , R_c and R_s , respectively) of the formulations at 25°C.

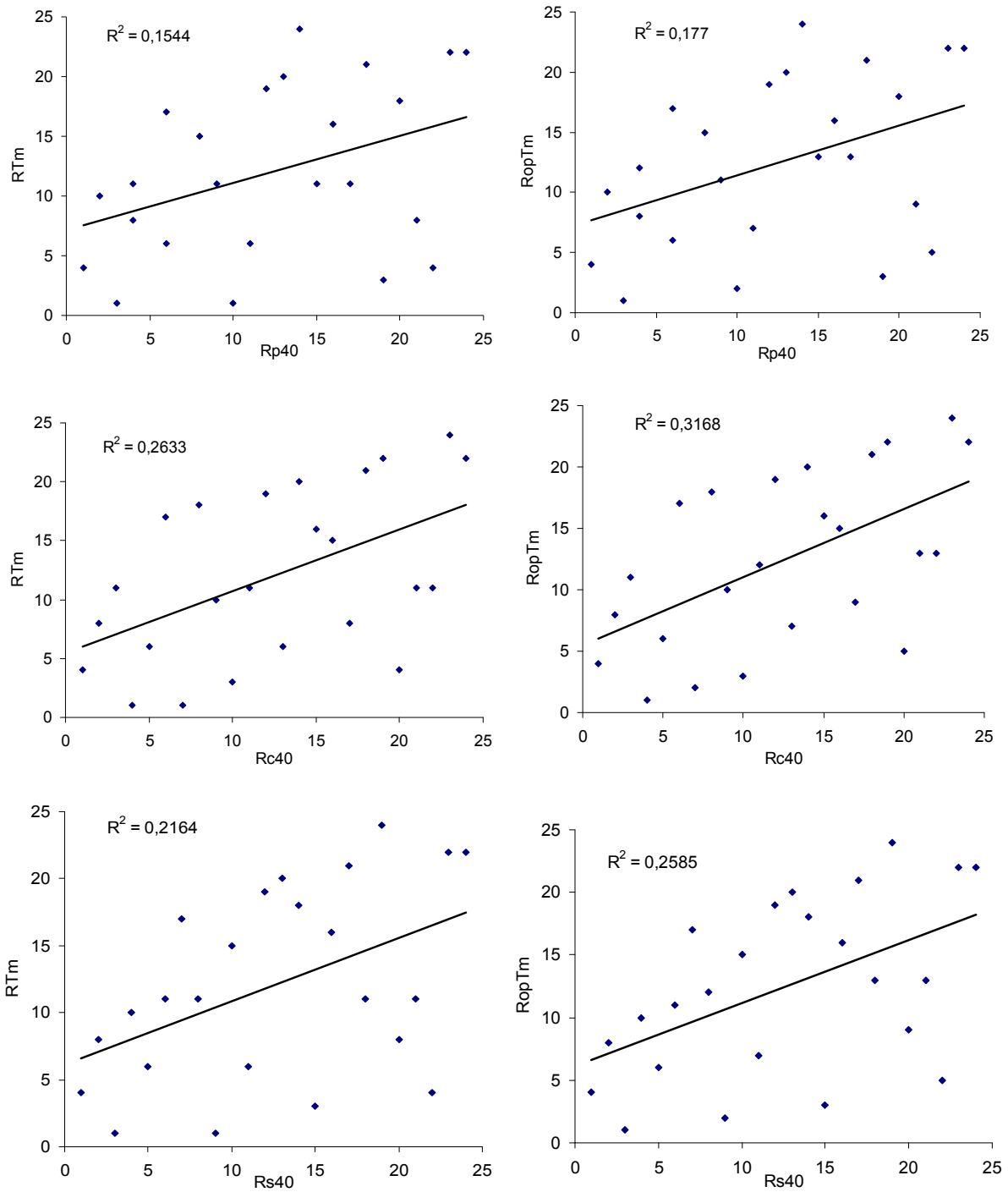


Figure 3.II. 13: Correlation curves of 24 GCSF formulations in DOEa, DOEb and DOEc. That includes correlation between R_{Tm} (ranking based on T_m) or R_{opTm} (ranking after optimization of R_{Tm} using the degree of unfolding reversibility), and physical, chemical or overall stabilities (R_p , R_c and R_s , respectively) of the formulations at 40°C.

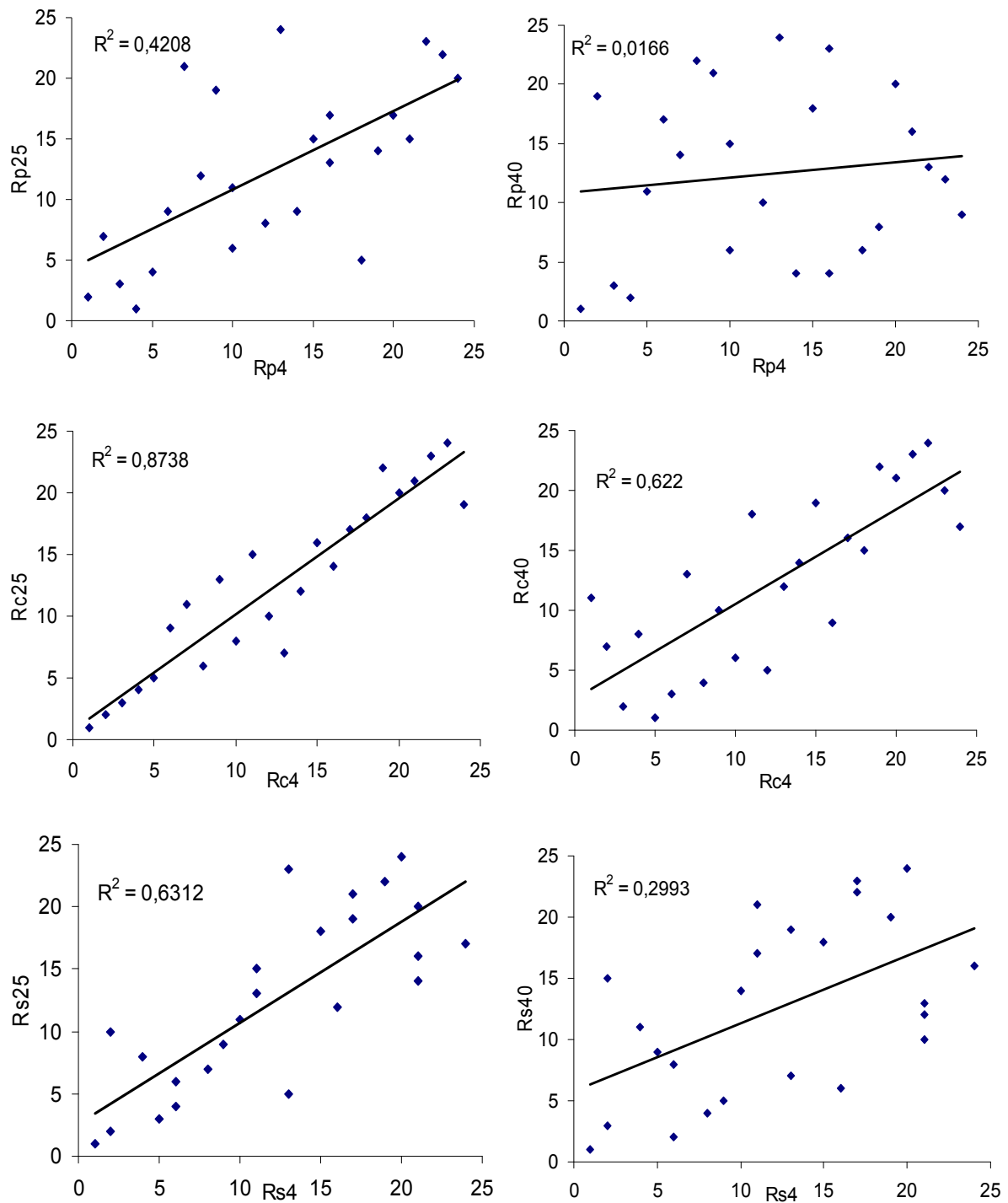


Figure 3.II. 14: Correlation curves of 24 GCSF formulations in DOEa, DOEb and DOEc. That includes correlation between ranking based on IsoSS at 4°C (R_p4 , R_c4 and R_s4) and ranking based on different IsoSS at 25°C (R_p25 , R_c25 and R_s25) and at 40°C (R_p40 , R_c40 and R_s40).

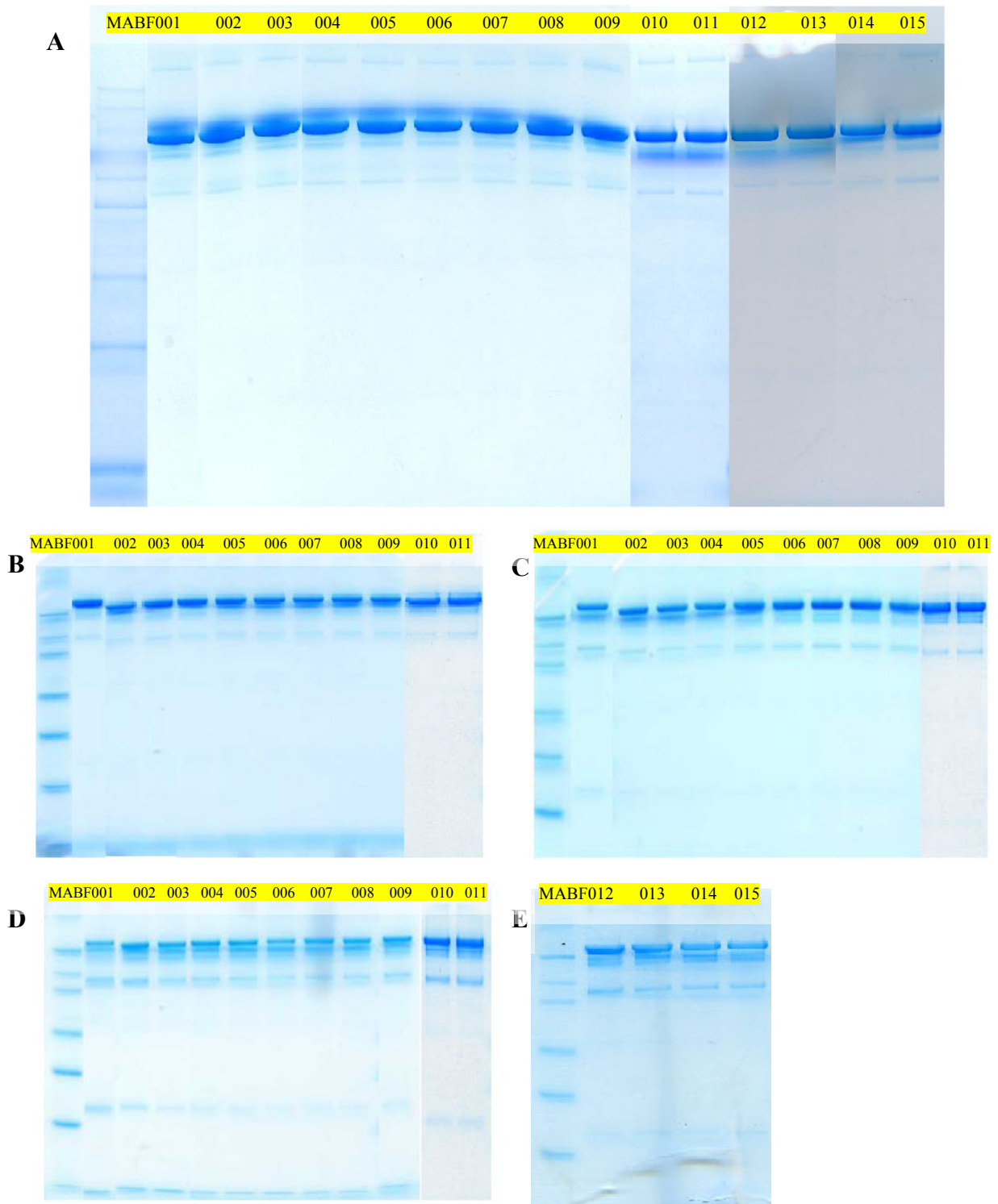


Figure 3.II. 15: SDS-PAGE for the whole 15 MAB formulations at the beginning (A) of the IsoSS and after 12 months storage at 4°C (B) and 25°C (C) and 40°C (D) for 11 MAB formulations and after 6 months storage at 40°C for 4 MAB formulations (E).

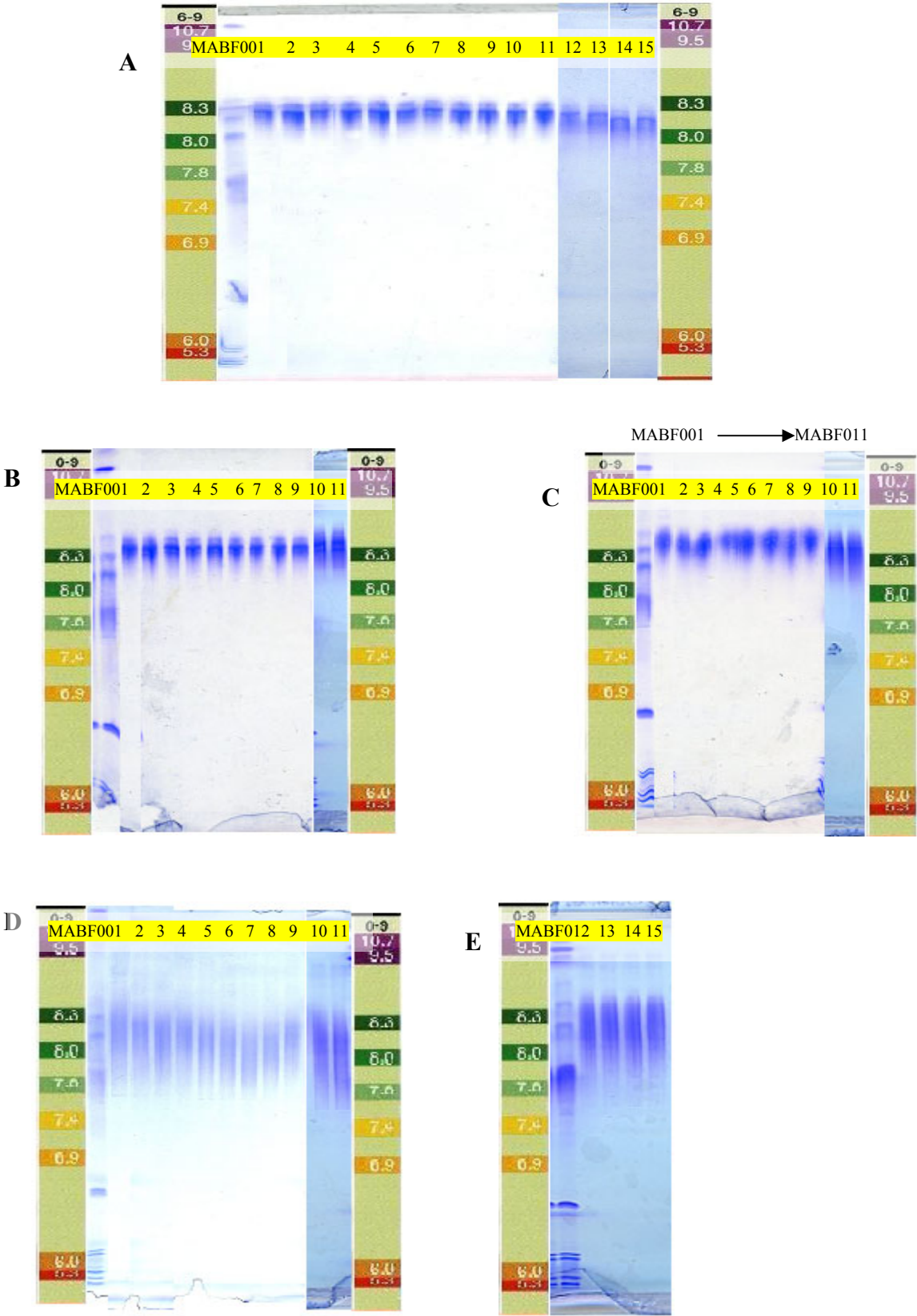


Figure 3.II. 16: IEF for the whole 15 MAB formulations at the beginning (A) of the IsoSS and after 12 months storage at 4°C (B) and 25°C (C) and 40°C (D) for 11 MAB formulations and after 6 months storage at 40°C for 4 MAB formulations (E).

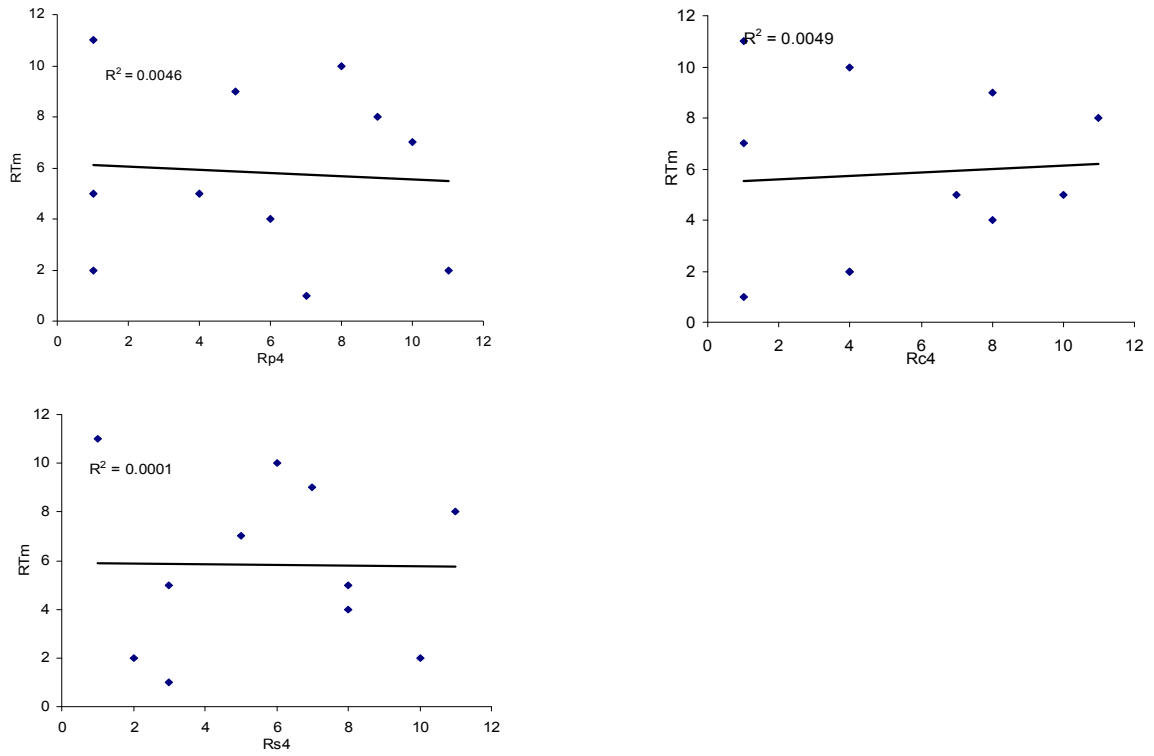


Figure 3.II. 17: Correlation curves of 11 PEG-INF formulations. That includes correlation between T_m based ranking (R_{T_m}) and rankings based on IsoSS at 4°C ($R_{p,4}$, $R_{c,4}$ and $R_{s,4}$) after 12 months

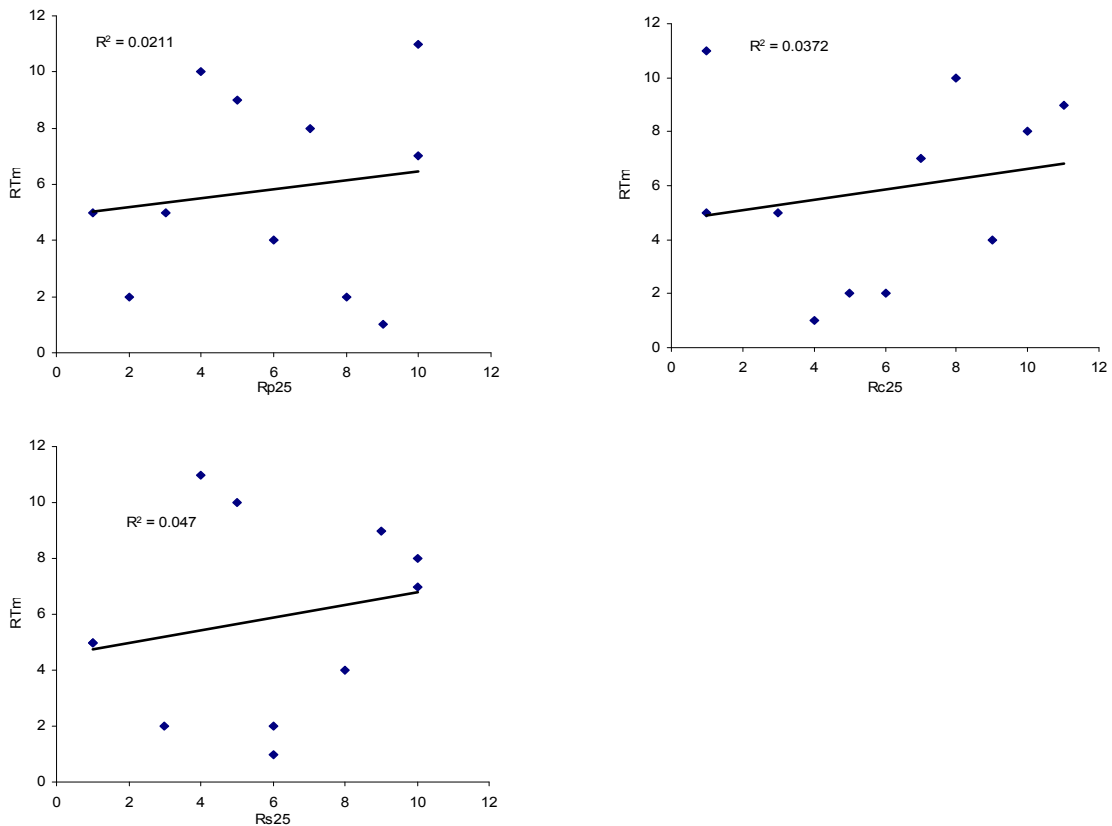


Figure 3.II. 18: Correlation curves of 11 PEG-INF formulations. That includes correlation between T_m based ranking (R_{T_m}) and rankings based on IsoSS at 25°C ($R_{p,25}$, $R_{c,25}$ and $R_{s,25}$) after 12 months

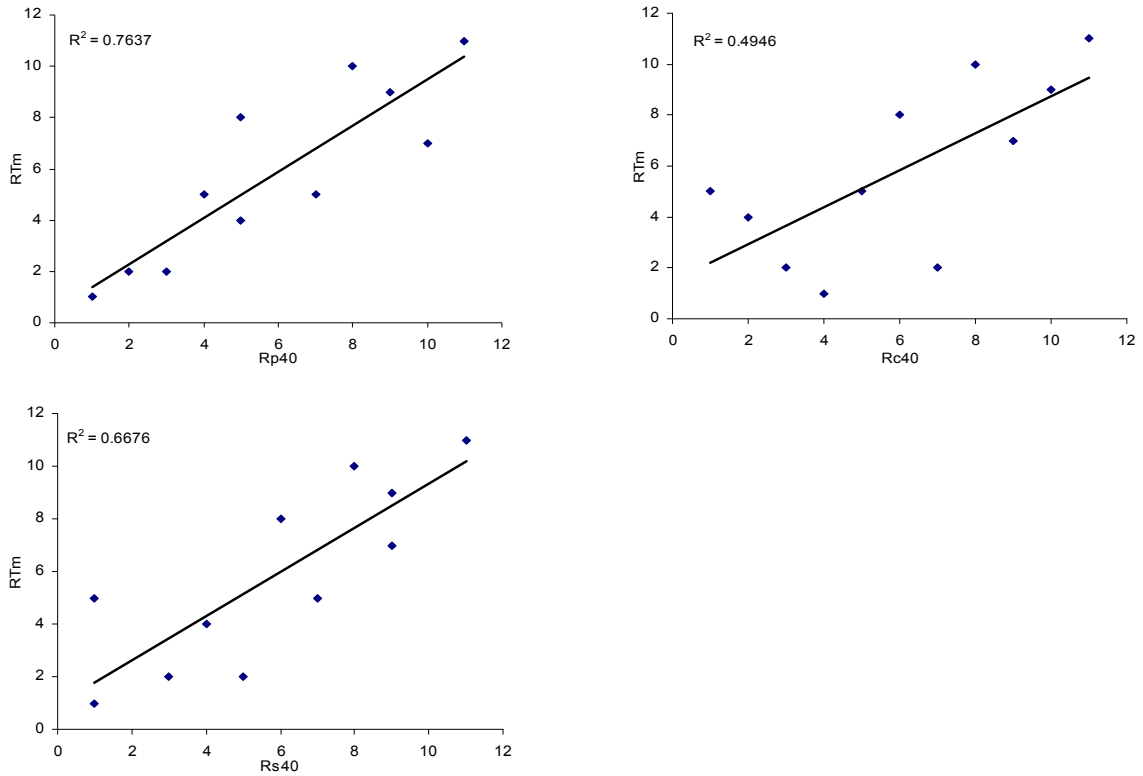


Figure 3.II. 19: Correlation curves of 11 PEG-INF formulations. That includes correlation between T_m based ranking (R_{Tm}) and rankings based on IsoSS at 40°C (R_{p40} , R_{c40} and R_{s40}) after 6 months

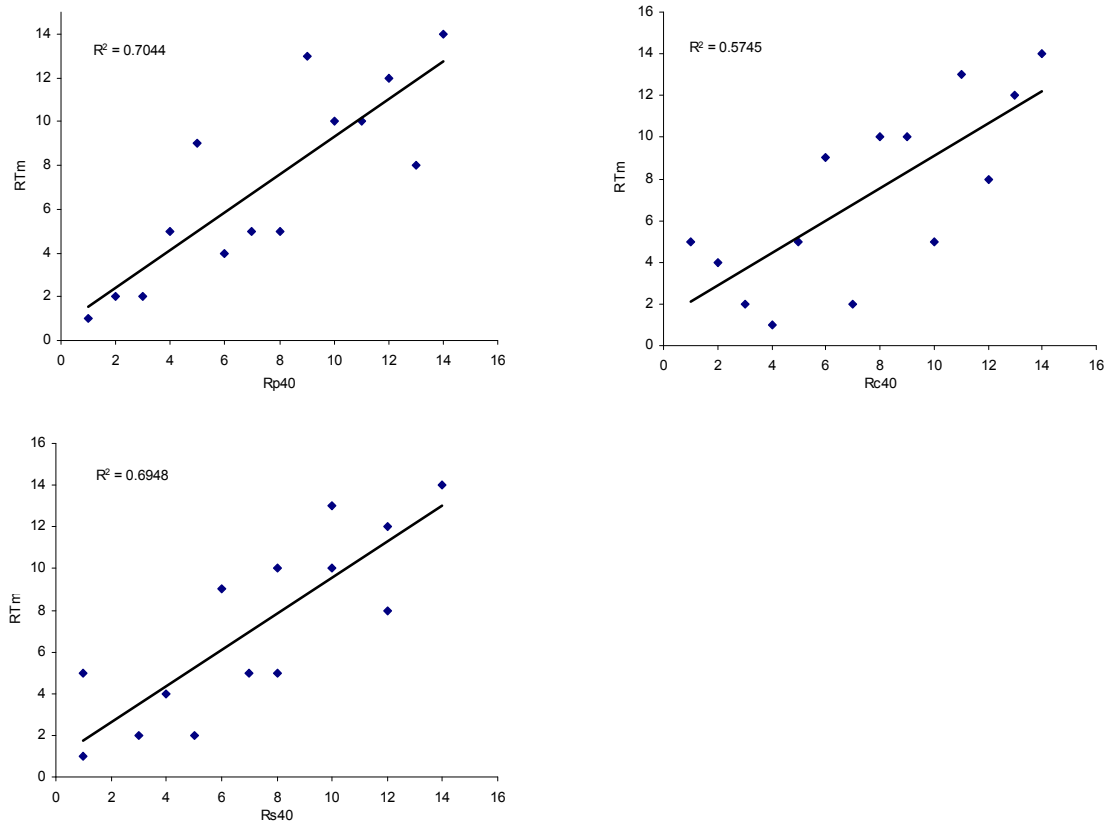


Figure 3.II. 20: Correlation curves of 14 PEG-INF formulations. That includes correlation between T_m based ranking (R_{Tm}) and rankings based on IsoSS at 40°C (R_{p40} , R_{c40} and R_{s40}) after 6 months

Chapter 4

Other strategies for the prediction of long term stability of GCSF liquid formulations

1. Introduction:

As mentioned before proteins undergo many degradation pathways mainly physical or chemical. The main degradation pathway for protein is, as considered in most cases, physical denaturation and aggregates formation. In fact such assumption should be justified according to each individual protein. The extent to which either physical or chemical stability is involved in overall stability can vary from one protein molecule to another. Furthermore, stabilizing excipients may affect the protein degradation either through chemical, physical or even both mechanisms. In the last chapter a systematic study to evaluate the predictive power of T_m (measured by μ DSC) as a stability marker for three different proteins was presented. That was furthermore evaluated in comparison to the predictive power of the classical accelerated stability studies where T_m proved to be more powerful in predicting long term physical stability. On the other hand classical accelerated stability studies showed higher power in predicting chemical stability.

Other methods to predict stability are also used in protein formulation development. Such methods aim mainly to determine the protein unfolding temperature (T_m) based on spectroscopic measurements. Those include Fourier transform infrared spectroscopy (FTIR), 2nd derivative UV spectroscopy, circular dichroism and fluorescence spectroscopy¹⁻⁴. Predictive studies with such techniques are not published intensively. However, all such studies evaluate either μ DSC or spectroscopic T_m s depending on comparing T_m s with accelerated stability data.

In this chapter 16 GCSF formulations were selected to evaluate the predictive power of other strategies. Both isothermal stability data at 40°C and μ DSC T_m s determined in the previous work were used and added to that T_m measurements from both FTIR and 2nd derivative UV spectroscopy. Moreover, we developed a new method where the temperature at which 50% of GCSF monomer is denatured was measured by non-isothermal strategies. All the above mentioned methods were tested for their predictive power of the isothermal stability study at 4°C.

2. Materials and methods:

2.1. Materials:

Granulocyte Colony stimulating factor (GCSF) was obtained as a gift from Roche diagnostics GmbH (D-Penzberg). All other materials and solvent were of analytical grade. Deionised double-distilled water was used throughout the study.

2.2. Formulations:

In the present work we have selected 16 GCSF formulations from the previously, in chapter 3 part I, studied set to evaluate other high throughput stability predictive strategies. The formulations were included in 2 designs of experiments (DOE), DOEb and DOEc, which are already presented in chapter 3, page 55, in tables 3.2 and 3.3, respectively. The effect of acetate and citrate buffers in different concentrations, different pH values, and the effect of different concentrations of Tween 80 or HPBCD were studied. These 2 DOEs were designed as fractional factorial designs based on the partition of a 2⁴ full factorial design using the (-1) generator from the third order interaction (-ABCD)⁵.

GCSF was obtained in Phosphate buffer 20 mM at pH 4 with a concentration of 4.2 mg/ml. The original solution was dialyzed using Slide-A-Lyzer^R Dialysis Cassette 2000 MWCO, 12-30 ml Capacity (Pierce, Rockford, USA), to remove the buffer salt. After dialysis the sample concentration was examined using an Uvikon 810 UV spectrophotometer (Tegimenta, Rotkreutz, Switzerland.). To the dialyzed stock the intended buffer salt and excipients were added and the final GCSF concentration was adjusted to 0.2 mg/ml for 2nd derivative UV spectroscopic measurements, and for the non-isothermal accelerated stability study. For FTIR measurements the final concentration was adjusted to 2 mg/ml. The final pH of the sample was adjusted and rechecked with a Mettler Toledo MP220 pH meter (Mettler-Toledo GmbH, Schwezenbach, Switzerland). After preparation all formulations were filtered through low protein binding syringe filters (25 mm, 0.2 µm, polyvinylidene fluoride (PVDF) membrane, Pall Corporation, MI, USA). A reference for each formulation containing the same buffer and the same excipients was also prepared and filtered using cellulose acetate disk filters, 0.2 µm pore size (VWR international, USA).

2.3. Fourier Transform Infrared Spectroscopy (FTIR):

The temperature-induced changes in the secondary structure of GCSF were monitored by attenuated total reflection (ATR)-FTIR, using Bio-ART unit. The spectra were collected in the

wave-number range from of 4000 to 850 cm^{-1} . The temperature was ramped according to thermal profile of each formula as revealed from μDSC previous measurements. Generally the temperature range was between 20-80 $^{\circ}\text{C}$. The secondary structure was monitored in closer intervals near μDSC T_m .

Before recording the spectrum the cell was equilibrated for 60 seconds. Each spectrum was obtained with 120 scans at a resolution of 4 cm^{-1} . The protein spectra were automatically background corrected by the buffer spectra at the respective temperature. The adsorption spectra were further processed by vector-normalisation. Afterwards, the second derivatives were calculated and again vector-normalised (OPUS, Bruker Optik, Ettlingen, Germany).

Figure 4.1 A shows the vector normalized 2nd derivative spectra for one of the tested formulations (GCSFDb1) in a temperature range of 20 to 80 $^{\circ}\text{C}$. Different interpretation methods are available in the literature to extract the unfolding temperature (T_{mFTIR}) from the spectral changes⁴. Plotting the intensities of the increasing β -sheet band at 1620 cm^{-1} (T_{mFTIR1} in figure 4.1 B), Plotting the intensities of the decreasing α -helix band at 1655 cm^{-1} (T_{mFTIR2} in figure 4.1 C) and using the cross section point between the increasing β -sheet band at 1620 cm^{-1} and the decreasing α -helix band at 1655 cm^{-1} (T_{mFTIR3} in figure 4.1 D). The midpoints of thermal denaturation in figure 4.1 B and C were obtained by performing sigmoid fit.

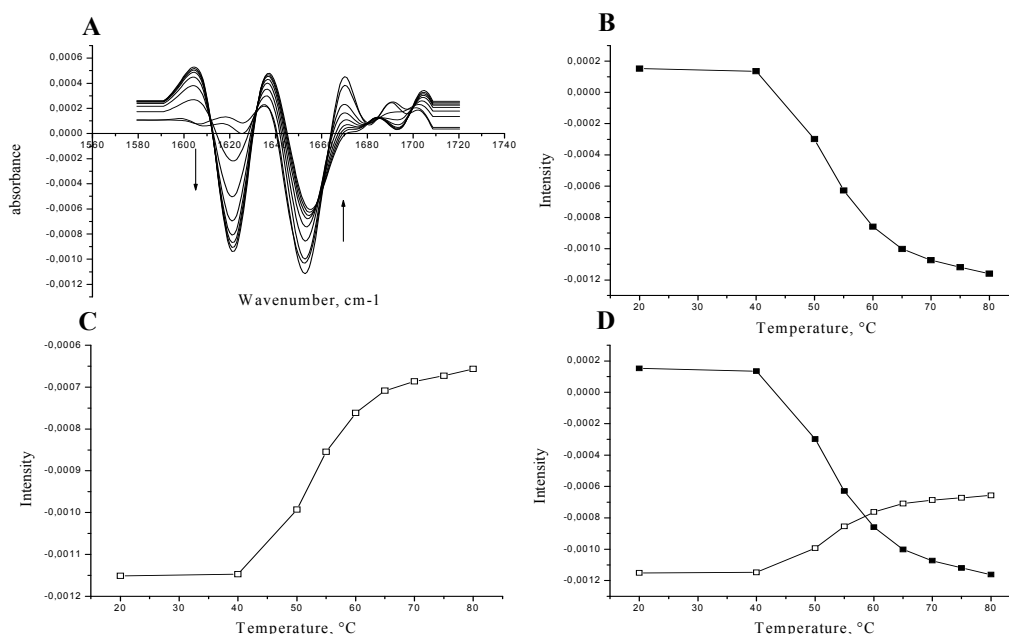


Figure 4. 1: FTIR measurement for GCSFDb1 formulation. Vector normalized second derivative spectra (A), Intensity change of the β -sheet band at 1620 cm^{-1} (B), Intensity change of α -helix band at 1655 cm^{-1} (C) and cross section point between increasing β -sheet and decreasing α -helix intensities(D).

2.4. 2nd derivative UV spectroscopy:

UV absorption spectra were obtained generally from 20 - 80 °C. The exact temperature range was selected according to the previously measured μ DSC T_m . Absorption spectra were recorded in a 5°C interval and in 2 °C intervals in the area just before and during unfolding. Measurements were done using Agilent 8453 UV spectrophotometer equipped with an Agilent 89090A temperature control device. Second derivatives of the absorption spectra were obtained employing a nine data point, quadratic-cubic formula using UV-Visible Chemstation® software from Agilent Technologies™. Second derivative spectra were fit to spline functions with 99 points of interpolation. The combined tyrosine and tryptophan peak near 284 nm and the tryptophan peak near 292 nm were used to monitor change in the tertiary structure of different GCSF formulations. As an effect of increasing temperature the above mentioned minima perform either blue (towards lower wavelengths) or red (towards higher wavelengths) shift indicating either unfolding or aggregation, respectively⁶. The position of each minimum was plotted as a function of temperature (figure 4.2 B and C) and the midpoints of thermal denaturation (T_{mUV}) were obtained by performing sigmoid fit. Accordingly, two different T_m s were obtained T_{mUV1} and T_{mUV2} for combined tyrosine tryptophan peak and tryptophan peak, respectively (figure 4.2 B and C). Moreover, the optical density at 350nm (turbidity) was monitored over the same temperature range to assess the aggregation behaviour of the formulation (figure 4.2 A). The resulted curves were fitted to exponential growth fitting function.

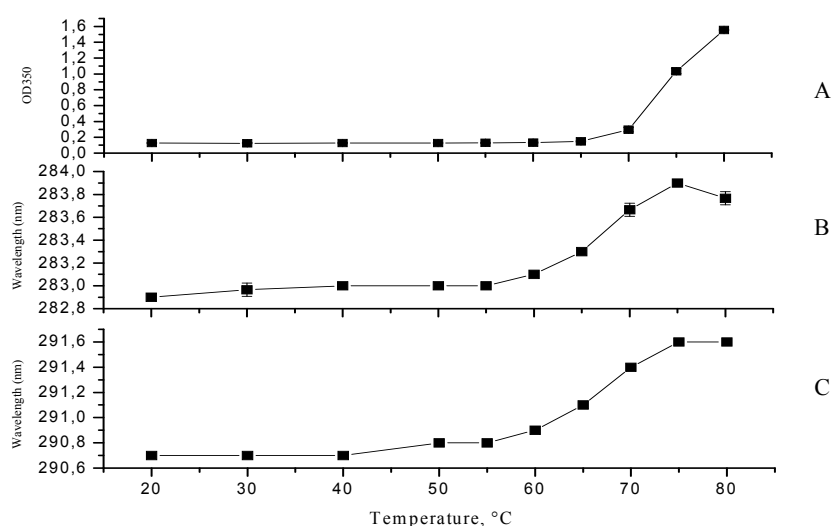


Figure 4. 2: Denaturation of GCSFDb1 monitored by 2nd derivative UV spectroscopy. Optical density at 350 nm (OD) versus temperature (A). Negative peak positions as a function of temperature near 282 nm (B) and 290 nm (C) for the absorbance of a combination of Tyr/Trp and Trp, respectively.

2.5. Non-isothermal accelerated stability study (Non-IsoSS):

Non-IsoSS was reported as a fast alternative to obtain linear Arrhenius parameters^{7,8} for small drug molecules and also for protein drugs. These studies considered monitoring the chemical degradation of a drug substance during heating and from the collected data the degradation rate at each temperature could be determined from which a linear Arrhenius plot is calculated. Protein physical denaturation doesn't obey a linear Arrhenius behaviour⁹ therefore, we didn't aim to determine any Arrhenius parameters. Using non-isothermal procedures we aimed to determine the temperature at which 50% of the native monomer is denatured (we called it in this work Temp⁵⁰ to differentiate it from thermal or spectroscopic determined T_ms) but instead thermal or spectroscopic measurements the monomer content was monitored during the heating cycle using size exclusion chromatography (SE-HPLC).

GCSF formulations were heated from 20 to Ca. 80°C using a Thermo-mixer device (ComfortTM, Eppendorf AG 2233, Hamburg). No mixing was applied during the whole ramp. Each formulation was divided in small aliquots each in an Eppendorf tube and left in the thermo-mixer to equilibrate at 20°C for 5 min. The temperature was increased according to a programmed temperature ramps. At several temperature intervals the set was left to equilibrate for 5 min and one tube was withdrawn, centrifuged at 14000 rpm for 5 min using Neo lab 16/18TM centrifuge (Hermle labortechnik, Wehingen, Germany). SE-HPLC analysis was performed to monitor the monomer content of each formulation at each temperature. Separation was achieved using Spectra-Physics HPLC system and a TSKgel G3000SWXL 7.8 mm ID x 30.0 cm L (Tosoh Bioscience). A flow rate of 0.6 ml/min was used, and the protein was detected at a wavelength of 215 nm. Mobile phase consists of 100 mM phosphate buffer pH 7. At each temperature the found monomer content was plotted against temperature. It was noticed that the monomer content decreased slowly at the early phase and then suddenly the monomer content drops very fast. Fitting such a curve was achieved by dividing it into two parts and each part was fitted using two terms polynomial fitting using Excel® software. An example of such a fitting is presented in figure 4.3. The temperature at which 50% of monomer is denatured (Temp⁵⁰) is calculated from the polynomial equation:

$$y = ax^2 + bx + c \quad (1)$$

By knowing y equal to 50 then two value of x can be calculated:

$$x_1 = \frac{-b - \sqrt{b^2 - 4a(c - y)}}{2a} \quad (2)$$

$$x_2 = \frac{-b + \sqrt{b^2 - 4a(c - y)}}{2a} \quad (3)$$

In all cases Temp⁵⁰ was determined by x_1 .

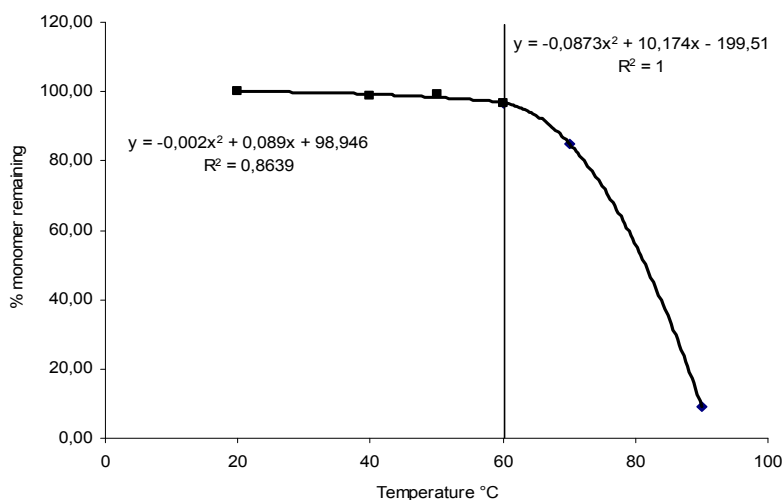


Figure 4. 3: Monomer content during Non-Iso-thermal stress for GCSFDb1 formulation. The curve left part is the slow degradation part and the right part the fast part.

2.6. Isothermal stability study (IsoSS):

All formulations were subjected to IsoSS at 4°C (20 months) and 40°C (3 months). At several time intervals formulations were analyzed for their monomer denaturation rate, turbidity, and chemical degradations rates. All methods and formulations were described in the last chapter in details. The results from chapter 3 part I are again used in this study too.

2.7. Ranking:

2.7.1. Ranking for the IsoSS:

This was described in details in the chapter 3 part I. in section I.1.5.2, pages 58 - 60. Table 4.1 show the ranking procedures for the 16 formulations included in 2 DOEs (DOEb and DOEc) based on IsoSS stability study at 4°C. The formulations were ranked with regards to physical stability (R_p4), chemical stability (R_c4) and the overall stability (R_s4).

Table 4. 1: Ranking of GCSF formulations in DOEb and DOEc after 20 months storage at 4°C

Formulations	K_p4	R_14	$Tur.4$	R_24	Avr. (R_14+R_24)/2	R_p4	K_c4	R_c4	Avr. (R_p4+R_c4)/2	R_s4
GCSFDb1	-0.0003	3	1	8	5.5	5	-0.0056	13	9	10
GCSFDb2	-0.0001	2	0.7	1	1.5	2	-0.0012	12	7	5
GCSFDb3	-0.0007	6	0.6	1	3.5	3	-0.00005	4	3.5	2
GCSFDb4	-0.0011	8	0.8	1	4.5	4	-0.0066	14	9	10
GCSFDb5	-0.0009	7	1.6	8	7.5	10	-0.0005	7	8.5	8
GCSFDb6	-0.0006	5	1	8	6.5	8	-0.0119	16	12	15
GCSFDb7	-0.0017	11	0.8	1	6	6	-0.0101	15	10.5	12
GCSFDb8	-0.0011	8	1.2	8	8	11	-0.0011	11	11	13
GCSFDc1	-0.0387	15	0.7	1	8	11	0.0003	2	6.5	4
GCSFDc2	-0.0005	4	1.1	8	6	6	0.0004	1	3.5	2
GCSFDc3	0.00004	1	0.9	1	1	1	-0.0002	5	3	1
GCSFDc4	-0.0377	13	0.7	1	7	9	-0.0005	7	8	6
GCSFDc5	-0.0011	8	1.1	8	8	11	-0.0004	6	8.5	8
GCSFDc6	-0.0383	14	2.9	15	14.5	16	-0.0005	7	11.5	14
GCSFDc7	-0.0398	16	1.6	8	12	14	0.0003	2	8	6
GCSFDc8	-0.0021	12	5.2	16	14	15	-0.0006	10	12.5	16

2.7.2. Predictive rankings:

In this chapter, 5 different stability studies were evaluated for their predictive power of the real time stability ranking (table 4.1.). Consequently, different ranking methods were studied.

2.7.2.1. Individual ranking:

For 16 GCSF formulations 5 different predictive rankings were calculated. Each of those was based on one of the studied predictive strategies. In table 4.2 rankings based on $T_{m\mu DSC}$, T_{mUV} , T_{mFTIR} and $Temp^{50}$ are presented. Furthermore, the accelerated stability study at 40°C was

also evaluated as a predictive method and the ranking based on it is presented also in table 4.2 (IsoSS40°C ranking) for physical (R_p40), chemical (R_c40) and overall (R_s40) stability.

Table 4. 2: Individual ranking based on different stability predictive strategies

Formulations	μ DSC		2 nd UV		FTIR		Temp ⁵⁰		IsoSS40°C ranking		
	$T_{m\mu DSC}$	Rank	T_{mUVav}	Rank	T_{mFTIR1}	Rank	Temp ⁵⁰	Rank	R_p40	R_c40	R_s40
GCSFDb1	69,5	7	66,2	7	52,9	8	81,5	3	11	14	13
GCSFDb2	69,9	6	68,4	3	53	7	82,7	2	1	7	4
GCSFDb3	71,5	3	67,1	6	50,7	13	79	4	7	9	7
GCSFDb4	69,6	7	66	8	50,9	12	72,8	6	12	13	13
GCSFDb5	59	13	57,9	13	48,5	15	58,2	12	13	11	11
GCSFDb6	57,3	15	55,6	15	51,4	11	54,4	15	16	16	16
GCSFDb7	56,3	16	54,4	16	47,3	16	53,2	16	9	15	11
GCSFDb8	57,5	14	56,9	14	50,2	14	57,9	14	15	12	15
GCSFDC1	70,3	5	68	4	53,1	6	70,8	7	3	1	1
GCSFDC2	72,5	1	71	1	62,9	1	86,4	1	6	5	6
GCSFDC3	72,6	1	70,1	2	56	4	74,5	5	2	2	1
GCSFDC4	71,2	4	67,7	5	57,14	2	70,4	8	5	3	4
GCSFDC5	66,2	9	62,2	9	56,8	3	63,9	9	3	4	3
GCSFDC6	61,7	11	59	11	52	9	61,1	11	8	8	7
GCSFDC7	62,9	10	59,8	10	53,4	5	62	10	13	6	9
GCSFDC8	60,5	12	58,2	12	51,9	10	58	13	9	10	9

2.7.2.2. Combined ranking:

In a trial to improve the predictive power of each method a combined ranking was performed in which the average of two or more rankings was calculated and compared with the IsoSS4°C ranking. The number of possible combinations was huge. Therefore, and due to limited space, not all ranking tables are presented but only a representative table for the combined ranking between $T_{m\mu DSC}$ and T_{mUV} is presented in table 4.3.

Table 4. 3: Combined μ DSC and 2nd derivative UV ranking for 16 GCSF formulations

Formulations	μ DSC		2 nd UV		Average ($R_{\mu\text{DSC}} + R_{\text{UV}}$)/2	
	T_m	Rank	$T_{m\text{UVav}}$	Rank	Aver.	Rank
GCSFDb1	69,5	7	66,2	7	7,5	7
GCSFDb2	69,9	6	68,4	3	4,5	3
GCSFDb3	71,5	3	67,1	6	4,5	3
GCSFDb4	69,6	7	66	8	7,5	7
GCSFDb5	59	13	57,9	13	13	13
GCSFDb6	57,3	15	55,6	15	15	15
GCSFDb7	56,3	16	54,4	16	16	16
GCSFDb8	57,5	14	56,9	14	14	14
GCSFdc1	70,3	5	68	4	4,5	3
GCSFdc2	72,5	1	71	1	1,5	1
GCSFdc3	72,6	1	70,1	2	1,5	1
GCSFdc4	71,2	4	67,7	5	4,5	3
GCSFdc5	66,2	9	62,2	9	9	9
GCSFdc6	61,7	11	59	11	11	11
GCSFdc7	62,9	10	59,8	10	10	10
GCSFdc8	60,5	12	58,2	12	12	12

2.8. Correlation:

The correlations were judged as in chapter 3 according to two parameters.

- 1- Pearson product moment correlation coefficient obtained from correlation curves between each predictive rankings and ranking based on IsoSS at 4°C
- 2- The 50% and 20% prediction quality.

3. Results and discussion:

3.1. Measured parameters:

Table 4.4 shows different T_m s measured using UV and FTIR for 16 GCSF liquid formulations involved in our study. μ DSC measured T_m and Temp⁵⁰ were listed in table 4.2.

Table 4. 4: T_{mUV} and T_{mFTIR} for 16 GCSF formulations of DOEb and DOEc

Formulations	2 nd derivative UV			FTIR		
	T_{mUV1}	T_{mUV2}	T_{mUVav}	T_{mFTIR1}	T_{mFTIR2}	T_{mFTIR3}
GCSFDb1	66,1	66,2	66,2	52,9	52,8	58,8
GCSFDb2	68,7	68,0	68,4	53	51,2	58,5
GCSFDb3	67,5	66,7	67,1	50,7	47,1	57
GCSFDb4	66,3	65,7	66	50,9	51,18	59,8
GCSFDb5	57,3	58,5	57,9	48,5	46,9	59,4
GCSFDb6	56	55,1	55,6	51,4	58,8	60,4
GCSFDb7	52,9	55,9	54,4	47,3	44,2	60,3
GCSFDb8	56	57,8	56,9	50,2	49,4	59,8
GCSFDc1	68,4	67,6	68	53,1	64	64,3
GCSFDc2	72,1	69,8	71	62,9	63,9	64,7
GCSFDc3	70,7	69,5	70,1	56	65,6	59,3
GCSFDc4	67,7	67,6	67,7	57,14	58,3	59,2
GCSFDc5	62,4	61,9	62,2	56,8	57,9	58,3
GCSFDc6	59,5	58,5	59	52	55,4	55,5
GCSFDc7	59,7	59,9	59,8	53,4	54,1	57
GCSFDc8	57,2	59,1	58,2	51,9	51,5	56

3.2. Correlation:

In this section it should be highlighted, as explained in chapter 3, that the stability of the GCSF molecule is affected by both physical and chemical stability. In DOEb physical stability of the formulations was driven from chemical stability, due to the oxidative effect of the peroxide residue in Tween 80, which was not the case in DOEc formulations.

Normally in protein formulation development the objective is not to develop physically or chemically stable formulation but one that is both physically and chemically stable. In such a situation, the prediction power of a method would be rather judged based on its ability to predict the overall stability rather than either physical or chemical stability alone.

Theoretically most of the studied parameters in this chapter should only be able to reflect the changes in physical properties. Therefore, prediction of the overall stability will be a great challenge.

In the following section the predictive power of each method will be discussed.

3.2.1. Prediction based on individual rankings:

Ranking based on each parameter was correlated to rankings based on IsoSS 4°C for physical, chemical, and overall stabilities. The predictive power of each method was judged based primarily on correlation coefficients, and second on the 50 % as well as 20 % prediction quality. Figure 4.4 shows an overview of the resulting correlation coefficients and figure 4.5 shows the 50% and 20% prediction quality. (Due to the huge number of correlation curves obtained in this chapter as well as the limited space no correlation curves are presented).

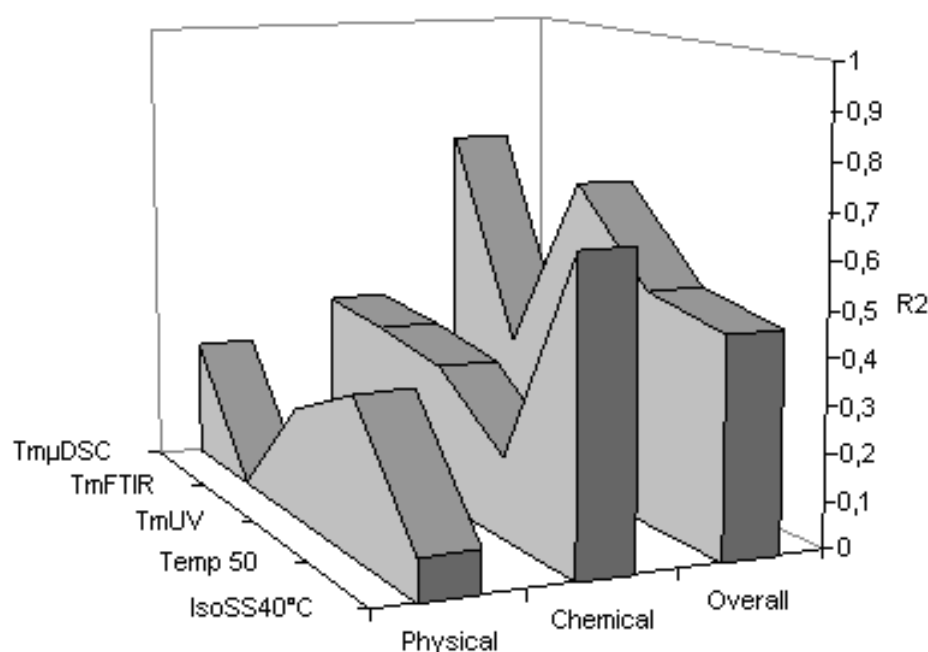


Figure 4. 4: An overview of the correlation coefficients resulting from correlating rankings based on different predictive methods and IsoSS at 4°C (physical, chemical, or overall) based rankings.

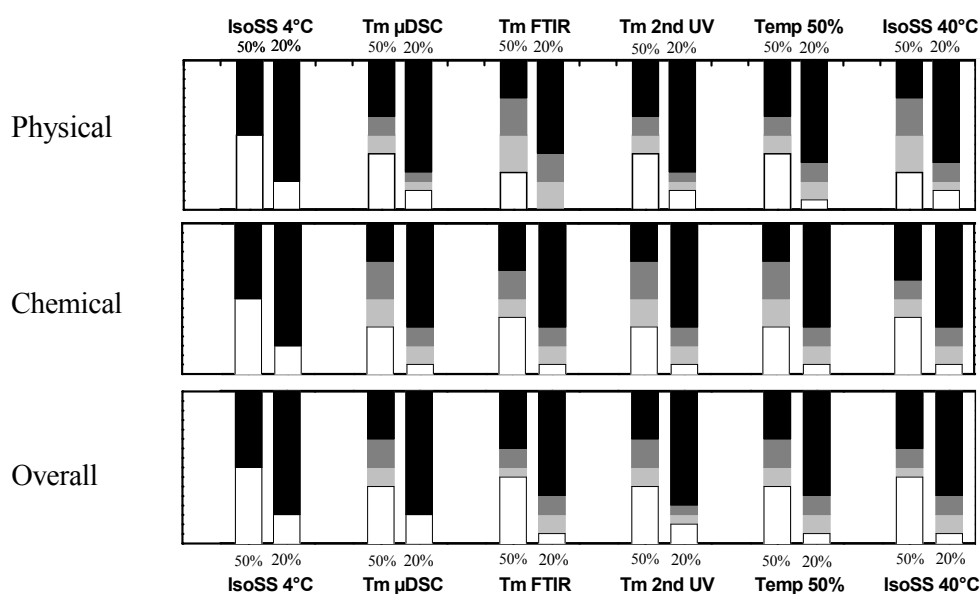


Figure 4. 5: Prediction quality of different methods in predicting physical, chemical or overall IsoSS at 4°C. 50% as well as 20 % prediction quality are shown beside each other for each method.

3.2.1.1. Differential scanning microcalorimetry (μ DSC):

$T_{m\mu DSC}$ showed a slightly lower correlation coefficient for physical than that for chemical stabilities (figure 4.4). Despite lower correlation coefficient, $T_{m\mu DSC}$ showed a higher 50% and 20% quality in predicting the physical stability (figure 4.5). $T_{m\mu DSC}$ measurement was affected by chemical oxidation of GCSF formulations in DOEb (8 from the total 16 formulations) and that caused (when ranking both DOEb and DOEc as one group) a reduced correlation to physical stability than to chemical stability and therefore, lower correlation coefficient for physical stability has been observed. Predicting the overall stability ranking, $T_{m\mu DSC}$ showed a significantly strong predictive power revealed by a high correlation coefficient, a very high 50% prediction quality and surprisingly a full 20% prediction quality. $T_{m\mu DSC}$ was able without error to select the best 3 formulations and to exclude the worst 13 from a group of 16 GCSF liquid formulations (figure 4.5)

3.2.1.2. *Fourier Transform Infrared spectroscopy (FTIR):*

In order to choose which of the FTIR measured T_m s shall be used preferably, rankings based on each of the different T_m s was studied in correlation to the IsoSS rankings at 4°C (appendix 4.I figure 4.I.1). T_{mFTIR1} , which showed the highest correlation coefficients, was used further in the correlation study (the ranking shown in table 4.2 is made based on T_{mFTIR1}). T_{mFTIR} based ranking showed a very low correlation coefficient and a bad prediction quality especially for physical stability as shown in figures 4.4 and figure 4.5, respectively. The correlation with chemical stability was better. For measuring the unfolding temperature (T_{mFTIR}) of liquid protein formulations high protein concentration is needed to omit the interference of the water absorption peak in the amide I region¹⁰. In this study the concentration used for T_{mFTIR} measurements was 2 mg/ml while only 0.2 mg/ml GCSF was included in formulations for IsoSS. This higher concentration most probably would affect the measured T_m and consequently false ranking may be obtained. Furthermore, the measurement in the Bio-ART unit takes place on the crystal surface and not in solution bulk and therefore the measured T_m would be mainly affected by protein stability at interfaces^{1,10}. In the presence of factors like Tween80 and HPBCD where they act on both levels (interface and solution bulk) the effect on the interface would be exaggerated leading to a wrong determination of T_m s. The reason for the high correlation with chemical stability is not clear. A possible explanation can be that FTIR monitors changes in secondary structure which take place mainly through breaking of hydrogen bonds^{11,12}. Such bonds might break due to other covalent chemical reactions and thus would also cause secondary structure changes and T_m would be highly affected by chemical changes.

3.2.1.3. *2nd derivative UV spectroscopy:*

As mentioned in section 2.4, page 152, two different T_m s were obtained: T_{mUV1} and T_{mUV2} (figure 4.2 B and C). Each one was tested for its correlation to the IsoSS 4°C. Moreover, the average of these two T_{mUV} (T_{mUVav}) listed in table 4.4 was also tested to find out which T_m could be used further in the correlation studies. Figure 4.I.2 in appendix 4.I shows the comparison based on correlation coefficients of the two T_{mUV1} and T_{mUV2} as well as the average T_{mUVav} . All three were found to be equal in terms of correlation coefficients and for further correlation studies T_{mUVav} was used (the ranking shown in table 4.2 is made based on T_{mUVav}). The prediction quality was very similar to that for T_{mDSC} . Physical stability was predicted with a slightly lower correlation coefficient than chemical stability with higher prediction quality to physical stability prediction, and a high correlation to overall stability

prediction was obtained (figure 4.4 and 4.5). This ability to reflect some chemical degradation process gave this method an advantage in predicting the overall stability ranking of GCSF formulations.

3.2.1.4. *Non-IsoSS measured Temp⁵⁰*:

The monomer content of each formulation was monitored during a temperature ramp from 20 to ca. 80°C as described in section 2.5. Temp⁵⁰, which is the temperature at which 50% of the monomer is denatured, should in theory be equal to T_ms determined from other techniques but practically that was not true as shown in table 4.2. It was noticed that T_ms determined from other techniques (μ DSC, UV or FTIR) are also not identical. A reason for this deviation might be due to the different measuring principles in each technique. However, Temp⁵⁰ is a direct measure for the monomer content and therefore it would represent the true temperature at which really 50% of the protein molecule is denatured.

Temp⁵⁰ showed, in comparison to other predictive strategies, the highest correlation coefficient to physical stability and the lowest to chemical stability (figure 4.4). Temp⁵⁰ based rankings were not that good in predicting the overall stability of the studied GCSF formulations.

3.2.1.5. *IsoSS40°C*:

IsoSS40°C showed the best correlation to chemical stability and very weak correlation to physical stability with a middle correlation to overall stability (figure 4.4). The same behaviour was noticed when studying the correlation of the whole 24 GCSF formulation set in chapter 3, part I (figure 3.7. page 72). The chemical degradation, of many proteins showed linear Arrhenius plots¹³⁻¹⁵ which should allow us to apply extrapolation of the Arrhenius curve to predict shelf life at real storage temperature. And that agrees with the strong predictive power of IsoSS40°C to chemical stability of GCSF formulations. In contrast, for physical denaturation involving conformational changes, only phenomenological extrapolation approaches for aggregation rate prediction were published¹⁶. An excellent review criticizing the application of the Arrhenius plot in predicting aggregation rates under real time conditions is available from Weiss et al⁹. This review explains how protein molecules show non Arrhenius behaviour and there are many concerns in predicting aggregation rate using extrapolation Arrhenius approaches. That might explain the bad prediction observed by using IsoSS40°C in predicting physical stability not only in the present study but also in chapter 3 with three different proteins. IsoSS40°C is chemically biased

method therefore the prediction of the overall stability was not satisfactory in comparison with other predictive methods like μ DSC and 2nd derivative UV spectroscopy.

3.2.2. Prediction based on combined-ranking:

In this section it was investigated if the predictive power would be improved by combining of more than one method in a combined predictive ranking.. Effects of such combinations on both correlation coefficients and prediction quality of each predictive method are studied. The effect of combined rankings on the predictive power of $T_{m\mu DSC}$ is graphically presented in figures 4.6, 4.7 and 4.8 for the effect on correlation coefficients, 50% and 20% prediction quality, respectively. The effect on predictive powers of the other techniques (UV, FTIR, Temp⁵⁰ and IsoSS40°C) is presented in figures 4.I.3 – 14 in appendix 4.I.

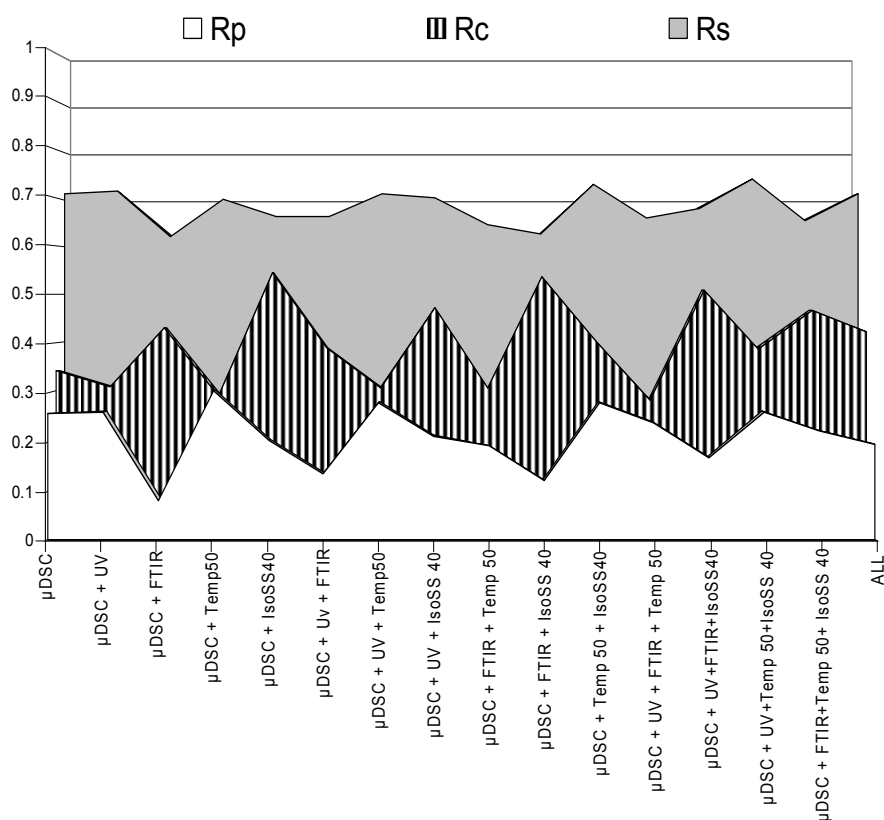


Figure 4. 6: Effect of combining different predictive rankings with ranking based on $T_{m\mu DSC}$ on the correlation coefficients resulting from correlating each combined ranking with the real stability based ranking. R_p states for ranking based on physical stability, R_c for ranking based on chemical stability and R_s for ranking based on overall stability

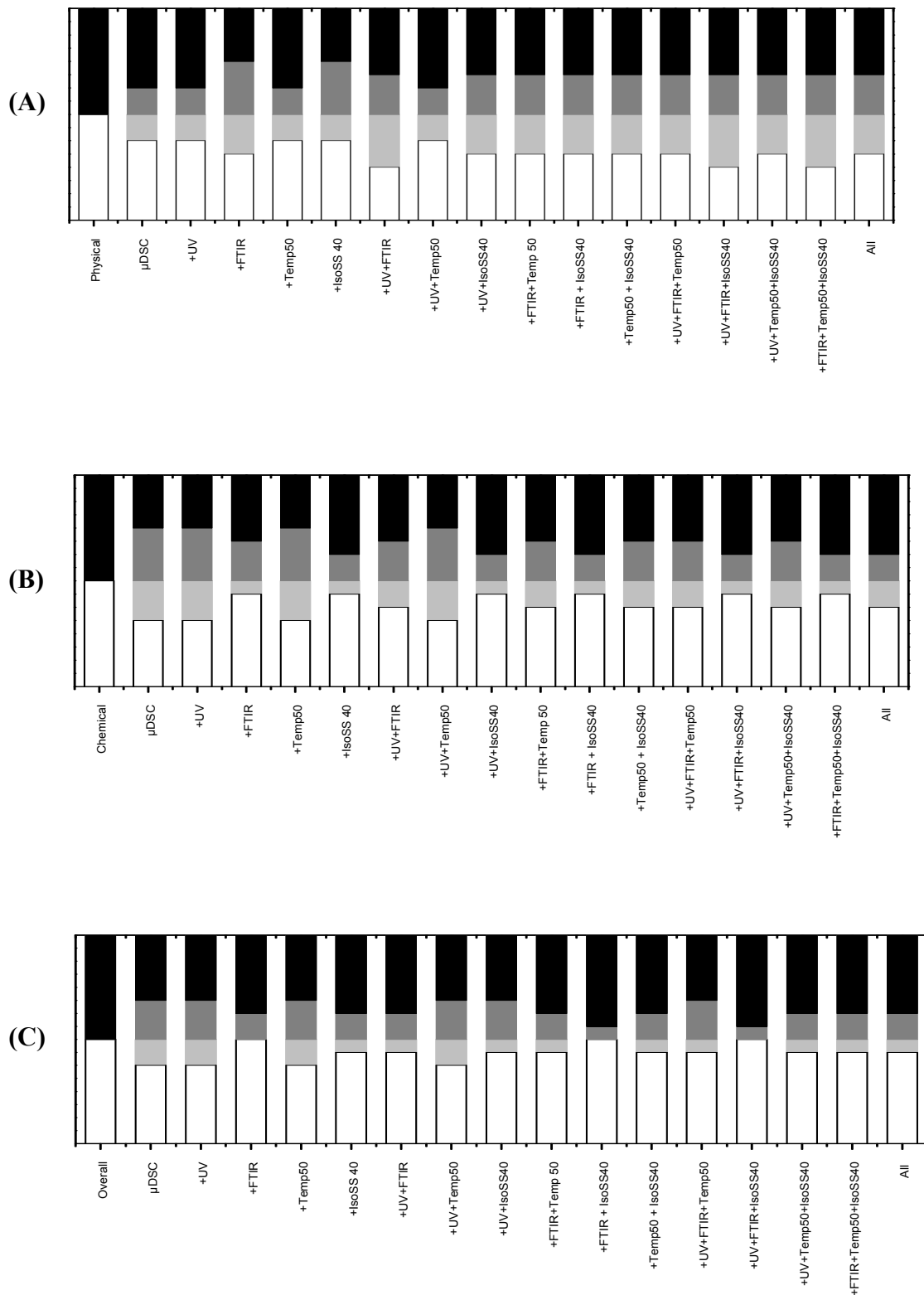


Figure 4. 7: Effect of combined rankings on the 50% prediction quality of $T_{m,\mu DSC}$ in predicting physical stability (A), chemical stability (B) and the overall stability ranking (C) of 16 GCSF formulations after 20 months storage at 4°C

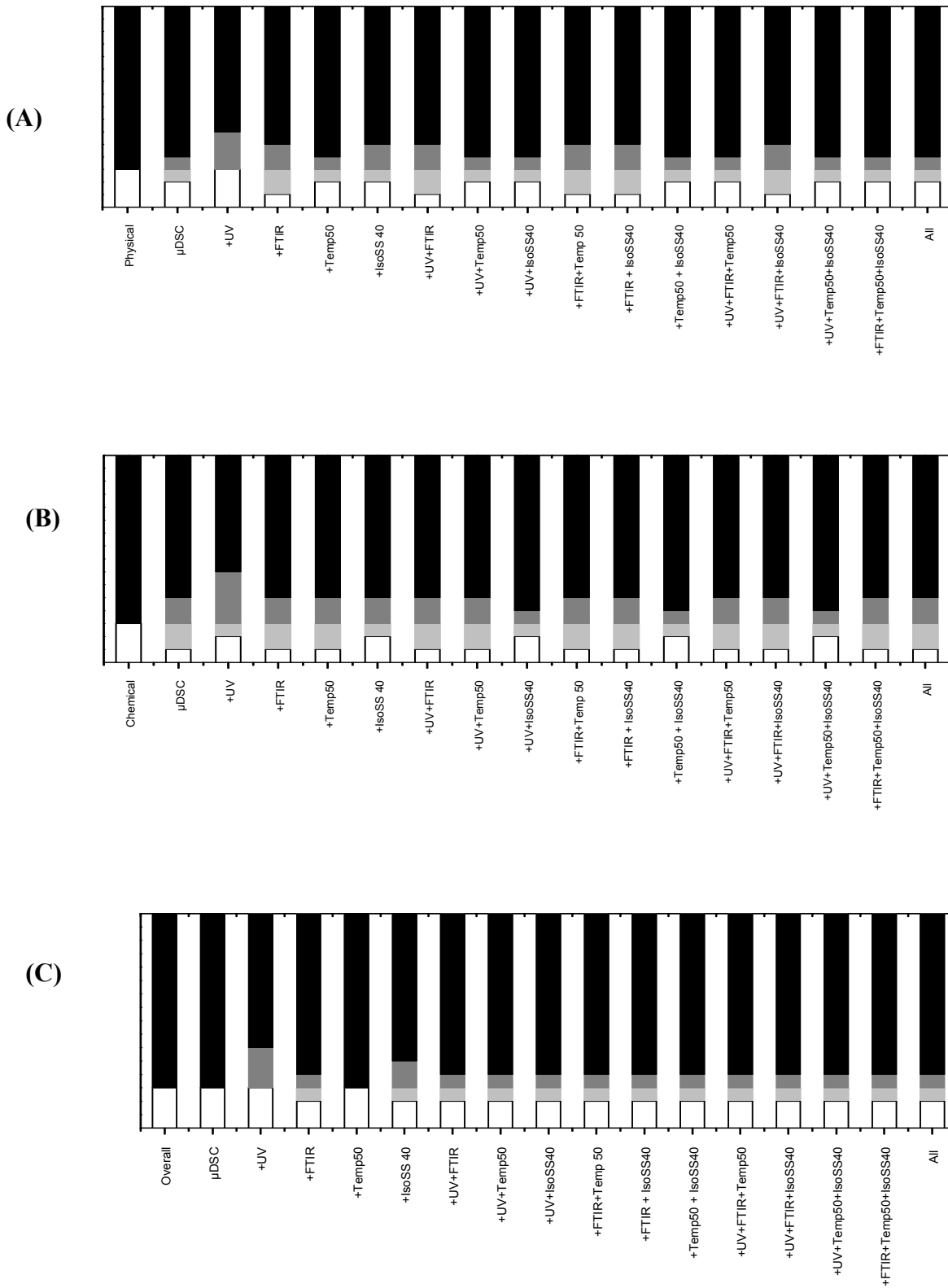


Figure 4. 8: Effect of combined rankings on the 20% prediction quality of $T_{m,\mu DSC}$ in predicting physical stability (A), chemical stability (B) and the overall stability ranking (C) of 16 GCSF formulations after 20 months storage at 4°C

3.2.2.1. *Physical stability:*

No significant improvement in physical stability prediction of $T_{m\mu\text{DSC}}$, as observed on the correlation coefficients, by combining rankings from other predictive techniques (figure 4.6). The same was also observed for $T_{m\text{UV}}$ and Temp^{50} based rankings (figures 4.I.3, page 171 and figure 4.I.9, page 177, respectively). $T_{m\text{FTIR}}$ and accelerated stability studies (IsoSS 40°C) based rankings showed improvement in correlation coefficients when combined with one or more of $T_{m\mu\text{DSC}}$, $T_{m\text{UV}}$ and Temp^{50} based rankings (figure 4.I.6, page 174 and Figure 4.I.12, page 180, respectively). Studying both 50% and 20% prediction qualities, no improvement was observed for $T_{m\mu\text{DSC}}$ (Figure 4.7 A and 4.8 A), $T_{m\text{UV}}$ (Figures 4.I.4 A and 4.I.5 A, pages 172 and 173) and Temp^{50} (figures 4.I.10 A and 4.I.11 A, pages 178 and 179) by combined ranking approach. $T_{m\text{FTIR}}$ (figure 4.I.7 A and 4.I.8 A, pages 175 and 176) and IsoSS 40°C (figure 4.I.14 A and 4.I.15 A, pages 181 and 182) physical stability prediction quality improved when one or more of $T_{m\mu\text{DSC}}$, $T_{m\text{UV}}$ and Temp^{50} based rankings are included.

3.2.2.2. *Chemical stability:*

No significant improvement in chemical stability prediction of IsoSS40°C based ranking by combining with other predictive rankings (figures 4.I.12, 4.I.13 B and 4.I.14 B, pages 180 – 182). On the other hand improvements were achieved in the predictive power of other methods when combined with IsoSS 40°C ranking. This can be seen on the higher correlation coefficients as well as the better prediction quality when rankings based on $T_{m\mu\text{DSC}}$ (figures 4.6, 4.7 B and 4.8 B, pages 163 – 165), $T_{m\text{UV}}$ (figures 4.I.3, 4.I.4 B and 4.I.5 B, pages 171 – 173), $T_{m\text{FTIR}}$ (figures 4.I.6, 4.I.7 B and 4.I.8 B, pages 174 – 176) or Temp^{50} (figures 4.I.9, 4.I.10 B and 4.I.11 B, pages 177 – 179) is combined with IsoSS 40°C based ranking.

3.2.2.3. *Overall stability:*

No significant improvement in the overall stability prediction of $T_{m\mu\text{DSC}}$ (Figure 4.6) and $T_{m\text{UV}}$ (figure 4.I.3, page 171) by combining rankings from other techniques. $T_{m\text{FTIR}}$ (figure 4.I.6, page 174), Temp^{50} (figure 4.I.9, page 177) and IsoSS 40°C (figure 4.I.12, page 180) based rankings showed significantly higher correlation coefficients when $T_{m\mu\text{DSC}}$ and/or $T_{m\text{UV}}$ are included. $T_{m\mu\text{DSC}}$ 50% prediction quality (figure 4.7 C) showed improvement by combining with either $T_{m\text{FTIR}}$ or IsoSS40°C. However, the best 20% selection quality was obtained by individual $T_{m\mu\text{DSC}}$ based ranking with no falsely predicted formulations (figure 4.8 C). $T_{m\text{UV}}$ showed similar improvement in 50% and no improvement in 20 % prediction

quality by combining with other predictive rankings (figures 4.I.4 C and 4.I.5 C, pages 172 and 173). Improvements in prediction quality of T_{mFTIR} (figure 4.I.7 C and 4.I.8 C, pages 175 and 176), $Temp^{50}$ (figures 4.I.10 C and 4.I.11 C, pages 178 and 179) and IsoSS 40°C (figure 4.I.14 C and 4.I.15 C, pages 181 and 182) by combining with either $T_{m\mu DSC}$ and/or T_{mUV} based rankings were observed.

4. Conclusion:

Stability of a protein formulation is determined by both physical and chemical issues. Formulation conditions as well as stabilizing excipients affect both physical and chemical stabilities variably. However, to reach the right decision in a big formulation set in order to end up with a small group where the most stable candidates are included many issues should be considered. Whether chemical or physical stability would have the upper hand in the overall stability decision is very crucial to reach such a decision. This is dependant on protein structure, nature and action of the studied excipients, and effect of other formulation conditions. Being aware of such information this study would provide the formulator with a suitable guideline to choose the method that would be suitable for the studied protein and/or experimental design. The predictive powers of five analytical strategies towards both physical and chemical stabilities were tested. Furthermore, the predictive powers of these methods towards an overall stability ranking were also evaluated. Each method showed different behaviour in predicting the long term stability of 16 GCSF liquid formulations. μDSC and UV spectroscopy were able to equally predict both physical and chemical stabilities and therefore have an advantage in predicting the overall stability of the formulation set. However, μDSC based rankings were able to predict the best 3 stable formulations without false prediction. $Temp^{50}$ which represent the temperature at which 50% of the monomer in the formulation is denatured, after non-isothermal stress from 20 to ca. 80°C, was more biased to physical stability. On the other hand IsoSS40 was extremely biased to chemical stability. FTIR showed unclear correlation behaviour due to reasons addressed in the discussion. However, including FTIR in combined rankings resulted in a significant improvement of the selection quality. Considering ranking based on FTIR, $Temp^{50}$ or IsoSS40°C didn't improve the predictive power of μDSC or UV.

5. References:

1. Matheus, S.; Mahler, H. C.; Friess, W. A Critical Evaluation of Tm(FTIR) Measurements of High-Concentration IgG1 Antibody Formulations as a Formulation Development Tool. *Pharmaceutical Research* 23[7], 1617-1627. 2006.
2. Kuelzto, L. A.; Ersoy, B.; Ralston, J. P.; Middaugh, C. R. Derivative absorbance spectroscopy and protein phase diagrams as tools for comprehensive protein characterization: A bGCSF case study. *J.Pharm.Sci.* 92[9], 1805-1820. 2003.
3. Kuelzto, L. A.; Middaugh, C. R. Structural characterization of bovine granulocyte colony stimulating factor: Effect of temperature and pH. *Journal of Pharmaceutical Sciences* 92[9], 1793-1804. 2003.
4. Matheus, S.; Friess, W.; Mahler, H. C. FTIR and nDSC as Analytical Tools for High-Concentration Protein Formulations. *Pharmaceutical Research* 23[6], 1350-1363. 2006.
5. Gareth A.Lewis; Didier Mathieu; Roger Phan-Tan-Luu . *Pharmaceutical Experimental Design.* 23-150. 1999. Marcel Dekker, Inc.
6. Ausar, S. F.; Rexroad, J.; Frolov, V. G.; Look, J. L.; Konar, N.; Middaugh, C. R. Analysis of the Thermal and pH Stability of Human Respiratory Syncytial Virus. *Molecular Pharmaceutics* 2[6], 491-499. 2005.
7. Kipp, J. E.; Jensen, M. M.; Kronholm, K.; McHalsky, M. Automated liquid chromatography for non-isothermal kinetic studies. *Int.J.Pharm.* 34[1-2], 1-8. 1986.
8. Lee, M. L.; Stavchansky, S. Isothermal and nonisothermal decomposition of thymopentin and its analogs in aqueous solution. *Pharm.Res.* 15[11], 1702-1707. 1998.
9. Weiss, W. F., IV; Young, T. M.; Roberts, C. J. Principles, approaches, and challenges for predicting protein aggregation rates and shelf life. *J.Pharm.Sci.* 98[4], 1246-1277. 2009.
10. Cooper, E. A.; Knutson, K. Fourier transform infrared spectroscopy investigations of protein structure. *Pharmaceutical Biotechnology* 7[Physical Methods to Characterize Pharmaceutical Proteins], 101-143. 1995.
11. Pelton, J. T.; McLean, L. R. Spectroscopic Methods for Analysis of Protein Secondary Structure. *Anal.Biochem.* 277[2], 167-176. 2000.
12. van de Weert, M.; Hering, J. A.; Haris, P. I. Fourier transform infrared spectroscopy. *Biotechnol.: Pharm.Aspects* 3[Methods for Structural Analysis of Protein Pharmaceuticals], 131-166. 2005.
13. Patel, K.; Borchardt, R. T. Chemical pathways of peptide degradation. II. Kinetics of deamidation of an asparaginyl residue in a model hexapeptide. *Pharm.Res.* 7[7], 703-711. 1990.
14. Lee, K. C.; Lee, Y. J.; Song, H. M.; Chun, C. J.; DeLuca, P. P. Degradation of synthetic salmon calcitonin in aqueous solution. *Pharm Res* 9[11], 1521-1523. 1992.

15. Helm, V. J.; Mueller, B. W. Stability of gonadorelin and triptorelin in aqueous solution. *Pharm.Res.* 7[12], 1253-1256. 1990.
16. Yoshioka, S.; Aso, Y.; Izutsu, K. i.; Kojima, S. Is stability prediction possible for protein drugs? Denaturation kinetics of beta -galactosidase in solution. *Pharm.Res.* 11[12], 1721-1725. 1994.

6. Appendix 4.I:



Figure 4.I. 1: Comparison between correlation coefficients resulting from correlating different FTIR measured T_m s based ranking with physical (R_p), chemical (R_c), or overall (R_s) stability based rankings of the studied 16 GCSF formulations.

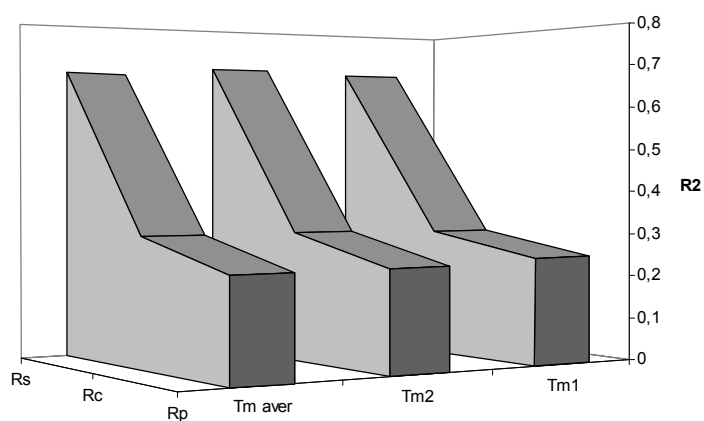


Figure 4.I. 2: Comparison between correlation coefficients resulting from correlating different UV determined T_m s based ranking with physical (R_p), chemical (R_c), or overall (R_s) stability based rankings of the studied 16 GCSF formulations.

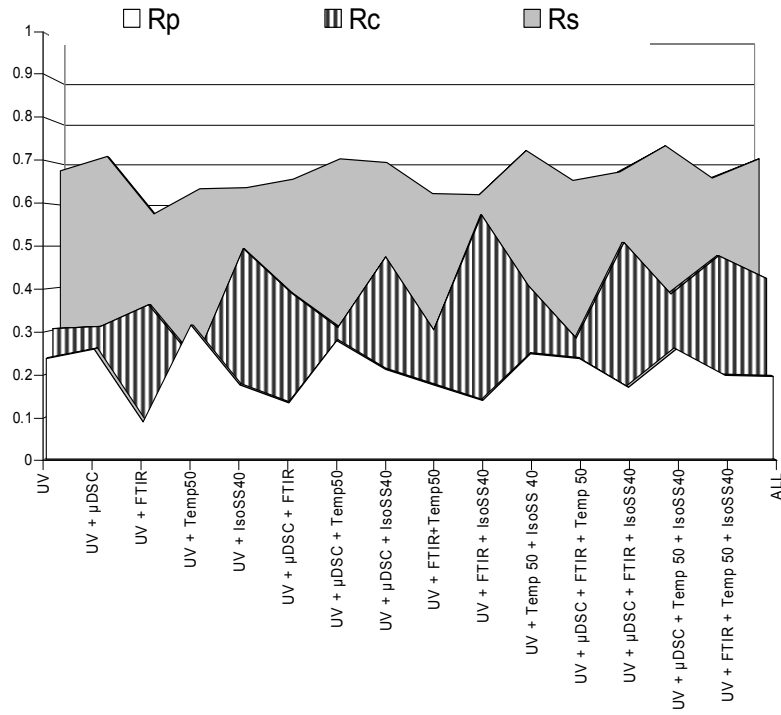


Figure 4.I. 3: Effect of combining different predictive rankings with ranking based on T_{mUV} on the correlation coefficients resulting from correlating each combined ranking with the real stability based ranking. R_p states for ranking based on physical stability, R_c for ranking based on chemical stability and R_s for ranking based on overall stability

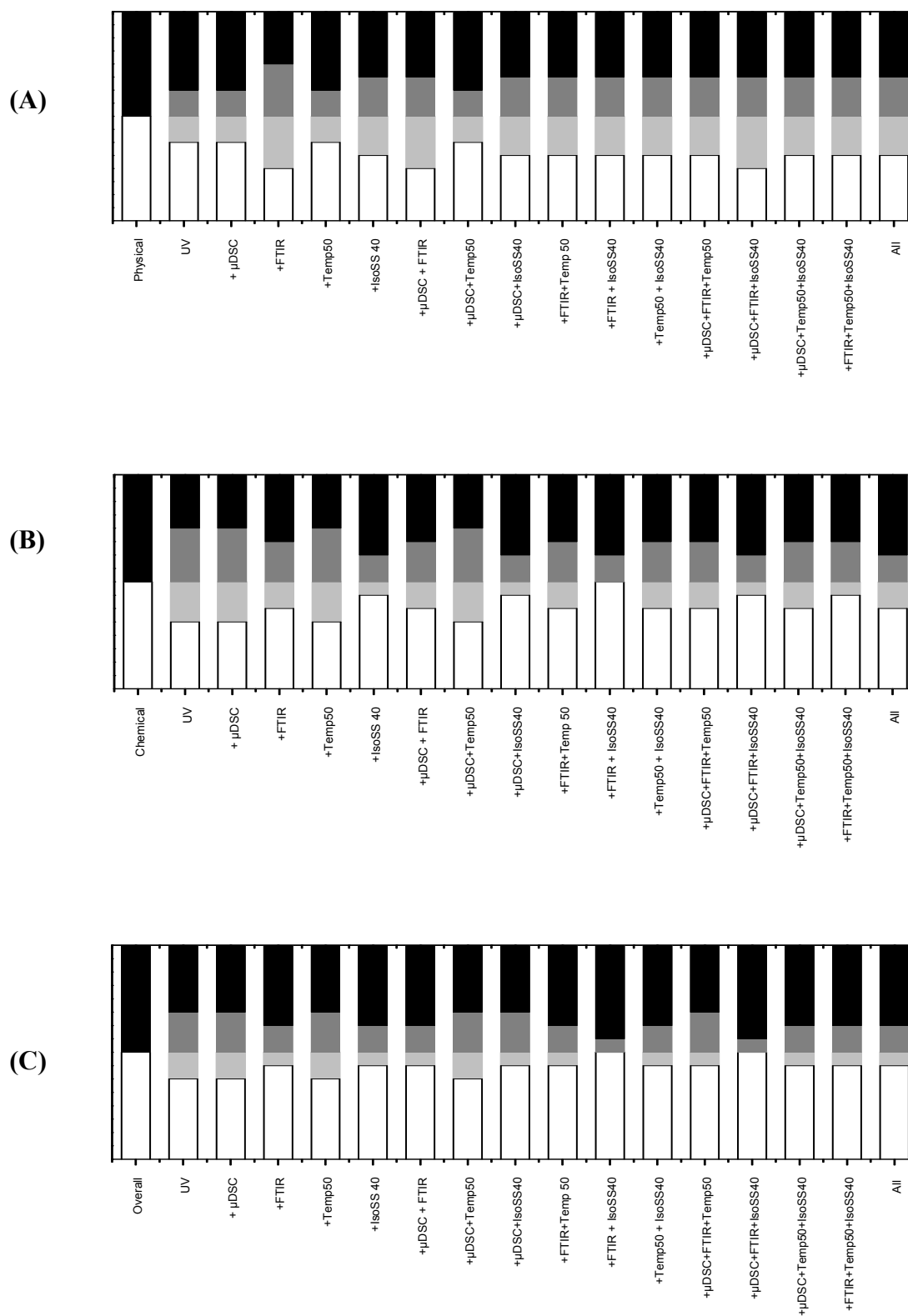


Figure 4.I. 4: Effect of combined rankings on the 50% prediction quality of T_{mUV} in predicting physical stability (A), chemical stability (B) and the overall stability ranking (C) of 16 GCSF formulations after 20 months storage at 4°C

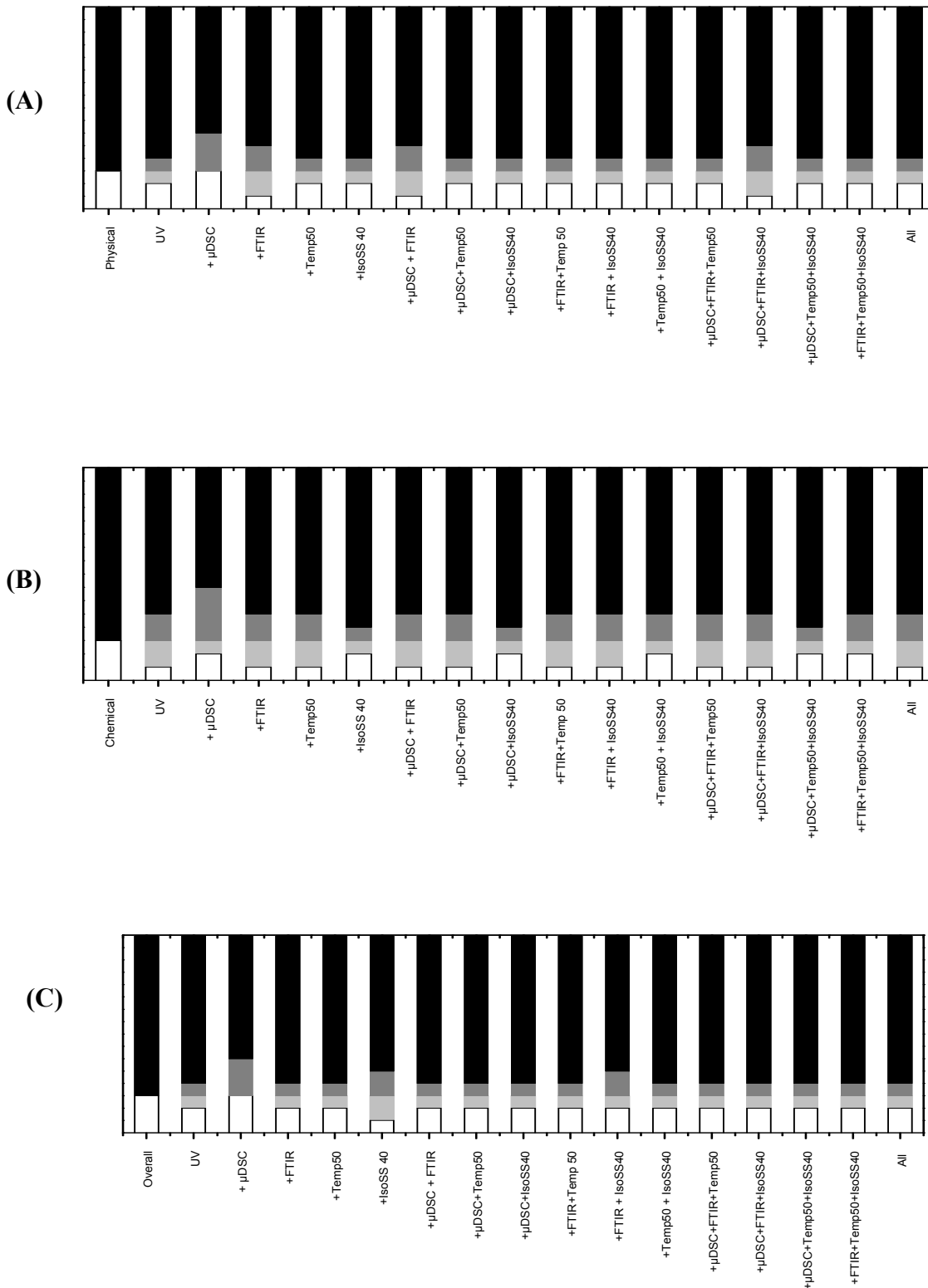


Figure 4.I. 5: Effect of combined rankings on the 20% prediction quality of T_{mUV} in predicting physical stability (A), chemical stability (B) and the overall stability ranking (C) of 16 GCSF formulations after 20 months storage at 4°C

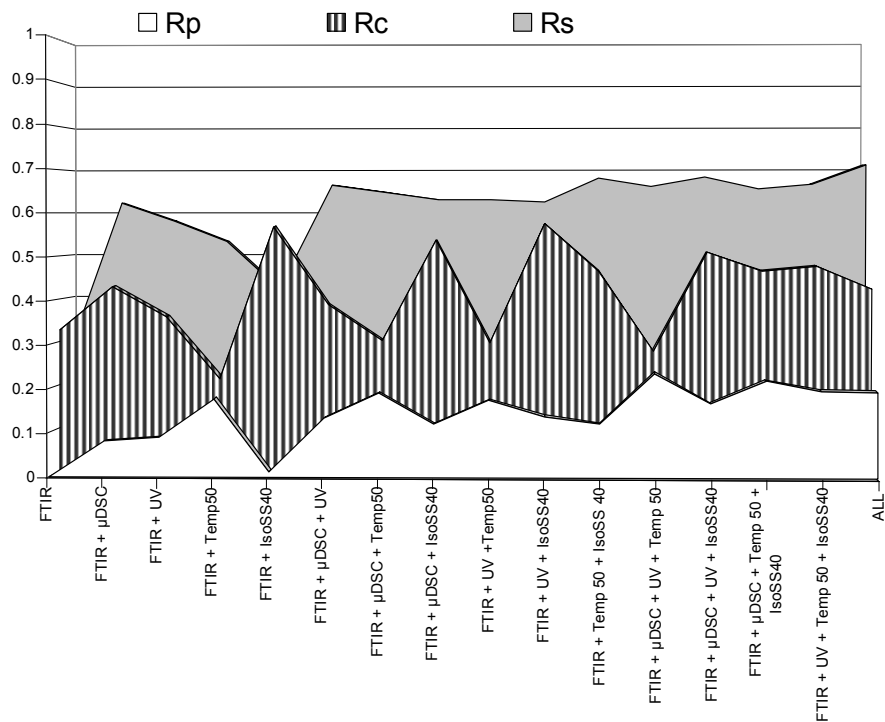


Figure 4.I. 6: Effect of combining different predictive rankings with ranking based on T_{mFTIR} on the correlation coefficients resulting from correlating each combined ranking with the real stability based ranking. R_p states for ranking based on physical stability, R_c for ranking based on chemical stability and R_s for ranking based on overall stability

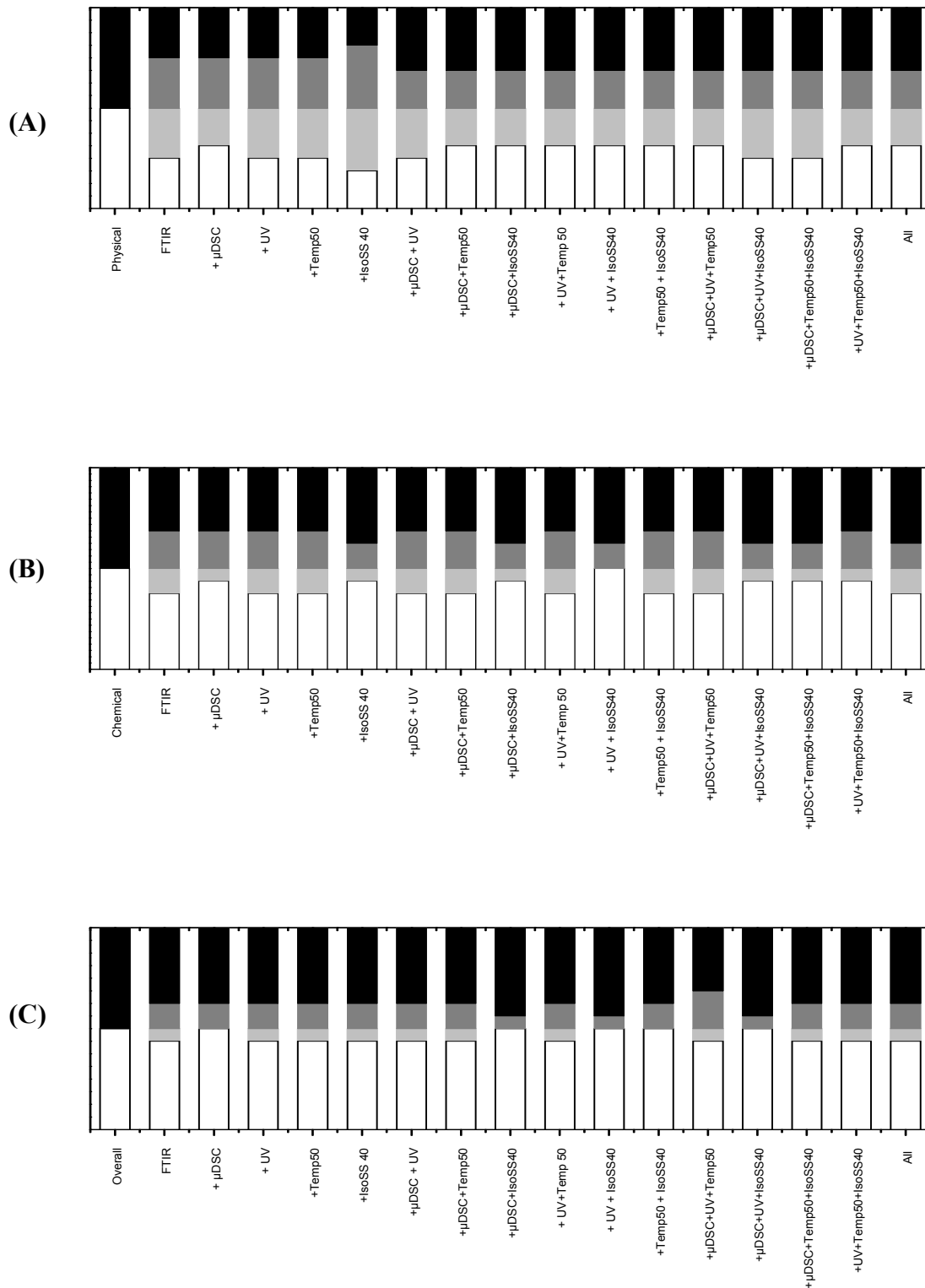


Figure 4.I. 7: Effect of combined rankings on the 50% prediction quality of T_{mFTIR} in predicting physical stability (A), chemical stability (B) and the overall stability ranking (C) of 16 GCSF formulations after 20 months storage at 4°C

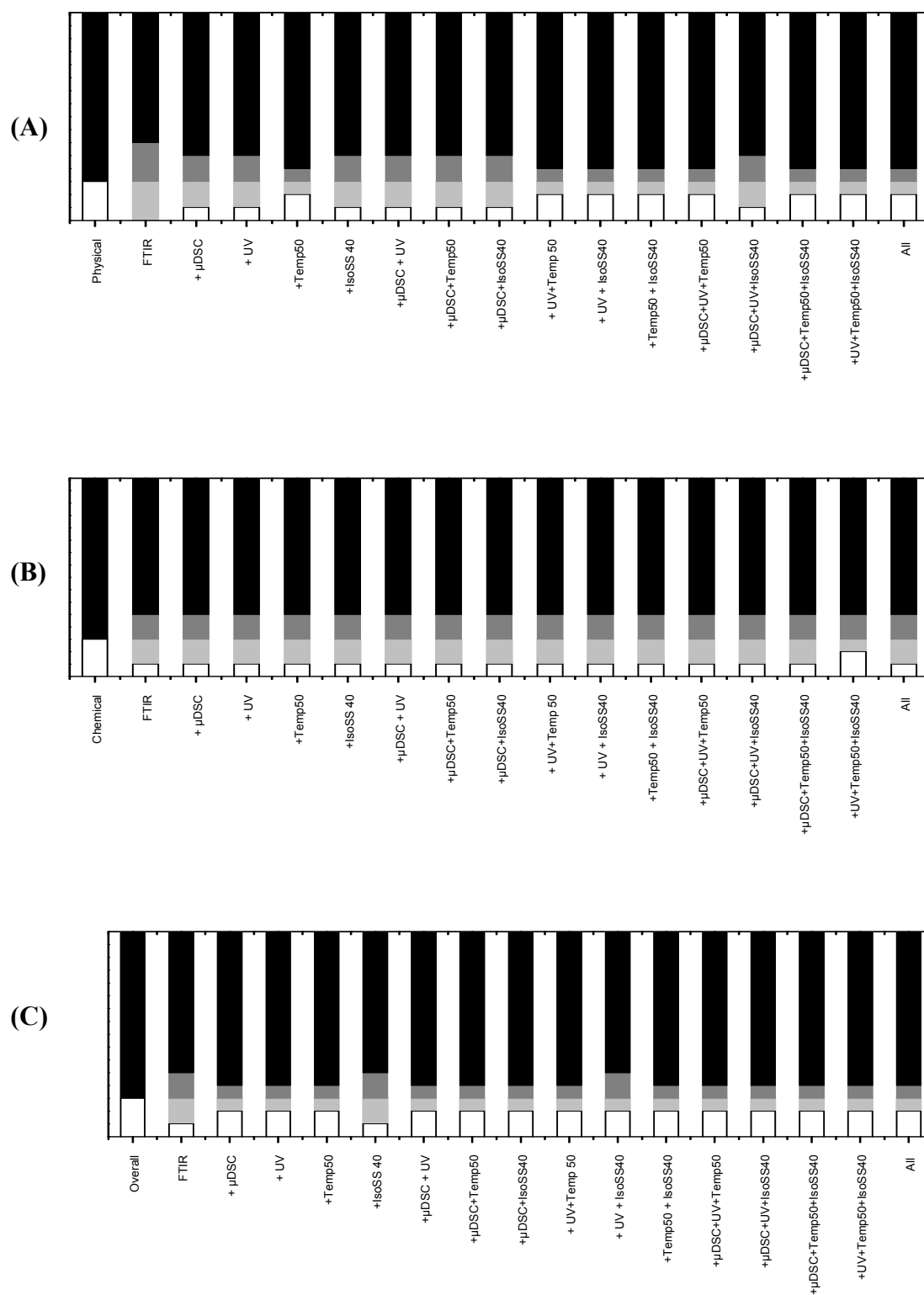


Figure 4.I. 8: Effect of combined rankings on the 20% prediction quality of T_{mFTIR} in predicting physical stability (A), chemical stability (B) and the overall stability ranking (C) of 16 GCSF formulations after 20 months storage at 4°C

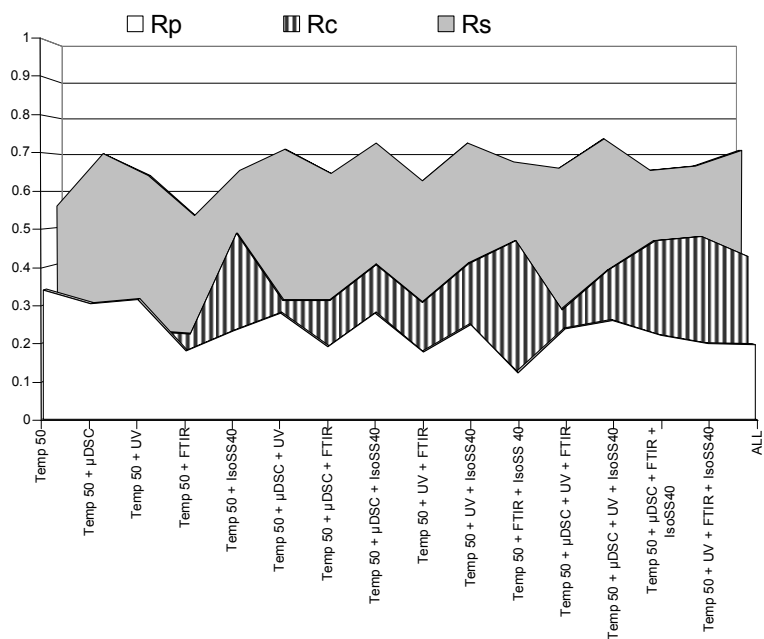


Figure 4.I. 9: Effect of combining different predictive rankings with ranking based on Temp⁵⁰ on the correlation coefficients resulting from correlating each combined ranking with the real stability based ranking. R_p states for ranking based on physical stability, R_c for ranking based on chemical stability and R_s for ranking based on overall stability

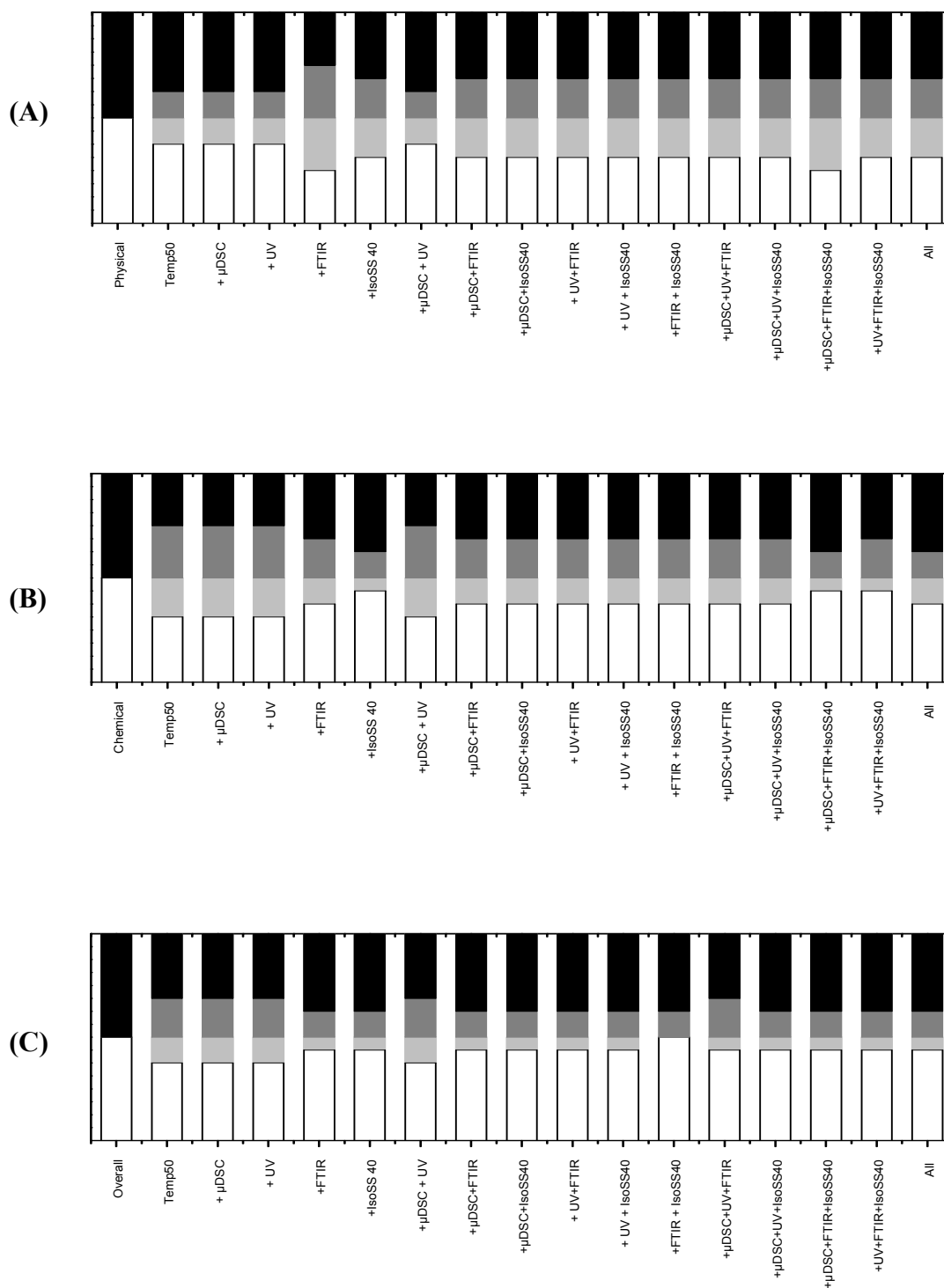


Figure 4.I. 10: Effect of combined rankings on the 50% prediction quality of Temp⁵⁰ in predicting physical stability (A), chemical stability (B) and the overall stability ranking (C) of 16 GCSF formulations after 20 months storage at 4°C

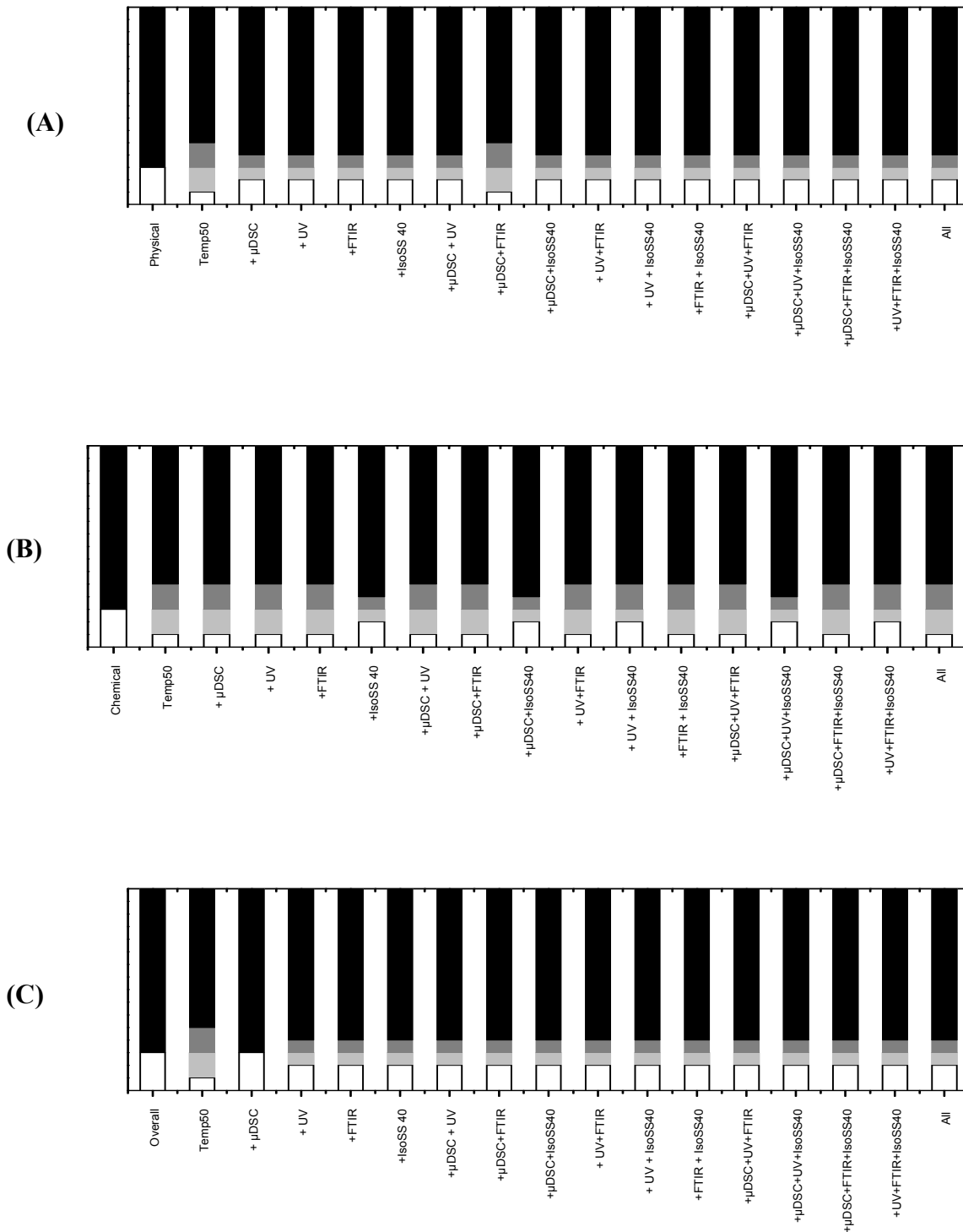


Figure 4.I. 11: Effect of combined rankings on the 20% prediction quality of Temp⁵⁰ in predicting physical stability (A), chemical stability (B) and the overall stability ranking (C) of 16 GCSF formulations after 20 months storage at 4°C

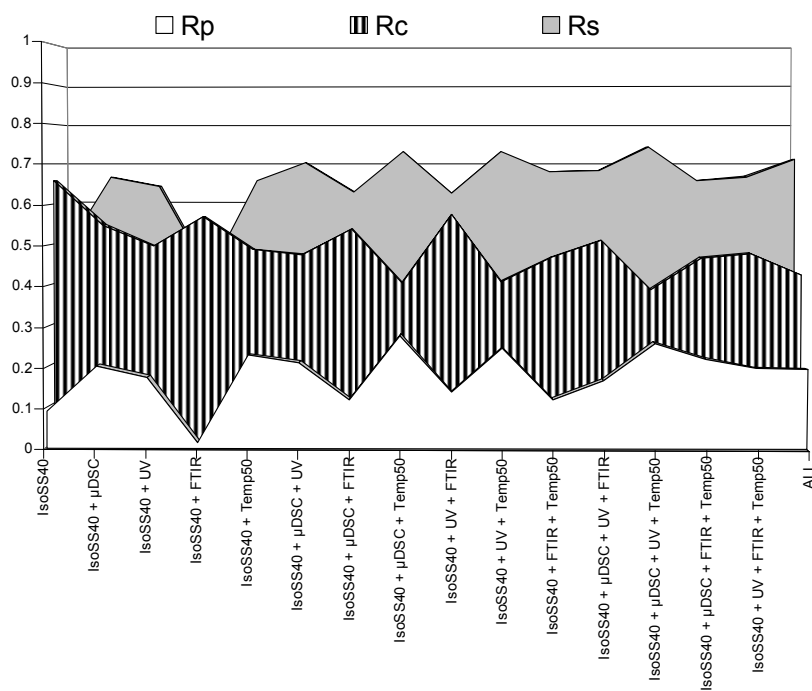


Figure 4.I. 12: Effect of combining different predictive rankings with ranking based on IsoSS40°C on the correlation coefficients resulting from correlating each combined ranking with the real stability based ranking. R_p states for ranking based on physical stability, R_c for ranking based on chemical stability and R_s for ranking based on overall stability

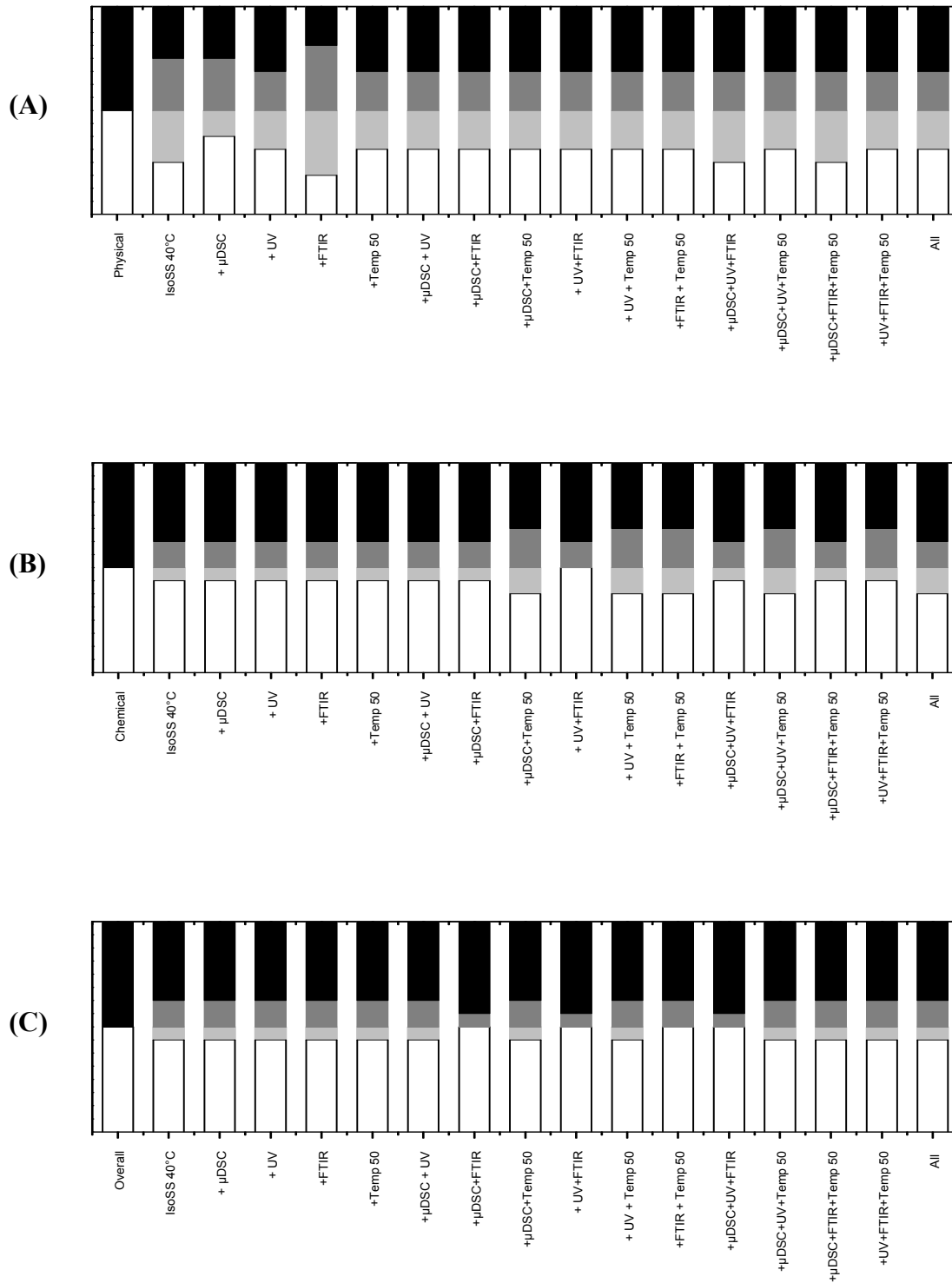


Figure 4.I. 13: Effect of combined rankings on the 50% prediction quality of IsoSS40°C in predicting physical stability (A), chemical stability (B) and the overall stability ranking (C) of 16 GCSF formulations after 20 months storage at 4°C

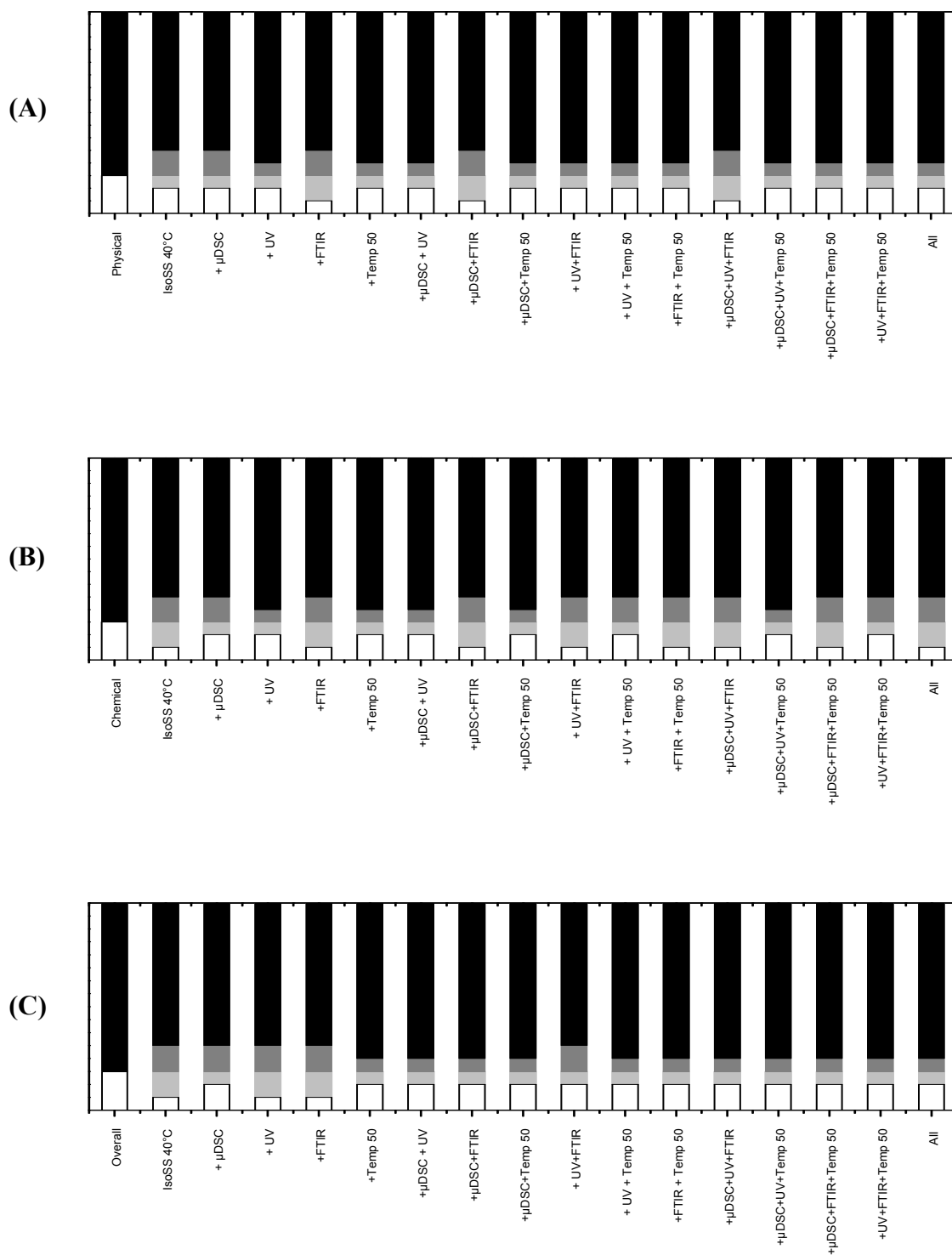


Figure 4.I. 14: Effect of combined rankings on the 20% prediction quality of IsoSS40°C in predicting physical stability (A), chemical stability (B) and the overall stability ranking (C) of 16 GCSF formulations after 20 months storage at 4°C

Chapter 5

Summary of the thesis

The prediction of the overall protein stability is not trivial before the real time stability studies are conducted, which are very costly and time consuming. Due to the complex formation mechanisms and structure of protein degradation products it is quite hard to characterize and furthermore to quantify such species accurately with a single analytical method. In fact, many analytical techniques have to be involved to get reliable decisions. Moreover, predictive strategies are still not well evaluated with respect to real long term stability of proteins. For successful prediction of protein long term stability the selected analytical method(s) should be able to predict the rates of main protein degradation processes. In chapter 1 some general aspects on protein stability are summarized including mechanisms and factors involved in protein stabilization and/or destabilization processes. Furthermore, an overview on analytical techniques used in protein formulation development is presented.

μ DSC represents a predictive tool which is believed to be successful depending on measured Unfolding temperatures (T_m) but till now comprehensive, systematic data from real time studies correlated with T_m determined by μ DSC have not been published.

Therefore, the main objective of this study is to find out how far a formulator can rely on T_m as a predictive marker for protein stability. Systematic studies to correlate μ DSC data with long term stability as well as short term stress studies are performed and the quality of the obtained prediction is evaluated.

1. Microcalorimetry as a predictive tool for physical stability of granulocyte colony stimulating factor (GCSF) in solution at different pH values (chapter2).

T_m and degree of unfolding reversibility were determined using differential scanning microcalorimetry (μ DSC) for 12 unbuffered GCSF formulations over a pH range from 2 – 7. T_m showed no significant difference in the range from pH 3.5 – 4, below and above these pH values T_m is significantly reduced. The degree of unfolding reversibility showed a clear reduction with increasing the pH values till pH 3.9. Further increasing the pH value, GCSF

showed no reversibility any more. Now the applicability of both T_m and degree of unfolding reversibility in predicting physical stability of GCSF was evaluated. Two accelerated stress stability studies applying either isothermal or mechanical stress were performed and the results were compared with the μ DSC parameters. The results showed excellent predictive power of T_m for the isothermal stability study at elevated temperature which was further improved by considering the degree of unfolding reversibility. The degree of unfolding reversibility was even significantly better than T_m in predicting the outcome of the mechanical stress stability study.

2. Critical evaluation of μ DSC as a predictive tool for the long term stability of different protein classes (Chapter 3).

A systematic stability study on up to 24 different Granulocyte colony stimulating factor (GCSF), 15 Monoclonal antibody (MAB) and 14 Pegylated Interferon α 2a (PEG-INF) formulations was performed. The formulations were tested with respect to different factors. For all formulations T_m and unfolding reversibility, when applicable, were determined. The same formulations were used for isothermal stability studies (IsoSS) at ICH temperatures (4, 25, and 40°C) for a period of up to 24 months in GCSF and 12 months for MAB and PEG-INF. At different time intervals the formulations were analyzed using classical analytical methods (size exclusion chromatography, turbidimetry, light blockage, gel electrophoresis, and reversed phase chromatography). Finally, microcalorimetric data were correlated with IsoSS data

In large groups of formulations T_m was not able to predict the exact rank order, but selecting the good formulations and excluding the bad ones was an excellent approach to reduce the work load in long term stability studies. Surprisingly, T_m showed stronger correlation and more reliability than routinely applied accelerated stability studies. Such conclusions should encourage many changes in routinely applied formulation development scenarios in biopharmaceutics.

In 24 GCSF formulations, where T_m and unfolding reversibility could be determined, further optimization of T_m based ranking by considering the degree of unfolding reversibility did not show any significant benefit on predictions. T_m showed superior predictive power, in predicting the overall stability ranking especially at 4°C. Although ranking based on IsoSS at

25°C showed higher correlation coefficients and higher prediction quality toward real time stability at 4°C, 9 to 12 months are needed to reach predictive results. Predictive studies using μ DSC for 24 formulations can be carried out in an experimental plan which needs less than 4 weeks to be done and show approximately similar predictive power compared to IsoSS at 25°C. Concerning chemical stability, IsoSS at elevated temperatures (e.g. 40°C) showed significantly higher correlation coefficients and high prediction quality.

In a μ DSC study for 15 MAB formulations three different transitions were determined. Selecting the good formulations and excluding the bad ones was very successful based on the earliest transition (T_{m1}) especially for long term stability at 4°C. Predictive studies based on T_{m1} measurements had proved superiority in predicting physical stability ranking to the routinely performed accelerated isothermal stability studies at elevated temperatures.

For PEG-INF formulations T_{ms} were not able to predict the long term stability at 4°C but selecting the good formulations and excluding the bad still did work. Pegylation of a protein molecule seems to prevent accurate prediction of the long term stability at 4°C.

3. Other strategies for the prediction of long term stability of GCSF liquid formulations (Chapter 4).

In this study the long term stability data of 16 from the previously studied 24 GCSF liquid formulations were used to evaluate other predictive methods. Those include Fourier Transform Infrared Spectroscopy (FTIR), 2nd Derivative UV spectroscopy and non-isothermal stability studies. Improvement of the predictive power was also tested by a combined ranking approach.

The predictive powers of five analytical strategies towards both physical and chemical stabilities were tested. Furthermore, the predictive powers of these methods towards an overall stability ranking were also evaluated. Each method showed different behaviour in predicting the long term stability of 16 GCSF liquid formulations. μ DSC and UV spectroscopy were able to equally predict both physical and chemical stabilities and therefore have an advantage in predicting the overall stability of the formulation set. However, μ DSC based rankings were able to predict the best 3 stable formulations without false prediction. $Temp^{50}$ which represent the temperature at which 50% of the monomer in the formulation is

denatured, after non-isothermal stress from 20 to ca. 80°C, was more biased to physical stability. On the other hand IsoSS40 was extremely biased to chemical stability. FTIR showed unclear correlation behaviour due to reasons addressed in the discussion. However, including FTIR in combined rankings resulted in a significant improvement of the selection quality. Considering ranking based on FTIR, Temp⁵⁰ or IsoSS40°C didn't improve the predictive power of μ DSC or UV.

For a better quality of candidate selection during protein formulation development a formulation selection scheme was suggested and shown in figure 5.1

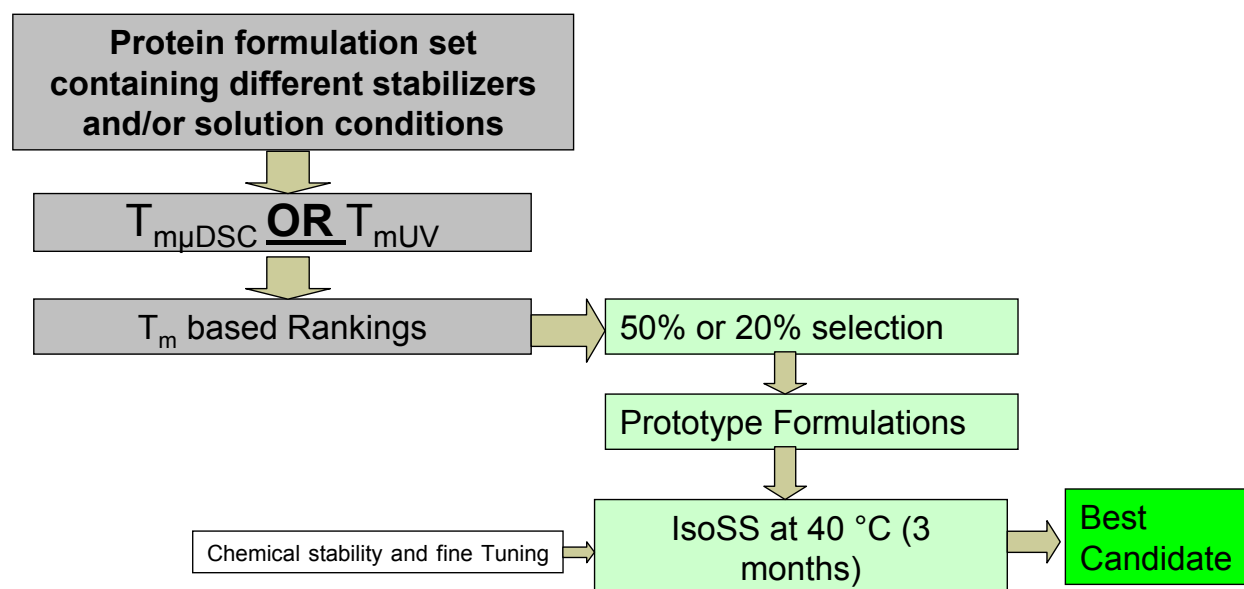


Figure 5. 1: Formulation selection scheme for better quality of candidate selection

Presentations and publications associated with this thesis

Poster presentations

A Youssef, G. Winter. The use of Microcalorimetry for prediction of the physical stability of a Monoclonal antibody. Application of Bio-calorimetry (abc6), Heidelberg, Germany, 7th-10th July 2008.

A. Youssef, F. Gruber, G. Winter. Systematic correlation study of thermodynamic parameters determined by μ DSC for liquid GCSF formulations with conventional isothermal stability study. 6th World Meeting on Pharmaceutics, Biopharmaceutics, and Pharmaceutical Technology, Barcelona, Spain, April, 6th-10th 2008

A. Youssef, F. Gruber, G. Winter. Systematic Correlation of Microcalorimetry Data with Conventional Stability Study Results for Protein Drug Formulations: Liquid GCSF formulations. AAPS Annual Meeting and Exposition, San Diego, CA, November 11th - 15th 2007

Oral presentations

A. Youssef, G. Winter. Prediction of real time stability of GCSF liquid formulations: Comparison of microcalorimetry (T_m) vs. accelerated stability studies. 7th World Meeting on Pharmaceutics, Biopharmaceutics and Pharmaceutical Technology, Valleta, Malta, 8th – 11th March 2010

A. Youssef, G. Winter. Is T_m a good marker for predicting biopharmaceutical formulation stability? Application of Bio-calorimetry (abc6), Heidelberg, Germany, 7th-10th July 2008

Curriculum Vitae

Ahmed Moustafa Kamal Youssef Mohamed

Personal details

Date of birth: 02.11.1973

Place of Birth: Assiut, Egypt.

Nationality: Egyptian.

Education:

10/2009 – Now Laboratory Head ,Pharmaceutical Sciences Dept., Sanofi-Aventis,
Frankfurt, Germany

04/2006 – 10/2009 PhD student, Dept. of Pharmaceutical sciences, Ludwig-
Maximilians-University, Munich, Germany
Title: *Systematic studies to correlate Microcalorimetry with
stability studies on liquid formulation of various protein drugs.*
Under the scientific advisory of: Prof. Dr. Gerhard Winter.

01/2002 - 07/2004 Master of Pharmaceutical Science (Pharmaceutical Technology),
Faculty of Pharmacy, University of Tanta, Egypt.
Title: Study of the inclusion complexes of certain drug systems

10/1996 - 06/1998 Preparatory courses for master degree, Faculty of Pharmacy,
University of Tanta, Egypt

09/1991 - 05/1996 Bachelor of Pharmaceutical Science (Grade: very good), Faculty of
Pharmacy, University of Tanta, Egypt